Evolutionary patterns derived from 150 million years of morphological and functional evolution in neopterygian fishes

John T. Clarke

St Hugh's College

Department of Earth Sciences

University of Oxford

Submitted to the University of Oxford for the degree

Doctor of Philosophy in Earth Sciences

Trinity 2015

Supervised by Prof. Matt Friedman

Thesis Contents

Acknowledgements

It seems impossible for me now to fully contemplate the efforts made by my supervisor, Matt Friedman, over the course of my DPhil research. To feel in some way responsible for my progress and wellbeing for four years must require staggering levels of patience and care that I cannot truly comprehend unless I am placed in a similar position. I thank him deeply for all of his guidance in so many areas, from assistance in framing project ideas, providing carefully considered methodological advice, and taking the time to provide detailed feedback on talks, to all of the fantastic comments he has provided on numerous abstracts, reports and thesis chapters. He has always supported me in any way he could, and I thank him for coping with my rambling e-mails and other quirks in a positive and well-humoured manner. I am fully aware of how lucky I have been in these respects, and will be forever grateful.

Graeme made a huge contribution to this work, and it is difficult for me to imagine what I could have produced without his guidance. I was delighted to learn some years ago that he would be joining the lab in Oxford, although it was a decision he would learn to regret! How he coped with the sheer quantity of method (and football) related questions, I'm not sure. Having discovered fairly early on that I lay at the tail of a distribution with regards to 'natural' programming ability, Graeme helped me to paper over the cracks and kick on, to the point that he has been freed from the tyranny of providing programming tips for over a year! I can only hope I didn't factor into his decision to move to Australia. I am indebted to Graeme for his help, and hope I can return the favour in future.

I remember meeting Roger Benson for the first time at SVPCA in Lyme Regis, and sought him out at subsequent conferences. Rogers's arrival in Oxford has brought great energy and

evermore rigour to the lab, and I have greatly enjoyed the lab meetings and pub trips alike where he shared his insights into a plethora of evolutionary topics and methodological questions. Roger has shown great patience with me in particular, taking the time to provide in depth discussion pertaining to particular methods, and providing assistance in their execution. I thank him for his time, patience, and ability to convey complex ideas in an intuitive manner.

The Palaeobiology lab in Oxford has changed dramatically from my arrival. I'm grateful to have caught the tail end of Martin Brasier's lab, including Leila Battison, Alex Liu, Jack Matthews, Latha Menon, Renee Hoekzema and of course, Martin himself, who did much make me feel welcome when I arrived. It was great to see Laura Soul and Sam Giles join the lab, and both have inspired aspects of my own work. Laura has taken the time to discuss many methodological topics with me, enthusiastically explaining tricky concepts and helping with problematic pieces of code. Sam has always been eager to offer insights and assistance whenever I have needed it, especially in the final stages of writing, where she regularly offered to look over aspects of my work. There may even come a day when Sam stops berating me for everything I do…but I'm not going to count on it! It's clearly an act of admiration!

The lab continued to grow with the arrival of molecular systematist Rich Harrington, and palaeontologist Roger Close. Both have been generous with their time, and fortunately there has been sufficient overlap in our projects to allow for useful discussions and help in all directions. Then there was the arrival of Daniel Delbarre and Andrzej Wolniewicz. Dan has kept a low profile since his arrival due to his sneaky library working exploits, although Christmas parties are useful for revealing another side to people! Andrzej seems to be taking after Sam, berating me in all aspects of vertebrate palaeontology, including my inspirational

abilities to place dots around fishes. He has provided great company since his arrival, and I look forward to more fun times with Andrzej and the rest of the lab after submission. I am grateful to those who gave their time to proofread various chapters (Sam, Laura, Roger, Rich and Graeme), including two new members of the lab, Gemma Benevento and Mimi Beckett.

Although much of my time as a postgraduate has been spent welded to my office chair and claiming the department as my home, this has been counterbalanced by wonderful opportunities for travel to numerous collections around the world to conduct my research. These trips would, of course, not have been impossible without funding, and I am thankful to NERC and the Palaeontological Association (Whittington Award) for making them possible. I thank all of the curators and museum staff who allowed me access to the specimens in their care, often greatly assisting data collection through equipment provision and much more, at the following institutions:

Australian National University, Canberra: Lynne Bean

Austrailian Museum, Syndey: Yong Yi Zhe, Tina Goh

Geological Survey of NSW, Londonderry: Ian Percival

Stuttgart State Museum of Natural History: Ronald Böttcher

Urweltmuseum Hauff, Holzmaden: Rolf Hauff

Steve Etches collection of Kimmeridge Clay fossils

Natural History Museum, London: Zerina Johanson, Martha Richter and Sally Young

Museum of Natural History, Milan: Cristiano Dal Sasso

Museum of Natural Sciences, Bergamo: Anna Paganoni and Annalisa Aiello

Friulian Museum of Natural History, Udine: Luca Simonetto and Fabio Dallavecchia

University of Milan: Andrea Tintori and Cristina Lombardo

Paleontological Institute and Museum, Zurich: Heinz Furrer and Carlo Romano

American Museum of Natural History: Alana Gishlick

Peabody Museum, Yale: Daniel Brinkman

Museum of Comparative Zoology, Harvard: Jessica Cundiff

Beyond the fantastic help of these curators, there is a small army of people to thank who helped me on my travels, providing much needed assistance, entertainment and most commonly a place to sleep as it became inevitable that the student stipend alone would not cover the full costs.

In Australia, I am particularly grateful to Niki Sabel and Trevor Croft, Lynne Bean, Ian Percival and Tina Goh. I cannot thank enough my hosts in Syndey, Niki Sabel and her partner Trevor. They put me up for almost three weeks, allowing me to tackle jetlag prior to the paleobiology database course, visit numerous local collections, and take a short Gondwanan holiday. The only downside was the monster cockroaches that were attracted to the insecticide sprayed on my bedroom floor. It's a special type of fear. Lynne Bean was kind enough to put me up for a few days at her Canberra home, allowing me to examine her own collection as well as those at ANU. I also appreciate the time she took to show me around some of the sights, and I've developed a bit of a habit for ANZAC biscuits ever since. I'm still surprised to learn that she used to teach at my old school…although her comments on the place were far from complimentary! Ian Percival provided great assistance, advising me on the stratigraphy of the Sydney basin and its various fish localities as well as picking me up from the station when I travelled to Londonderry each day. I also thank Tina Goh, who seemed more than happy to mother me during my time at the Australian Museum, inviting me to museum events and treating me to a meal at her favourite new restaurant! Finally, I am grateful to the demonstrators on the palaeobiology database course (Gene Hunt, John Alroy, Pete Wagner,

Tom Olszewski and David Polly) for taking the time to prepare vast amounts of teaching material, and opening the door to a wide array of methods that I will continue to use in my research.

In Germany, I am indebted to Detlev Theis for facilitating my trip to Holzmaden and Stuttgart, picking me up from the airport, arranging accommodation in Holzmaden, and accompanying me to both museums. He also converted me from a cider drinker to a beer drinker in the space of a single day, and I haven't looked back since!

In the US, I am particularly thankful to the grad students at AMNH, Harvard and Yale for helping me out during my time there. Jo Wolfe helped me settle in New York, while Simon Darroch, Rachel Racicot and Joseph Panzik all put me up in New Haven, and Eric Sperling and his housemates were kind enough to provide me with a sofa for a few nights in Boston.

In Italy, I reserve special thanks to Marco Castiello and his family. I remember adding something fossil fish related to my Academia.edu account the week before I was due to head to Milan, provoking a message from this enthusiastic former student of Andrea Tintori. Learning of my trip to Milan, Marco happily welcomed me into his home, where I shared a room with him and his sister for over two weeks. I must admit that I struggled with evening conversations over dinner, although I still managed to convey my appreciation for homemade orange schnapps! I can only hope I helped Marco in some small way by encouraging him to attend SVPCA and meet with those that share his interests, and was delighted to learn he had joined Martin Brazeau's lab at Imperial. In Udine, I thank Luca Simonetto for kindly collecting me from the station, taking me around the various fossil stores, and providing me with my very own tour of the town.

In London, I am thankful to Sally Young, who agreed to watch over me each evening, allowing me to work late at the museum. Even closer to home, I thank all of those at Oxford that have helped make my time here a pleasure, from fancy college meals and five-a-side football to baking extraordinary Christmas cakes. Particular thanks go to my office mates Gemma Prata and Alison Small for boosting morale throughout. I must single out Stefan Lachowycz for special praise for being a brother in arms throughout the entirety of the DPhil, providing company on the countless late nights, forever armed with well-informed, cutting insights into politics and current affairs, and for becoming something of a personal shopper in the latter stages of thesis preparation, it made all the difference!

I would like to thank my partner Rhiannon Davies for the love, care and consideration she has shown throughout the years, including temporarily bailing me out financially during my first year when the MSc repayments combined with college rents became too difficult to handle. How she has put up with all my work related ramblings and other habits I will never know. I can only hope I acted to support her with as much care as she has supported me.

Finally, I am thankful to my parents for everything they have done for me over the years, setting me free to pursue whatever I wished. The frequent phone calls of an evening helped me feel at least a little socially active towards the end, and I apologise for not visiting often as I would like, I will put that right soon enough.

Abstract

Neopterygian fishes represent over half of vertebrate richness in the Recent and display staggering phenotypic variety, yet little is known about the first 150 million years of their evolution. Furthermore, neopterygian richness and disparity is highly unevenly partitioned between teleost fishes, with ~29,000 species expressing a plethora of phenotypes, and holostean fishes, with 8 species and just two morphological styles. Fossil phenotypes have the unique ability to illuminate the assembly of neopterygian disparity, and can reveal the pattern by which the uneven partitioning of disparity arose.

Morphology and function were quantified with landmarks and six functional traits, respectively, for 356 neopterygian species known globally throughout the first 150 million years of their history. The main axes of morphological and functional variation were derived and used to examine a series of evolutionary questions. Pertinently, they revealed how disparity was accumulated for 60% of the neopterygian radiation; morphological disparity increased through time, whereas functional disparity remained stable.

The morphological dataset was expanded to include shape data for 398 species and size data for 471 species. Time scaled supertrees containing 671 mostly Mesozoic, but also living neopterygian species, were created. Together, the trees and traits were used to quantify evolutionary rates and innovation and test the predictions of genome duplication enhanced morphological diversification in teleosts, and the presence of 'living fossil' characteristics in holosteans. The analyses revealed higher rates and greater innovation in teleosts guaranteed to possess duplicated genomes, consistent with the predictions of genome duplication enhanced diversification. The only 'living fossil' characteristic of holosteans is their poor capacity for size innovation, yet they possess relatively high rates of shape evolution. However, estimates of rates and innovation are heavily influenced by timescale choice, emphasising the need for workers to perform their analyses on a variety of plausible timescales to determine the limits of their conclusions.

Extended abstract

A fundamental goal of evolutionary biology is to explain the diversity of life on Earth. Key to achieving this goal is to understand why species diversity (richness) and anatomical form (disparity) are so unevenly distributed across the tree of life. Particularly noteworthy are cases where closely related groups strongly differ in richness and disparity. The two monophyletic divisions of 'advanced' ray-finned fishes (neopterygians) provide one of the clearest examples of this pattern. Teleosts comprise approximately 29,000 species (about half of all living vertebrates), assume a bewildering array of morphologies, and have come to occupy nearly every aquatic environment imaginable, from alpine streams to the deepest ocean trench. In dramatic contrast, holosteans number a mere eight living species and are geographically restricted to the freshwaters of eastern North America. The asymmetry between these two clades has provided the basis for assertions of teleost 'superiority' and fuelled a series of evolutionary scenarios. However, these assertions lack any historical data, and even a cursory examination of the neopterygian Mesozoic fossil record points to patterns of diversification very different from those inferable from living taxa, as holosteans show far greater richness and disparity compared with the Recent. Unfortunately, a cursory examination is all that is currently possible regarding the morphological and functional history of Neopterygii, since, for the first 150 million years of this radiation, there has been no broad examination of their global disparity. This thesis aims to addresses this situation through examination of over 400 Mesozoic species, to document the morphological and functional variety of Mesozoic neopterygians, reveal the pattern by which this diversity was assembled for the first 150 million years, and then use this data to address a series of evolutionary scenarios.

There are currently no broad scale hypotheses of phylogeny for Mesozoic neopterygians, yet such a framework is essential in order to illuminate the diversification history of the

Neopterygii. Instead, many smaller scale phylogenies exist that rarely overlap in scope. Furthermore, most taxa have never been included in a formal, or informal (hand-drawn) phylogenetic hypothesis. A supertree of 671 Mesozoic and living neopterygians (Chapter 2) was therefore created for two purposes. The first was as a means to summarise the state of knowledge on the interrelationships of Mesozoic neopterygians, and the second was to derive topologies for later comparative analysis and simulations. The 10,500 supertrees revealed that, although there was relatively reasonable levels of agreement within well-defined clades (although some of this agreement itself often derives from the rarity of solutions), the relationships between major clades within Halecomorphi, Ginglymodi and Teleostei were poorly resolved, even under a majority rule consensus. Especially poor regions of resolution include the majority of the teleost stem, and the considerable diversity of Ginglymodi *incertae sedis* and Neopterygii *incertae sedis* taxa.

Morphology and function were quantified by landmarks and six functional traits, respectively, for 356 neopterygian species known globally throughout the Triassic, Jurassic and Early Cretaceous. Ordination of these respective datasets yielded the major axes of variation which were used to examine patterns of disparity and ordination space occupation through time. Disparity through time plots (Chapter 4) indicate that morphological disparity in Neopterygii increases through the Mesozoic, whereas functional disparity remains stable, observations that are clearest when *Lagerstätten* are removed, or with genus range data. Trajectories for Holostei and Teleostei individually are broadly consistent with these observations.

Early high disparity is a common feature of palaeontological datasets, and three definitions of this phenomenon were created (1. shared maximum, 2.uniquely early and 3.bottom heavy early high disparity) and sought for in the trajectories (Chapter 4). Whereas morphology

tended to show no clear indications of early high disparity, since all trajectories appear top heavy (there is potential for 'shared maximum disparity' in Teleostei and Holostei), functional data exhibit relatively flat trajectories, implying that all clade trajectories (Neopterygii, Holostei, Teleostei) show 'shared maximum disparity' (there is potential that holosteans also show 'uniquely early maximum' and 'bottom heavy' early high disparity).

The pattern of ordination space occupation through time was examined (Chapter 3), delivering three pertinent observations. First, the extremities of morphospace and functionspace are discovered gradually through time, even though functional data showed a greater capacity for early high disparity. For example, the first deep-bodied forms with large jaw-closing and jaw-opening mechanical advantage appear in the Mid-Triassic, and the first slender-bodied taxa with small jaw-closing and jaw-opening mechanical advantage appear in the Early-Mid Jurassic. Furthermore, once extremities of morphospace are discovered, they are generally retained, whereas this is not the case for functionspace. Second, particular regions of phenotypic space were occupied in every time slice in both morphology and function, pertaining to fusiform fishes with dorsal fins inserting more anteriorly than the anal fin (for morphology), and taxa with small jaw-closing mechanical advantages and relatively long lower jaws (for function). Third, it was not until the Late Jurassic that the overall pattern of occupancy in morphological and functional space began to stabilise, rather than showing dramatic differences in the regions occupied between time bins.

Evidence for any changes over the Triassic-Jurassic boundary has proved elusive in fishes, mainly due to a lack of research attention. Changes in disparity and ordination space occupation were therefore examined for neopterygians as a whole (Chapter 4). The pattern largely depends upon insights from a Late Triassic and an Early Jurassic *Lagerstätte*, and

removal of these sites signals a decline in morphological and functional disparity over the boundary, as all deep-bodied taxa disappear. With these *Lagerstätten* retained, disparity and ordination space occupation of the Late Triassic and Early Jurassic are comparable, albeit with some new taxonomic actors (holosteans) in previous roles ('pholidophorid' regions). The most notable change was a shift from a diverse assemblage of deep-bodied taxa to a deep-bodied assemblage consisting entirely of *Dapedium* species. Furthermore, if Dapedidae are teleosts, the boundary marks the disappearance of deep-bodied holosteans.

In addition to themes already discussed that pertain mainly to Neopterygii as a whole, numerous scenarios exist relating specifically to the holostean and teleost lineages that comprise Neoptergii. One such scenario is a transition from a holostean dominated (taken here to mean greater richness and disparity) world to a teleost dominated world (Chapter 4), driven by competitive replacement of holosteans by teleosts (Chapter 3). First, the issue of transition was addressed, not just from a taxonomic perspective (on which the scenario was originally proposed), but also from the perspective of disparity. The taxonomic pattern is relatively clear; holosteans dominate the Early and Middle Triassic world prior to equivalence in the Late Triassic and Early Jurassic, and teleosts form the majority of global diversity from the Toarcian onwards. For disparity, two scenarios are possible dependent upon the placement of Dapedidae. If Dapedidae are holosteans, holosteans show greater phenotypic disparity than teleosts across the entire Triassic and most of the Jurassic, only giving way to teleosts in the latest Jurassic (Kimmeridgian – Tithonian), after which teleosts possess marginally higher disparity in all Lower Cretaceous time bins. If Dapedidae are teleosts, the holostean period of dominance is brief, restricted only to the Early and Middle Triassic, after which, in the Late Triassic potentially, but Early Jurassic definitively, teleosts obtain greater phenotypic disparity and maintain this for the rest of the Jurassic and Lower Cretaceous. Nevertheless,

there clearly is a transition from a higher diversity holostean world, to a higher diversity teleost world.

Regarding a competitive replacement of holosteans by teleosts, nearest-neighbour distances between holosteans and teleosts were examined to determine whether, under the assumption that morphology and/or function loosely correlate with ecology, there was any evidence of the ecological "swamping" of holosteans by teleosts. The analysis revealed no substantial change in these distances through time. This finding, in combination with an examination of the ordination space plots, suggested there was no compelling evidence that holosteans were increasingly "swamped" through time, nor had holosteans circumvented teleost encroachment by moving to phenotypic refugia far away from any teleost phenotypes (with the exception of the Late Jurassic proliferation of Macrosemiiformes). The need to better map the link between morphology, function and ecology in living taxa is emphasised.

Beyond scenarios that focus upon the interactions between holosteans and teleosts, numerous evolutionary scenarios have sought to explain the extant diversity of holosteans and teleosts individually (Chapter 1). The predictions of two scenarios were tested. The first scenario implies teleost phenotypic diversification was enhanced by a genome duplication event. This inherently predicts that taxa possessing duplicate genomes should show higher rates of phenotypic change and greater phenotypic innovation compared with closely related taxa lacking duplicated genomes. The second scenario is that holosteans represent 'living fossils', and as such, should exhibit low rates of phenotypic change and innovation.

The innovation aspect of these scenarios was examined in a non-phylogenetic framework simply to document the historical pattern of morphologies and functions seen in holosteans

and teleosts over the Mesozoic, using the dataset of 356 species (Chapter 3). Holosteans and teleosts commonly occupy similar regions of morphological and functional space. However, teleosts occupy far more unique regions of the ordination spaces than holosteans, in both morphology and function. The morphological dataset was expanded to include shape data for 398 species and size data from 471 species to examine evolutionary rates and innovation in a phylogenetic comparative framework (Chapter 5). The analyses recovered higher rates and greater innovation in teleosts known to possess duplicated genomes (i.e. the crown group), consistent with the predictions of a genome enhanced diversification. However, the results provide only correlational support for a link between the duplication and phenotypic diversification, and numerous other candidate explanations could be invoked to explain the pattern, such as reproductive innovations unique to crown teleosts. Furthermore, high rates within crown group teleosts follow a prolonged period of low rates within the teleost stem linage, suggesting that highly successful lineages can still arise from those that appear to be evolutionary dead-ends. Regarding holosteans, their only 'living fossil' characteristic is their poor capacity for size innovation, otherwise they possess relatively high rates of shape evolution, and their relative capabilities for shape innovation and size rates are entirely dependent on the evolutionary timescale. More broadly, these analyses highlight the importance of timescale choice in phylogenetic comparative methods, emphasising the need for workers to perform their analyses on a variety of plausible timescales to determine the limits of their conclusions.

The relationship between morphological and functional disparity is poorly understood, and previous work suggests the relationship is complex, and the two measures can become decoupled. The morphological and functional dataset pertaining to the same 356 species allowed further investigation of this relationship. Morphospace possessed greater structure

than functionspace, with dense clusters of taxa in extreme regions. By contrast, functionspace appeared relatively symmetrical in all directions with a relatively even spread of forms throughout the space. Correlations between all morphological and functional axes revealed good correspondence between the first axis of morphospace and functionspace, illustrating that deep-bodied taxa possess high jaw-closing and opening mechanical advantages and large eyes relative to length, whereas slender-bodied taxa tend to possess the inverse of these traits. Another correlation revealed an association between dorsal fin base length and relative jaw and eye size, where taxa with long dorsal fin bases possess larger relative jaw and eye sizes compared with those with small dorsal fin bases. A correlation of distance matrices revealed no association between morphological distances and functional distances, allowing huge scope for decoupling of these measures. An asymmetry was apparent, suggesting it is easier for morphologically divergent taxa to be functionally convergent, but difficult for morphological convergent taxa to be hugely functionally divergent. Correlations of first differences in mean disparity through eleven Mesozoic time bins demonstrated a moderate correlation between morphological and functional measures in Neopterygii and Teleostei, but poor correlation in Holostei. Nevertheless, the actual disparity trajectories between morphology and function differed in numerous important features in every clade. Most notably, morphological disparity tended to increase with time, whereas functional disparity tended to remain stable. All of the findings corroborate those of previous workers, highlighting that distances between taxa and disparity in morphospace cannot easily be used to infer distances and disparity in functionspace. As such, traits should be carefully selected for the question at hand. At the very least, authors should state their assumptions clearly and not place significant weight on any conclusions that require inference of one measure of disparity from another, including the relationship of these measures to ecology.

A growing significance (richness, disparity and increasing destructiveness) of durophagous neopterygian fishes forms a key line of evidence supporting the notion of a Mesozoic Marine Revolution, yet these three attributes have not been quantified in neopterygian fishes. First, the proportion of neopterygian taxa with clearly identifiable crushing dentitions peaked in the Late Triassic, falling to a consistent low in the Early Cretaceous, while absolute numbers of these species remained comparable throughout the Triassic, Jurassic and Lower Cretaceous. Second, mean jaw-closing mechanical advantage, quantified for all neopterygians to assess whether taxa on average became more destructive in their feeding capabilities through time, remained stable throughout the Mesozoic (although a general expansion in the capabilities of taxa was observed in the Albian, when taxa with the largest and smallest recorded jaw-closing mechanical advantages appear). Third, the maximum jaw-closing MA of neopterygians increases in the Late Jurassic and remains high throughout the Early Cretaceous. Forth, an analysis into the disparity of potential durophages revealed higher levels of disparity late in the Mesozoic compared with the Early and Middle Triassic, illustrating that durophages may have presented a more varied threat later in the Mesozoic. Taken together, the findings from maximum jaw-closing MA and disparity provide some support for a neopterygian contribution to the Mesozoic Marine Revolution, consistent with other proxies cited in support of this event within invertebrates.

The findings summarised above outline the utility of fossil fishes for studies of diversification, and a host of other evolutionary questions in deep-time. The quality, quantity, and duration of their record, spanning most of the Phanerozoic, render them a model system for palaeobiological research, yet they remain a poorly understood portion of the vertebrate tree of life. This thesis contributes to a growing momentum of macroevolutionary work in

fishes, which combined with their huge potential for systematic work, suggests they will form a major frontier of vertebrate palaeontology research in years to come.

Chapter 1
Understanding the diversity of life - concepts, progress, the importance of fossils and the utility of Mesozoic fishes.

PREFACE

One broad goal of evolutionary biology is to explain the diversity of life on Earth. Key to achieving this goal is to understand why diversity is so unevenly distributed across the tree of life. Diversity itself can be measured in numerous ways, be it the number of species (richness), the variety in gross morphology (morphological disparity) or the variation in biomechanical traits of organisms (functional disparity). All of these measures can be applied to both living and fossil organisms to document changes in diversity over time, documentation which is essential to establish the basic pattern of 'what happened' before seeking to understand the processes underlying the pattern. Unfortunately, establishing the pattern is notoriously difficult, as biological data are inherently incomplete due to difficulties in sampling all living species coupled with the fact that most species ever to have lived are now extinct. The problem is further exacerbated when data is available for extinct taxa, yet is ignored entirely, with ancestral traits being inferred solely from living species. Nevertheless, deterministic explanations underlying the perceived success or failure of clades are commonly created based upon Recent biological diversity in the absence of any historical data.

Fortunately, methods now exist to include fossil data within the same phylogenetic comparative framework as living taxa, and the small (but growing) number of studies in this field highlight the importance of fossil data, demonstrating how it can outright reject results based upon living species alone (Finarelli and Flynn 2006, Quental and Marshall 2010). Fossil fishes represent a group with arguably the greatest potential for such methods, given that we possess a reasonably good understanding of their interrelationships and huge numbers of species in museum collections represented by multiple articulated specimens. Despite their potential, only a handful of studies have utilised this resource in a phylogenetic comparative framework to date. This thesis aims to fill that void by focussing upon the first 150 million years of the neopterygian radiation, a period of time where no taxa (with the exception of pachycormids, Friedman 2012) have been subjected to any phylogenetic comparative method concerning phenotype. Furthermore, neopterygians represent over half of all vertebrate species in the Recent, yet their diversity is highly unevenly partitioned between teleost fishes, with 29,000 species and a plethora of morphologies recovered from nearly every aquatic environment, and holostean fishes, with 8 species and two morphological styles that are restricted to the freshwaters of eastern North America. This dramatic contrast has fuelled a series of evolutionary scenarios, many of which make testable phenotypic predictions. Thus, Neopterygii provide a golden opportunity to examine historical patterns of evolution, specifically from the perspective of morphology and function, in order to constrain scenarios regarding the asymmetries that exist between holosteans and teleosts in the Recent.

This thesis seeks to embrace this opportunity by quantifying historical patterns of morphological and functional evolution in Mesozoic neopterygians to constrain numerous evolutionary scenarios. First I create a supertree that broadly summarises the uncertainty regarding neopterygian relationships, and simultaneously provides a framework in which

fossils can be subject to phylogenetic comparative methods. I then quantify the morphological and functional diversity present in these taxa, examine the diversity present, and use this information to constrain hypotheses concerning pattern. Finally, I use this dataset to examine rates and mode of morphological change to test the prediction that an ancient genome duplication brought about higher rates and greater innovation in teleosts, a theory which represents one of the most pervasive deterministic scenarios in the evolution of fishes.

MEASURING DIVERSITY

To make any progress towards understanding the diversity of organisms, it is first necessary to quantify that diversity in some form to provide a means of comparison. Diversity measured by counting the number of species, also referred to as richness, is by far the most commonly used measure of diversity (May 1994). Several attempts have been made to ascertain the richness of species alive on the planet today (Mora et al. 2011) along with efforts to calculate richness across geological time (Sepkoski 1978, 1979, Alroy et al. 2001). However species and lineage counts are not the focus in this thesis. Instead, I focus entirely upon morphological and functional measures of diversity.

Morphological diversity

Morphological diversity pertains to variation in organismal form, and is more commonly referred to as morphological 'disparity' (Gould 1989, 1991, Foote 1990). Although qualitative descriptions of morphology have always formed the cornerstone of palaeontology, it was not until the early 1990's that methods to quantify and compare the morphological diversity of organisms were adopted and popularised (Foote 1990, 1992, 1993, 1994, Briggs et al. 1992). The early 1990s also coincided with the revolution in geometric morphometrics (Rohlf and Marcus 1993), which saw an explosion in the number of landmark based techniques focussed

upon analysis of shape (Adams et al. 2004). Landmark methods have long since matured into a set protocol (Adams et al. 2004), and both discrete and landmark based measures remain popular in studies of disparity today. However, discrete characters, often based upon the identical character matrices created for the purpose of phylogenetic work, have emerged as the data of choice for large scale analyses of disparity, due to the ready availability of data and its ability to compare drastic body plans (Wills et al. 1994). However, partially as a result of disparity studies focusing upon cladistic datasets, there is a relative paucity of broad scale, shape based measures of disparity from groups with relatively well constrained relationships (e.g. vertebrates). Of the few broader scale studies in existence, with the exception of Friedman (2010; 605 species), most average around 100 taxa (Wesley-Hunt 2005, Drake and Klingenberg 2010, Goswami and Polly 2010), illustrating the need for more large scale analyses of shape disparity. This thesis will help to address the imbalance between studies of cladistic and shape disparity by quantifying shape for 356 neopterygian fishes across the Mesozoic.

Functional diversity

Functional diversity (= functional disparity) seeks to quantify the variation in specific morphological traits that possess either a known or presumed ecological or biomechanical function. A classic example of a functional trait is the mechanical advantage of the lower jaw, which is the ratio of the input to the output arm when the jaw is modelled as a simple lever (see 'functional traits' in Chapter 3 for full details). This ratio captures the trade-off between bite force and bite velocity, providing broad information on feeding capabilities, and can be readily applied to fossil taxa (e.g. Wainwright and Bellwood 2002, Bellwood 2003). Traditionally, functional traits have been studied in isolation (e.g. Lighthill 1975), or as bivariate plots to examine the functional variety present, and the potential ecological

correlates of those functions (e.g. Bellwood 2003, Goatley 2010). In contrast, the combination of numerous functional traits within an ordination to examine functional disparity over a fossil record time series appears to be a relatively recent phenomenon (Anderson et al. 2011, Stubbs et al. 2013). Therefore, in comparison with analyses of morphological disparity over fossil time series, there is a paucity of comparable functional analyses, and the available evidence suggests it is important to examine both, since morphological disparity can bear poor correspondence to functional disparity (e.g. Anderson 2009). This thesis helps address the imbalance by quantifying functional disparity in the same 356 Mesozoic neopterygians used to examine morphological disparity.

Reading Diversity Patterns: progress delimiting stochastic verses deterministic explanations

Why are some groups so diverse (taxonomically, morphologically and functionally) whereas others are not? The uneven partitioning of diversity is a prevalent feature across the tree of life, and understanding its causes would represent an important milestone towards explaining the diversity of life on Earth. At present, two end-member explanations attempt to explain how this unevenness is generated. The first argues that successful groups achieve their success through possession of some key features or a greater capacity to evolve, whereas the second claims that the unevenness is generated purely by stochastic mechanisms. The first represents a deterministic view of the evolutionary process, whereas the latter is entirely to do with chance, yet our ability to distinguish between the two for large groups of organisms over long timescales has only become possible relatively recently with the continued development of phylogenetic comparative methods (e.g. Alfaro et al. 2009, Eastman et al. 2011).

Deterministic views of evolution have long been pervasive in evolutionary thought. The earliest formalisation of such views in an evolutionary framework can be traced to Jean-Baptiste Lamarck (1744-1829), specifically in the form of his 'complexifying force' rooted in the principles of alchemy, whereby the movement of fluids within organisms would drive them to greater complexity (Lamarck 1815).

Even in the shadow of Darwin's 'Origin of Species', deterministic views of evolutionary change remained, best encapsulated under the broad banner of orthogenesis, popular in the late 1800s and early 1900s. Orthogenesis under most definitions characterises some form of directional, non-adaptive evolutionary change (Levit and Olsson 2006), and was popularised by Eimer in the 1890s (Bowler 1989). It was evidenced by perceived trends in the evolution of fossil (e.g. the evolution of progressively larger horns or antlers throughout geological time) and living organisms (e.g. common themes of butterfly patterning), what we would now refer to as convergent evolution or mimicry. However, true determinism came in the form of the explanations put forward for such trends, such as teleological views that nature has goals, in a 'drive to perfection' (Nägeli 1884, Levit and Olsson 2006), or that they were driven by ontogeny (Eimer 1888, Levit and Olsson 2006).

The arrival of the modern evolutionary synthesis saw a decline in directional views of evolution, yet there remains ample room within this framework for deterministic explanations for the perceived success or failure of clades. These are most clearly apparent in the variety of key innovations suggested throughout the second half of the 20th century, prominent examples of which include the evolution of flight in birds (Mayr 1963), the flower in angiosperms (Stebbins 1974) and hypocone in mammals (Hunter and Jernvall 1995). Concurrent with these deterministic explanations was a growing realisation that stochastic

explanations, captured by simplistic null models, can provide equally good or better explanations for observed patterns, and as such, any deterministic scenarios should be tested against a stochastic null model (MacArthur and Wilson 1967, Levins 1968, May 1973, Raup et al. 1973, Gould et al. 1977).

The importance of null models has since become well established across the sciences, and a wide array of null models have been developed to aid studies of biological diversity. Included amongst these are: the unified neutral theory of biodiversity and biogeography (Hubbels 2001) to explain diversity and relative abundance of species in ecological communities; multiple models regarding taxonomic diversification, concerning clade shape (Gould et al. 1977), palaeontological richness relating to species-area effects (Sepkoski 1976) and rock record sampling (Smith and McGowan 2007, Benson et al. 2009, Lloyd 2011); and multiple models regarding phenotypic diversification, including rates, mode, disparity (Sidlauskas 2007, Sidlauskas 2008, Eastman et. al. 2011), phenotypic trends (Wagner 1995), and convergence (Stayton 2008).

These studies and others like them have enabled great progress towards identifying those aspects of biodiversity than can be accounted for by 'chance', and those that require alternative explanations. For example, it appears we can reject the null hypothesis that species-area effects are the principal driver of latitudinal biodiversity gradients (Roy et. al 1998), which led to suggestions that solar energy input (via its assumed temperature and productivity consequences) may provide a better explanation. Conversely, there are many instances where a null cannot be rejected (likely to be underreported in the literature), such as a failure to detect higher rates of change (i.e. departing from those obtainable under a null model), as was expected under the deterministic scenario that possession of a highly modified pharyngeal jaw

apparatus in labrid fishes drove taxonomic and morphological diversification (Alfaro et al. 2009, Price et al. 2009).

All of these approaches set the tone for this thesis, as they make clear that deterministic explanations should only be entertained where a stochastic hypothesis of evolutionary change can be rejected. In the light of such approaches, I briefly touch upon some areas of progress regarding explanations for the unevenness of biodiversity, highlighting the difficulties they face. I then focus upon what the consensus of evidence suggests is the best way forward to illustrate the utility of Mesozoic neopterygians to this broad ranging yet fundamental area of evolutionary biology.

Progress understanding the unevenness of biological diversity

Nearly all of the literature investigating the uneven partitioning of diversity to date has focused upon taxonomic diversification. The resulting explosion of studies exploring net rates of diversification implicitly assume that differences in net diversification rates are responsible for the differing richness of clades, and that numerous explanations may explain why clades have differing rates, including external factors such as energy (Davies et al.2005) and climate (Weir and Schluter 2007); internal factors such as polyploidy (Mayrose et al. 2011, Zhan et al. 2014) or anatomical innovations (e.g. Hodges and Arnold 1995); or a mixture of both internal and external factors, such as co-evolutionary interactions (Farrell 1998). However, it has been highlighted that a focus on the net diversification rate alone can be highly misleading, as it struggles to capture historical patterns of species accumulation, and the influence of ecological limits (Rabosky 2010).

A second major explanation for unevenness is clade age. Under a stochastic model of diversification, clade richness should increase with time, which should result in a clear correlation between clade age and richness (in living clades only), where older clades are more diverse (Stephens and Wiens, 2003, McPeek and Brown 2007). Yet a study of the relationship between age and diversity in 1,397 clades argues that we should reject this claim (Rabosky et al. 2012).

A third broad explanation as to why clades differ in diversity pertains to ecological limits/ density dependence, the idea that different clades may essentially have different limits to their diversity (Rabosky 2009a, 2009b), analogous to carrying capacity of population growth. Although an appealing conceptual framework has been outlined (Rabosky et al. 2013) and reference made to instances of apparent stability in the fossil record of fishes (Friedman and Sallan 2012) and marine invertebrate genera for large swathes of the Phanerozoic (Alroy et al. 2008) that might reflect ecological limits, a convincing case of the mechanisms and its widespread relevance across the tree of life still needs to be made (Wiens 2011).

Therefore, despite considerable efforts to understand the unevenness of diversity, clear generalities are yet to emerge. Instead, a range of smaller scale, clade specific explanations are making more successful inroads, especially in scenarios where proposed effects of a deterministic driver can be identified across multiple groups on multiple occasions, such as the importance of reefs on the diversification of fishes (Alfaro et al. 2007), the co-evolutionary interactions of plants promoting beetle diversification (Farrell 1998), or the negative effects of genome duplication on plant diversification (Mayrose et al. 2011, *but see* Soltis et al. 2014). However, the vast majority of diversification studies focus solely upon

living taxa, and as such, their analyses are blind to historical patterns of diversification. This means that the findings of such studies, particularly those involving deep time divergences, are vulnerable, since the consensus of evidence indicates that the integration of fossils is essential to capture diversity dynamics over long time scales (Rabosky 2010, Alfaro et al. 2009, Rabosky 2014, Tarver and Donoghue 2011, Quental and Marshall 2010, Losos 2011 Benson et al. 2013). Despite this, very few broad scale analysis including fossils in a phylogenetic framework have been performed, and those that have indicate that even small amounts of fossil data can alter results (Finarelli and Flynn 2006, Slater et al. 2012). Furthermore, the majority of diversification studies conducted thus far have focused upon taxonomic diversification, whereas exploring unevenness in morphological and functional traits has received comparatively little attention (Wainright 2007). This is unfortunate, since morphology and function possess some clear advantages of over species counts. First, since similar morphological and functional traits are often shared by numerous species due to phylogeny, it should be easier to sample most of the broad categories of phenotypes present through time than it would be to capture accurate species diversity. Second, they allow workers to ask fundamentally different types of questions, as phenotypes provide information on functional capabilities and ecology. Third, and perhaps most pertinently, a framework already exists to include phenotypic information alongside living representatives, or to analyse the fossil data in isolation (e.g. Eastman et al. 2011).

To address both the need for fossil data in the study of diversification, and the paucity of studies examining morphological and functional diversification in a comparative framework, I sought a group with a large number of fossil species and reasonably good constraints on their phylogenetic relationships, at a time in geological history that is pertinent to live evolutionary hypotheses. Fishes fulfil the first two criteria, and it is the Mesozoic neopterygian fishes in

particular that can deliver a unique perspective on live hypotheses regarding the success of teleosts fishes and perceived failure of holostean fishes, and thus, Mesozoic neopterygians form the focus of this thesis.

Fishes as a model system for studies of diversification

Extant fishes have emerged as a model system for studies of diversification in recent years, having been the focus of numerous large scale analyses. Significant findings based solely upon living taxa include: the identification of diversification rate increases underpinning the evolution of crown Teleostei, Percomorpha and Ostariophysi (Alfaro et al. 2009, Santini et al. 2009); the importance of reefs in driving taxonomic and morphological diversification (Alfaro et al. 2007, Cowman and Bellwood 2011, Price et al. 2011) and morphological convergence (Price et al. 2014); and the close relationship between speciation rates and rates of morphological evolution (Rabosky et al. 2013). Importantly, these studies are quick to highlight the vulnerability of their conclusions in the absence of fossil data (Alfaro et al. 2009) and look, where possible, to corroborate their findings with the fossil record (Price et al. 2014), illustrating the importance of palaeontological data.

Since living fishes already provide a good model system, the potential of this system is even greater when we recognise the sheer quantity of fossil material available. It has been claimed that the number of fossil teleost species alone is of the same order of magnitude as mammals (Patterson 1977), thus the record of all fishes will outnumber them considerably. Yet the fossil record of fishes offers more than quantity, as it is the quality of the material that makes them a good choice of model system. There are huge numbers of fossil fishes preserved as fully articulated specimens for which we can obtain a wealth of morphological and functional information. Again, it was claimed that there were more articulated teleost fossils than

mammals (Patterson 1977), and I suspect there are more articulated fishes than all other vertebrate groups combined. They therefore represent an ideal resource for studies of morphological and functional diversification in deep time, especially because the wealth of living forms enables us to better constrain the relationship between morphology, function and ecology of fishes. Furthermore, essential to the phylogenetic comparative method required to study diversification is a relatively well constrained hypothesis of phylogeny. Although work on the phylogenetic relationships of fishes lags somewhat behind other vertebrate groups, it is still vastly better constrained than a host of invertebrate groups from which we could sample large amounts of trait data. Therefore it represents a trade-off between the quantity of trait information, and the quality of phylogeny. Fortunately, supertree methods (Bininda-Emonds et al. 2002) offer a way to capture the variety of live phylogenetic hypotheses for a given group, and by performing diversification analyses on the full variety of topologies, the robustness of results to changing phylogeny can be assessed. The phylogeny of fishes is sufficiently well resolved to be amenable to such methods, rendering fishes a powerful resource, when combined with the quantity and quality of their fossil record, for diversification studies.

Despite the potential of the fossil fish record, few have made use of it for studies of diversification. Yet these few studies make a powerful case for its importance in revealing patterns that we would otherwise be unable to ascertain. These include demonstrating the stability of jaw functionality in the Devonian (Anderson et al. 2011) and the selective extinction and subsequent refilling of vacated ecospace over the K-Pg boundary (Friedman 2009, 2010), to a variety of investigations examining the origins and proliferation of herbivory (Bellwood 2003, Bellwood and Hoey 2004, Bellwood et al. 2014a), nocturnal

feeding, high-precision benthic feeding (Goatley et al. 2010) and detritivory (Bellwood et al. 2014b).

This thesis makes use of the exceptional record of fossil fishes by focusing on the Triassic, Jurassic and Lower Cretaceous record of the neopterygian fishes, to document the morphological and functional capabilities for the first 150 million years (60%) of the neopterygian radiation that today represents over half of all vertebrate species. In the Recent, neopterygians comprise the depauperate holostean lineage, represented by 8 species (7 sp. of gar and the bowfin *Amia calva*) restricted to the freshwaters of North America, and the highly diverse teleost lineage, represented by ~29,000 species (96% of all 'fishes') that occupy nearly every aquatic environment on the planet. Specifically, I seek to compare the holostean fishes, regarded as 'living fossils' in the Recent (Darwin 1859), assumed to have always been conservative in their morphological and functional capabilities, with the teleost fishes, which exhibit staggering phenotypic variety in the Recent, assumed to always have been more innovative than holosteans (e.g. Romer 1966, Colbert 1969). For a brief historical review of how the scientific community arrived at its current understanding of living neopterygian relationships, followed by a supertree analysis that seeks to summarise progress assigning fossil forms, see Chapter 2. Timescales for neopterygian evolution are also presented in Chapter 2.

Neopterygian phenotypic diversity and evolutionary scenarios

Neopterygians are often cited for their huge taxonomic diversity, yet they clearly also possess staggering morphological and ecological variety. Within Neopterygii exist the heaviest (1

tonne ocean sunfish *Mola mola*) and longest (oarfish *Regalecus glesne* growing up to 11 metres) of all known ray-finned fishes, as well as the shortest (male anglerfish *Photocorynus spiniceps* at 6.2mm, Pietsch 2005) and lightest (gobioid *Schindleria brevipinguis* at 2mg, Watson and Walker 2004) vertebrates on the planet. Among vertebrates, they display the greatest diversity of colour pigmentation (Braasch et al. 2008), possess both the largest (elephantnose fish: Osteoglossiformes, Nilsson 1996) and smallest (bony-eared assfish: Ophidiiformes, Fine et al. 1987) brain to body size ratios, and have amongst the longest (Koi > 200 years, Rougheye rockfish: Scorpaeniformes 205 years, Cailliet et al. 2001) but definitely the shortest (Depczynski and Bellwood, 2005) lifespans. They exhibit bizarre architectures as distinct as inflatable porcupinefish, deep sea anglerfish, asymmetrical flounder, flying fish and the elaborate seahorse. Furthermore, they express a bewildering array of sexual and ecological strategies. Sexual strategies include internal fertilization and live birth (e.g. guppies), the ability to change sex (Ross 1990), mouth brooding (multiple families across phylogeny) and male brooding (seahorses: Syngnathiformes) and the ability to reach sexual maturity faster than any other vertebrate (*Nothobranchius kadleci*: Cyprinodontiformes, Blažek et al. 2013). From the plethora of ecological strategies, some of the most bizarre include forms that consume prey larger than themselves (gulper eels: Saccopharyngiformes; chiasmodontids: Gartner et al. 1997), see both above and below water simultaneously (four-eyed fishes: Cyprinodontiformes, Sivak 1976), emit light (>20 families; Herring 1987), fire jets of water to catch prey (Archerfish: Perciformes, Triggerfish: Tetraodontiformes), transmit electric shocks (e.g. stargazers: Perciformes) and toxic stings (e.g. reef stonefish: Scorpaeniformes, lionfish: Scorpaeniformes), climb waterfalls (Nopoli rockclimbing goby), see vertically upwards through a transparent head covering (barreleyes: Argentiniformes), 'walk' on land and underwater (Renous et. al 2000, Graham 1973), glide

anywhere from 50 to 400 metres at a time (Piper 2007) and swim at speeds of up to 110 km/h (sailfish, Walford 1937), faster than any other vertebrate.

However, the entirety of the diversity outlined above is encompassed within the teleost radiation, whereas the holosteans consist solely of 8 predatory freshwater taxa restricted to the freshwaters of North America. This dramatic contrast, gleaned from living taxa alone, has fuelled a series of deterministic evolutionary scenarios to explain the perceived success of teleosts, and relative failure of holosteans. I discuss some of the most prominent scenarios below, to assess what progress has been made and the contribution that fossil neopterygians can make toward testing these scenarios.

Holosteans as 'living fossils'

The term 'living fossil' was first coined by Darwin (1859), in specific reference to gars, to characterise 'aberrant'[1] taxa/groups expressing character combinations that appear intermediate between more easily definable existing groups, just 'like fossils'[2]. These taxa/groups are said to arise from ancient or intermediate forms, transmitted to the present day with little modification[3]. Thus, implicit in Darwin's own characterisation of living fossils, we should expect them to exhibit low rates of morphological change over long timescales. This has been empirically examined in 'living fossil' groups based upon both palaeontological (e.g. lungfish, Lloyd et al. 2013, Cavin and Guinot 2014) and neontological (e.g. tuatara, Hay et al. 2008) datasets. Holosteans too have been examined as part of broad scale neontological

[1] Defined in Darwin (1859) as 'Forms or groups of animals or plants which deviate in important characters from their nearest allies, so as not to be easily included in the same group with them, are said to be aberrant.'
[2] 'some of the most anomalous forms now known in the world, as the Ornithorhynchus and Lepidosiren, which, like fossils, connect to a certain extent orders at present widely separated in the natural scale.'
[3] 'the more ancient forms of life often present characters in some degree intermediate between existing groups. As some few of the old and intermediate forms having transmitted to the present day descendants but little modified, these constitute our so-called osculant or aberrant groups.'

datasets of vertebrates (Alfaro et al. 2009) and fishes (Rabosky et al. 2013), which infer that they must have displayed incredibly low rates of taxonomic and morphological diversification over long timescales. Despite this finding, they openly admit that they cannot account for historical patterns of diversification, and stress the need for the incorporation of paleontological data (Alfaro et al. 2009). Thus, only the fossil record of holosteans can complete our insights into their rates of morphological evolution time. Although this investigation could be performed on holosteans alone, this would only provide information on relative changes in rate within holosteans, not whether holosteans overall exhibit lower rates than other neopterygians. Thus, by utilising the record of all Mesozoic neopterygians, holostean and teleost rates can be compared to test whether holosteans really do evolve phenotypes slower their close relatives (performed in Chapter 5). However, rates do not capture everything, since low rates in a single direction could, theoretically, amount to vast morphological changes over time. Therefore I test a second prediction of holosteans as 'living fossils', that they have remained phenotypically conservative over long timescales, with little capacity for morphological innovation. I test this by examining 1) the degree to which holosteans evolve unique phenotypes (Chapter 3), 2) the levels of phenotypic diversity they obtain through time (Chapter 4) and 3) whether, in a phylogenetic context, they exhibit low phenotypic innovation in comparison with teleosts (Chapter 5).

Scenarios for teleost success

Multiple scenarios have been devised to explain the success of teleost fishes. Many traditional explanations focus upon evolutionary trends, such as general improvements to locomotion due to loss of heavy scales, development of a homocercal tail, or gradual increases in the flexibility of the maxilla (e.g. Romer 1966, Colbert 1969). However, many of these changes are broadly framed and poorly defined, and/or the proposed benefits are unclear (e.g. is there

any functional difference in how the homocercal tail of stem teleosts creates propulsion compared with the symmetrical tails of many holostean species?). These trends stand in contrast to other theories that focus upon key innovations, which possess clear definitions, modes of action, and phenotypic predictions, and thus are imminently testable. Three of the most popular key innovations are briefly discussed below:

Protrusible jaws – The ability to eject the oral jaws forwards, possible through the structural decoupling of the jaws from the neurocranium, is referred to as jaw protrusion. It is a feature of a great number of teleost fishes, and has been linked to the success of the Acanthomorpha (~16,000 species) and the Cypriniformes (~3200 species) (Schaeffer and Rosen, 1961; Rosen, 1982). However, jaw protrusion is not a discrete trait; there is huge variation in the jaw protrusion abilities and mechanisms of taxa (Alexander, 1967; Motta 1984, Westneat and Wainwright, 1989), hindering the immediate formalisation of testable hypotheses. Furthermore, although jaw protrusion has evolved multiple times (Westneat 2004), ever changing hypotheses of phylogeny have hampered attempts to articulate how many, and there is no clear overview regarding the jaw protrusion abilities of teleost fishes. Variability in degrees of protrusion combined with phylogenetic uncertainty has meant there is no clear framework in place to test jaw protrusion as a driver of diversification, and no studies of diversification have specifically targeted jaw protrusion. However, the potential remains, in the light of recent phylogenies, to develop a clear and testable framework for the role of jaw protrusion in diversification, but this has not been attempted to date. Instead, workers have focused mainly upon the mechanisms and capabilities of jaw protrusion of individual taxa (e.g. Waltzek and Wainwright 2003, Wainwright and Day 2007, Staab et al. 2012). Neopterygian fossils will prove useful for future studies into the relationship between jaw

protrusion and diversification, since both clades that possess and lack jaw protrusion (occasionally due to secondary loss) are known from fossils.

Pharyngeal Jaws – The best explored key innovation to date pertains to pharyngeal jaws. Percomorph fishes, which represent over half of all teleost species, possess, in addition to their oral jaws, pharyngeal jaws at the back of the mouth, which process and move food to the oesophagus. Considering that Percomorpha represent over half of all teleost species (~15,000), this alone could be seen as sufficient to arouse suspicion regarding the role of the pharyngeal jaws in diversification. Indeed, a huge shift in taxonomic diversification rate has been identified for Percomorpha, the largest rate shift of all vertebrates (Alfaro et al. 2009). Although this result was not discussed in reference to pharyngeal jaws, it is certainly consistent with its predictions of increased diversification, although there could be many other explanations (including jaw protrusibility). Instead, work has tended to focus specifically upon taxa possessing a highly modified version of the pharyngeal jaw apparatus, referred to as pharyngognathy (Liem 1973, Stiassny and Jensen 1987). Pharyngognathy characterises some of the most speciose percomorph clades, including Labridae (Wrasses ~ 600 sp), Cichlidae (~1600 sp) and Pomacentridae (damselfishes ~387 sp), yet their interrelationships have proved difficult to establish. Nevertheless, studies of diversification have examined clades in isolation to test the role of pharyngognathy, principally the Labridae, and found that increases in rates of taxonomic and phenotypic change did not correspond to the evolution of pharyngognathy (Alfaro et al. 2009, Price et al. 2009). However, these studies are limited in scope, as they fail to compare families with pharyngognathy to those without. This is especially significant when we consider that pharyngognathy appears to have evolved at least six times independently (Wainwright et al. 2012) and should represent an ideal framework for testing its role in diversification. However, as the authors of this discovery stress, rigorous

testing of pharyngognathy requires further clarification on the sister group relationships of these groups (Wainwright et al. 2012). Therefore, just as for protrusible jaws, efforts are still somewhat hindered by the uncertainty of phylogeny.

Genome duplication – The notion that the duplicate genomes of teleosts (relative to all other jawed vertebrates) are the primary driver of their success is by far the most popular theory to date (Amores et al. 1998: Taylor et al 2001; Postlethwait et al. 2004; Volff 2005, Semon and Wolfe 2007, Van de Peer 2009). Specifically, authors cite genome duplication as a driver of phenotypic diversification in teleosts (Wittbrodt et al. 1998, Hoegg et al. 2004, Van de Peer 2004, Meyer and Van de Peer 2005). Fortunately, the phylogenetic position of the duplication is known; it must have occurred in the teleost stem lineage or *the* last common ancestor of crown teleosts, in order to be a shared trait of all living teleosts (Meyer and Van de Peer 2005). This renders the predictions of a genome duplication driven phenotypic diversification imminently testable. However, it will be difficult to address this with neontological datasets due to the vast amount of phenotypic data that needs to be collected and the paucity of data obtainable from species poor teleost outgroups. In addition, any neontological analysis would be blind to historical patterns of diversification. Mesozoic neopterygian fossil data provide the key, as rates of phenotypic change and the degree of phenotypic innovation can be assessed directly in stem teleosts and early crown teleosts. Furthermore, the new consensus that a monophyletic Holostei forms the teleost sister group allows for a pairwise comparison between a clade with duplicated genomes and one without (Chapter 5).

THESIS STRUCTURE

Chapter 1 – Introduction.

Chapter 2 – Provides a historical account of living neopterygian relationships, followed by a supertree analysis to summarise progress in placing fossil taxa. Two timescales for neopterygian evolution are presented.

Chapter 3 – Captures the major axes of variation in morphology and function within Mesozoic neopterygians, and their anatomical correlates. The degree to which morphological and functional axes covary is then compared, as are the distances between taxa in the two spaces. Levels of uniqueness and convergence are then compared between holosteans and teleosts, followed by a historical account of ordination space occupation through time. The potential for a competitive replacement of holosteans by teleosts is then assessed.

Chapter 4 – Quantifies the morphological and functional disparity of Mesozoic neopterygians with numerous trajectories to interrogate the pattern. This information is then used to address five questions, relating to the relationship between morphology and functional disparity, early high disparity, whether the trajectories capture the Mesozoic fall of holosteans and rise of teleosts as predicted by previous taxonomic accounts, the potential influence of the Triassic-Jurassic extinction boundary on neopterygians, and the implications of the data for the Mesozoic Marine Revolution.

Chapter 5 – Quantifies rates and mode of evolution to test the predictions of a genome duplication enhanced diversification in teleost fishes. The extent to which holosteans fulfil their 'living fossil' stereotype is also assessed.

Chapter 6 – Thesis summary.

Appendix – Disparity trajectories and statistics pertaining to Chapter 4.

Chapter 2
Assembling a supertree of Mesozoic neopterygians

Introduction

Although the neopterygian fishes represent over half of all vertebrate species in the Recent, broad scale hypotheses of phylogeny among their fossil representatives are lacking. There are numerous explanations for why this might be the case. First, although the scope of the problem could be seen as motivation for broad scale work, in reality, the vast taxonomic and phenotypic variety of neopterygians presents a large and difficult challenge for any practitioner of phylogenetic methods. Second, although the fossil record of fishes is vast, there is only a small community of fossil fish workers, meaning the record is understudied in relative terms (Friedman and Sallan 2012). Third, a series of works by Colin Patterson argued for the secondary importance of fossils relative to living taxa, often in explicit reference to fishes, in resolving phylogenetic relationships (Patterson 1977, Patterson 1981, Patterson 1987). This may have dissuaded some workers from pursuing phylogenetic work programmes with fossil fishes. As a consequence of these, and no doubt numerous other factors, the literature of fishes is populated by a variety of smaller scale hypotheses, and the same is true of the Mesozoic neopterygians that form the basis of this thesis. Some groups have proved popular for study, such as the Osteoglossomorpha (e.g. Cavin and Forey 2001, Zhang 2004, Wilson and Murray 2008, Xu and Chang 2009), and Ginglymodi (Cavin 2010, Lopez-Arbarello 2012, Cavin et al 2013, Deesri et al. 2013), yet the broadest analyses (e.g. those

examining total group teleosts, such as Arratia 2013) still contain relatively small numbers of taxa (< 45) given the diversity present. Furthermore, the majority of Mesozoic neopterygian fossil taxa have never been included in a formal phylogenetic analysis, leaving only the taxonomic information available with their description to inform their placement.

To date, there has been little attempt to summarise these local solutions into a broad neopterygian framework, in part due to the paucity of macroevolutionary studies in fishes (Friedman and Sallan 2012). A notable exception is the appendix of Cavin et al. (2007), which presents a genus level composite tree of Middle Jurassic to Late Cretaceous actinopterygians, although the branching structure between all genera, especially those outside of the apomorphy based definition of teleosts, are not clearly visible (in part due to the timescale).

Given the lack of a broad, accessible and clearly interpretable summary of Mesozoic neopterygian relationships, the main goal of this chapter is to derive the first formal supertrees for the group. However, supertrees constructed via matrix representation with parsimony (MRP) have received numerous criticisms, such as the non-independence of the underlying data between source trees, variation in the quality of source trees, and the challenges of applying cladistic principles to trees rather than character data (Bryant 2004, Gatesy and Springer 2004). Although these criticisms form a strong argument that supertrees should not be used to actually infer relationships between organisms, both authors accept they are defensible as a means to summarise previous hypotheses on relationships (Bryant 2004, Gatesy and Springer 2004). The latter is clearly the intention of this chapter, where I do not attempt to infer neopterygian relationships, but instead seek to derive a population of supertrees to summarise systematic progress to date, supertrees that, by capturing a range

different topologies, provide an ideal framework for the broad scale comparative analyses performed in Chapters 4 and 5.

Creation of these supertrees required the use of many literature solutions and information from taxonomy. However, the lack of overlap between these solutions necessitated the use of a constraint (i.e. backbone) phylogeny. Beyond mere necessity, the constraint offers an opportunity to enforce some recent and well-supported findings regarding the interrelationships of living groups upon the supertree analysis, particularly important given historical uncertainty regarding the relationships of gars, *Amia* and teleosts that permeate the source trees. To justify this move, I provide a brief, historical review of living neopterygian interrelationships to emphasise the strength of the current consensus in contrast to previous times of consensus. I then conduct a supertree analysis to summarise progress in fossil neopterygian systematics to date, and highlight the considerable areas of uncertainty that remain. Finally, I use information from both fossils and molecular clocks to generate two alternative timescales for neopterygian evolution.

Arriving at the modern understanding of Neopterygii: there and back again.

The current consensus is that holosteans are monophyletic and consist of 7 species of gar and the bowfin *Amia calva*. Teleosts represent the holostean sister group, and comprise ~29,000 species. Together they represent crown group Neopterygii. Historical reviews of neopterygian relationships are presented by Patterson (1973, 1977, 1981), Grande and Bemis (1998), Grande (2010) and Sallan (2014). Here I summarise only those developments pertinent to understanding the relationships between gars, *Amia* and teleosts (**Table 2.1**).

Early concepts and acceptance of Holostei

The first specific reference to holosteans and teleosts came in 1844 (English translation 1846a) when Johannes Müller named and characterised Holostei and Teleostei for the first time, based solely upon the soft anatomy of living species. His definition of living teleosts matches our modern definition (although *Amia* was included amongst herrings in Clupeidae); however his Holostei differed, consisting of Lepisosteidae (*Lepisosteus* only) and Polypteridae (*Polypterus* only). Following additional information regarding the heart of *Amia* (Vogt 1845), Müller (1846b) removed *Amia* from the Clupeidae and added it to Holostei.

Holostei (Amia, gars), teleosts) Fig.2.1a	Halecostomi (Amia, gars), teleosts) Fig.2.1b	Ancient Fish Clade (Sturgeon+paddlefish, gar, Amia), teleosts) Fig.2.1d	Unnamed (gars, teleosts), Amia) Fig.2.1c
Huxley 1861			
Regan 1923			
Goodrich 1930			
	Westoll 1944 p94		
Romer 1945			
Jarvik 1959			
	Gardiner 1960 fig.79		
	Jollie 1962:155		
	Gardiner 1963:317		
Romer 1966			
Andrews et al. 1967	Gardiner 1967a fig.8		
McAllister 1968			
Nelson 1969a, b			
Jessen 1972			
	Patterson 1973		
	Wiley 1976		
	Nelson 1976		
	Bartram 1977		
	Patterson and Rosen 1977		
Jarvik 1980			
	Rosen et al. 1981		
	Lauder & Liem 1983		
Jollie 1984	Wiley & Schultz 1984		Olsen 1984
	Nelson 1984		
	Gardner 1984		
	Nolf 1985		
	Verran 1988		
Normark et al. 1991*			Olsen & McCune 1991
Lê et al. 1994:fig.3*			
Lecointre 1994:fig.1*		**Lecointre 1994**	
	Gardner et al. 1996		
	Bemis et al. 1997		
Venkatesh et al. 1999*			
	Liem et al. 2001	**Venkatesh et al. 2001***	
		Inoue et al. 2003*	
Kikugawa et al. 2004*			
Grande 2005		**Inoue et al. 2005***	
Crow et al. 2006*			
Hurley et al. 2007:fig.2	Hurley et al. 2007:fig.3*	**Hurley et al. 2007:SI.fig.12***	
Azuma et al. 2008*			
Alfaro et al. 2009*		**Near & Miya 2009***	
Inoue et al. 2009*			
Santini et al. 2009*			
Grande 2010		**Inoue et al. 2010***	
Raincrow et al. 2011*			
Saitoh et al. 2011*			
Near et al. 2012*			
Betancur-R et al. 2013*			
Broughton et al. 2013*			
Faircloth et al. 2013*			
Rabosky et al. 2013*			

Table 2.1. Studies, listed in chronological order, in support of the four phylogenetic topologies outlined in **Fig. 2.1.** Studies in **bold** font support a monophyletic Holostei. Studies followed by an **asterisk** are based upon molecular data.

It took one final step, in 1861, to arrive at our current definition of Holostei and Teleostei, when Huxley removed Polypteridae from Holostei. However, recognition of these two groups in isolation did not state that they represent each other's closest living relatives. On the contrary, Müller had grouped Holostei with Chrondrostei rather than teleosts. However, the link between holostean and teleosts was established, in all but modern tree thinking parlance, when Neopterygii was erected by C. Tate Regan in 1923 as the group containing holosteans and teleosts. The view of a monophyletic Holostei, sister to Teleostei (**Fig. 2.1a**), although doubted, with holosteans commonly referred to as a grade in the early part of the 20th century (see discussion in Patterson 1973 and Sallan 2014), appeared relatively unchallenged by alternative, tree thinking scenarios until the 1960's, since more studies can be cited in support of Holostei prior to this time (**Table 2.1**).

The birth of Halecostomi

Although a minority of workers had suggested *Amia* might be more closely related to teleosts than holosteans prior to the 1970's (**Table 2.1**), it was not until the 1973 publication of *Interrelationships of Fishes* containing Colin Patterson's review of holosteans relationships that skeletal characters supporting a close relationship between *Amia* and teleosts in a phylogenetic framework came to light. Patterson argued that *Amia* was the sister-group of teleosts, to the exclusion of gars, and adopted the term Halecostomi for this clade. This work rendered the Holostei redundant, a name only useful for historical discussions or those regarding evolutionary grades, and established Halecostomi as the new consensus, adopted by many subsequent works in the 70's and 80's that cited Patterson's synapomorphies without obtaining or clearly presenting additional evidence (Grande 2010:804).

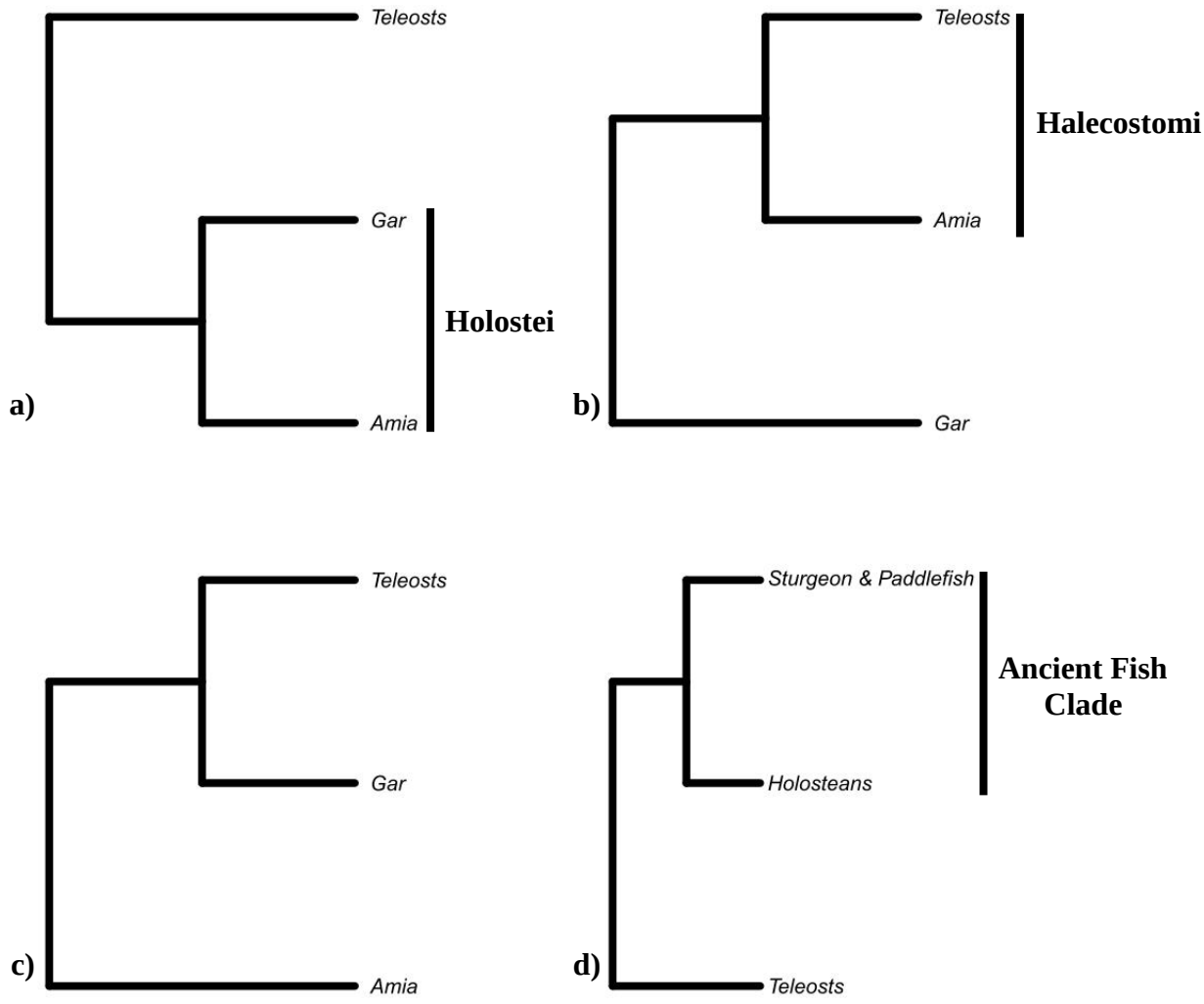

Fig. 2.1. Proposed phylogenetic relationships of gars, *Amia* and teleosts. **a)** The modern consensus, with gars and *Amia* forming a monophyletic Holostei, sister to teleosts. **b)** The Halecostomi topology, where *Amia* are more closely related to teleosts (clade Halecostomi) to the exclusion of gars. **c)** Topology suggested by Olsen (1984) and Olsen and McCune (1991) in which gars form an unnamed clade with teleosts to the exclusion of Amia. **d)** The "Ancient Fish Clade", formed by a sister group relationship between holosteans and chondrosteans, represents the teleost outgroup.

A tired consensus

The acceptance of Halecostomi throughout the 70's and 80's gave way to increasing uncertainty regarding the relationships of gars, *Amia* and teleosts in the 90's and early 2000's (**Table 2.1**). The implementation of formal, algorithm-based cladistic analysis (Olsen and McCune 1991) and the arrival of molecular phylogenetic analyses (e.g. Venkatesh et al. 2001) offered new and varied results regarding Neopterygii, such as a gar-teleost sister relationship (**Fig.2.1c**), or (regarding the relationships of actinopterygians as a whole) solutions such as the Ancient Fish Clade (**Fig.2.1d**). Despite this variety, holostean monophyly was a common feature of most analyses (**Table 2.1**, studies in bold font). Many authors openly discussed the uncertainty present (Grande 2010:804), and in the absence of new evidence, could not distinguish between the available topologies.

The resurrection of Holostei

The mid 2000's onwards saw the arrival of more morphological and molecular evidence, almost all of which converged upon a monophyletic Holostei sister to teleosts (**Fig.2.1a, Table 2.1**), marking the onset of a new consensus. Unlike previous times of consensus, where influential publications (e.g. Patterson 1973) presenting one set of evidence were largely adopted by the wider community without much scrutiny or additional support, the new consensus is evidence led, with data from a wide diversity of sources using varied methodologies on differing and overall, larger datasets. Thus, the new consensus provides the ideal foundation for any examination of neopterygian diversification, providing a clear, comparative framework in which to test hypotheses pertaining to holosteans and teleosts.

MATERIALS AND METHODS

Constructing neopterygian supertrees

i) Source trees

The quality and non-independence of source trees have been highlighted as issues to consider when constructing MRP supertrees (Bryant 2004, Gatesy and Springer 2004). For example, it was noted that a single transferrin immunology dataset was effectively up-weighted through its incorporation in five separate source trees in the bat supertree of Liu et al. (2001) (Springer and de Jong 2001, Gatesy and Springer 2004). However, it has already been stated that such issues are essentially unavoidable for fossil phylogenies where most studies will share at least some underlying character data (Gatesy and Springer 2004). I do not see this as an obstacle to supertree construction where the aim is to summarise the topologies available in the literature, rather than to assess which datasets might be the most reliable. One can envisage other scenarios where source tree selection might influence which arrangements are most common in the resultant supertrees. For example, the inclusion of multiples trees from a single author would up-weight their solutions relative to a single solution for the same clade from another author. One might also question whether hand-drawn solutions should be included alongside those derived from cladistic analyses. While all of the observations above are interesting to consider, the state of Mesozoic neopterygian phylogenetics influences the decision here not to weight/remove multiple contributions by single authors or ignore hand drawn solutions and solutions for which a cladistic data matrix has not been provided. There are several reasons for this. First, there are relatively few solutions available for Mesozoic neopterygians, and many are restricted in scope to particular families or orders. Given this situation, any procedures that act to throw phylogenetic information away are of secondary importance to

my objective to incorporate solutions for as many unique Mesozoic neopterygian taxa as possible. Removing hand drawn solutions or those that fail to provide a cladistic data matrix would involve a huge loss of phylogentic information, influencing my decision to retain such datasets. Decisions to weight or remove multiple contributions from the same author face similar difficulties; many authors have continually altered the taxonomic sample of their datasets, rather than continually growing the taxonomic sample for their dataset over time. In this situation, new solutions by the same author can conflict with their previous solutions in any case, and often contain novel information in the form of new taxa. Under these conditions, it is not clear what advantage down-weighting contributions by a given author would bring.

Given all of the considerations outlined above, I decided not to weight or remove topologies for this first attempt at a formal supertree for Mesozoic neopterygians. This is not to say that these steps are unimportant; future versions of supertree would benefit from such measures, especially when more, larger scale hypotheses of phylogeny containing considerably larger taxon sets (along with the cladistics dataset used to create them) become available. Instead, my aim here was to include all known topologies pertaining to crown group neopterygian taxa from the Permian, Triassic, Jurassic and Early Cretaceous. 120 topologies were obtained in total. As previously noted, numerous trees lacked the data matrix used to create them (e.g. Lambers 1995) and others were hand-constructed cladograms (e.g. Taverne 2011), thus, all trees were redrawn manually in Mesquite v.2.75 (Maddison and Maddison 2008). Many source trees contained taxon names which have since been superseded. To address this, I created a list of all junior synonyms present in the source trees alongside their corresponding senior synonyms, replacing the former with the latter in R prior to supertree assembly.

ii) Taxonomic and molecular constraint tree

Poor overlap between source trees necessitated that I include a "seed" (i.e. backbone) tree based upon taxonomic information containing every species in the dataset, an approach demonstrated to improve supertree construction (Bininda-Emonds and Sanderson 2001). This also provided a means to include species not represented in any source trees because they have never been included in a formal phylogenetic analysis.

The taxonomy seed tree was also treated as a constraint on the supertree analysis to ensure that some basic interrelationships could not be overruled by the source trees. This was desirable as it was not uncommon for older source trees to conflict with more recent trees over some fundamental interrelationships that are no longer controversial. For example, numerous source trees resolve Halecostomi (**Fig.2.1b**) instead of the holostean-teleost sister group relationship (**Fig.2.1a**), yet as discussed in detail above, the latter represents the current consensus. Therefore I ensured the taxonomy constraint tree reflected the latter, and the same principle is applied to other areas of the tree where there is a strong consensus.

The taxonomy constraint tree was also constructed to match the most recent molecular phylogenetic hypotheses for Neopterygii. Within crown teleosts, relationships between some living taxa could not be enforced on the taxonomy tree without forcing fossil crown teleosts with uncertain affinities into specific positions from which they would be unable to move during phylogenetic inference. To avoid fixing such fossils, the molecular phylogeny of Near et al. (2012) was included as a source tree (one of the 120), and implemented as a constraint (was fully upweighted in TNT), enabling teleosts fossils that would otherwise have been fixed in one position to resolve in a variety of positions relative to living clades, more accurately capturing the uncertainty present.

Because the taxonomy tree was implemented as a constraint, great care was taken to ensure that it was quite poorly resolved so that the source trees could act to resolve relationships where there was genuine uncertainty. To illustrate this, I refer to the situation within the gar total group, Ginglymodi. In nearly every case, taxa can be reliably assigned to Ginglymodi, yet relationships within Ginglymodi are uncertain. For example, the relative position of the order Macrosemiiformes with respect to the rest of Ginglymodi is unclear, resolved as either nesting within Ginglymodi (López-Arbarello 2012) or sister to all other Ginglymodians (Cavin et al. 2013). Therefore, while the constraint tree does enforce the uncontroversial assignment of Macrosemiiformes to the Ginglymodi, the position of the clade amongst other Ginglymodian taxa was left as a large polytomy, allowing the source trees to inform its placement within Ginglymodi. Where there was no dissenting topology in source trees, I often ensured the monophyly of genera and occasionally families where the evidence was unchallenged, although in the most part, interrelationships between proposed families were left unresolved.

iii) Running the supertree analysis

671 neoptergian species, living and fossil, were included in the analysis. I employ an optimization supertree approach via matrix representation using parsimony (MRP, Bininda-Emonds 2004). This approach involves the conversion of tree topologies into something closely resembling a character matrix, where nodes behave as characters. There are different methods for coding this matrix, I apply what is referred to as the standard method (Baum 1992, Regan 1992), which codes descendants of nodes as 1, non-descendants as zero, and taxa missing from that source tree (but present in other source trees or the taxonomy constraint tree) as question marks. I chose the standard method as it has been shown to produce

supertrees that receive greater support according to the V index (Lloyd et al. 2008), which measures the relative proportion of input trees that support supertree clades (Wilkinson et al. 2005).

Safe taxonomic reduction (Wilkinson 1995) was then performed on the MRP matrix in order to remove taxa that have no effect upon the relationships inferred for other taxa, but would act to increase the number of MPTs and computation time for the inference step. To ensure that the relationships suggested by the constraint tree and molecular backbone tree would be reflected in all MPTs, nodes capturing the relationships amongst these taxa were upweighted to 1000 (the maximum) in the nexus file required for TNT, created in R.

Phylogenetic inference based upon the MRP matrix was performed in TNT v1.1 (Goloboff et al. 2008). Twenty replicates of new technology searches were performed, saving 1000 each time, with each replicate starting from a random tree. 10,000 MPTs were then obtained from these saved replicates, followed by a final search for remaining MPTs with tree bisection and reconnection, resulting in a total of 10,500 MPTs. Taxa removed by safe taxonomic reduction were then reinserted into every MPT. A strict consensus (**Fig. 2.3b**) and a 50% majority rule consensus (**Fig. 2.3c**) were then obtained based upon the 10,500 MPTs. 100 of the 10,500 MPTs were selected at random, and used as the bases for the simulations and comparative analyses presented in Chapters 4 and 5.

c) Time scaling the supertrees

i) Steps required for both fossil and molecular time scaling procedures

The starting point for both time scaling procedures was to obtain an age for every fossil species in the supertree, dates that define the tip age for that species. Tip ages reflect the first

appearance of that species in the fossil record, yet the first appearance of any fossil has age uncertainty associated with it. To reflect this uncertainty, I derive first occurrence time spans for every species, ranging from the oldest possible age interpretation for that species until the reliable minimum age estimate for that species. Finding the oldest possible interpretation involves identifying all rock units containing the species, obtaining their lower boundary age (i.e. oldest possible age), and selecting the oldest. Finding the reliable minimum age involves identifying all rock units containing the species, obtaining their upper boundary age (i.e. youngest possible age), and selecting the oldest – identical to the minima derived for fossils in molecular clock calibration (e.g. Clarke et al. 2011). Together these provide first appearance time spans, and taxon ages were then drawn from a uniform distribution within their respective spans. This was repeated 100 times so that tip ages would be slightly different in every supertree. These tip ages have been saved for reproducibility. A second set of 100 randomised tip ages were derived, and saved, for use in the molecular based time scaling procedure.

ii) Fossil based time scaling procedure

I used the node dating procedure of Hedman (2010) to provide an estimate for the neopterygian crown node. This technique requires the age of successive outgroups to the focal clade, and estimated a time of origin for crown Neopterygii of 280 Ma. Given this result, the variable 'vartime' in *timePaleoPhy* function of the *paleotree* package in R was set to constrain the root age to 280 Ma in every time scaled supertree. This constraint on the root combined with the randomised fossil ages outlined above, were used to derive 100 fossil based timescales.

iii) Molecular based time scaling procedure

The variable 'node.mins' in *timePaleoPhy* was used to constrain the age of three nodes in every supertree according to clock estimates obtained from Near et al. (2012). These nodes were 1) crown Neopterygii at 361.2 Ma, 2) crown Holostei at 271.9 Ma and 3) crown Teleostei at 307.1 Ma. These three constraints combined with the randomised fossil ages outlined above were used to derive 100 molecular based timescales.

RESULTS

i) Constraint tree and major areas of uncertainty

Figure 2.2 presents a pruned summary of the constraint tree applied in the analysis. The constraint tree looked to impose only the most uncontroversial relationships, and used information from taxonomy to include all 671 species. As a result, there are many polytomies, even for the relationship between the major clades, especially apparent on the teleost stem. The constraint tree, in combination with 120 source trees provided 10,500 (a number determined *a priori*) MPTs upon which a strict consensus (**Fig. 2.3b**) and 50% majority rule consensus (**Fig. 2.3c**) could be obtained.

Compared with the constraint tree (**Fig. 2.3a**), the strict consensus tree adds little extra resolution to the topology, with the exception of two regions (highlighted in red, **Fig. 2.3b)**. The first regards the basal most stem teleost lineages Aspidorhynchiformes, Pachycormiformes and Pycnodontiformes, and suggests that Aspidorhynchiformes are sister

to Pycnodontiformes (**Fig. 2.3b**). This results from the fact that little attempt has been made to address the interrelationships of these three clades in the same analysis, and so the few studies that have included all three clades (Arratia 2000a, Arratia 2000b, Arratia 2008) inform the result that Aspidorhynchiformes and Pycnodontiformes are sister group. The second area of improved resolution was simply due to action of the molecular constraint that was imposed, which resolves the relationship amongst the Otocephala. The origin of Otocephala therefore represents the divergence of total group Clupeiformes (i.e. Clupeomorpha) from total group Ostariophysi, represented in the Recent by five orders, but known from the Mesozoic only by two, the Gonorhynciformes (milkfishes) and Characiformes (tetras). *Tischlingerichthys* was consistently resolved as the earliest diverging member of total group Ostariophysi in this framework.

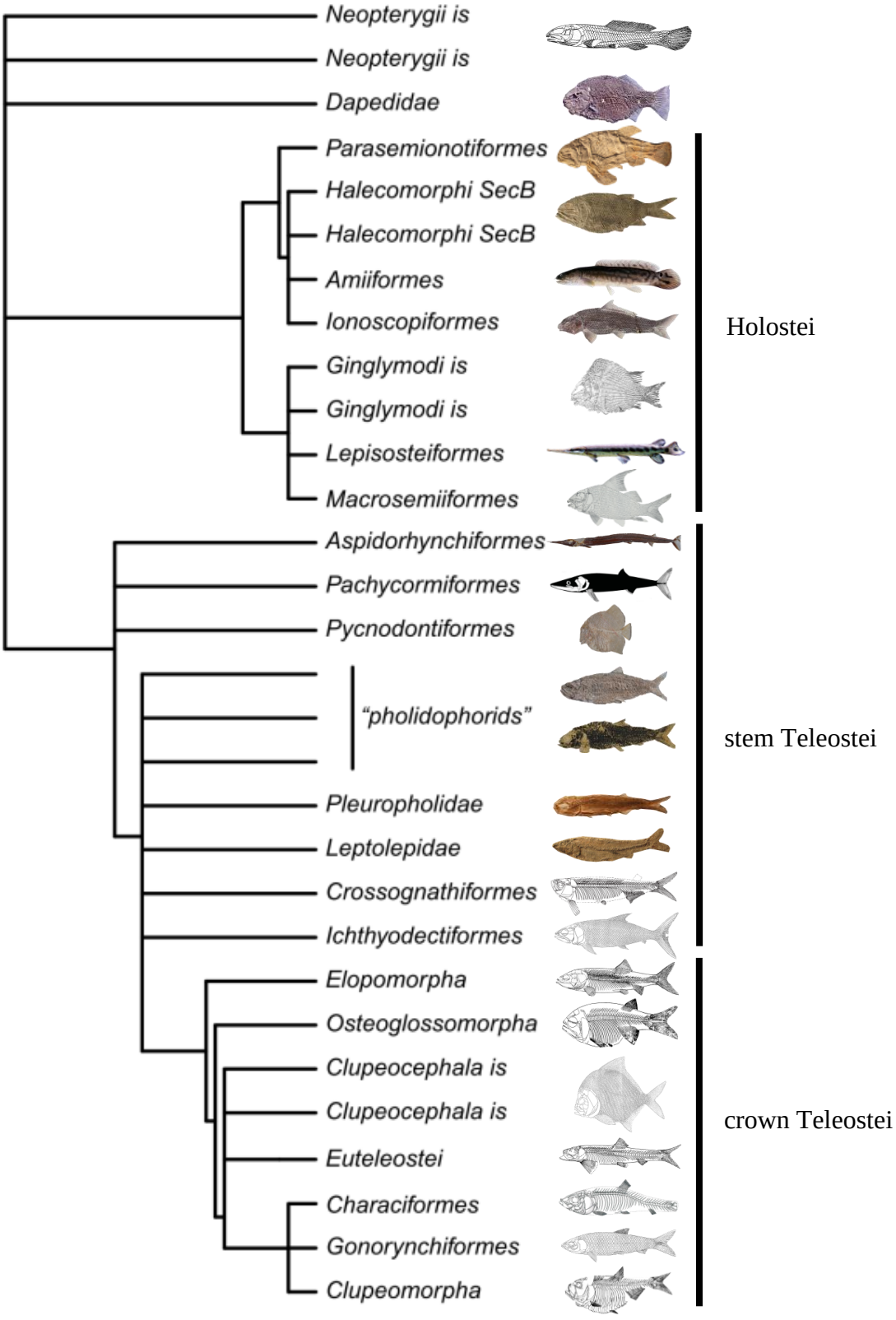

Fig. 2.2. A pruned version of the constraint tree used in the supertree analysis.

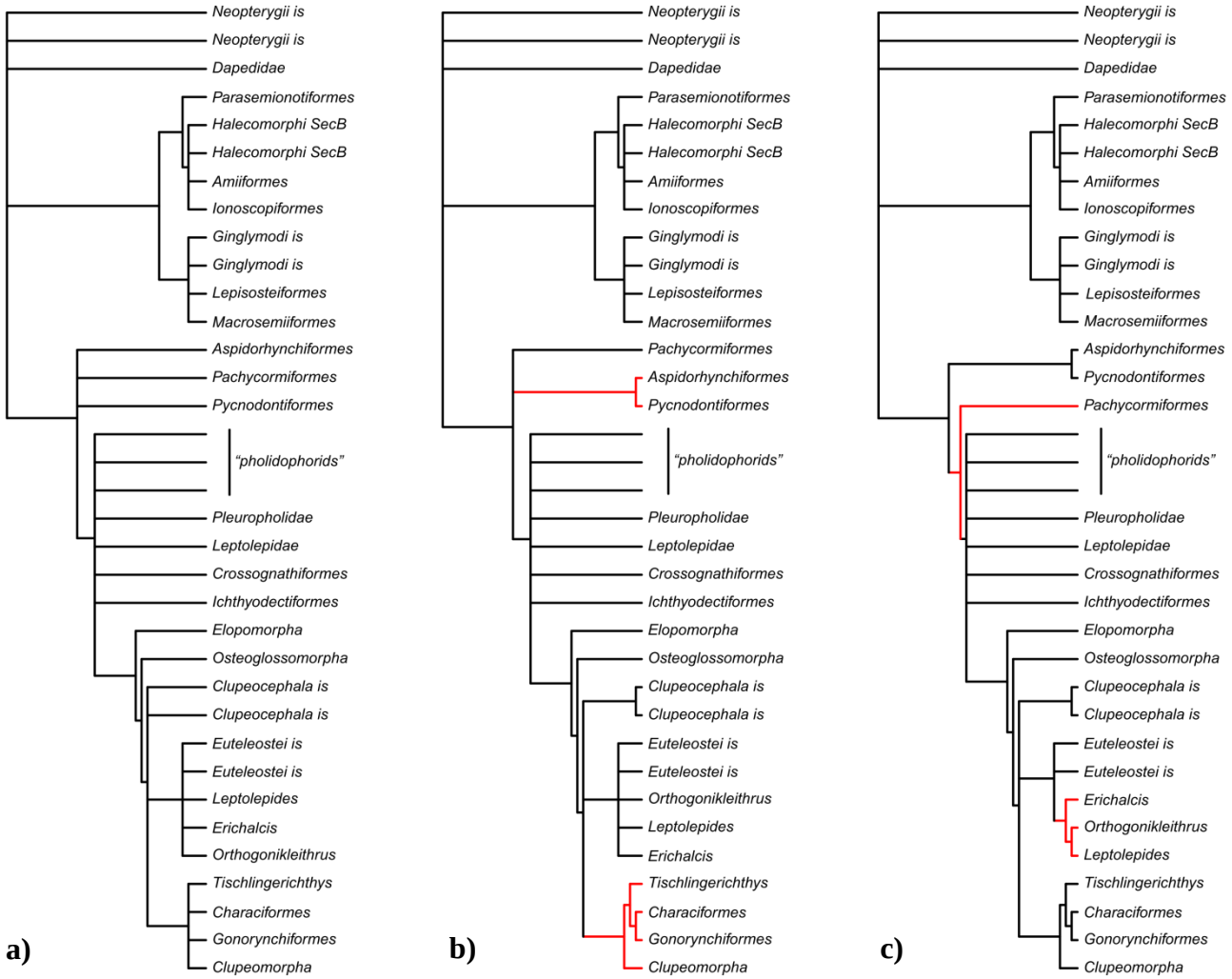

Fig. 2.3. Pruned versions of the supertree that illustrate the level of resolution recovered between the major groups of Mesozoic neopterygians. Branches in red illustrate regions of increases resolution relative to the tree immediately to the left. **a)** The constraint tree prior to the analysis. **b)** The strict consensus supertree based upon 10500 MPTs. **c)** The 50% majority rule consensus based upon 10500 MPTs.

No additional resolution between the major clades of Mesozoic neopterygians is seen in the majority rule consensus (**Fig 2c**). Instead, the next change worthy of note sees a few select genera of euteleosts (*Erichalcis*, *Orthogonikleithrus*, *Leptolepides*) form a clade.

ii) A supertree of Mesozoic neopterygians and within clade uncertainty

A single, unpruned majority rule consensus tree is presented in **Figure 2.4** to illustrate: 1) the main clades of neopterygians present in the Mesozoic, 2) the taxonomic diversity of these clades with select examples of their morphological variety, 3) where extinct fall relative to living clades, and 4) areas of uncertainty within clades.

Visual inspection of the tree indicates that some of the most speciose orders of Mesozoic fishes are found amongst the Holostei, especially within the bowfin total group (Halecomorphi), where the Amiiformes and Ionoscopiformes appear particularly diverse. Other particularly large orders include the Pycnodontiformes and the Ichthyodectiformes, both stem teleosts. Amongst crown teleosts, above the level of order, the Osteoglossomorpha, Clupeomorpha and Elopomorpha all contain a considerable diversity of Mesozoic forms.

Regarding the degree of resolution, I comment on the tree beginning at the top of **Figure 2.4a**, working downwards to the bottom of **Figure 2.4f**. **Figure 2.4a** shows taxa that have been rendered by the analysis to be Neopterygii *incertae sedis*, and thus, cannot confidentially be placed as either holosteans or teleosts. Surprisingly, this collection does not purely consist of oddball, or early appearing taxa, as one might expect, but an entire family, Dapedidae, known from many articulated species and specimens. The lack of resolution within the family

provides some explanation as to why. Very few taxa have been described in detail, and only *Dapedium*, usually coded as a composite OTU, has been used in any phylogenetic analysis to date.

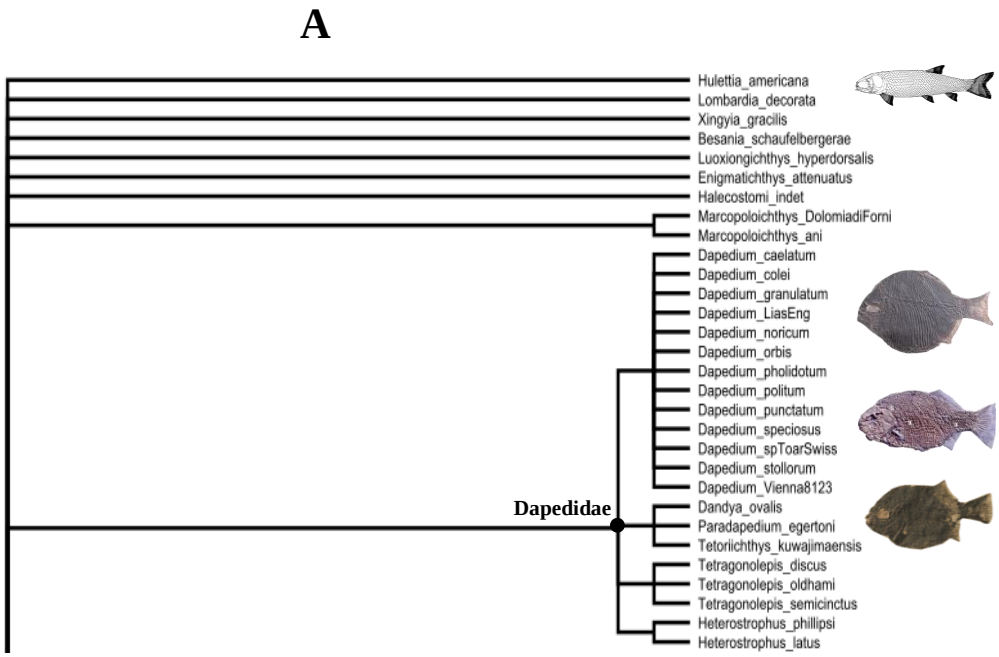

Fig. 2.4. Phylogeny of 671 neopterygian species derived from 120 source trees and a constraint tree which contained all 671 taxa. The phylogeny is presented in six parts **A**, **B**, **C**, **D**, and **E**.

Figure 2.4b captures the entire Triassic, Jurassic and Lower Cretaceous diversity of Halecomorphi. At the top, there is a clade of three Halecomorphi *incertae sedis* forms, even though none have ever been included in a formal analysis. Below this are Parasemionotiformes, a clade restricted to the Triassic, amongst which are the first occurrences of the Halecomorphi in the fossil record. Only a single taxon, *Watsonulus eugnathoides*, has been included in phylogenetic analyses to date, explaining the lack of resolution within the clade. Apart from Parasemionotiformes, only two other orders of Halecomorphi are recognised, Ionoscopiformes and Amiiformes. Both contain a considerable diversity of taxa, and compared with most other Mesozoic neopterygian clades, their interrelationships appear relatively stable.

Figure 2.4c depicts all Ginglymodian taxa in the supertree. As for Halecomorphi, two clear orders are recognised, Lepisosteiformes and Macrosemiiformes. Striking is the large proportion of taxa which are essentially Ginglymodi *incertae sedis*. Many taxa have been proposed to form a pinnate structure from which Lepisosteiformes and Lepidotes represent the final divergence in the series (Deesri et al. 2013, Cavin et al. 2013), whereas other analyses propose numerous taxa form clades within a third order, Semionotiformes (López-Arbarello 2012). These conflicts deliver the uncertainty present in the supertree, although there is consistent evidence that some species of Lepidotes (generally regarded as a wastebasket taxon from which taxa are slowly being removed) are sister to the Lepisosteiformes (**Fig. 2.4c**). As for Halecomorphi, the relationships within well-established orders (Lepisosteiformes and Macrosemiiformes) appear relatively stable.

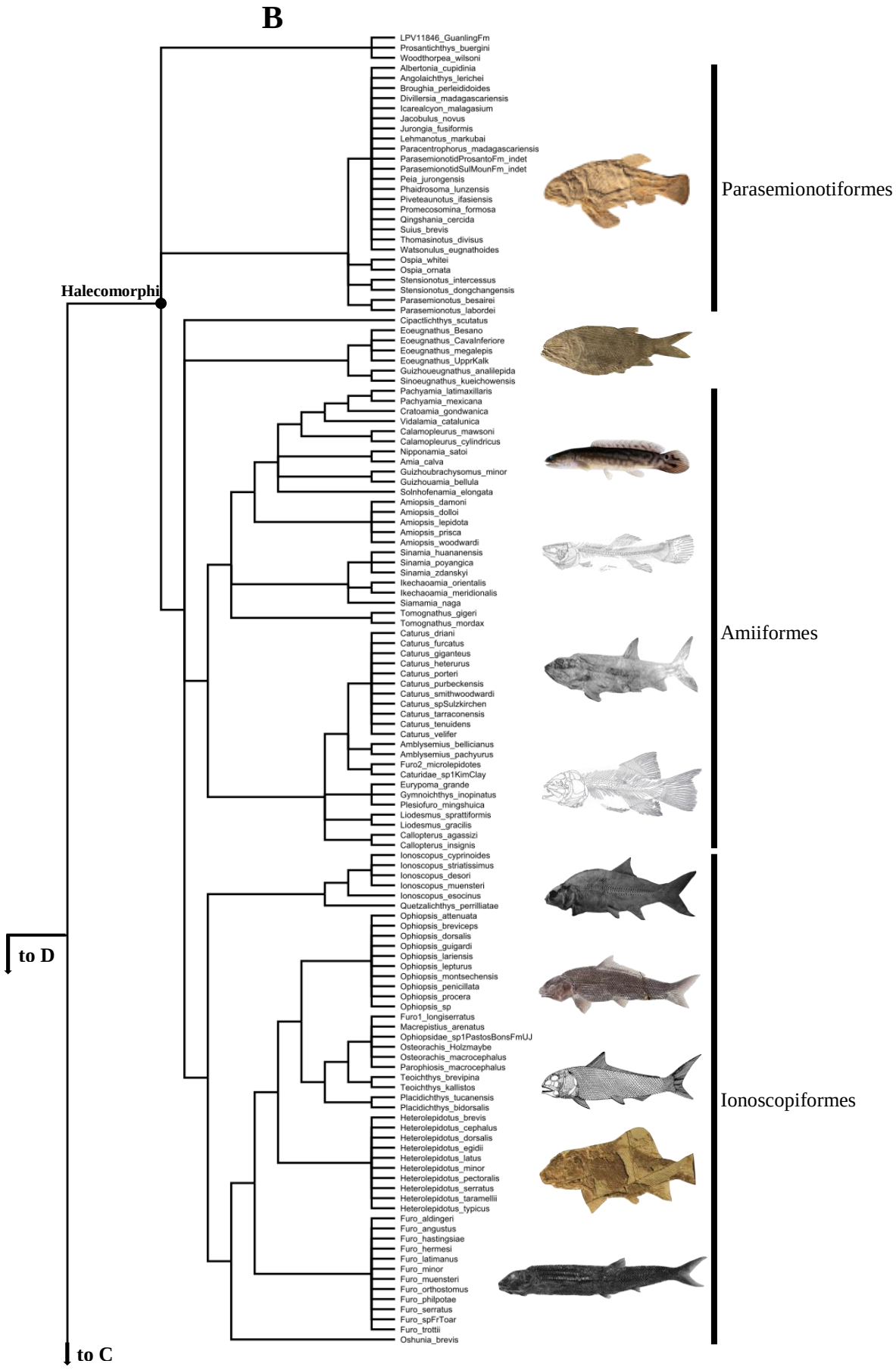

Fig. 2.4. (continued).

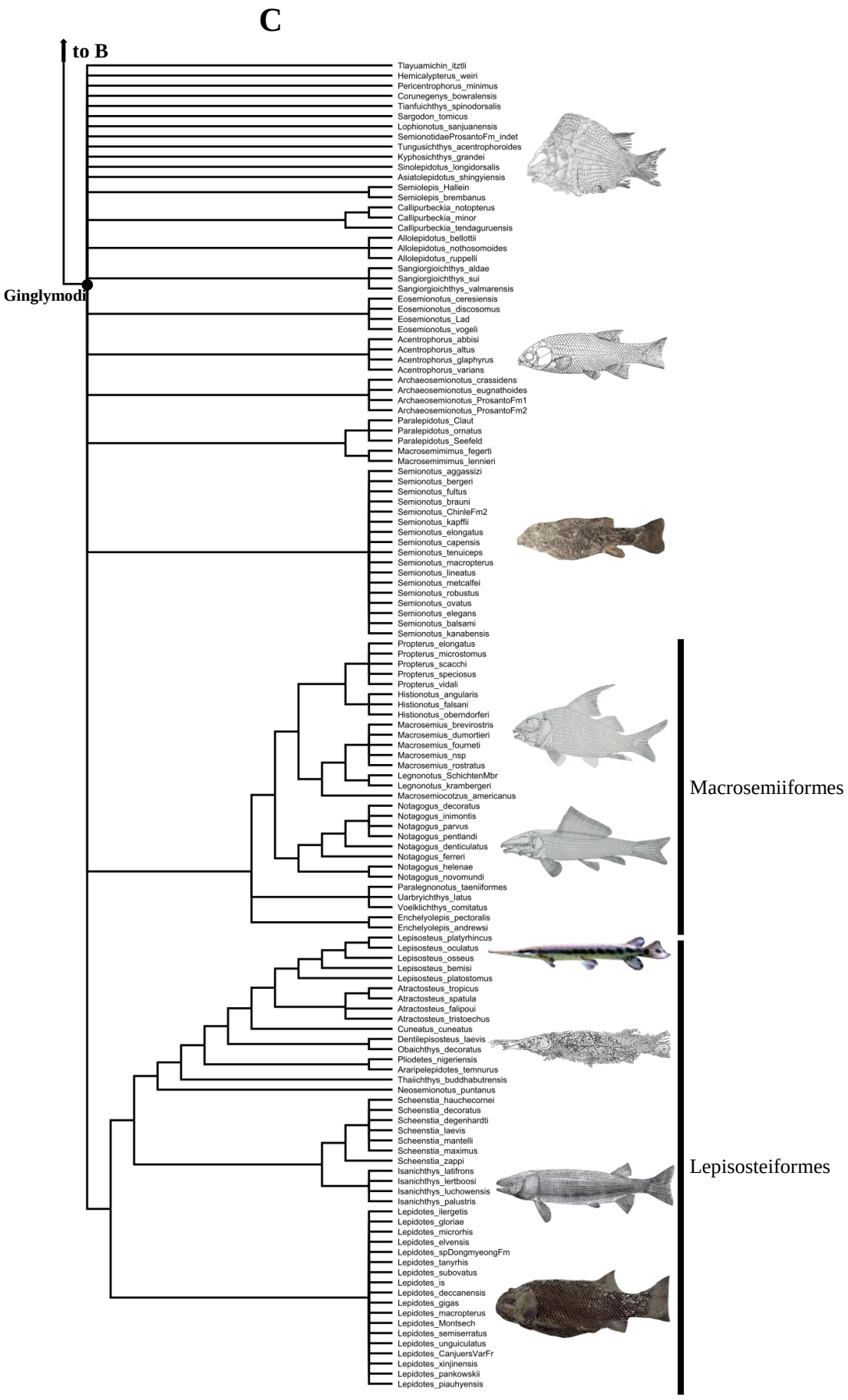

Fig. 2.4. (continued).

Figure 2.4d represents the lower half of the teleost stem lineage, and most notably contains the three enigmatic and morphologically distinct orders Pycnodontiformes, Aspidorhychiformes and Pachycormiformes. The sister group relationship between Pycnodontiformes and Aspidorhychiformes has already been highlighted, and the relationships within these orders are relatively well-constrained. This is in stark contrast to the rest of the teleost stem taxa in **Figure 2.4d**, where there is no overriding consensus regarding the relationships of taxa. This problem is exacerbated due to the wastebasket genus *Pholidophorus*, to which many species have been assigned, even though detailed descriptions and phylogenetic analysis often remove taxa from the genus, rendering it paraphyletic (Arratia 2013). Many other unresolved genera have been considered closely related to *Pholidophorus*, sometimes within the order Pholidophoriformes, however, this order has long been considered paraphyletic (Arratia 2000), and as a result, these taxa may instead be referred to as 'pholidophoriforms' (see Arratia 2013 for a review).

The first half of **Figure 2.4e** is a continuation of the list of unresolved genera presented in **Figure 2.4d**, many of which have been considered 'pholidophoriforms'. The potential, poorly understood (Arratia 2013) clades Archaeomaenidae and Pleuropholidae have also been considered 'pholidophoriforms'. The Leptolepidae, characterised by the genus *Leptolepis*, is not considered a 'pholidophoriform', and often appears in fairly derived positions on the teleost stem (e.g. Patterson 1977, Taverne 2011b. Arratia 2013), yet a lack of consensus still prevents confident placement. The final two clades at the base of **Figure 2.4e** are the orders Crossognathiformes and Ichthyodectiformes. Like the Leptolepidae, they tend to occupy derived positions on the teleost stem, and Ichthyodectiformes commonly resolve as the sister group to crown teleosts in source trees (e.g. Arratia and Tischlinger 2012).

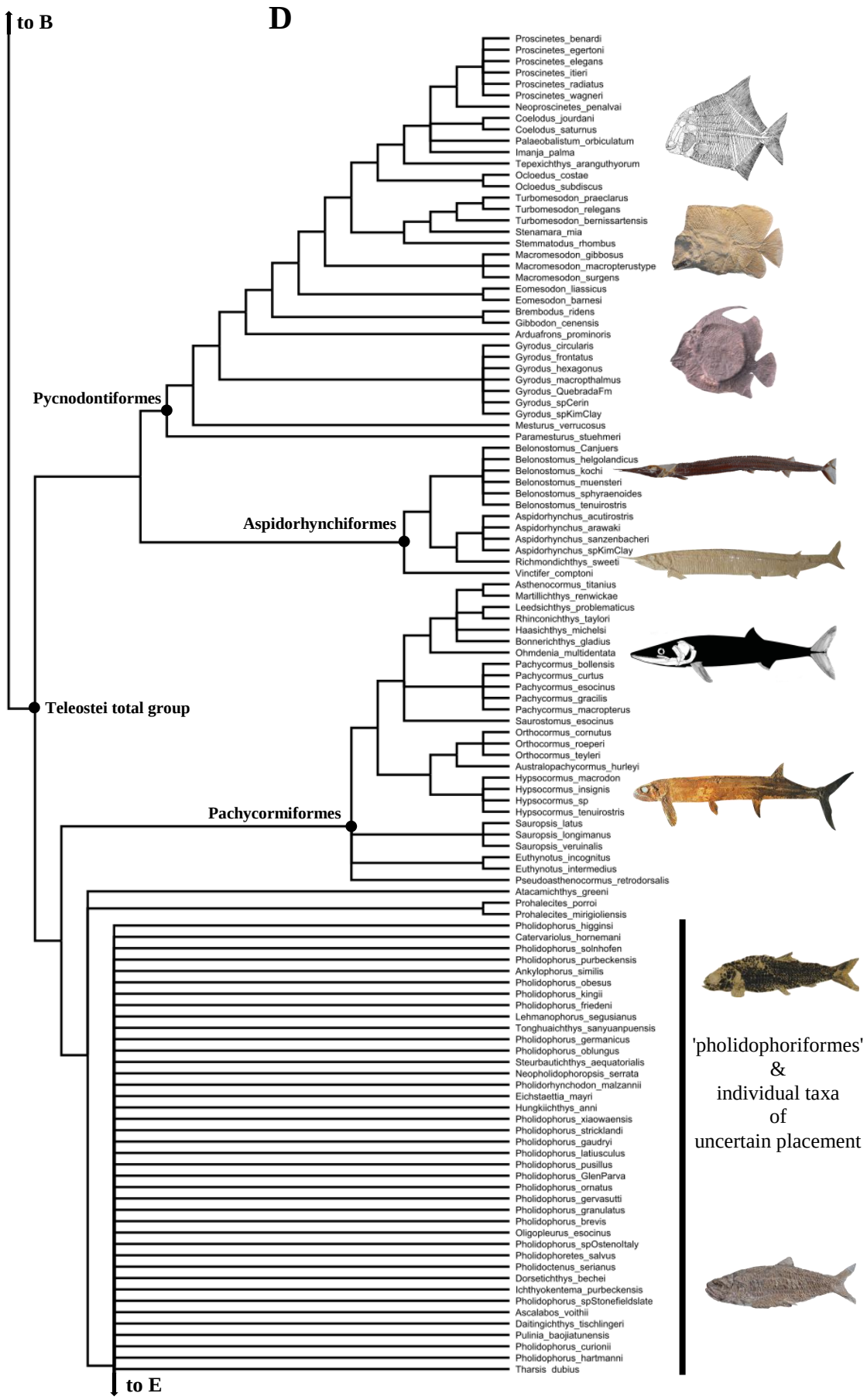

Fig. 2.4 (continued).

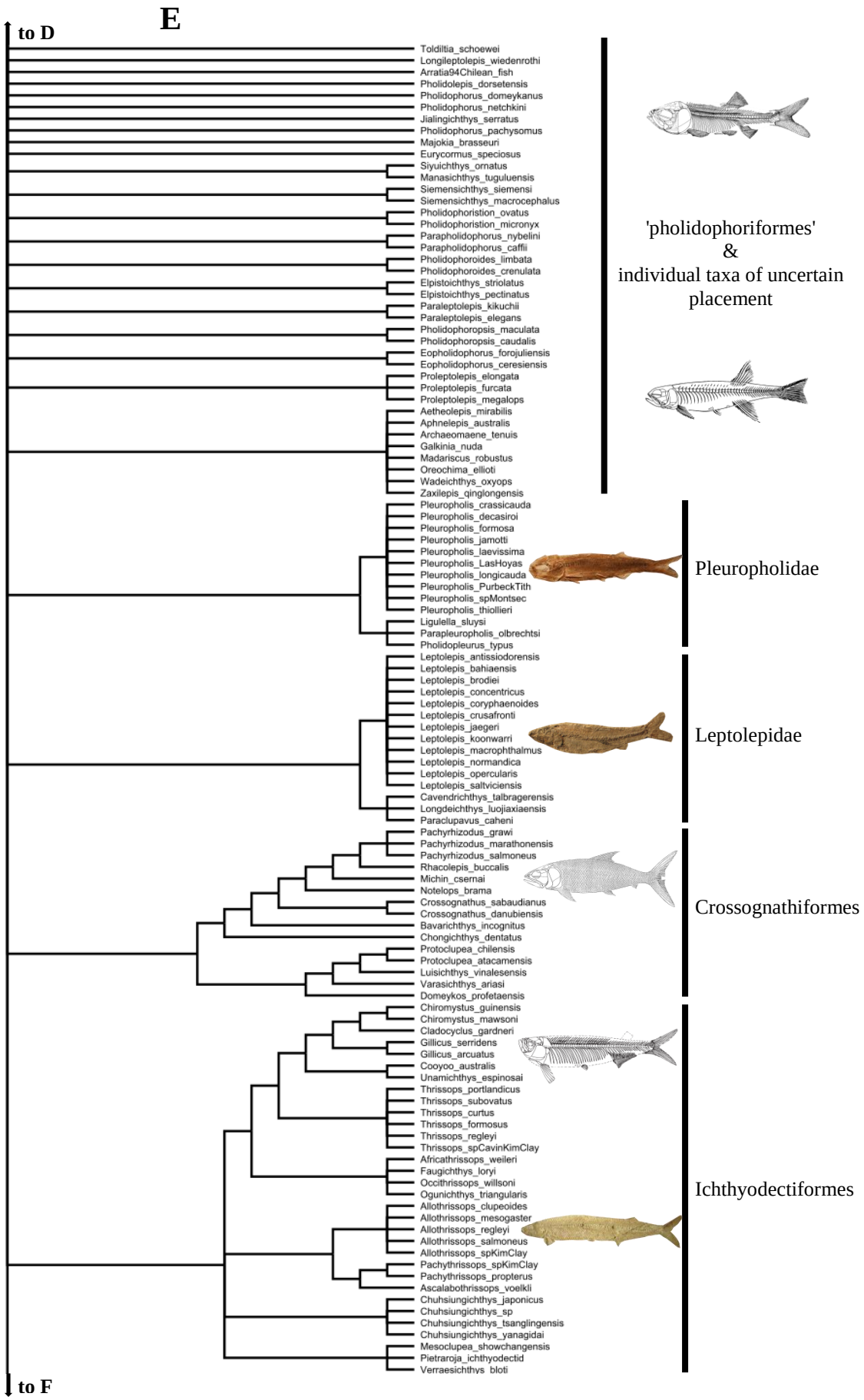

Fig. 2.4. (continued).

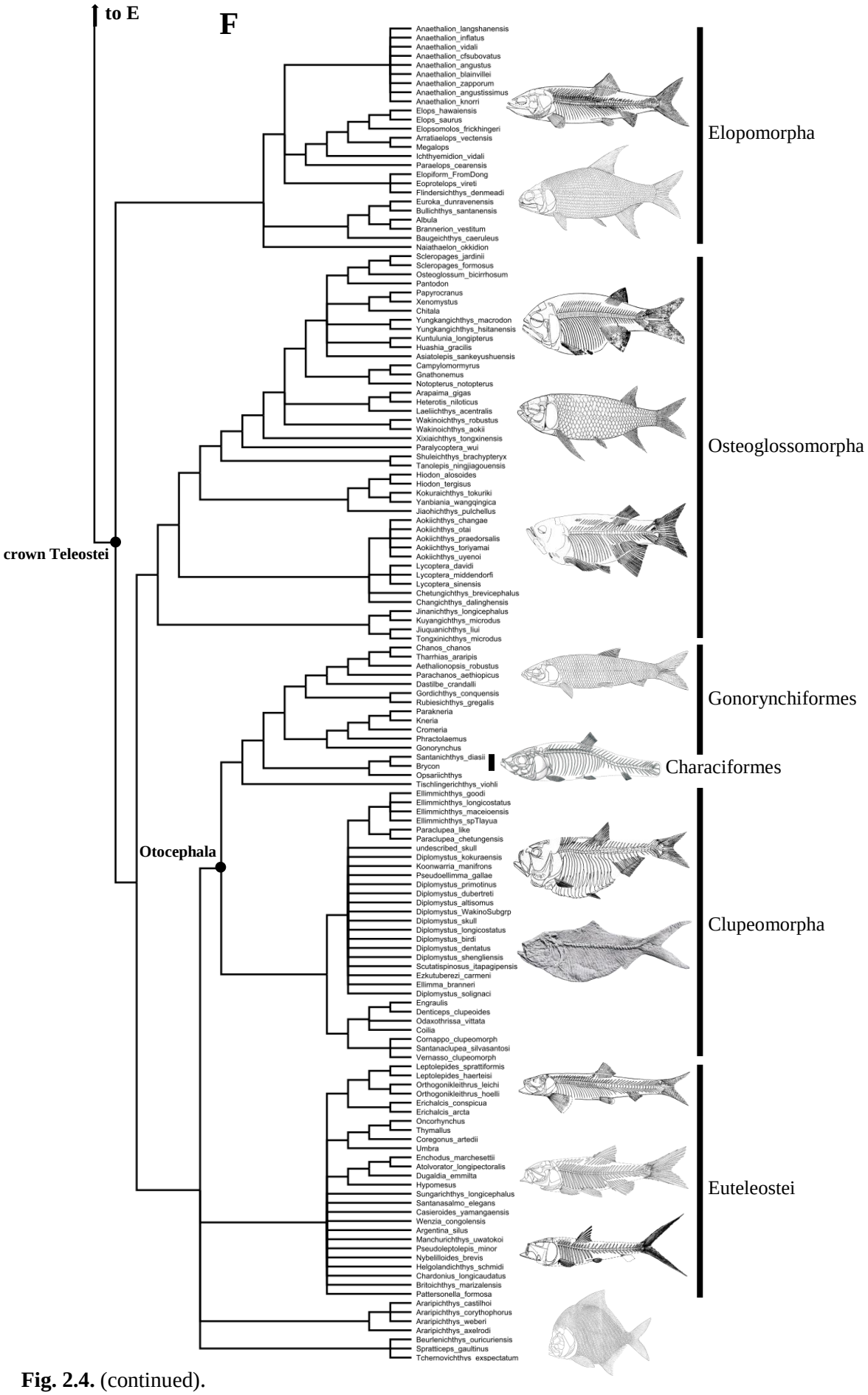

Fig. 2.4. (continued).

Figure 2.4f depicts the teleost crown group, and numerous extant representatives have been retained in the supertree to aid interpretation of where fossil taxa fall relative to living taxa. Within crown teleosts as a whole, relationships look relatively well resolved in comparison to much of the stem lineage, although part of this stability derives from constraining the living taxa according to molecular constraint tree (Near et al. 2012). Nevertheless, the relationships of fossil Elopomorpha appear relatively well-contained, as do many members of the Osteoglossomorpha. Otocephala presents a contrast between the well-resolved Ostariophysi taxa, and the poorly resolved Clupeomorpha. However, this is not unexpected; there are far more fossil clupeomorphs than ostariophysians present in the tree. Even so, resolution among fossil clupeomorphs is particularly poor in comparison to other clades mostly known from fossils (e.g. Pynodontiformes). Similarly, the relationships amongst most euteleost fossils remain unresolved.

ii) Alternative timescales for neopterygian evolution

Fossil based and molecular based timescales for neopterygian evolution are presented in **Figure 2.5**, along with the known stratigraphic ranges for the major clades. The contrast between the fossil (**Fig. 2.5a**) and molecular (**Fig. 2.5b**) based timescales can be dramatic. There is ~150Ma difference between the origin of crown teleosts, and a ~90Ma difference in the age of Neopterygii, even though fossil sampling, via the method of Hedman (2010), was used to estimate the root age for the fossil tree. Despite this, some nodes remain similar, such as the holostean crown node.

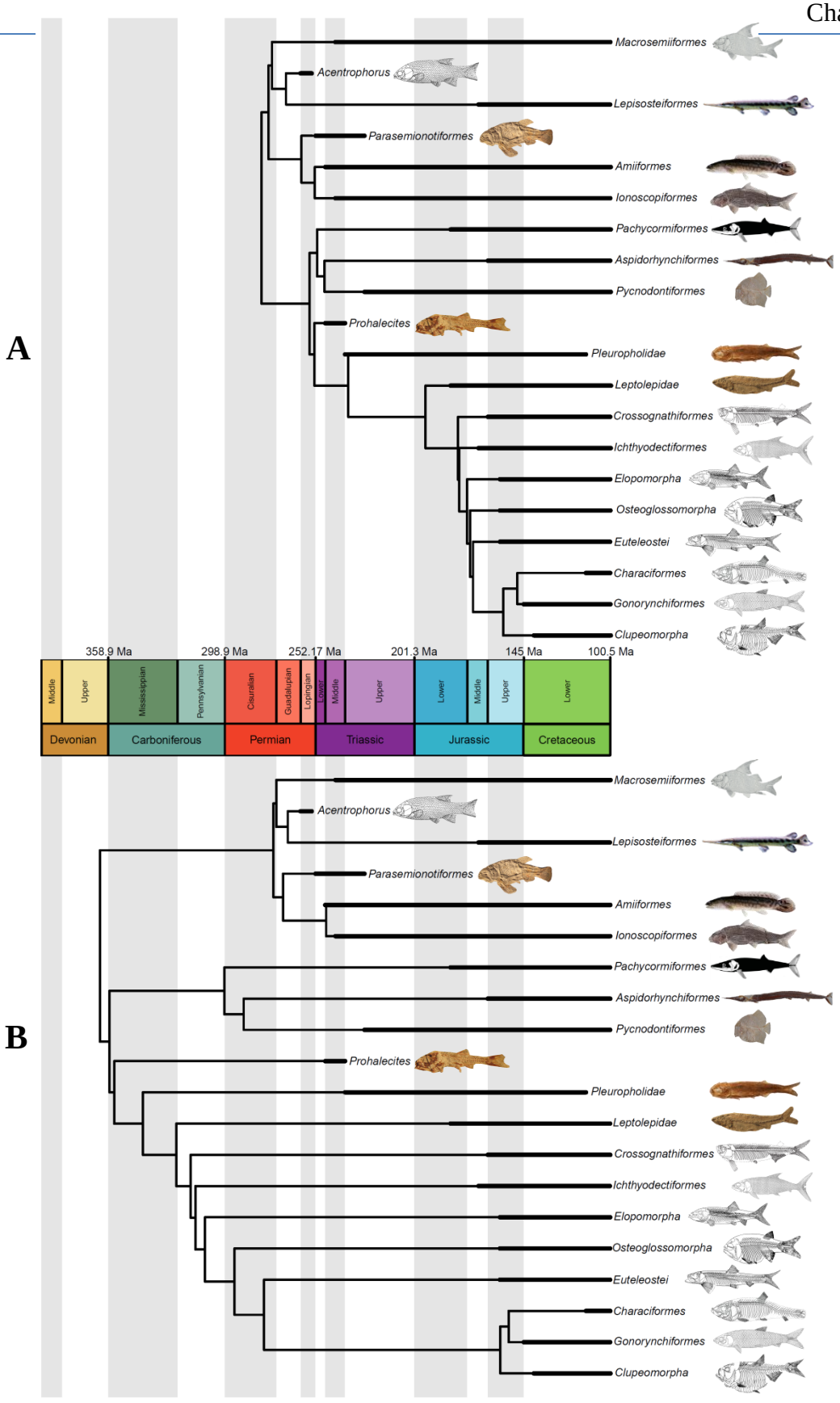

Fig. 2.5. Timescales for neopterygian evolution. **A)** Fossil based timescale, derived solely from fossil data using the method of Hedman (2010) to estimate the root node, and the "equal" method in R package paleotree. **B)** Molecular based timescale, where the ages of Neopterygii, Teleostei and Holostei were constrained to match the mean molecular clock estimates from Near et al. 2012, also performed in paleotree with the "equal" method.

Beyond the differences in timescale, the stratigraphic ranges of the main lineages illustrate some interesting patterns. First, the record of Ginglymodi is older than Halecomorphi; the oldest representatives of these groups derived from the Late Permian (*Acentrophorus*) and the Early Triassic (*Watsonulus*) respectively. Second, although the first teleost fossils are commonly cited as Late Triassic (Arratia 2004, Penga et al. 2009, Tintori 2011), the oldest teleost fossil actually occurs in the first stage of the Middle Triassic (*Prohalcites*, Anisian 242 - 247.2 Ma, Arratia 2013). Third, the first appearances of three main clades of crown teleosts appear simultaneously in the Kimmerdigian, all reported from the *Laggerstätten* of Solnhofen and Cerin. This would suggest that the origins of crown teleosts are deeper within the Mesozoic, especially true if the euteleost species present are found, after formal phylogenetic analysis, to be fairly derived. Fourth, despite the early divergences estimated for the basal stem teleost lineages Pycnodontiformes, Pachycormiformes and Aspidorhynchiformes, the fossil records of the latter two appear relatively late, suggesting either that we might expect to find considerably older representatives of these clades, or that further work on their phylogenetic relationships may break these long branches through insertion of new taxa, or find the current scheme of relationships to be incorrect.

DISCUSSION

The state of Mesozoic neopterygian systematics and future directions

The main purpose of the supertree analysis presented here was not to infer the relationships amongst Mesozoic neopterygians, but simply to summarise the progress that has been made. The results are sobering, suggesting large scale uncertainty throughout the neopterygian tree even with the use of a constraint tree to enforce uncontroversial relationships and molecular findings upon the analysis. The majority of fossil neopterygians have never been included in a formal analysis. Of the 671 taxa presented in the supertree, well over half (460 taxa) do not

appear by their species name in any source tree (although a minority of these will have informed a composite genus or family OTU). Many families have never been subject to formal phylogenetic treatment, and even entire orders have been neglected (e.g., Parasemionotiformes). Even more pertinently, the relationships between many of the major clades and orders of neopterygians are in flux. However, this uncertainty is not balanced. Whereas holostean relationships are relatively well-constrained (with the exceptions of the Parasemionotiformes and an array of Ginglymodians that fall outside of the order Lepisosteiformes), there is huge uncertainty across the entire teleost stem lineage. Vast numbers of stem teleost taxa have been considered to be 'pholidophoriforms', yet the paucity of formal analyses combined with a poor knowledge of many taxa has acted as a barrier to progress. Even where the supertrees suggest regions of stability on the teleost stem, such as the interrelationships between Pycnodontiformes, Pachycormiformes and Aspidorhynchiformes, this situation has arisen mainly due to the lack of analyses, because only a handful of studies by the same author have performed formal analyses including all three clades simultaneously. Indeed, numerous workers still stress the uncertainties regarding the affinities of these specific orders (e.g. Arratia and Schultze 2013:Pachycormiformes).

Despite these challenges, there is room for optimism. Where orders and other large clades have been defined, the interrelationships within these clades appear relatively stable. Furthermore, given these taxa are already described in sufficient detail to resolve within group relationships, further advances may come from including all of these major clades within the same analysis. To date, different analyses have tended to contain quite varied taxon sets. This has created a situation where most analyses are local, with little overlap between datasets, part of the reason a constraint needed to be employed in the supertree analysis. Thus, by including all the taxa known in sufficient detail in the same analysis, rarely tested regions of the tree

could face further scrutiny, such as the relationship between Pycnodontiformes, Pachycormiformes and Aspidorhynchiformes, or the position of Dapedidae.

Priorities for future systematic work, as stated above, could start by taking all of the available data, and including these within the same analysis. Additional taxa that have already been well described can also be incorporated. Beyond this, priority regions for research should be the taxa that currently populate the teleost stem, and Neopterygii *incertae sedis*, work which could also include the Parasemionotiformes for which little is known. This focus would deliver multiple benefits. First, it would establish which taxa are definitely holostean and teleost, which has clear implications for the macroevolutionary questions examined in this thesis. Second, it will dissipate the current fossil haze that populates the teleosts stem, delivering information on the actual sequence of character evolution in one of the most successful vertebrate radiations. Third, it may result in the addition of fossil taxa to the teleost crown group, which in turn may help to reconcile the differences between fossil and molecular timescales for neopterygian evolution.

Implications of the variable neopterygian evolutionary timescale

Clearly the fossil based, and molecular based timescales for neopterygians presented here differ markedly. This presents a challenge for any study where the tempo of neopterygian evolution is important for testing evolutionary or environmental hypotheses, such as those presented in chapters 4 and 5 of this thesis. To accommodate this uncertainty, analyses will be performed on both timescales, to determine their influence on the results.

It is also important to put both evolutionary timescales into context. Although the fossil based timescale was derived by comparable methodology to those employed in comparative

analyses of fossils (e.g. Lloyd et al. 2012, Benson and Choiniere 2013, Anderson et al. 2013), divergences between clades in such trees are usually close in age to the first fossil occurrence of either clade. However, the first fossil occurrence can only act as a minimum estimate for clade age (Benton and Ayala, 2003), and probabilistic estimates based upon sampling often infer considerably older times of origin for clades than suggested by their fossil minima (Marshall 1990, Friedman and Brazeau 2011). Even though steps were taken to address this through probabilistic estimation of the neopterygian root node (280 Ma) and a time scaling method that seeks to distribute this additional duration throughout the tree (the "equal" method of Lloyd et al. 2012), the influence of the method appears negligible in more derived portions of the tree. Thus, the fossil timescale is likely still too young in places. Regarding the molecular time scaling approach, the ages of Neopterygii, Holostei and Teleostei were constrained to match the molecular estimates of Near et al. (2012). While not the absolute oldest, the clock estimates of Near et al. (2012) are close to the oldest interpretation of neopterygian evolution ever proposed, with a Lower Carboniferous origin of Neopterygii, and an Upper Carboniferous origin of crown teleosts. More recent clock studies are shifting towards younger interpretations of these nodes, suggesting an Upper Carboniferous age and a mid-upper Permian age for Neopterygii and Teleostei respectively (Broughton et al. 2013, Betancur-R. et al. 2013, Faircloth et al. 2013, Dornburg et al. 2014). Therefore the two timescales presented here span the full range of interpretation for the neopterygian timescale, and if particular macroevolutionary findings hold for both, we can have greater confidence that these findings will be applicable to most of the alternatives that lie in between. Furthermore, by examining tempo and mode on both time scales, it is possible to learn whether time scaling derived solely from fossil data, as is routinely performed by palaeontologists, produces results that are at all comparable to those derived from molecular timescales. These considerations are addressed in Chapter 5.

Chapter 3
Patterns of morphological and functional space occupation in Mesozoic neopterygians

Introduction

The neopterygian fishes represent over half of all vertebrate species alive today and display a staggering array of morphological and functional variety (see chapters 1 and 2). Despite their prolific diversity in the Recent, there is no comprehensive quantitative overview of the morphological and functional diversity of neopterygians during the first 150 million years of their evolution. In this chapter, I seek to address this through the construction of a morphological and functional dataset based upon 356 neopterygian species recovered globally from the Triassic, Jurassic and Early Cretaceous.

In the Recent, neopterygian taxonomic diversity is unevenly split between teleost fishes with ca. 29,000 species from over 400 families, and the holostean fishes with just 8 species from 2 families. Holostean rarity combined with the presence of fossil species that resemble living ones has branded holosteans 'living fossils' (Darwin 1859, Schultze and Wiley 1984, Wiley and Schultze, 1984), with the implication that they have been always been morphologically and functionally conservative, a claim that has received empirical support based upon living species (Rabosky et al. 2013). However, broad taxonomic surveys indicate that there were upwards of 12 holostean families present in the Mesozoic, and that, during particular periods in the early and middle Mesozoic, there were more holostean families present than teleost

families (Gardiner 1993). Comparable levels of Mesozoic taxonomic diversity between holosteans and teleosts allows for a fairer comparison of these groups, providing opportunities to examine questions regarding the potential for competitive interactions, their convergent and divergent morphologies, and whether or not holosteans were always phenotypically conservative. The morphological and functional dataset itself can provide broader insights regarding the main anatomical correlates of morphological and functional diversity in fishes, the relationship between morphological and functional measures, and the patterns of morphospace occupation through time. Each question is outlined in further detail below.

Q1. What are the main axes of morphological and functional variation in Mesozoic neopterygians? Given a set of morphological landmarks and functional traits, it is unclear from the raw data alone where the main variation lies within those traits. Subjecting these datasets to ordinations reveals these main axes of variation, which can then be examined to determine what changes in morphology and function they characterise. Fossil neopterygians have only rarely been explored morphologically (*but see* Friedman 2010), but have received considerably more attention from a functional perspective, albeit usually restricted to *Lagerstätten* (Bellwood 2003, Bellwood and Hoey 2004, Bellwood et al. 2014a, Goatley et al. 2010 and Bellwood et al. 2014b, *but see* Friedman 2009 for a broad sampling of depositional settings). Deriving and describing the major axes of variation will deliver new information regarding the major anatomical changes that underlie diversity in neopterygian fishes.

Q2.To what extent does morphospace reflect functional space? Evidence bearing on the relationship between morphology, function and ecology has received growing attention in recent years (see Wainwright 2007 for a review, Anderson 2009, Stubbs et al. 2013). Understanding this relationship is of particular importance for palaeontologists, who often

lack any direct information regarding ecology and thus are dependent upon morphological and functional traits alone. Fishes in particular represent a model system for such investigations, since their prolific diversity in the Recent provides a wide range of morphologies and ecologies from which to establish such relationships, with the added benefit that many fossil forms appear, superficially at least, to possess modern analogues. The hope that we might quite reliably infer ecology from positions of taxa in morphospace, initially advocated by (Ricklefs and Miles, 1994) and seemingly adopted by a range of recent studies (e.g. Brusatte et al. 2008, Prentice et al. 2011, Thorne et al. 2011), is dependent on a range of assumptions that are poorly understood. It has proved difficult enough to reliably infer function from morphology, even in instances where morphological and functional traits are measured from the same piece of anatomy (e.g. Hulsey and Wainwright 2002, Anderson 2009). Thus, inferring ecology is an even more challenging task, dependant not solely upon functional capabilities, but the realisation of those capabilities.

Mesozoic neopterygians offer a rare example in fossil vertebrates to examine the relationship between morphology and function in hundreds of species over broad scales. Most commonly, the disparity of morphology and function are compared. I leave this comparison until Chapter 4. Here, I ask two questions: 1) how do morphological and functional axes of variation covary?; and 2) to what extent do distances between taxa in morphological space reflect distances between the same taxa in functional space? The first question seeks to establish which (if any) major axes of shape and functional variation are correlated with one another. This, in combination with an understanding of the anatomical and functional correlates of these axes (Q1 of this chapter) provides a means to establish associations between specific shape and trait changes, quantifying associations which are often based upon anecdote rather than derived from any broad scale analysis. These correlations should provide a better

understanding of the relationship between shape and function for fishes in general, rather than simply Mesozoic representatives.

Q3. How similar are Mesozoic teleosts and holosteans morphologically and functionally?

Given the huge diversity of teleosts alive today, it is unsurprising that most teleost morphologies and functions are unique relative to holosteans in the Recent. In contrast, almost all living holosteans appear to have teleost analogues. Bowfin analogues include the snakeheads (Channidae), whereas pike characins (Ctenoluciidae) represent gar analogues (yet the alligator gar *Atractosteus spatula* does appear relatively distinct owing to its large size). Across the Triassic, Jurassic and Early Cretaceous, numbers of holostean and teleost taxa are far more comparable, and allow for a fairer examination of the unique and convergent morphologies and functions in these two clades. This will help determine whether teleosts have always been better at discovering relatively unique morphologies and functions, or whether holosteans appeared more innovative during this interval.

Q4. What is the pattern of ordination space occupation through time?

Quantification of Mesozoic neopterygian morphology and function provides a unique opportunity to examine the appearance of particular morphologies and functions as they enter the fossil record through time. Although sampling may not allow documentation of the exact sequence in which phenotypes evolved through time, it can at least provide a minimum constraint on the appearance of those phenotypes, and should help to establish whether a wide range of phenotypes were present early on, or whether they were accumulated more gradually through time. It can also highlight those persistently occupied regions of phenotypic space, regions that remain occupied despite the variability of rock record sampling, as well as those

phenotypes that appear briefly and are never rediscovered within the time series. All of these aspects are examined within holosteans and teleosts for comparison.

Q5) Is there any evidence for a competitive replacement of holosteans by teleosts?

Textbook accounts of fish evolution argue for a competitive replacement of holosteans by teleost fishes (e.g. Romer 1966, Colbert 1969). Specifically, they depict a scenario where teleosts increasingly encroach upon holostean ecologies, outnumber them in these ecologies with more efficient forms, essentially swamping them, and as a result, drive a holostean decline through competition (Colbert 1969:60-63). However, except for rare instances where clade competition can be directly observed in the fossil record (encrusting bryozoans, Lingard et al. 1993, Sepkoski et al. 2000), competition is otherwise incredibly difficult to establish (Benton 1991). Even the search for potential candidates reveals that they are rare (Benton 1996). Some of these difficulties derive from a historical focus on entire clades and heavy reliance upon taxonomic data in isolation. Studies that focus instead upon the morphological and functional traits of individual taxa, traits which offer some insights into the ecology, provide more compelling arguments for competition (e.g. Ward 1980 on nautilod *versus* ammonoid shell patterning, Benson et al. 2014b on body size in pterosaurs and birds). However, links between morphology, function and ecology in ordination spaces remain poorly constrained (see Q2 above). Nevertheless, some correspondence is expected between phenotype and ecology, and with this assumption clearly stated, the distances between holostean and teleosts in ordination space is used as a proxy for potential competitive interactions. Although such methods applied to fossil taxa may never truly confirm competitive interactions between species, they do possess the potential to reject them. Here, I consider nearest neighbour and average distances between holosteans and teleosts to

determine whether there is a change in this relationship over time, consistent with the proposed 'swamping' of holosteans by teleosts.

MATERIALS AND METHODS

Taxon selection

Taxa derive from the 150 million year period between the Early Triassic (base of the Induan, 252.17 Ma) and the end of the Early Cretaceous (Albian, 100.5 Ma). Over 600 neopterygian species are known from this period, but the priority here was to select species from which the full complement of morphological landmarks and all six functional traits could be collected. This resulted in selection of 356 species.

Morphological dataset and ordination

i) Landmarking

There are two basic types of landmarks in geometric morphometrics, the traditional landmark pertaining to a specific corresponding point between specimens, and the semilandmark/sliding landmark, which can be used to characterise corresponding curves and surfaces between specimens (Gunz & Mitteroecker 2013). Semilandmarks can be further subdivided historically, between those applied to 2D curves (Bookstein 1991, 1997), and the subsequent extension of the principle to three-dimensional curves and surfaces (Gunz et al. 2005). Discussions regarding what might constitute a corresponding point for a traditional landmark, and how this relates to homology, is discussed elsewhere (Zelditch et al. 2004). Zelditch et al. (2004) outline that landmarks need to be homologous in the sense that they are discrete recognisable anatomical loci, such as the tips and centres of structures, or the intersects between structures, that are identifiable in all specimens. These together then characterise a shape, and allow the mapping of one set of point onto those corresponding points for a

different organism. However, these needn't be homologous from a histological point of view (i.e. the same developmental population of cells), simply a homology of that anatomical part (i.e. the anterior tip of the premaxilla). However, numerous structures cannot be characterised by homologous points, such as the dorsal curvature of a fish, or the 3D surface of a cranium (e.g. Gunz & Mitteroecker 2013). In these instances, these can be treated as homologous curves or surfaces, and the same number of semilandmarks can be used to characterise that curve or surface. They are then slid along the tangent to the curve they attempt to characterise to minimise deformation from the reference (mean) configuration, thus, semilandmarks are treated somewhat differently to traditional landmarks. In conclusion, landmark positions and types need to be selected based upon the question at hand.

A scheme of 25 2D landmarks (**Fig. 3.1**) was applied to images of 735 individuals assigned to 356 species using the software package TPSDIG2 (Rohlf 2013). Two classes of landmarks were used: fixed points marking discrete morphological features, and sliding semilandmarks. The landmark positions, and the choice to include semilandmarks alongside traditional landmarks, are designed primarily to capture overall body shape and fin positions. The semilandmarks are particularly useful to this aim as they act to capture the dorsal and ventral curvature of the body outline. The landmark arrangement used here corresponds closely to those applied previously to both living (Kerschbaumer and Christian 2011) and fossil (Friedman 2010) fishes. As well as landmarks capturing overall body shape, additional landmarks captured structures of established functional and ecological importance, such as the position and size of the eye relative to the head and body (Goatley et al. 2010) and the size of the jaw relative to the head and body (Bellwood 2003). Most of the specimens landmarked preserved all of the relevant structures in life position. Imperfect material was considered on a case-by-case basis. The positions of landmarks in missing structures were occasionally

estimated when their position could easily be inferred from symmetrical parts of anatomy or from examination of closely related species. Where estimation was not possible, the specimen was excluded from the dataset altogether.

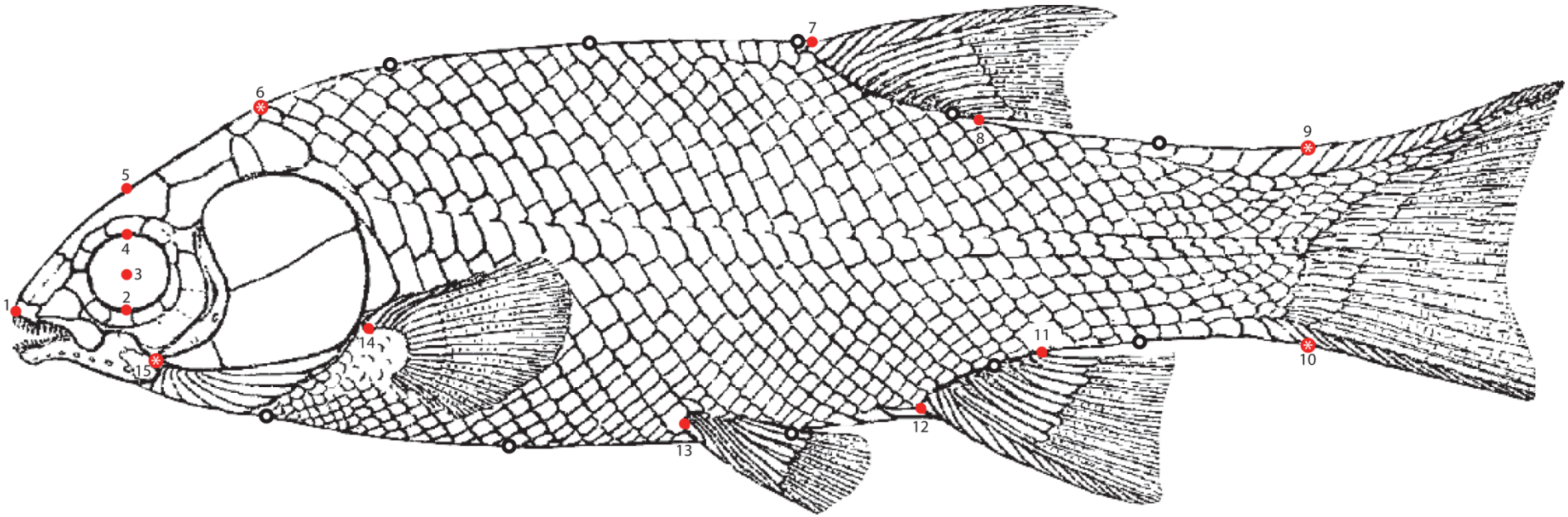

Fig. 3.1. Landmark scheme used to quantify morphological diversity in 356 neopterygian species. Fixed landmarks are marked by red circles, while semilandmarks are marked by black circles with white fill. Red circles containing a white asterisk act as anchor points for the semilandmarks in-between. Fixed landmarks document: 1) anterior tip of the upper jaw (premaxilla); 2) the central, ventral surface of the orbit; 3) the centre of the orbit; 4) the central, dorsal surface of the orbit; 5) the dorsal surface of the skull immediately above the eye; 6) postero-dorsal tip of braincase; 7) anterior insertion of dorsal fin; 8) posterior insertion of dorsal fin; 9) dorsal surface representation of the last vertebral centra; 10) ventral surface representation of the last vertebral centra; 11) posterior insertion of anal fin; 12, anterior insertion of anal fin; 13) anterior insertion of the pelvic fin; 14) anterior insertion of the pectoral fin; 15) lower jaw joint.

ii) Relative warp analysis

Landmarked specimen data was subjected to an initial alignment using an orthogonal generalised Procrustes superimposition analysis (GPA) as implemented in the program tpsRelw 1.49 (Rohlf 2010), where semilandmarks were 'slid' over 3 iterations using the 'chord – min BE' method. Aligned coordinates were then averaged in cases where species were represented by multiple individuals. This finalised set of coordinates formed the basis of a second GPA followed by a relative warps analysis executed in tpsRelw 1.49 (Rohlf 2010).

Functional dataset and ordination

The following six functional traits were collected from differing numbers of specimens. Where a given functional trait could be measured from multiple specimens, a species average was obtained. A joint total of 1261 unique specimens were examined.

i) Functional traits

1. Aspect ratio of the lower jaw – Aspect ratio of the lower jaw is calculated by dividing the square of jaw length by the area of the jaw. This measure can act as a proxy for the jaws second moment of area, which can be used as a measure of stiffness (Vogel 2003, Anderson et al. 2011).

2. Mechanical advantage of lower jaw closing – The lower jaw of Mesozoic neopterygians involves a rotational articulation with the suspensorium at the articular joint. As such, a force applied above the articulation will close the jaw, and below the articulation will close the jaw.

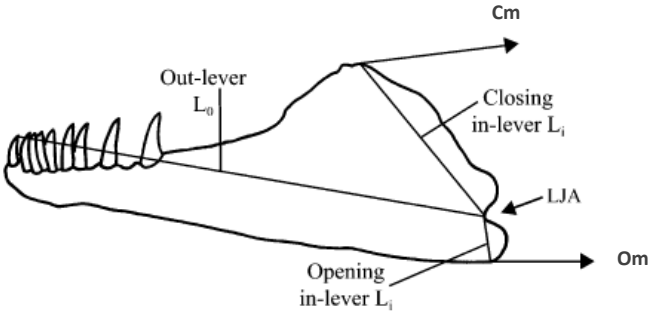

Fig. 3.2. Lower jaw lever ratios explained. Lower jaw labelled with the measurements required to calculate both the closing lever ratio (closing in-lever /out-lever) and opening lever-ratio (opening in-lever/out-lever). There is a muscle responsible for jaw-closing (closing muscle, Cm), and one for jaw-opening (opening muscle, Om), both muscles act via rotation of the jaw about the lower jaw articulation (LJA). The jaw-closing ratio determines the proportion of the opening muscles force that is felt at the jaw tip during jaw-closing, while the jaw-opening ratio determines the proportion of the closing muscle force felt at the jaw tip during jaw-opening. Modified from Bellwood (2003).

This understanding has led to lower jaw being modelled as a third-order lever (Barel 1983, Westneat 1994, **Fig. 3.2**). In this model, the force applied at the anterior tip of the jaw (at the dentition), is dependent on the distance of the relevant muscle attachment from the articular joint (the in-lever) and the distance of the anterior tip of the jaw from the articular joint (out-lever). The ratio of the in-lever to the out-lever is called the mechanical advantage, and represents the proportion of muscle force applied to the dentition. The mechanical advantage of jaw-closing is calculated by dividing the in-lever (which connects the dorsal-most region of muscle attachment on the lower jaw to the articular joint) by the out-lever. This ratio also captures the trade-off between bite force and bite velocity.

3. Mechanical advantage of lower jaw opening – To obtain the mechanical advantage of jaw-opening, the principle is the same as described above, only a different in-lever is selected. To calculate opening mechanical advantage, the in-lever (the distance between the most posteroventral part of the lower jaw and the jaw joint) is divided by the out-lever (**Fig. 3.2**).

4. Body aspect ratio – Body aspect ratio is calculated by dividing the square of body length (standard length) by the area of the body, where low aspect ratios indicate short, fat shapes and high ratios indicate long, thin shapes. Like fineness ratio (Lighthill 1975) it is correlated with drag (Bainbridge 1960) and in turn, locomotion style (Fletcher et al. 2014). Standard length (SL) is measured here from the anterior tip of the snout to the base of the caudal fin. This measurement permits fair comparison between all individuals, regardless of whether they have highly specialized, damaged, or missing caudal fins.

5. *Orbit length relative to standard length* – Calculated as the length of the orbit divided by standard length. In living taxa, large values in this trait have been linked to nocturnal lifestyles

(Goatley et al. 2010), whereas small values have been linked to suspension feeding (Sanderson and Wassersug 1993).

6. Lower jaw length relative to standard length – Calculated by dividing the length of the lower jaw by body length (standard length). It provides information on relative gape, a fundamental limit on relative prey size. Large relative gapes with small relative orbit sizes can characterise suspension feeders (Sanderson and Wassersug 1993), large relative eyes and gapes can characterise nocturnal reef taxa (Goatley et al. 2010) and small relative eyes and gapes can characterise reef generalists (Goatley et al. 2010).

ii) Transformation and Ordination

All six traits were standardised using the Z transformation using the scale() function in R. This ensured that each trait had an average value of 0 and standard deviation (and variance) equal to 1. These transformed traits were then subjected to a principal components analysis using the PCA() function of the R package 'FactoMineR' version1.27 (Lê et al. 2008).

Q1) Establishing anatomical correlates of morphological and functional axes

The anatomical correlates of morphological axes were determined from examination of grid plots from TPSRelW, extreme examples of which are presented in **Table 3.1**. There is no equivalent tool for functional traits. Instead, Spearman's rank correlations were conducted between every functional axis that explained more than 5% of the variance, and all six functional traits (**Table 3.2**). In addition, the magnitudes of each trait were plotted individually within functional space (**Figs. 3.6, 3.8**).

Q2) Assessing covariation in morphological and functional axes and distance matrices

I performed Spearman's rank order correlations to assess the extent of covarition between every morphological and functional axis. To examine the strength of the correlation between distances between taxa in the morphospace and distances between taxa in the functional space, two Mantel tests (Mantel, 1967) were performed. The first was based on Pearson's product moment correlation *r*, and the second using the Spearman's rank-order correlation coefficient *rho*.

Taxa from which these distances are calculated and correlations performed are not statistically independent owing to their shared evolutionary history (Felsenstein 1985). However, my goal at this stage is to establish whether morphology and function correspond, not to identify the source any potential correspondence. Furthermore, it allows me to compare my results directly with other analyses where shared evolutionary history was not accounted for (Anderson 2009, Anderson and Friedman 2012). All analyses were performed in R.

Q3) Examining unique and convergent areas of morphospace and functionspace

Bivariate plots derived from ordination spaces of morphological and functional variety provide a means to visualise the distributions of taxa for the major axes of variation. This is sufficient for an assessment of unique regions of morphospace and highly convergent regions of morphospace displayed by holosteans and teleosts.

Q4) Establishing the pattern of Mesozoic morphospace and functionspace occupation

The goal of this section is simply to document the main features of morphospace occupation in holosteans, teleosts, and neopterygians as a whole, across the Mesozoic. To examine morphospace and functionspace occupation through time, it was first necessary to define time bins to generate a time series. Since stratigraphic stage intervals can vary greatly in duration

(e.g. Norian 18.5 Ma compared with the Induan 0.97 Ma), stages were combined to create eleven composite bins of comparable duration while preserving period boundaries. Time bins were as follows: 1) Induan-Anisian, (duration: 10.17 Ma); 2) Ladinian-Carnian (duration: 15 Ma); 3) Norian-Rhaetian (duration: 25.7 Ma); 4) Hettangian-Pliensbachian (duration:18.6 Ma); 5) Toarcian- Bajocian (duration: 14.4 Ma); 6) Bathonian-Oxfordian (duration:11 Ma); 7) Kimmeridgian-Tithonian (duration:12.3 Ma); 8) Berriasian-Valanginian (duration:12.1 Ma); 9) Hauterivian-Barremian (duration: 7.9 Ma); 10) Aptian (duration: 12 Ma); 11) Albian (duration: 12.5 Ma).

I describe bivariate plots based upon those ordination axes that explain the majority of the variation in the dataset. This pertains to axes 1-3 for morphology (a cumulative ~77% of the variation) and axes 1-2 for function (a cumulative ~75% of the variation).

Q5) Nearest neighbour and mean distance comparisons

ii) Accounting for uncertainty in phylogeny and the ages of fossil deposits

In order to examine distances between holosteans and teleosts in ordination space throughout eleven Mesozoic time bins, it is first necessary to determine 1) which taxa are holosteans and teleosts, and 2) the age of these fossils to enable assignment to a time bin. However, for numerous taxa and deposits, there is uncertainty regarding their affinities and ages. The full detail for how this uncertainty was accounted for is provided in Chapter 4. In short, instead of making arbitrary, singular decisions regarding ages and affinities, I incorporate uncertainty by calculating distances based upon 100 replicates (i.e. 100 versions of events), pooling the distances calculated from all of them. These are the same 100 replicates outlined in Chapter 4.

ii) Calculating nearest neighbour distances.

To examine whether, on average, the phenotypes of holosteans and teleosts became closer or more distant through time, the closest phenotype (i.e. nearest neighbour) for a given clade (e.g. holosteans) to a member of the alternative clade (e.g. teleosts) was calculated for every taxon in every time bin. Nearest neighbour distances between two clades are inherently asymmetric, so the analysis was performed in both directions (i.e. obtain the distances between all holosteans and their closest teleost in a given time bin, then obtain the distances between all teleosts and their nearest holostean). For a given direction (I outline the holostean example here), the nearest neighbour distances for every holostean to its closest teleost were stored for each time bin across the 100 replicates. Distances across all 100 replicates were then pooled for each time bin, and used to derive a mean and 95% confidence intervals for the distribution. In this way, the confidence intervals presented in **Figures 3.19 and 3.21** are distributions of individual taxa, where those at the lower confidence limit represent taxa closely positioned to a holostean, and those at the upper limit are positioned far from a holostean.

iii) Calculating mean distances

In conjunction with obtaining nearest neighbour distances, mean distances (i.e. the mean distance of each holostean taxon from all the teleosts present in a given time bin) were also obtained. Mean distances provide complementary information regarding whether teleosts 'swamped' holosteans with time, not simply by asking whether most holosteans had a close teleost analogue (nearest neighbour) but whether holosteans and teleosts as a whole moved closer together (or further apart) throughout the Mesozoic. This should aid interpretation of changes in nearest neighbour distances.

Results and Discussion

RW	% variance	Anatomical correlate (negative scores)	Anatomical correlate (positive scores)
1.	42.53%	Slender body 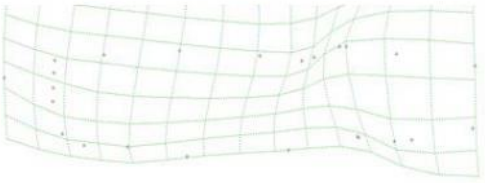	Deep body 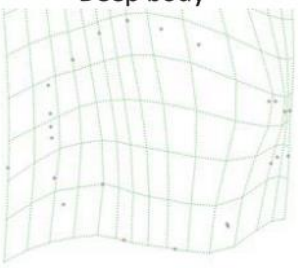
2.	21.43%	Dorsal fin inserts closer to head, anal fin inserts closer to tail. 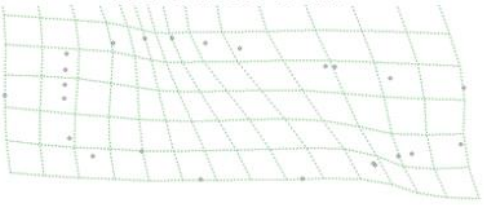	Dorsal fin inserts closer to tail, anal fin inserts closer to bodies centre. 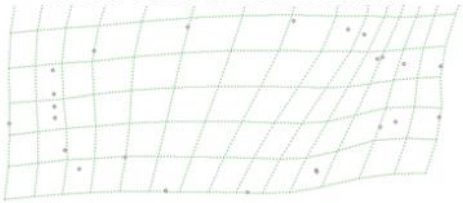
3.	13.52%	Large dorsal fin base 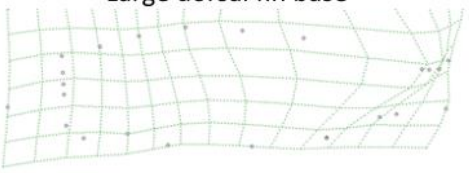	Short dorsal fin base 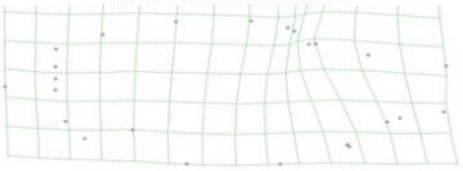
4.	6.10%	Ventral-dorsal flection i.e. bend 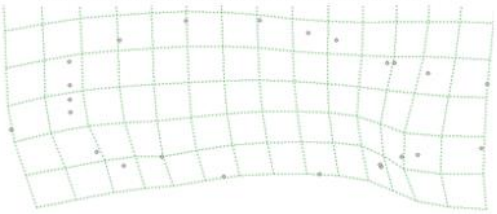	Ventral-dorsal flection i.e. bend 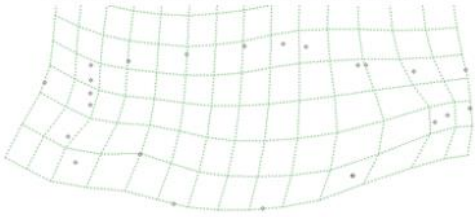

Table 3.1. Anatomical correlates of the four relative warp axes that explain more than 5% of the overall shape variation.

Q1.a Morphological axes of variation

Four axes explain >5% of the variation across the species sampled (**Table 3.1**). RW4, representing only 6.10% of the variation, appears to summarise ventral-dorsal flexion, commonly exhibited by some fish after death. Although care was taken to remove these distorted taxa from the dataset, some expressing mild degrees of bending clearly remain, and appear to inform this axis. Therefore I do not analyse variation in RW4, and instead focus upon RW1-3. Axes were plotted against one another to visualise morphospace to examine the spread of taxa across various axes (**Figs. 3.3, 3.4**).

RW1 captures 42.53% of the variance, reflecting changes from slender-bodied taxa to deep-bodied taxa. Highly positive scores on RW1 are dominated by pycnodonts (Pycnodontiformes), a highly diverse order of early stem teleosts. The only other taxa possessing high RW1 scores are members of the Dapedidae, the occasional ginglymodian (*Sargodon tomicus*, *Hemicalypterus weiri*), and a few other individual, distantly related genera. The most negative scores on RW1, characterising highly slender bodies, belong to the Aspidorhynchiformes, a stem teleost clade including four genera: *Aspidorhynchus*, *Belonostomus*, *Richmondichthys* and *Vinctifer*. Although Aspidorhynchiformes form the extreme, taxa from a wide number of distantly related groups possess highly negative scores, including a variety of stem teleost clades (Pachycormiformes, Leptolepidae, Pleuropholidae, Icthyodectiformes, Crossognathiformes), crown teleosts ('Salmoniformes', Gonorhynchiformes), Halecomorphi (Parasemionotiformes) and Ginglymodi (Early Cretaceous taxa with gar morphologies).

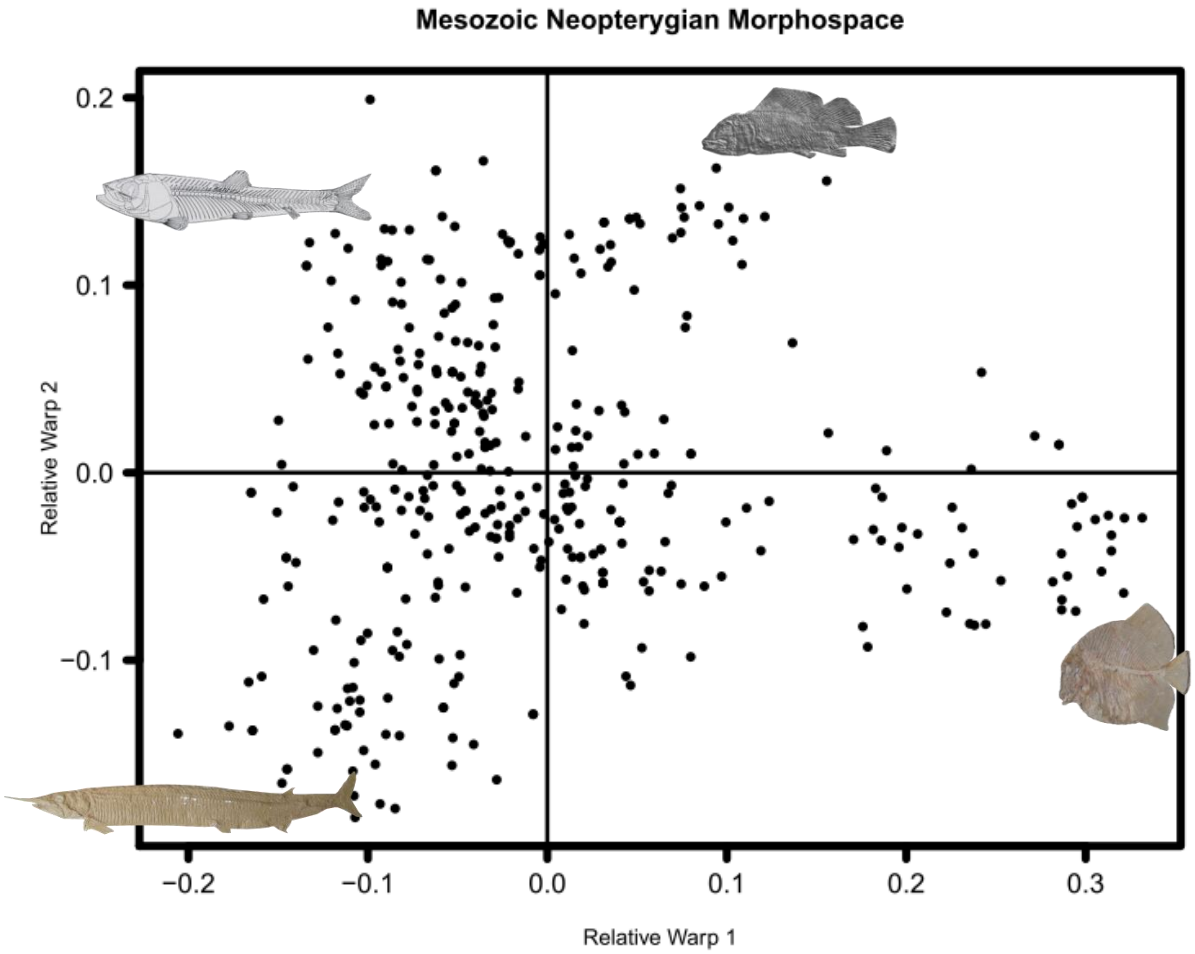

Fig. 3.3. A morphospace of relative warp axes 1 and 2 for the full dataset of 356 species.

RW2, representing 21.43% of variance, captures the position of the dorsal fin relative to the anal fin. Those taxa with highly positive scores have dorsal fins that insert much more anteriorly than the anal fin. The most extreme examples of this are the euteleost *Chardonius longicaudatus* and the halecomorph *Tomognathus mordax*. Highly positive scores are dominated by the Macrosemiiformes, a clade of stem gars, although numerous crown teleosts (e.g. some representatives from the Euteleostei and Clupeomorpha), halecomorphs (e.g. Caturidae, Ionoscopiformes, Amiidae) and stem teleosts (e.g. *Lehmanophorus segusianus*, *Pholidophorus germanicus*) are present in this region. Highly negative scores characterise taxa whose dorsal fin inserts more posteriorly than the anal fin, the most extreme example of which is the pachycormid *Euthynotus incognitus*. Highly negative scores are unique to teleosts, both from the stem group (Pachycormiformes, Ichthyodectiformes, Aspspidorhynchiformes, 'pholidophoriforms') and the crown group (Osteoglossomorpha)

Plotting RW1 versus 2 (**Fig. 3.3**) provides additional information on the spread of taxa throughout morphospace. The densest clusters occur close to the origin, especially in the top left, bottom left, and bottom right quadrants of the morphospace. Beyond specific clusters, it appears that a majority of taxa have negative scores on RW1 (215 taxa) as opposed to positive scores (141 taxa), indicating that somewhat slender morphologies are more common. Morphospaces can also provide information on how some aspects of morphology may be related. For example, the points form somewhat of an isosceles triangle in morphospace, with the broad base at the most negative RW1 scores, ever narrowing to a tip in the most positive RW1 scores. This indicates that, whereas the most elongate body forms show large variation in their relative dorsal and anal fin positions (i.e huge variation on RW2), the more deep-bodied a taxon becomes, the less variation in fin position they exhibit, resulting in a situation where the most positive RW1 values show tiny amounts of variability in RW2.

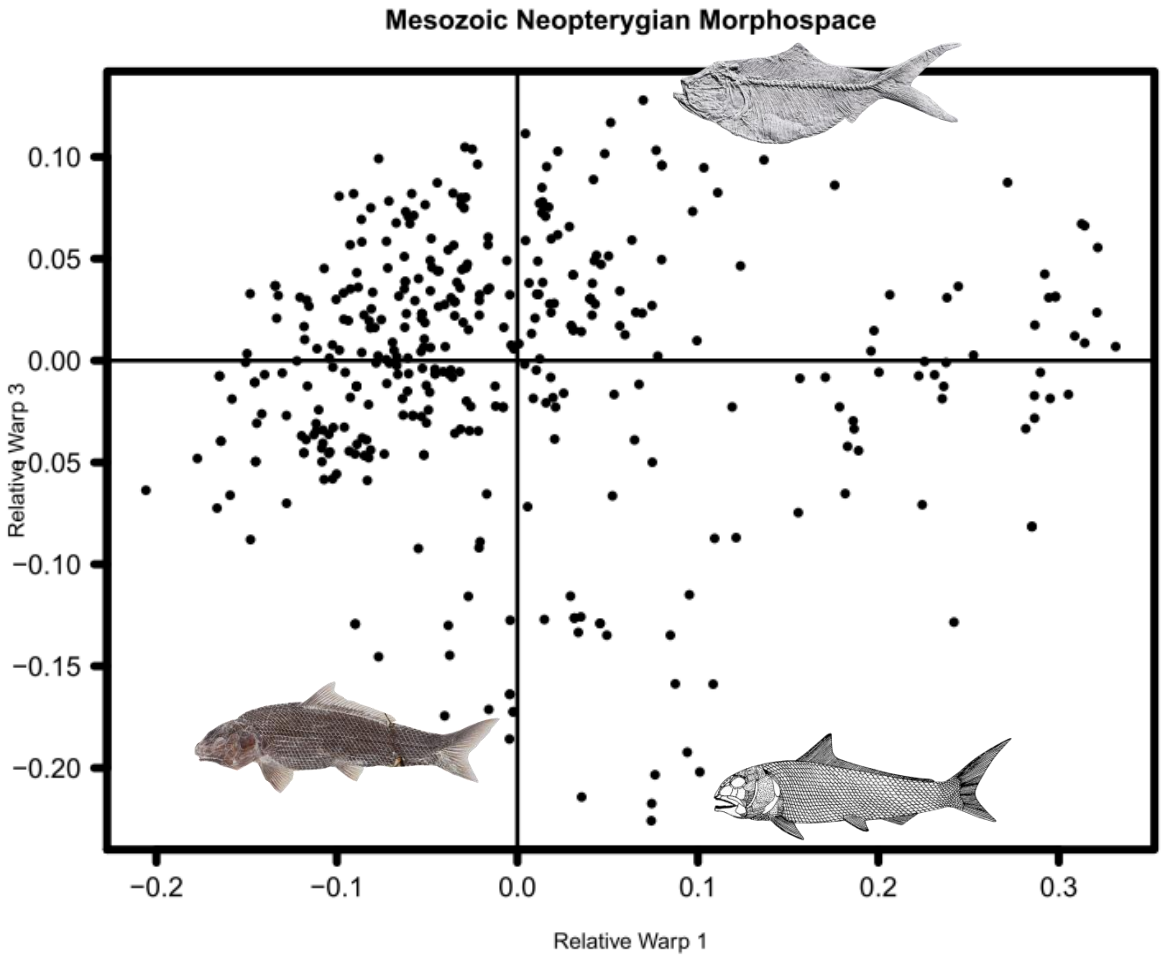

Fig. 3.4. A morphospace of relative warp axes 1 and 3 for the full dataset of 356 species.

RW3 explains 13.52% of variance and captures variation in the length of the dorsal fin base (**Table 3.1**). Highly positive scores on this axis characterise taxa with small dorsal fin bases relative to the length of the body's dorsal surface. The ellimichthyforms (Clupeomorpha) are quite common amongst these highly positive scores, yet numerous 'pholidophoriforms' and a few Ginglymodi and Halecomorphi are also present. The most negative scores (less than –0.2) are populated solely by ginglymodians (Macrosemiiformes) whose dorsal fin bases are large, extending along most of the dorsal surface of the body. Plotting RW1 verses RW3 (**Fig. 3.4**) illustrates that most taxa cluster tightly in the upper left quadrant, characterised by relatively slender bodies with a tendency to have relative short dorsal fin coverage. Both very slender and highly deep-bodied taxa lack a dorsal fin covering the majority of their dorsal surface (i.e. highly negative RW3 scores); the former is somewhat surprising given the large dorsal fin coverage expressed by eels in the Recent.

Q1.b Functional axes of variation

PCA of the six functional traits reveals that five axes explain more than 5% of the functional variation (**Table 3.2**). PC axes 1, 2, 3 and 4 are plotted against one another to visualise functionspace (**Figs. 3.5, 3.7**). Unfortunately, there is no way to directly visualise the functional changes that occur along axes as was possible for morphospace axes via deformation grids. Instead, I performed Spearman's rank correlations between functional traits of each PC axes to determine the importance of each trait to specific axes (**Table 3.2**). To visualise these relationships, I plotted each trait within functionspace by scaling the size of taxon points to the magnitude of each trait (**Figs. 3.6, 3.8**).

PC1 captures 50.37% of the variance, reflecting numerous coordinated functional changes (**Table 3.2**). Highly positive scores on PC1 represent deep-bodied taxa (small aspect ratios)

PC	% variance	Correlation to traits (Spearmans *rho*)		Anatomical correlates (negative scores)	Anatomical correlates (positive scores)
1.	50.37%	Jaw AR	- 0.92	Elongate jaws, elongate bodied, somewhat smaller eyes relative to body length, and mildly longer jaws relative to body length.	Short jaws, deep bodied, somewhat larger eyes relative to body length and mildly shorter jaws relative to body length.
		MA closing	0.80		
		MA opening	0.77		
		Body AR	- 0.65		
		Orb.SL	0.48		
		JL.SL	- 0.38		
2.	24.3%	JL.SL	0.80	Shorter jaws relative to body length, smaller eyes relative to body length, somewhat slender bodied, slightly more individuals with somewhat robust jaws.	Longer jaws relative to body length, larger eyes relative to body length, somewhat deeper bodied, slightly more individuals with somewhat elongate jaws.
		Orb.SL	0.62		
		Body AR	- 0.46		
		MA close	- 0.23		
		Jaw AR	0.21		
		MA open	- 0.09		
3.	9.37%	MA close	0.46	Small mechanical advantage of closing yet large mechanical advantage of jaw opening. Mildly smaller eyes relative to body length.	Large mechanical advantage of jaw closing yet small mechanical advantage of jaw opening. Mildly larger eyes relative to body length.
		MA open	- 0.41		
		Orb.SL	0.28		
		Body AR	0.18		
		Jaw AR	- 0.08		
		JL.SL	- 0.01		
4.	7.7%	Orb.SL	0.46	Tendency for smaller eyes yet longer jaws, both relative to body length. Some of these longer jaws maintain high closing MA.	Tendency for larger eyes yet shorter jaws, both relative to body length. Some of these shorter jaws maintain low closing MA.
		JL.SL	- 0.38		
		MA close	- 0.20		
		Jaw AR	0.11		
		Body AR	0.03		
		MA open	0.03		
5.	5.3%	Body AR	0.29	Presence of some deep bodied taxa with smaller eyes and low MA of jaw opening.	Presence of some slender bodied taxa with larger eyes and high MA of jaw opening.
		MA open	0.28		
		Orb.SL	0.20		
		Jaw AR	- 0.18		
		JL.SL	0.17		
		MA close	0.10		

Table 3.2. Functional trait correlates of the five principal component axes that explain more than 5% of the combined trait variation.

that possess short, robust jaws with large mechanical advantages of both jaw opening and jaw closing (**Fig. 3.6a-d**). These taxa also tend to possess somewhat larger eyes and shorter jaws relative to their body length (**Fig. 3.6e-f**). Taxa that best capture these traits are numerous species of Pycnodontiformes and members of Dapedidae (**Fig. 3.5**). Taxa with highly negative scores have slender bodies and relatively slender jaws, and a mild tendency to have smaller eyes and larger jaws relative to their body length (**Fig. 3.6a-f**). *Belonostomus* embodies these traits to the extreme (**Fig. 3.5**).

PC2 represents 24.3% of the variance and is most strongly associated with relative jaw and orbit size (**Table 3.2**). Highly positive scores are characterised by taxa with large jaws and large eyes relative to body length (**Fig. 3.6 e, f**). There is also a weak correlation with body aspect ratio and jaw-closing mechanical advantage, highlighting, some taxa with positive PC2 scores that possess deep-bodies and slender jaws; the halecomorph *Eoeugnathus* typifies this morphology. Taxa with highly negative scores have small eyes and jaws relative to body length, with a weak tendency to have slender bodies and jaws. Numerous taxa embody these traits, such as early and late diverging stem teleosts (*Aspidorhynchus*, *Allothrissops salmoneus*), crown teleosts (Gonorhychiformes *Tharrhias* and *Rubiesichthys*) and Ginglymodi morphologies that closely resemble extant gars (*Obaichthys*).

PC3, included in a second functionspace plot (**Fig. 3.7**), explains 9.37% of the variation, and highlights taxa that appear to deviate from some of the relationships between traits highlighted in PC1. Whereas highly positive scores in PC1 illustrated that many taxa with large mechanical advantages for jaw closing also had large mechanical advantages for jaw opening, highly positive PC3 highlight those taxa which show the inverse of this relationship, (i.e., large jaw-closing MAs, but small jaw-opening MAs; **Fig. 3.7b-c**). These taxa appear to

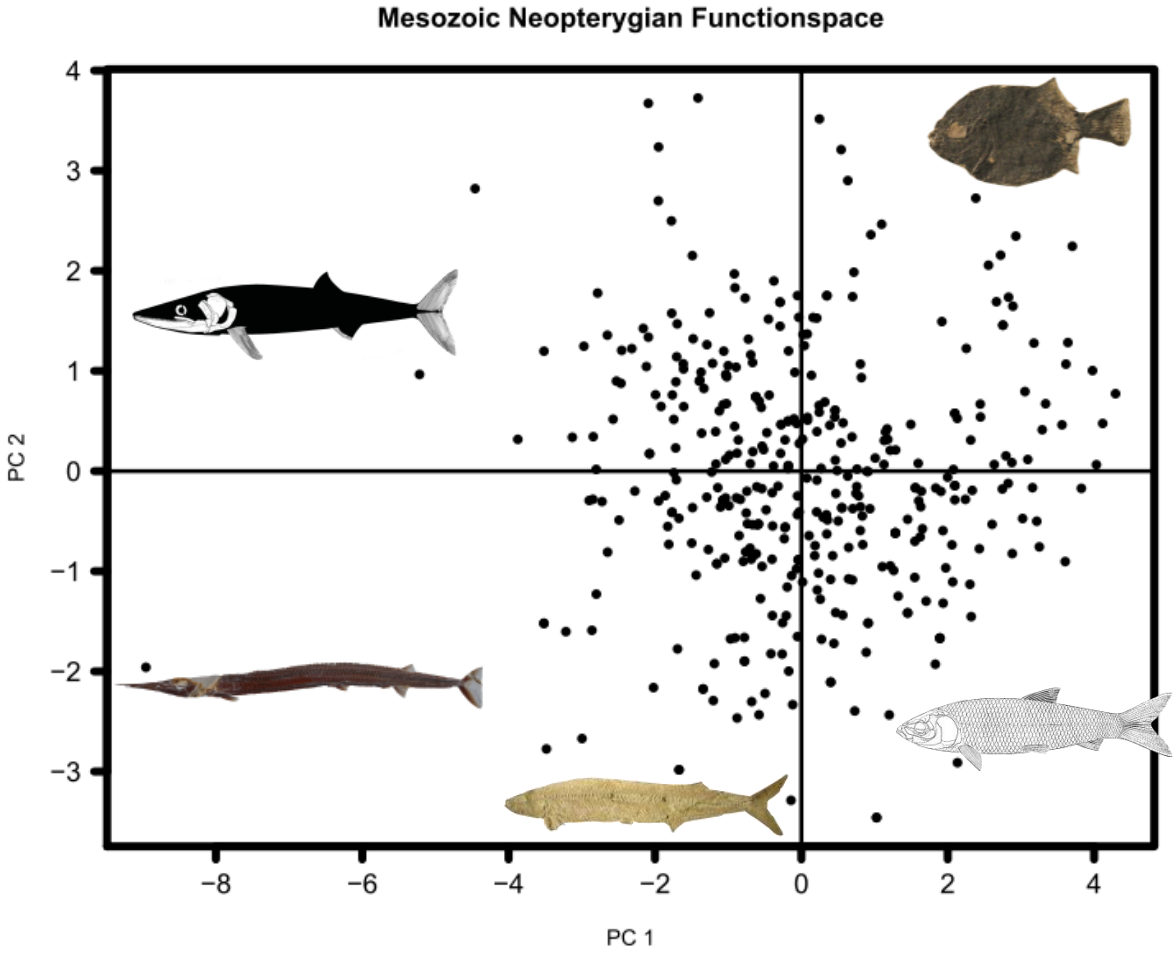

Fig. 3.5. A functionspace of principal component axes 1 and 2 for the full dataset of 356 species.

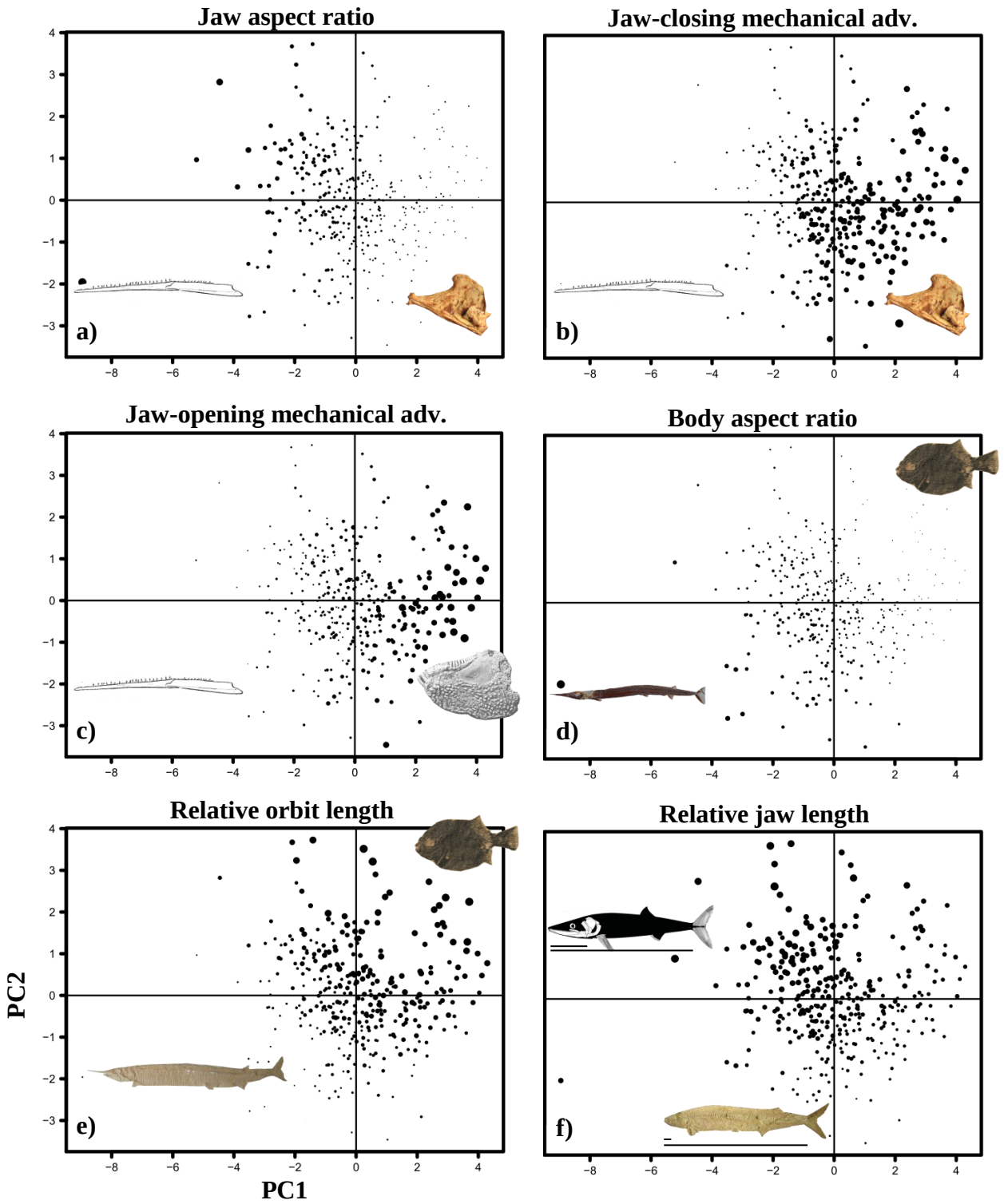

Fig. 3.6. All six individual functional traits, plotted with points scaled according to their magnitude, within the principal component 1 versus 2 functionspace for the full dataset of 356 species. Scaling of points exaggerates differences for clarity.

have posteriorly narrow lower jaws, and mildly expanded dorsal surfaces yielding an observable coronoid process (yet not necessarily the most prominent coronoid processes, such as in members of the Amiidae, since their opening MAs are not particularly small). However the relationship is not perfectly maintained across the axis, which is to be expected given that correlation coefficients for mechanical advantage are only ~0.4 (**Table 3.2**). Thus, although highly negative scores correspond to taxa with the largest jaw-opening MAs, they do not also possess the smallest jaw-closing MAs (which are intermediate in value). Highly negative scores are dominated by Dapedidae, a deep-bodied clade with uncertain phylogenetic placement (Chapter 2).

PC4 explains 7.7% of the variation and mostly captures the inverse of the positive relationship previously observed between relative eye and jaw size in PC2. As such, positive scores highlight taxa with large eyes yet short jaws and negative scores reflect taxa with small eyes and long jaws (**Table 3.2**). The correlations between these traits and PC4 are weak (~0.3), and so substantial deviations from this trend are expected. 'Pholidophoriforms' are common amongst the highly positive scores, although osteoglossomorphs (*Lycoptera*, *Yungkangichthys*) and a halecomorph (*Prosantichthys*) are also present. Taxa with long jaws and short eyes that populate the highly negative scores are drawn from a range of clades, including the Amiiformes (e.g. *Amblysemius pachyurus*, *Amiopsis prisca*), Pachycormiformes, Pyncodontiformes and Euteleostei, although the clearest embodiment of these traits is *Aokiichthys otai*, a member of Osteoglossomorpha.

PC5 explains just 5.3% of the variation, and appears to highlight further exceptions to the trends identified in RW1. Correlations between traits and PC5 scores are relatively weak (**Table 3.2**), making it difficult to find taxa that fit the pattern in all aspects, but positive

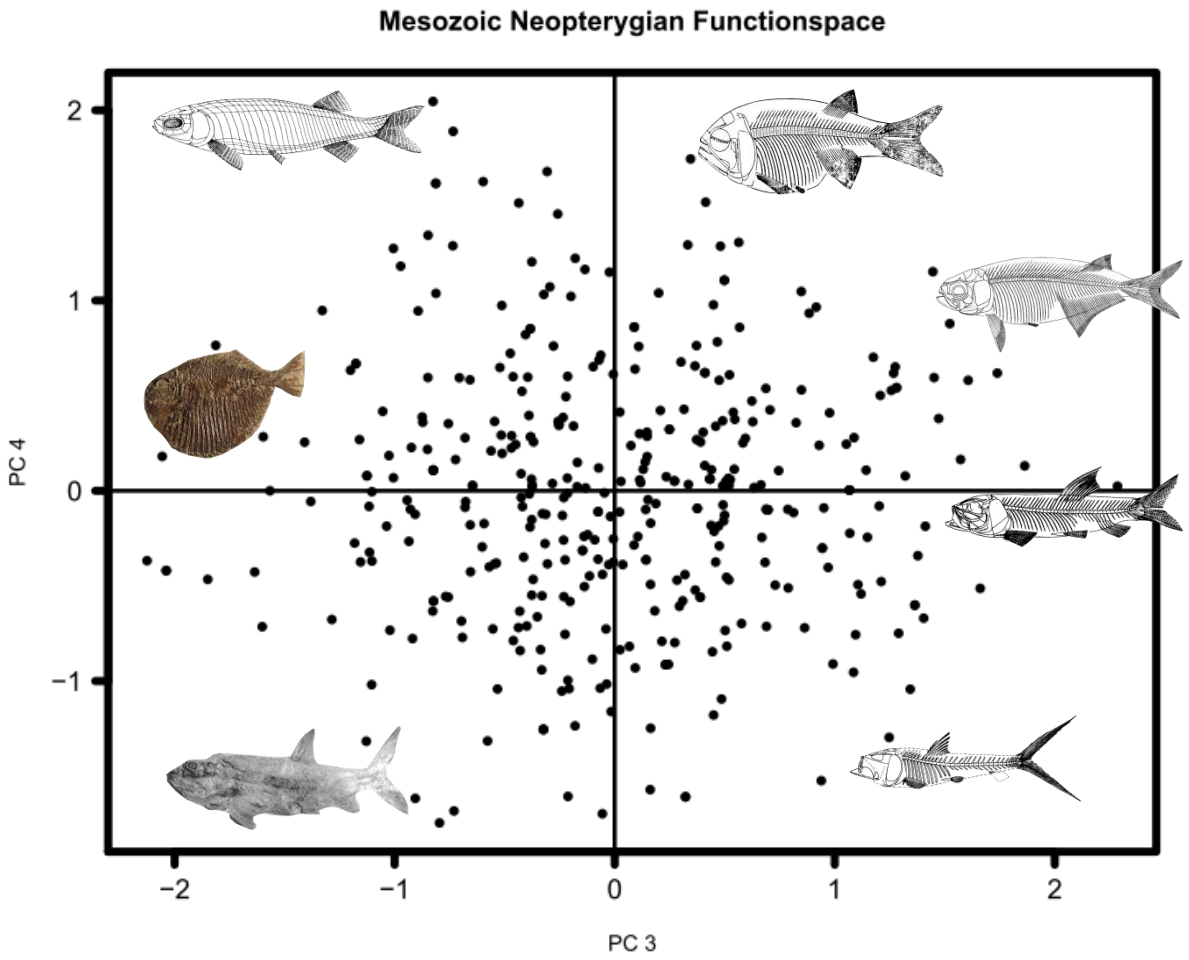

Fig. 3.7. A functionspace of principal component axes 3 and 4 for the full dataset of 356 species.

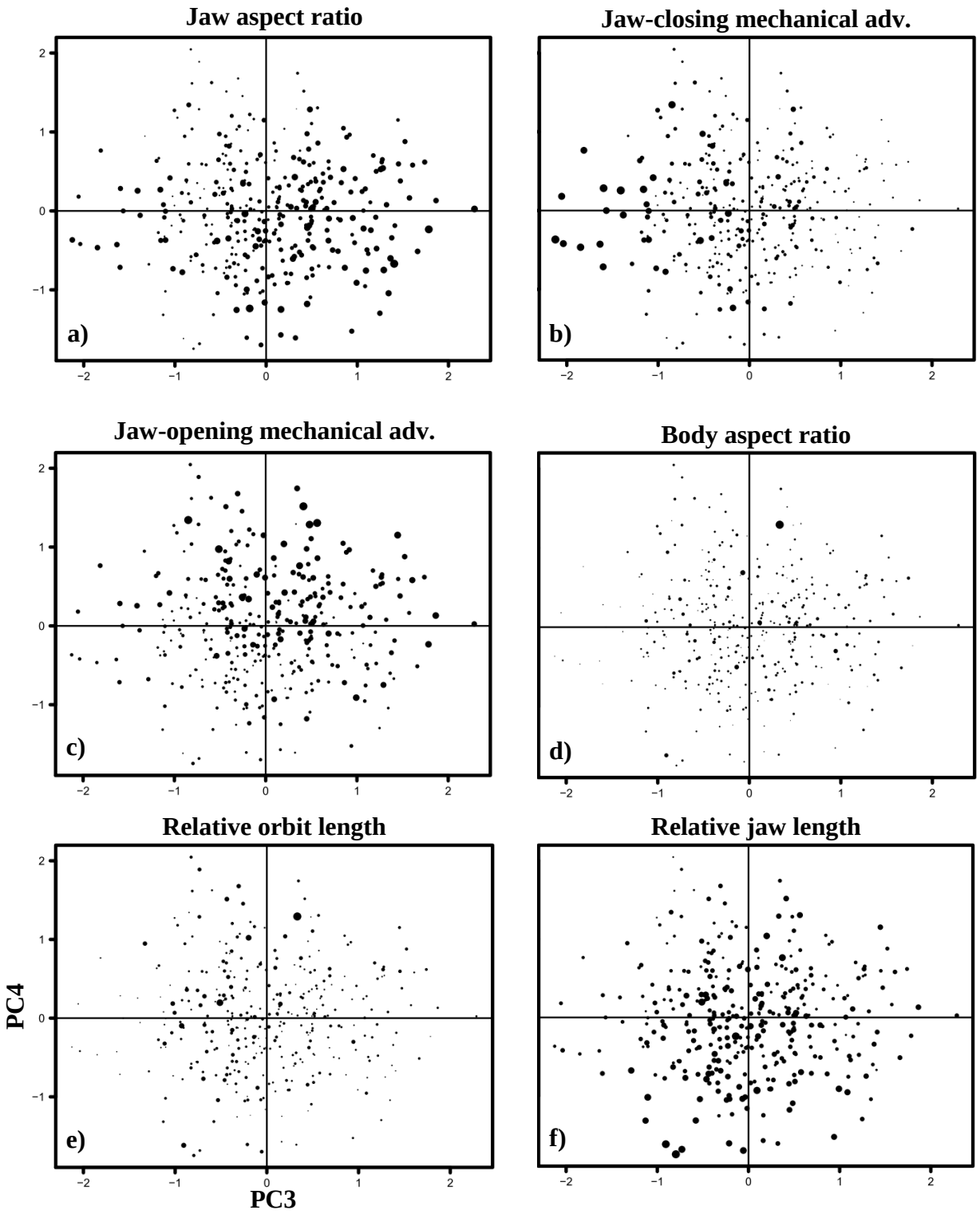

Fig. 3.8. All six individual functional traits, plotted with points scaled to their magnitude, within the principal component 3 versus 4 functionspace for the full dataset of 356 species. Scaling of points exaggerates differences for clarity.

scores weakly characterise taxa with some combination of the following traits: slender bodies, moderately large jaw-opening MAs, and relatively large eyes. *Belonostomus* possesses the most extreme positive score, and clearly has a slender body with a relatively large eye, but jaw-opening MA is very small. *Aspidorhynchus* fits the pattern slightly better, as it is similar in shape to *Belonostomus*, but possesses a shortened lower jaw, resulting in a larger jaw-opening MA. Amongst the negative scores there is a tendency for deeper bodies, relatively small eyes and small jaw-opening MAs. As for the positive scores, it is difficult to find taxa that embody all three traits simultaneously, yet many of the most negative scores characterise taxa with two, such as *Diplomystus longicostatus*, with its deep body and small jaw-opening MA, and *Sargodon tomicus*, with a deep body yet relatively small eyes.

Future work – Neopterygian fossil fishes provide a wealth of morphological information. Therefore further work on functional disparity could look to include a larger array of functional characteristics, such as the aspect ratio of the caudal fin, or discrete traits, such as information of tooth morphology. However, more traits will reduce the number of taxa that can be scored for such traits, which will necessitate either use of a principal coordinates analyses to account for missing data, or simply use of a smaller dataset. More generally, there is a need to broadly establish the morphological and functional correlates of living fishes, where inferences still tend to derive from anecdote rather than correlations.

Q2. To what extent does the morphospace reflect functional space?

First I calculated Spearman's *rho* between every morphological and functional axis (**Table 3.3**) to identify the functional correlates of morphological changes (and vice versa). The strongest association of all is found between RW1 and PC1, indicating that deep-bodied taxa tend to have deep robust jaws and large eyes, whereas slender taxa tend to have elongate jaws,

and smaller eyes relative to their body length. There is also a weak to moderate correlation between PC2 and RW1, which further captures a tendency for deep-bodied taxa to have large eyes and large jaws relative to their body length, and for some slender taxa to have smaller eyes and somewhat shorter jaws relative to their body length.

The third correlation of note is the weak to moderate association between RW3 and PC2, which suggests that there is a tendency for taxa with a short dorsal fin base to have larger eyes and jaws relative to their body length, whereas taxa with dorsal fins that cover the majority of their dorsal surface have small eyes and jaws relative to their body length (**Table 3.3**). This relationship is most clearly seen in the positive RW3 scores, where some taxa with short dorsal fins possess big eyes and jaws relative to their body length (e.g. *Pholidorhynchodon malzannii*). Examination of scatter plots indicates very weak associations between functional and morphological axes beyond the three discussed here.

Beyond seeking specific associations between axes, I examine whether the distances between taxa in morphospace are comparable to the distances between taxa in functionspace. A plot of Euclidean distances between all species in morphospace against functionspace is presented for both my observed data and a simulated dataset (**Fig. 3.9a-b**). A mantel test suggests no correlation between observed functional and morphological distances (Pearsons's r = 0.008, p = 0.36; Spearman's *rho* = 0.003, p = 0.47), illustrating that these are almost entirely decoupled from one another given the morphological (shape) and functional traits examined here. These results contrast with those from a Brownian null model of evolution, where morphological and functional distances show a weak yet significant correlation (Pearsons's r = 0.21, p = 0.001; Spearman's *rho* = 0.21, p = 0.001).

Morphological axis	Functional axis	Spearman's *rho*	Significance
RW1	PC1	0.690702	< 2.2e-16
	PC2	0.4218495	< 2.2e-16
	PC3	-0.1318233	0.01285
	PC4	-0.1101387	0.03784
	PC5	-0.09499482	0.07345
RW2	PC3	0.2187901	3.265e-05
	PC4	-0.136281	0.01009
	PC2	0.08842108	0.09576
	PC5	0.07946529	0.1345
	PC1	-0.02739131	0.6063
RW3	PC2	0.4041449	3.618e-16
	PC5	-0.2301465	1.219e-05
	PC4	-0.06676649	0.2087
	PC3	-0.01715036	0.747
	PC1	-0.009151538	0.8633
Functional axis	**Morphological axis**	**Spearman's *rho***	**Significance**
PC1	RW1	0.690702	< 2.2e-16
	RW2	-0.02739131	0.6063
	RW3	-0.009151538	0.8633
PC2	RW1	0.4218495	< 2.2e-16
	RW3	0.4041449	3.618e-16
	RW2	0.08842108	0.09576
PC3	RW2	0.2187901	3.265e-05
	RW1	-0.1318233	0.01285
	RW3	-0.01715036	0.747
PC4	RW2	-0.136281	0.01009
	RW1	-0.1101387	0.03784
	RW3	-0.06676649	0.2087
PC5	RW3	-0.2301465	1.219e-05
	RW1	-0.09499482	0.07345
	RW2	0.07946529	0.1345

Table 3.3. Correlation coefficients derived from comparison of all functional and morphological axes. For each axis, comparisons are ordered by the axes that correlate the most to those that correlate the least.

A plot of Euclidean distances between all species in morphospace against functionspace is presented for both my observed data and a simulated dataset (**Fig. 3.9**), and provides additional information on how morphological and functional distances are decoupled. For example, the clearest pattern is horizontally positioned sausage shaped scatter of points (**Fig. 3.9**) which implies the following three things regarding decoupling:

Four observations are made regarding the distributions of functional and morphological distances presented in **Fig. 3.9**:

i) *Divergent morphologies can be functionally convergent*

Small functional distances are present across the entire horizontal axis representing morphological distances (**Fig. 3.9a**). Therefore large morphological distances can correspond to highly similar functions (**Fig. 3.9a, box 1**), a feature absent from the Brownian null model distances (**Fig. 3.9b**). This form of decoupling, where many morphologies converge on similar functions, have been widely discussed in the context of many-to-one mapping (reviewed in Wainwright 2007), the phenomenon in which a complex functional system can produce the same measurable parameter (e.g. suction index) even with substantial variation in the morphology of its component parts. However, many-to-one-mapping is a specific cause of decoupling in a particular direction, and is not to be confused as a general descriptor of instances where divergent morphologies converge in function. Indeed, all of the functional traits employed in this study are based upon simple ratios or aspect ratios for which many-to-one-mapping does not apply on an individual basis. Nevertheless, we would expect some decoupling simply due to the choice of functional and morphological data. For example, body shape is not the best predictor of feeding ecology (e.g. Chakrabarty 2005). Therefore morphological data based upon gross body form and fin position would be expected to deviate

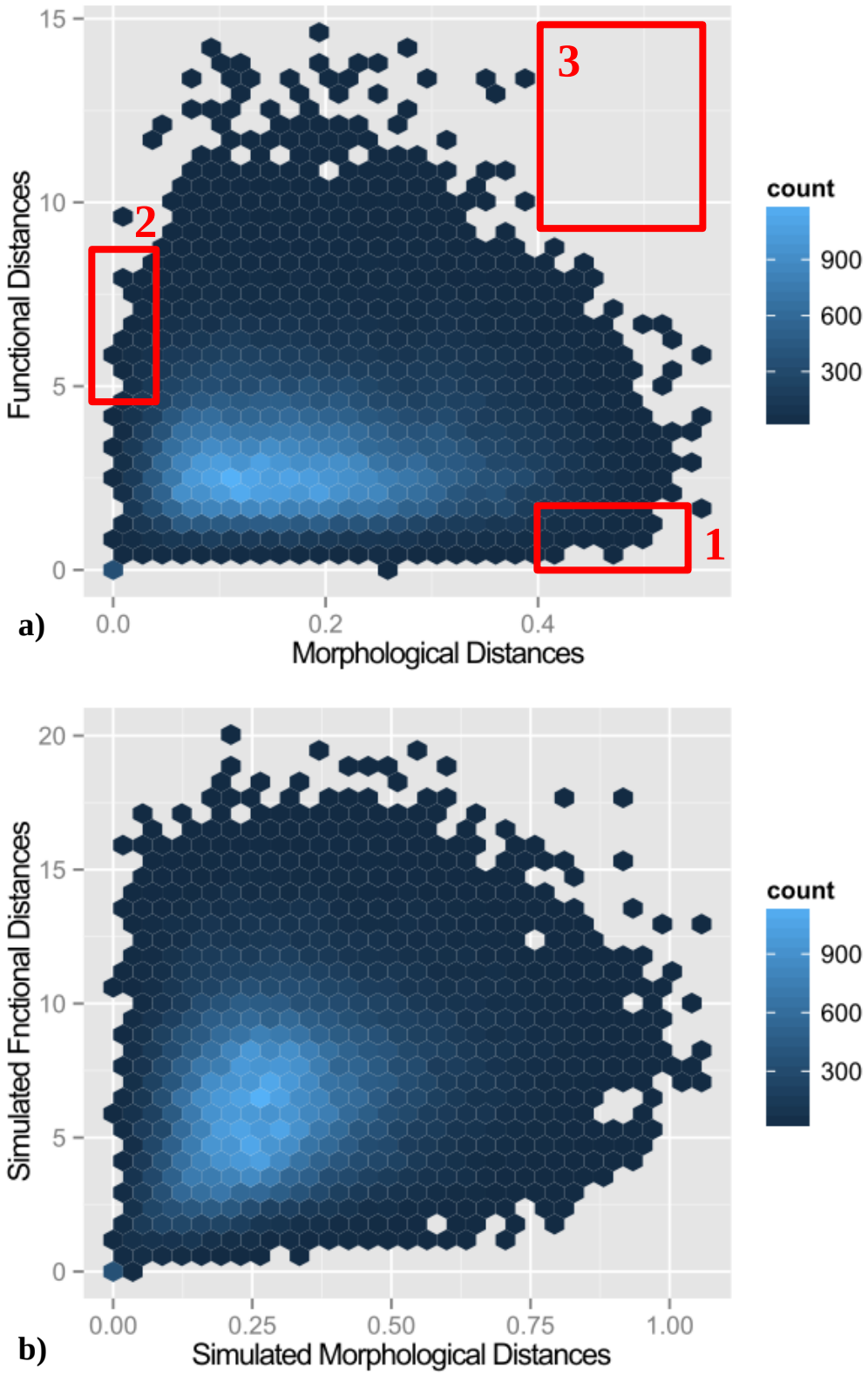

Fig. 3.9. Scatterplot depicting the Euclidean distances between all 356 species in morphospace (horizontal axis) and their corresponding distances in functionspace (vertical axis) from **a)** the observed dataset and **b)** a single simulated dataset using a Brownian null model. The red boxes highlight extreme decoupling of morphology and function distances. Box 1 highlights large morphological distances derived from taxa which are similar in function, whereas the box 2 highlights large functional distances derived from taxa that are morphologically similar. Box 3 highlights the absence of taxa which are highly distant in both morphology and function.

somewhat from traits regarding jaw lever ratios and relative eye diameters. There is further evidence for this disconnect in my datasets, gleaned from the correlation of morphological and functional ordination axes discussed above. For example, RW2 capturing relative anal to dorsal fin position was a poor predictor of any functional axes, and in turn, any functional trait (**Table 3.3**), although interestingly, gross body shape on RW1 was actually a moderate predictor of PC2 (**Table 3.3**) which best characterises relative jaw length (**Table 3.2**).

ii) Similar morphologies can be functionally divergent

Relatively large functional distances are present across the entire horizontal axis representing morphological distances (**Fig. 3.9a**). Therefore small morphological distances can correspond to large functional distances (**Fig. 3.9a, box 2**). As discussed above, the nature of ordination and the choice of data would lead us to expect this disconnect.

iii) Decoupling of morphology and function is asymmetric

Points 1 and 2 above discuss the instances of the greatest decoupling between form and function, labelled 1 and 2 in **Fig. 3.9a**. However, these extreme instances of decoupling do not appear equal; whereas small functional distances occur across the full range of morphological distances, small morphological distances only extend half way up the vertical axes. Thus, functionally convergent taxa have a greater capacity to arise from highly divergent morphologies than morphologically similar taxa have to produce functionally divergent taxa. This finding appears to be a common feature of datasets in the literature (Anderson 2009:Fig.7, Anderson and Friedman 2012:Fig.2). Interestingly, this asymmetry is not seen under a Brownian null model **Fig. 3.9b.** Perhaps part of the reason for this observed asymmetry derives not only from the presence of many-to-one mapping and the types of traits chosen more generally, but specifically due to the structure of the morphospaces and

functionspaces presented here. Whereas morphospace occupation appears highly structured, with specific regions of space densely populated with regions of empty space in between (**Figs. 3.3, 3.4**), functional space shows greater symmetry, with taxa more evenly spread along functional axes (**Figs. 3.5, 3.7**). Thus, taxa in morphospace are on average further apart than taxa in functional space, which could produce an asymmetry simply due to the probability of sampling taxa close together in the two spaces. For example, because morphospace has densely populated, far apart clusters, repeatedly sampling two taxa at random would commonly recover very large distances whenever taxa from two different extreme clusters were sampled. It would be much more difficult to recover the largest distances in functional space due to the lack of extreme clusters, dramatically lowering the chance of recovering two taxa at opposite extremes. Altogether, one might infer that functional traits evolve in a fundamentally different manner to shape traits, a claim that requires further investigation.

iv) *Rare to be both morphologically and functionally distant*

The observed distances reveal that no taxa which are highly morphologically divergent are also highly functionally divergent (Fig. **3.9a**, box 3). However, this is also rare under a null model (**Fig. 3.9b**), and so does not appear to be an unexpected outcome. Thus, the observation of this pattern under a null combined with fundamental differences in the distributions of morphological and functional distances (clumped versus more evenly distributed, respectively), may be sufficient to explain why taxa are rarely highly different in body shape and highly different across functional axes.

Conclusions

The anatomical and functional correlates of morphospace and functionspace have been established. Furthermore, the first axis of morphology and function show a relatively strong

correlation, highlighting the main functional correlates relating to changes from deep to slender bodies. However, remaining axes of variation show little correspondence, and this is reflected in the lack of correspondence between morphological distances between taxa and functional distances between taxa. Therefore, although broad claims about PC1 could be made based upon RW1, the general lack of correspondence advises against making any broad claims about distances in morphospace based upon functionspace and vice versa. This reinforces the findings and sentiments of other workers (Alfaro et al. 2004, Anderson 2009, Anderson and Friedman 2012), suggesting that data must carefully be chosen for the question at hand, and that clear inferences of morphological variety (body shape) cannot be made from multivariate measures of functional variety (or minimally, based upon the 6 traits selected here) and vice versa.

Future work – Additional work could test for further correlations in morphological and functional axes (but not their distribution in ordination space, the main intention of the above analyses) while accounting for the non-independence of morphology and function due to phylogeny. This could be achieved by calculating phylogenetically independent contrasts (PICs) for morphological and functional axes. Contrasts require trait values for terminal taxa, a time scaled phylogeny, and a model of trait evolution (e.g. Brownian-motion). For a multivariate ordination, this will require calculation of PICs for each individual axis, and comparison of these axes through correlations. For additional information on the relationship between morphology and function, see Q1 in Chapter 4 and its associated future work section.

Q3. How similar are Mesozoic teleosts and holosteans morphologically and functionally?

The prolific diversity of teleosts today renders any comparison to the depauperate holostean sister group straightforward yet uninformative; teleosts possess such a staggering array of

morphologies and functional characteristics that it would be impossible for holosteans to match. However, numbers of Mesozoic holosteans and teleosts are far more comparable, which lends itself to a more informative comparison of their capabilities throughout this time. Here I ask which morphologies and functions: 1) appear highly convergent in numerous holosteans and teleosts; and 2) appear unique to either holosteans or teleosts.

i) Unique regions of teleost and holostean morphospace

Holostean (blue) and teleost (red) taxa are identified within morphospace to highlight their distributions (**Fig. 3.10a**). Teleosts occupy the most extreme positive and negative scores in both RW1 and RW2. Not only do teleosts represent the ultimate extremes, but they also saturate three out of four of outer regions with respect to holosteans (RW1 scores below -0.1 and above 0.2, and RW2 scores less than -0.1). In addition to extreme and outer regions, there are more specific regions which appear entirely unique to teleosts, with no holostean analogue nearby. These regions are labelled in **Fig. 3.10b** from T1 to T7, and taxa that correspond to these regions displayed in **Fig. 3.12**.

Holosteans too occupy some unique regions, such as the densely populated cluster around the origin (0,0) and a small cluster at coordinates (1.5, 1.5). Examination of the third relative warp axis (**Fig. 3.11a**) reveals that taxa with longer than average dorsal fin bases are almost always holosteans (RW3 scores less than -0.1). Select regions of unique holostean morphologies are labelled from H1 to H4 (**Fig. 3.10b, 3.11b**), and taxa that correspond to these regions displayed in **Fig. 3.12**.

ii) Convergent regions of teleost and holostean morphospace

There are many instances of morphological convergence, where holostean and teleost taxa occur in close proximity in morphospace (**Fig. 3.10**). Some regions with particularly dense clusters of holosteans and teleosts are labelled from C1 to C4 (**Fig. 3.10b**), with example taxa illustrated in **Fig. 3.12**.

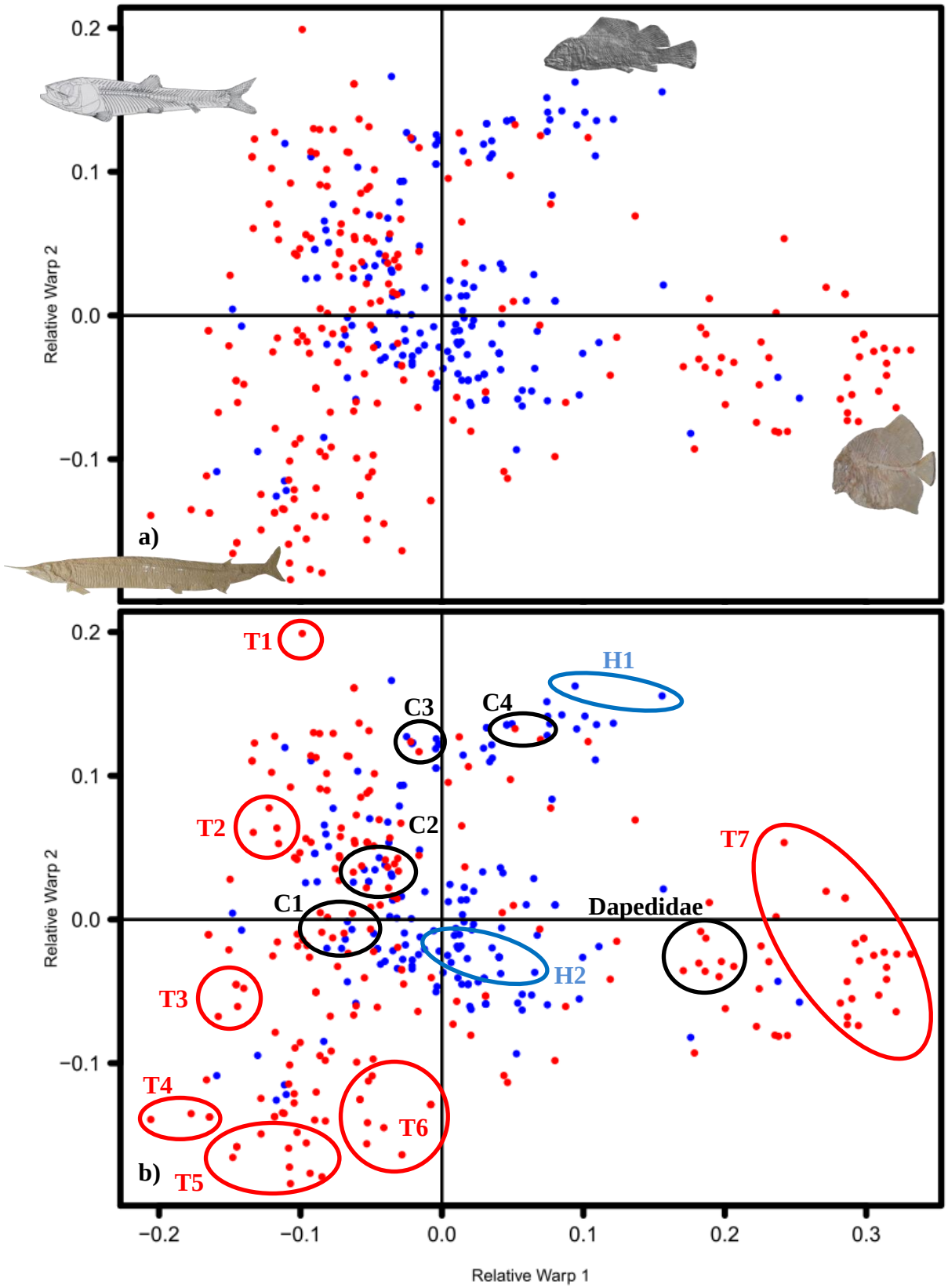

Fig. 3.10. A morphospace of relative warp axes 1 and 2 for the full dataset of 356 species, with holosteans denoted in blue, and teleosts in red. **a)** Morphospace with extreme taxa figured. **b)** Particularly unique regions of teleost (T) and holostean (H) space are noted, as are regions with many convergent holostean and teleost forms (C). Taxa from these regions are figured in Fig. 3.12.

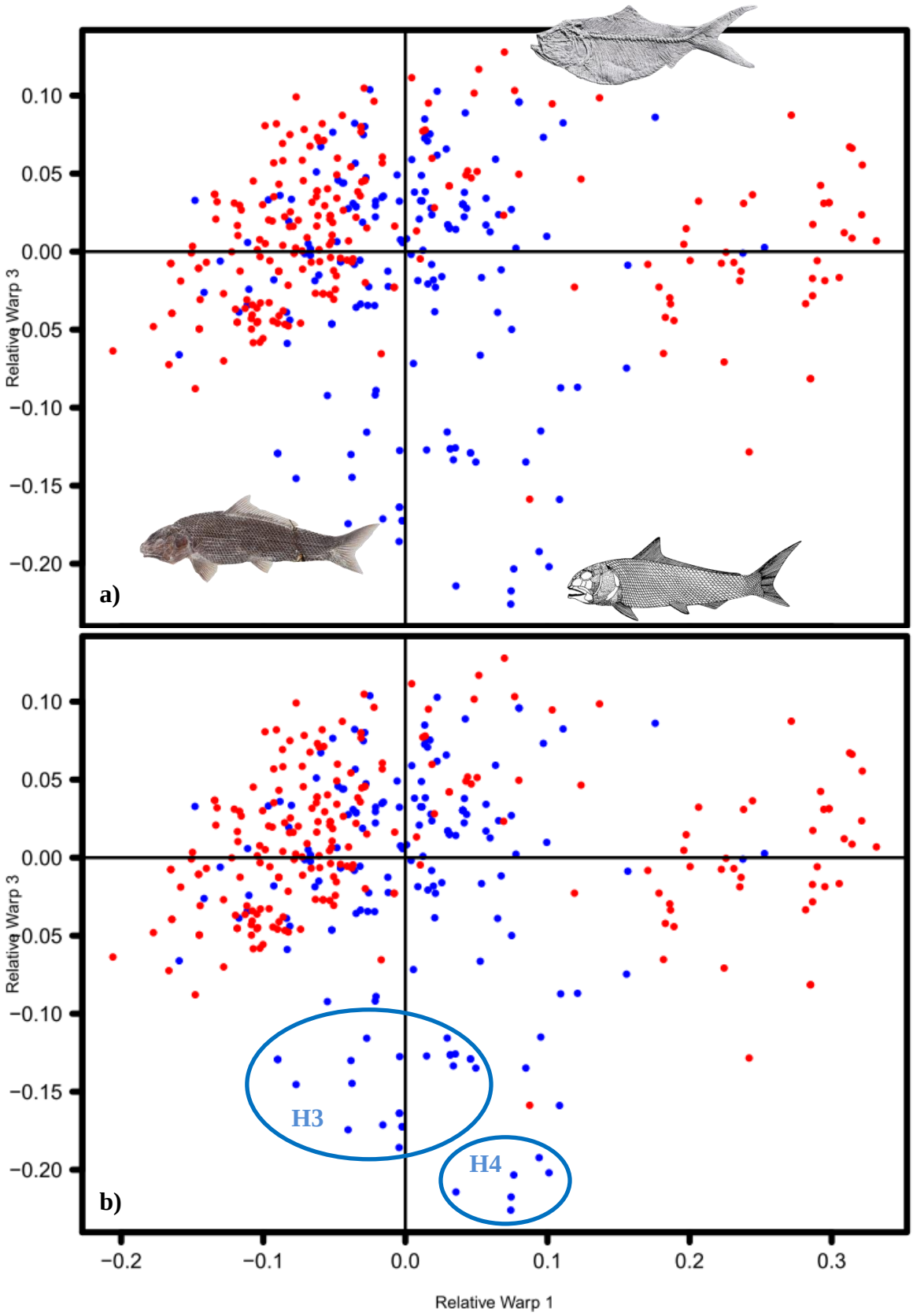

Fig. 3.11. A morphospace of relative warp axes 1 and 3 for the full dataset of 356 species, with holosteans denoted in blue, and teleosts in red. **a)** Morphospace with extreme taxa figured. **b)** Particularly unique regions of teleost (T) and holostean (H) space are noted, as are regions with many convergent holostean and teleost forms (C). Taxa from these regions are figured in Fig. 3.12.

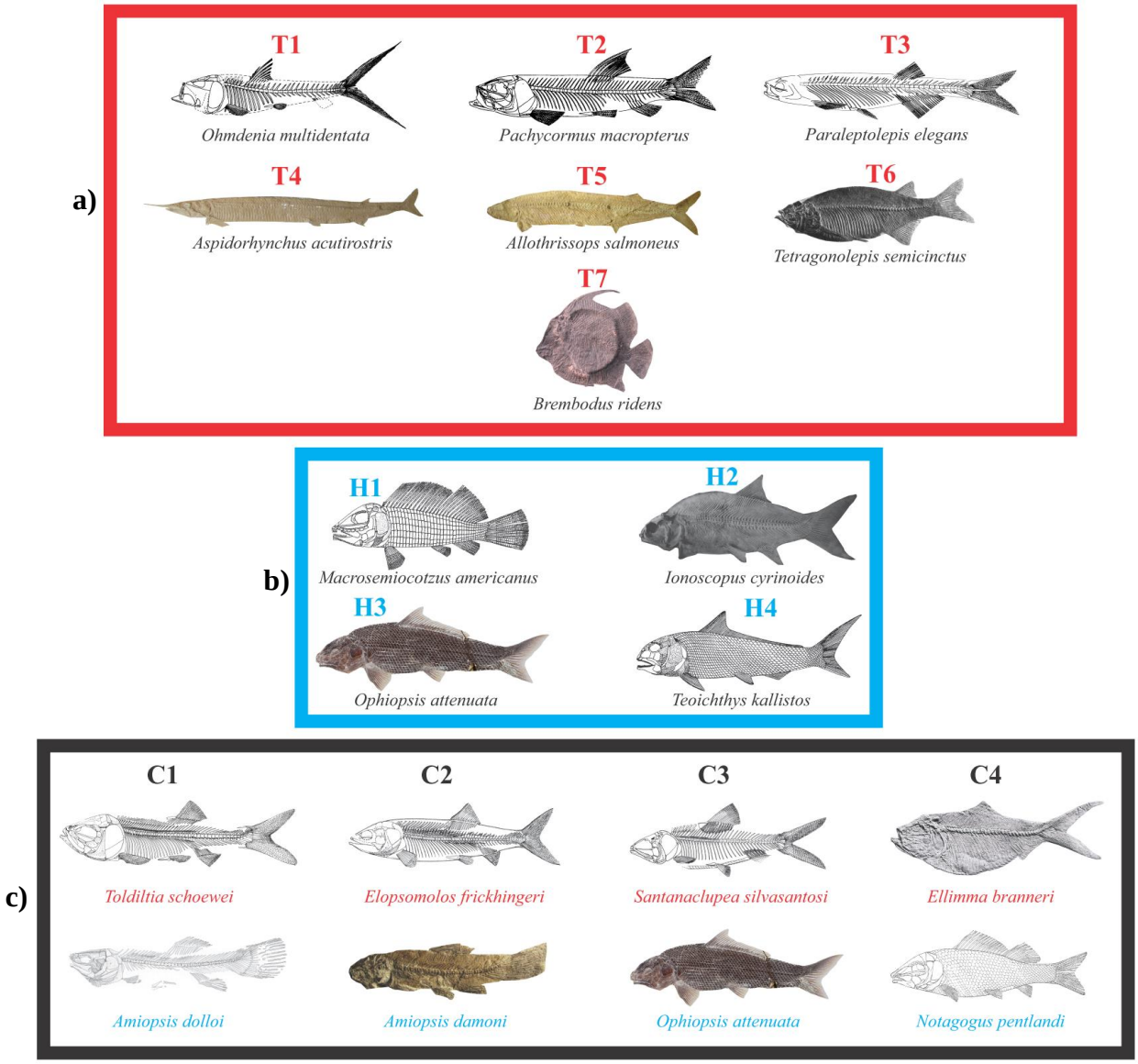

Fig. 3.12. Example taxa from regions of morphospace that are **a)** unique to teleosts. **b)** unique to holosteans and **c)** convergent between holosteans and teleosts. Numbers correspond to those regions identified in Fig. 13.10, 13.11.

iii) Unique regions of teleost and holostean functionspace

Holostean and teleost taxa are indicated within a functionspace of PC1-2 (**Fig. 3.13a**) and PC 3-4 (**Fig. 3.14a**). Teleosts represent the most extreme individuals on all four axes with the exception of the most positive value of PC2, which is a holostean. Teleosts also saturate six of the eight possible outer regions with respect to holosteans (PC1 < -3 and >3, PC2 <-3, PC3 < -1.25 and >1, PC4 >1), whereas holosteans saturate none. Specific regions of unique teleost and holostean morphospace are indicated in **Figures 3.13b and 3.14b** as T1-17 and H1-5 respectively. Examples of these regions are shown in **Fig. 3.15**.

iv) Convergent regions of teleost and holostean functionspace

Functional convergence is common as many holosteans and teleosts share many regions of functionspace (**Figs. 3.13a, 3.14a**), and particularly densely populated clusters are circled C1-C4 in **Figs. 3.13b, 3.14b**), and taxa from these regions are shown in **Fig. 3.15**.

v) Conclusions

1) Holosteans undoubtedly possessed a far greater variety of phenotypes in the past than they do in the Recent, suggesting that they were not always phenotypically conservative.

2) Despite the greater variety of holostean phenotypes in the Mesozoic, few of them appear particularly unique relative to teleosts. Whereas for most holostean phenotypes, there is a close teleost equivalent, the same cannot be said in reverse, since many more teleost phenotypes appear unique. There are numerous reasons why this might be the case, either due to greater teleost innovation, greater holostean constraint, or it could simply be the expectation under a null model of evolutionary change (see Future work). Chapter 5 examines some of these questions

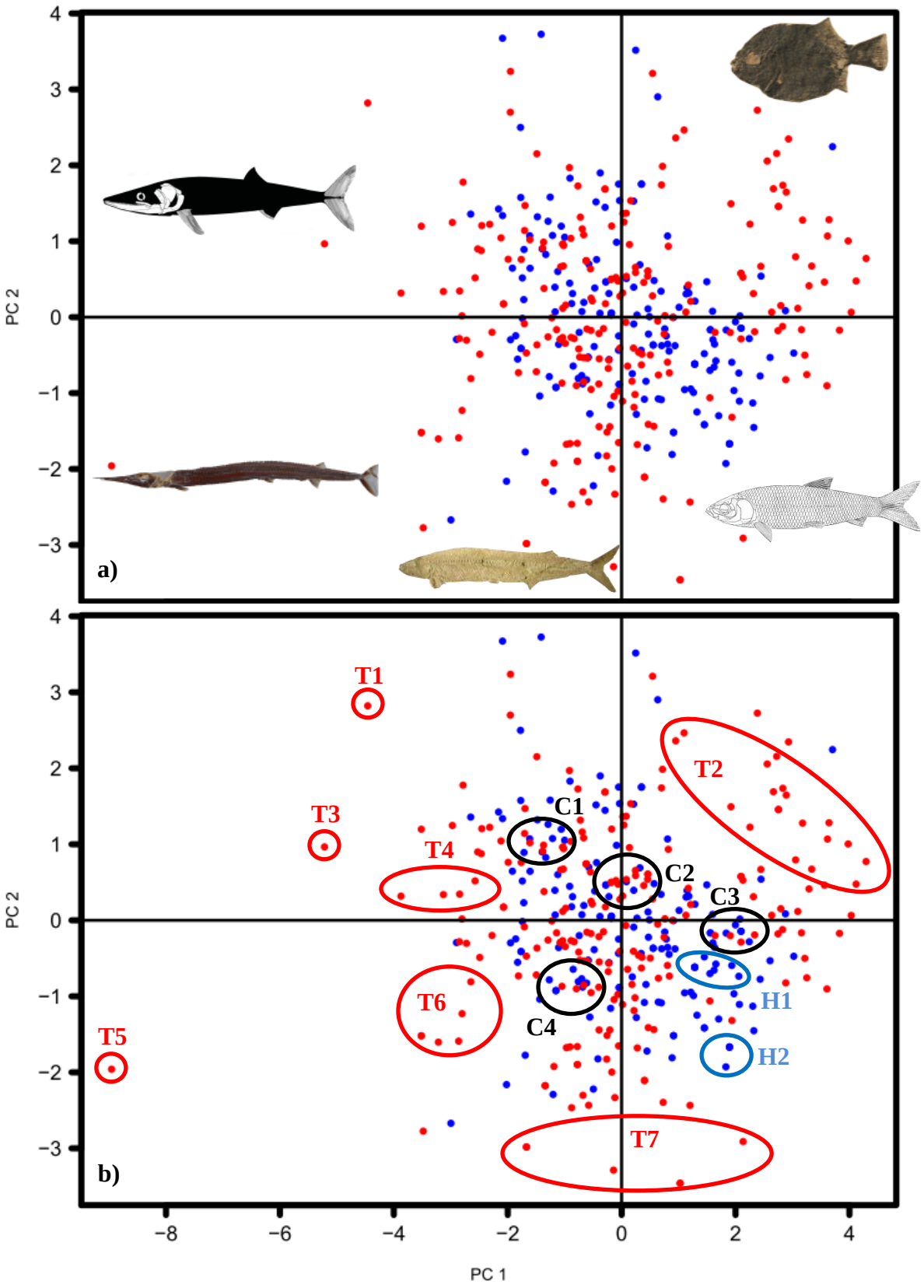

Fig. 3.13. A functionspace of principal component axes 1 and 2 for the full dataset of 356 species, with holosteans denoted in blue, and teleosts in red. **a)** Functionspace with extreme taxa figured. **b)** Particularly unique regions of teleost (T) and holostean (H) space are noted, as are regions with many convergent holostean and teleost forms (C). Taxa from these regions are figured in Fig. 3.15.

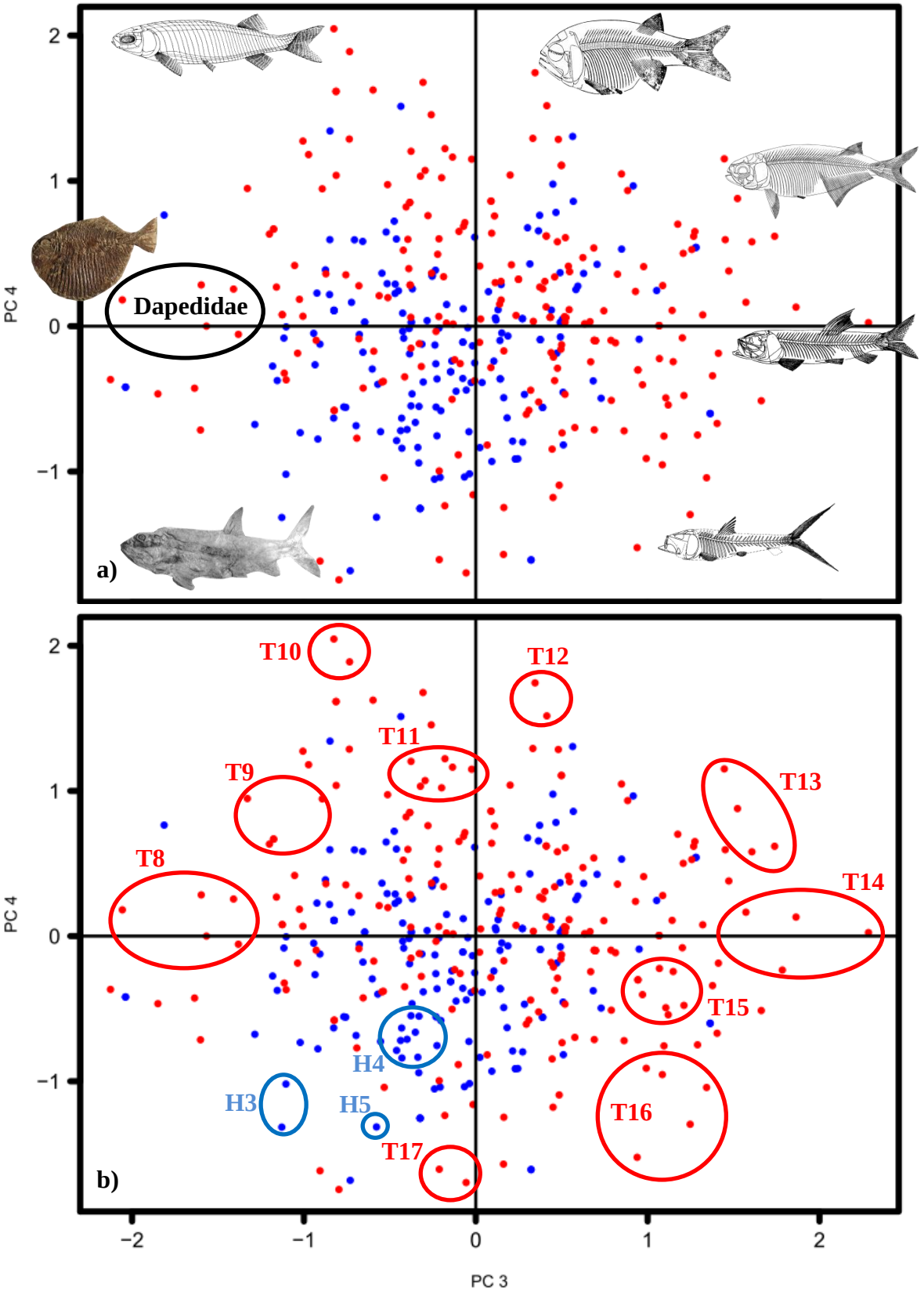

Fig. 3.14. A functionspace of principal component axes 3 and 4 for the full dataset of 356 species, with holosteans denoted in blue, and teleosts in red. **a)** Functionspace with extreme taxa shown. **b)** Particularly unique regions of teleost (T) and holostean (H) space are noted, as are regions with many convergent holostean and teleost forms (C). Taxa from these regions are figured in Fig. 3.15.

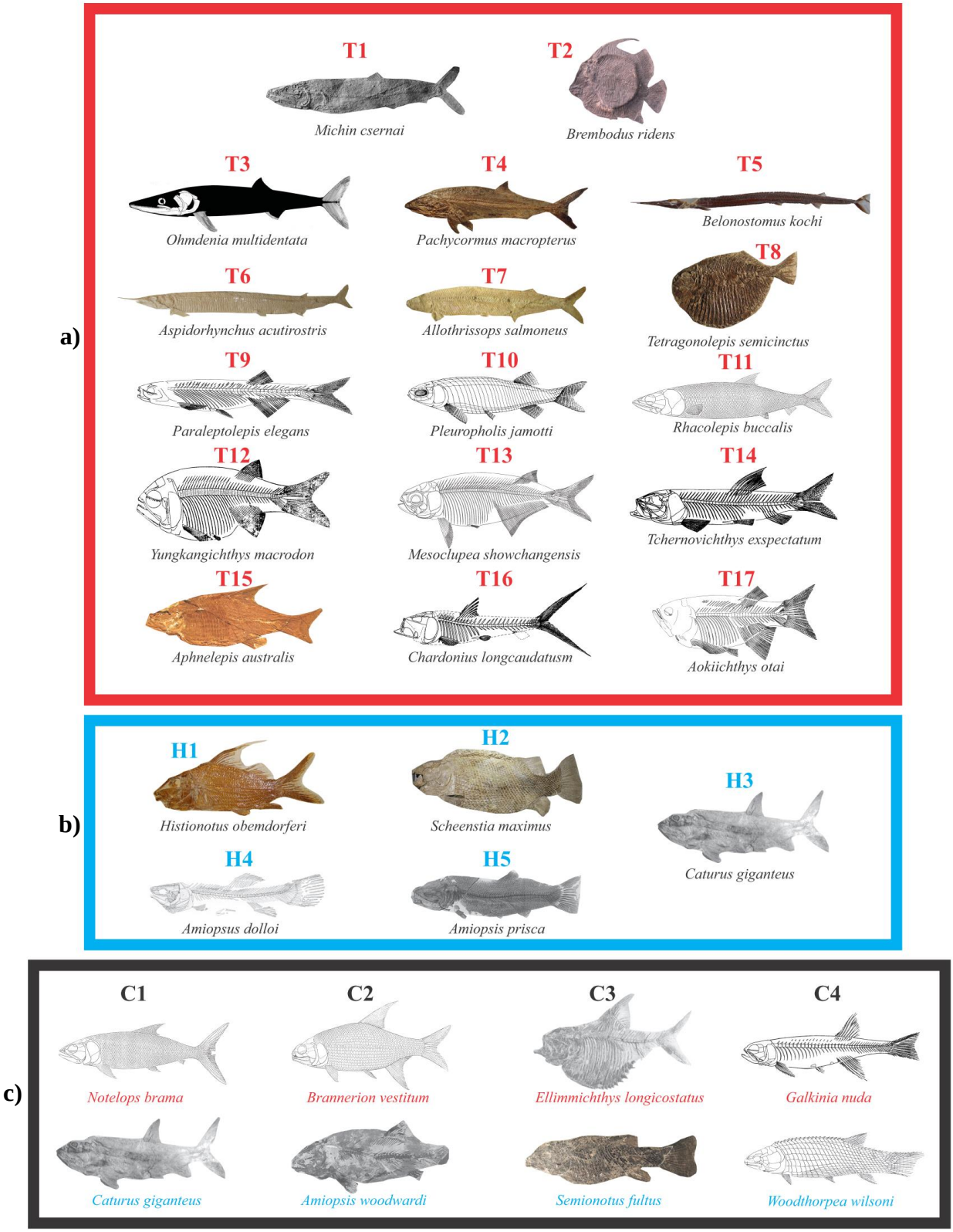

Fig. 3.15. Example taxa from regions of functionspace that are **a)** unique to teleosts. **b)** unique to holosteans and **c)** convergent between holosteans and teleosts. Numbers correspond to those regions identified in Fig. 13.13, 13.14.

by examining rates and innovation in holostean and teleost morphological traits in comparison with Brownian null models.

Future work – The signal that Mesozoic teleosts occupy considerably more unique regions of space appears strong enough to illustrate this point simply from observation of the ordination spaces alone, documenting the historical pattern. However, it would be beneficial to further quantify this relationship, and use distances between holosteans and teleosts to list all taxa from most unique to least unique in reference to a member of the other clade. This could also be applied to all neopterygian taxa individually, to investigate uniqueness more generally, outside of a clade comparison context. With such metrics in place, it would then be possible to derive these metrics from a null model and establish whether the degree of uniqueness (or convergence) observed might be expected under a null model, given the numbers of holostean and teleost taxa present and temporally scaled hypotheses of phylogeny (i.e. supertrees). Convergence has previously been examined in this way (Stayton 2008), and uniqueness would benefit from similar treatment. Such approaches could then be applied to a wide variety of clades to determine whether uniqueness is correlated with the abilities of a clade to innovate, or whether other drivers play a greater role. Such studies could also examine whether there is any real ecological significance to uniqueness, perhaps by defining a particularly unique ecology or whether these taxa have instead simply stumbled upon a rare solution to a common ecology. It could also be determined whether particular environments have a propensity to drive uniqueness, as they do for convergence (Price et al. 2014).

Q4.a The pattern of morphospace occupation through the Mesozoic.

Triassic (**Figs. 3.16, 3.17**) – The first Triassic bin is dominated by holosteans. These are centrally clustered, yet nearly all possess negative RW2 scores (**Fig. 3.16**). Interestingly, the

furthest lower left and lower right taxa represent two all-time extremes of holostean morphospace. The first (*Qingshania cercida*:Parasemionotiformes) is very gar-like in terms of body profile and fin position (but not in skull shape), a morphology that does not reappear until the Early Cretaceous. The second, a deep-bodied ginglymodian (*Kyphosichthys grandei*), occupies a fairly unique region of Mesozoic morphospace, rare not due to its deep body, but for possession of a dorsal fin which inserts more posteriorly than in most deep-bodied taxa. A few deep-bodied teleosts approach this morphology in the Late Jurassic, yet holosteans never regain this extreme. The second Triassic bin mainly contains holosteans, also clustered around the origin. This bin witnesses the first appearance of taxa with very long dorsal fin bases (*Besania*, *Guizhouamia*), a trait that does not reappear in such an extreme form until the Late Jurassic (**Fig. 3.17**). The Late Triassic, the first interval to contain numerous teleosts, witnesses a split between fusiform fishes and the first highly deep-bodied fishes, some of which are essentially circular in profile (e.g. *Brembodus ridens*).

Jurassic (**Figs. 3.16, 3.17**) – Regions of morphospace occupied by Early Jurassic neopterygians are essentially identical to those in the Late Triassic. Instead it is the second Jurassic bin which sees exploration of novel areas of morphospace, specifically the spread of taxa into the far left side, particularly in the lower left quadrant. This leftward expansion represents the proliferation of slender bodied forms (e.g. *Leptolepis antissiodorensis*, *Pleuropholis jamotti*), and amongst taxa in the lower left quadrant are the first ever neopterygians to possess anal fins that either insert at the same vertical position of the dorsal fin (e.g. the 'pholidophoriform' *Parapleuropholis olbrechtsi*), or, at the most extreme, insert more anteriorly than the dorsal fin (e.g. the pachycormid *Euthynotus incognitus*). The third Jurassic bin, which is poorly sampled in comparison to other bins, only shows taxa within previously explored regions of space, in dramatic contrast with the final Jurassic bin which

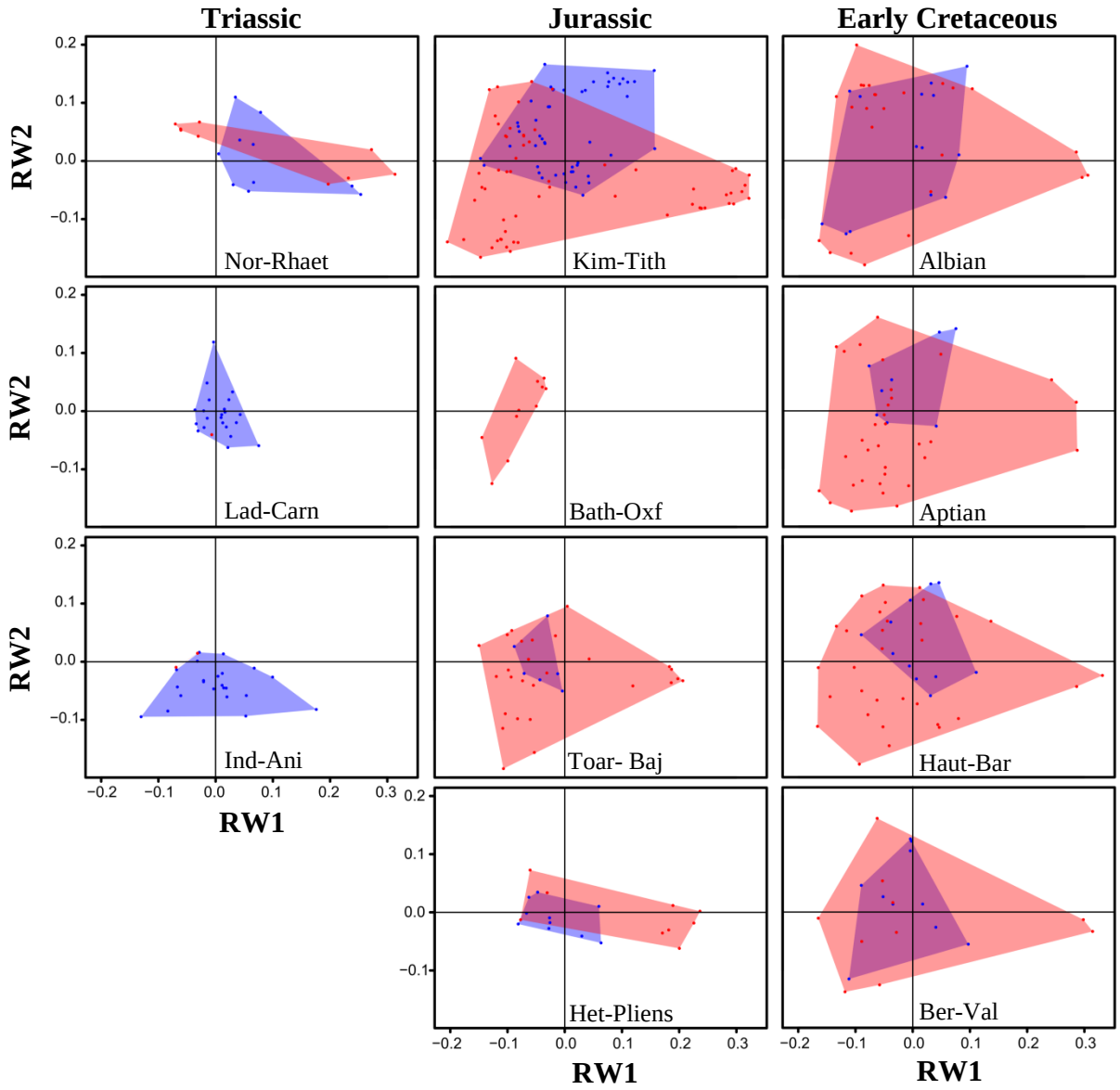

Fig. 3.16. Morphospace plots of relative warp axes 1 and 2 for the full dataset of 356 species divided over eleven Mesozoic time bins. Holosteans are denoted in blue, and teleosts in red, with convex hulls drawn for each.

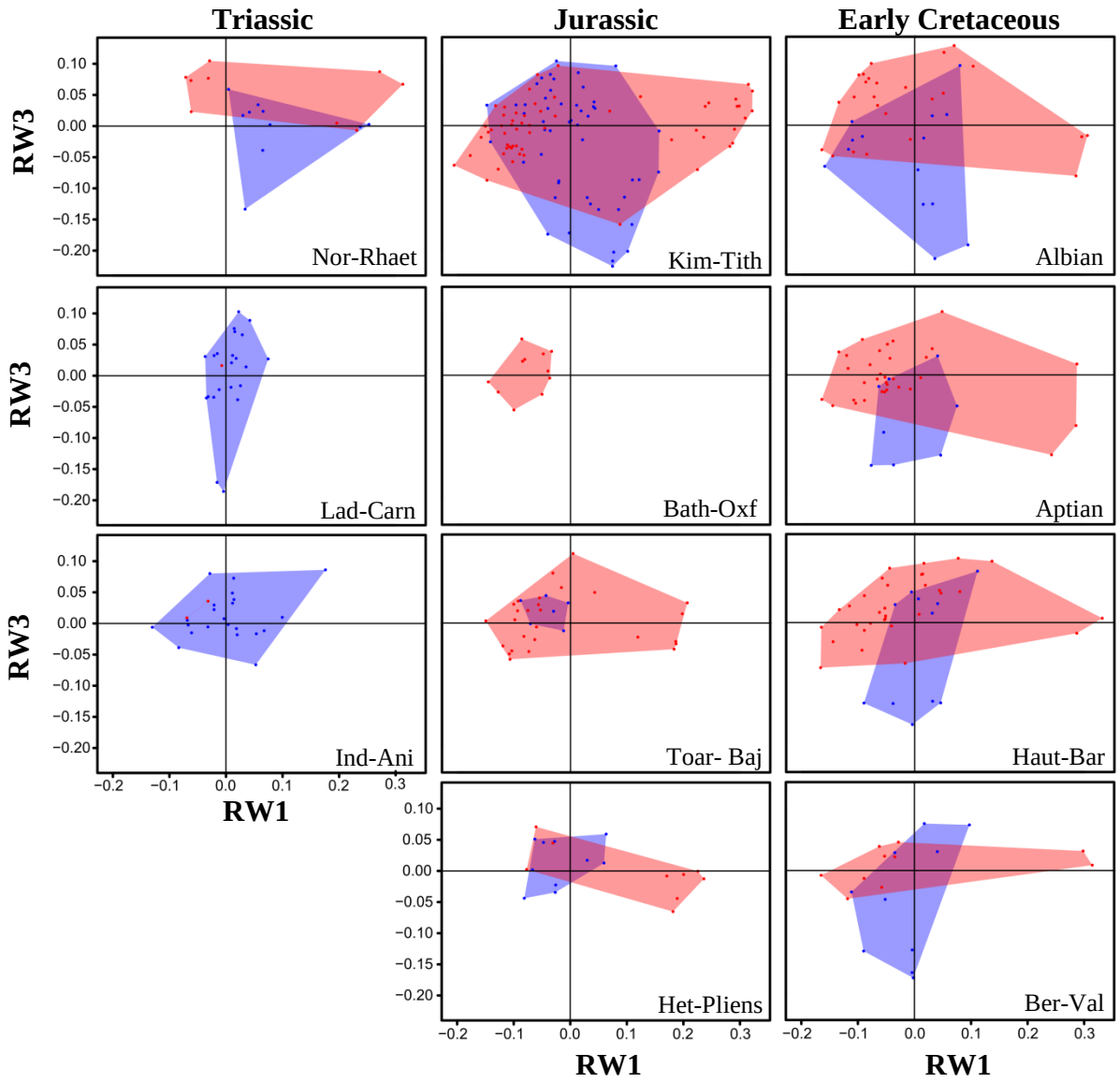

Fig. 3.17. Morphospace plots of relative warp axes 1 and 3 for the full dataset of 356 species divided over eleven Mesozoic time bins. Holosteans are denoted in blue, and teleosts in red, with convex hulls drawn for each.

sees the appearance of three novel areas of morphospace. One novel region is the further expansion into the lower left region, characterising highly elongate taxa with anal fins that insert more anteriorly than their dorsal fin (e.g. the apidorynchiform stem teleost *Belonostomus kochi*). The remaining two regions both share highly positive RW2 scores, plotting in the uppermost region of morphospace, and thus have dorsal fins that insert much closer to the head. The upper left combines this feature with an elongate body form (e.g. the euteleost *Orthogonikleithrus hoelli*), a region unique to teleosts in this bin, whereas the upper right is unique to holosteans, combining advanced dorsal fins with a deeper body form, typified by numerous Macrosemiiformes. Highly negative scores on RW3, representing a large dorsal fin base, also reappear in Late Jurassic holosteans and remain throughout the Early Cretaceous (**Fig. 3.17**).

Early Cretaceous (**Figs. 3.16, 3.17**) – Neopterygian taxa in this 50 million year period do not explore any particularly novel regions of space, largely adopting morphologies already seen in the Triassic and Jurassic. The pattern observed in the Late Jurassic, where teleosts occupy three extreme regions (top left, bottom left, far right), and holosteans occupy central regions with an upper extreme, is largely maintained across all Early Cretaceous bins, characterising a period of relative stability for holosteans, teleosts and neopterygians as a whole. There are, however, some subtle changes worthy of note. The first is the paucity of taxa with moderately positive RW1 values (0.1 – 0.025) sitting between the large density of taxa with negative scores on the left and the few highly deep-bodied taxa in the far right. This region was commonly occupied by both holosteans and teleosts in the Triassic and Jurassic, but is largely unexplored in the Early Cretaceous. Second, the lower left extreme of holostean morphospace seen in the Early Triassic returns in the Early Cretaceous, in both the first and final bin. Finally, holosteans in the Albian develop an upper left extreme for the first time

independently in two halecomorph genera (*Calamopleurus* [Amiidae] and *Teoichthys* [Ionoscopiformes]), invading what was previously a teleost specific region of space. This results in a situation where Albian holosteans express all but one (lower right) of their historical extremes simultaneously, an observation that runs contrary to notions of dwindling morphological variety in holosteans with over time.

Additional observations

Retaining extremes – All four extreme regions of relative warp 1 vs 2 morphospace (top left, bottom left, top right bottom right) are retained for the rest of the time series after their appearance, suggesting that extreme morphologies in this dataset become well-established and are relatively robust to the variability of fossil record sampling. Teleosts are represented in three of these extremes, and therefore teleosts are characterised by an ability to retain the extremities of their morphospace after their first appearance. The same applies to the fourth teleost (but not overall neopterygian) upper right extreme, which appears in the second Early Cretaceous bin and is maintained in subsequent bins. Holosteans, by contrast, frequently gain and lose regions of morphospace, especially extreme regions. This may be related to the low density of taxa within holostean extreme regions, since the single extreme region they do populate densely (i.e. the upper right excursion in the Late Jurassic) is retained.

Persistently occupied regions – Perhaps unsurprisingly, the regions surrounding the origin of morphospace are occupied in every time bin, suggesting it is not only common, but must be well-represented in a number of different depositional environments. More surprisingly, this region is almost entirely populated by holosteans; only a handful of teleost morphologies approach the origin.

Shifts in morphospace occupation – The positioning of taxa along relative warp 1 undergoes some dramatic shifts across the Mesozoic. Neopterygians are fairly evenly spread either side of zero on RW1 in the Early and Middle Triassic, before a shift to the right occurs (to positive RW1 scores) in the Late Triassic (**Fig. 3.16**). In the Early Jurassic, an even spread returns, yet in the second Jurassic bin, the vast majority of taxa have negative RW1 scores, and from this point onwards, a majority of taxa in every time bin have negative RW1 scores (i.e. more slender body shapes).

Notable absences – The first axis of morphospace establishes the dichotomy between slender (negative RW1 scores) and deep-bodied (positive RW1 scores) body plans. However, holosteans lose their deep-bodied forms during the Mesozoic. If Dapedidae are teleosts, this occurs after the Late Triassic. However, if Dapedidae are holosteans, this occurs after the Late Jurassic. A second observation is that the third bin of the Jurassic, which is the most poorly sampled time bin of the dataset, appears to selectively lack deep and semi deep-bodied taxa, even though range data predicts the presence of these forms during this interval (e.g. Pycnodontiformes). Holosteans, which typically possess semi deep-bodied forms, are therefore completely absent (in terms of articulated specimens) within this time bin.

Q4.b The pattern of functionspace occupation through the Mesozoic.

Triassic (**Fig. 3.18**) – Functionspace in the Early and Middle Triassic is dominated by holosteans clustered centrally, yet mainly within the upper half of the ordination (**Fig. 3.18**). However, there are some outliers which mark the first appearance of holosteans (two species of *Eoeugnathus*) and a teleost (*Eopholidophorus ceresiensis*) in the uppermost central region of morphospace, characterised by large jaws and eyes relative to their body length. Most notably, the Triassic witnesses exploration of the upper right regions of functionspace,

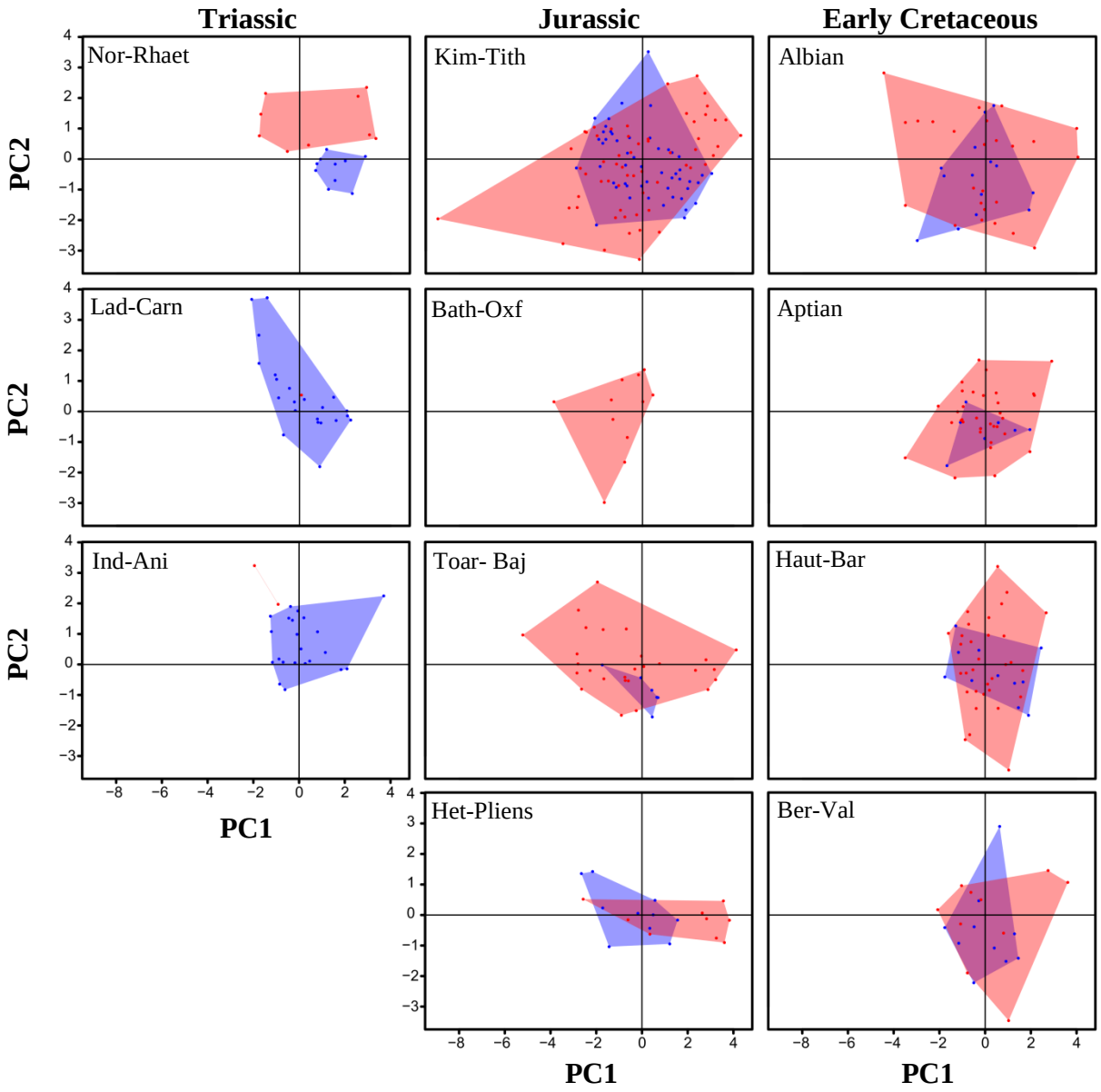

Fig. 3.18. Functionspace plots of principal component axes 1 and 2 for the full dataset of 356 species divided over eleven Mesozoic time bins. Holosteans are denoted in blue, and teleosts in red, with convex hulls drawn for each.

marking the appearance of highly deep-bodied fishes with large mechanical advantages of jaw closing and relatively large eyes. One deep-bodied form appears in the first Triassic bin, the ginglymodian (*Kyphosichthys grandei*), but most deep-bodied taxa make their first appearance in the Late Triassic. In addition, there is zero overlap between holostean and teleost PC1 vs PC2 functionspace in the Late Triassic.

Jurassic (**Fig. 3.18**) – Neopterygians in the first Jurassic time bin explore no new areas of functionspace compared with the Triassic, but the second Jurassic bin sees the reoccupation of the upper left region of morphospace that was commonly occupied in the Middle and Late Triassic (**Fig. 3.18)**. The taxa to the far left are characterised by more elongate jaws and slender bodies, some with large jaws relative to their length (e.g. *Ohmdenia multidentata*). The third Jurassic bin captures the appearance of the first taxa to venture into the bottom of the functionspace, again teleosts, characterised by small eyes and small jaws relative to body length with elongate bodies (e.g. *Occithrissops willsoni*). The Late Jurassic sees further expansion in the bottom left, bottom right, and top right quadrants of functionspace. The lower left quadrant contains taxa with even smaller eyes and jaws relative to body size and some of the more slender bodies, an extreme example of which is the teleost *Belonostomus kochi*. The bottom right quadrant expansion contains taxa with some of the largest mechanical advantages of jaw-closing, yet with small jaws relative to their overall length (**Fig. 3.6b,f**). This region is dominated by stem gars, including representatives of the Macrosemiiformes, and lone genera such as *Lepiodotes*, *Scheenstia* and *Callipurbeckia*. The top right expansion is purely a teleost one; all are pycondont taxa characterised by the smallest body aspect ratios, largest eyes relative to body length, and amongst the largest mechanical advantages of jaw opening and closing (**Fig. 3.6b-e**).

Early Cretaceous (**Fig. 3.18**) – No drastically new regions of functionspace are explored in the Early Cretaceous. The pattern of functional space occupation appears relatively stable compared to the Triassic and Jurassic, with taxa clustered around the origin and comparable numbers of taxa in each quadrant. The final time bin (Albian) is similar in overall pattern, but with a larger overall morphospace, representing the first time that all four quadrants are well explored simultaneously. Thus, it appears that taxa in the Albian were more functionally different from one another that at any previous time in the Mesozoic.

Additional observations

Retaining extremes – Extremes of holostean, teleost, and neopterygian functionspace are rarely retained after their initial discovery (although some are re-explored in a later time slice). This contrasts with the morphological pattern, in which extremes are often retained, and suggests that morphological extremes do not translate directly to functional extremes, but instead contain considerable functional variety.

Persistently occupied regions – Within the upper left quadrant of functionspace, a region close to the origin of functionspace is occupied in every time slice, some parts of which see high convergence between holosteans and teleosts (Q3). This region characterises taxa with small mechanical advantage of jaw-closing and with large jaws relative to their body length (**Fig. 3.6b,f**). These functional traits therefore appear common, relatively unaffected by variations in sampling and depositional environment over the Mesozoic.

Shifts in morphospace occupation –Shifts in either of the first two axes of functionspace are not as clearly apparent as for morphospace axes. Instead, functional axes appear more symmetrically occupied in most time bins. The one exception appears to be the absence of

taxa with positive PC1 scores in the third bin of the Jurassic (Bathonian-Oxfordian), due to the absence of articulated deep-bodied taxa, resulting in a shift to negative scores in PC1 (**Fig. 3.18**).

Notable absences – As discussed for morphospace, holosteans lose their deep-bodied forms in the Mesozoic, which corresponds to a cluster of low aspect ratio taxa with high jaw-closing mechanical advantages, and the assignment of Dapedidae determines when they are lost. Also discussed above is the absence of deep and semi deep-bodied articulated forms from the third Jurassic bin (**Fig. 3.18**).

Future work – The intention here was to highlight some of the pertinent features of neopterygian ordination space occupation across the Triassic, Jurassic and Early Cretaceous. Numerous metrics could be derived to further examine these patterns, although they would offer far more interesting insights if they were applied to a wide variety of clades simultaneously, rather than simply the three clades examined here. Two themes for further examination are: 1) Early unique morphologies. Many studies have discussed the notion of early high disparity (see Q2 in Chapter 4), but less effort has been made to quantify whether morphologies (including function) obtained by clades early in their history tend to be fundamentally different to those that arise later in their histories. For example, are most regions of space examined relatively early on, with later taxa revisiting previously established designs, or is it more common that clades keep discovering and expanding their overall ordination space with time? Another consideration is whether the first half of a clade's history delivers more all-time unique morphologies than the second half of their history. 2) Shifting of morphospace through time. How do clades move around ordination space over time? Are earlier time periods characterised by greater shifting of the ordinations centroid earlier in their

history, before becoming stable later in their history, and is the functional centroid through time more or less stable than the morphological centroid? Also, how common is it for multiple clades to exhibit shifts in their morphospace occupation in the same periods of geological time, and how many exhibit directional trends in their centroid over time? Null models should also be examined to determine the probability that any of these phenomena might occur by chance.

Q5. Do holosteans become crowded out by teleosts in morphological or functional space?

The scenario that teleosts swamped holosteans in ecological space through time, driving a holostean decline through competition, is compatible with two scenarios regarding nearest neighbour distances. The first is to observe declining distances through time between holosteans and their closest teleost in ordination space, as evidence that teleosts are increasingly encroaching upon holostean regions of space. The second is to observe increases in distances through time between holosteans and their closest teleost in ordination space, expected if teleosts drove ecologically comparable holosteans to extinction, leaving only a few exclusively holostean regions of space ('safe havens') that teleosts failed to swamp. Examination of ordination spaces should help determine which scenario, if any, is most likely. These tests for evidence of a changing relationship between holostean and teleost distances are considered below. I pay only minor attention to Early and Middle Triassic patterns, as teleosts are too rare to provide adequate comparison of distances with other Mesozoic bins, and do not discuss the third Jurassic bin, in which poor sampling prevents calculation of distances.

i) Morphological holostean and teleost distances

Nearest neighbour distances for holosteans (distance to closest teleost) are stable for the majority of the Mesozoic (**Fig. 3.19a**). Although slightly lowered values are observed in the first two Jurassic time bins, this pattern assumes that Dapedidae are teleosts, and disappears under the alternative holostean interpretation. Relative stability indicates holosteans were on average no closer to a teleost morphology later in the Mesozoic than they were early in the Mesozoic, rejecting the notion that teleosts consistently encroached upon holostean regions of morphospace through time.

Nearest neighbour distances for teleosts (distance to closest holostean) increase throughout the Triassic until the Early Jurassic, after which time their mean remains relatively stable (**Fig. 3.19b**). This reflects the observation that the first fossil teleosts are morphologically similar to holosteans, yet as they continued to explore morphospace, they also occupied regions further away from holosteans, increasing nearest neighbour distances. These observations are corroborated by morphospace plots (**Fig. 3.16**).

Average distances between holosteans and teleosts, regardless of the direction of comparison (i.e. holosteans to teleosts, or teleosts to holosteans, **Fig. 3.20**), are lowest in the Early and Middle Triassic, increase in the Late Triassic and stabilise until another increase occurs in the Late Jurassic, after which time distances remain stable (**Fig. 3.20**). Comparison of these trajectories with the nearest neighbour trajectories highlights that it was possible for teleost and holostean individuals to become increasingly different on average, whilst maintaining similar distances to a nearest neighbour (note the Late Jurassic increase in mean distances, but stability in nearest neighbour distances). Part of the explanation for this pattern is that, from the Late Jurassic onwards, holostean and teleost morphospace is larger than at any previous time (reflected in greater disparity, see Chapter 4), and so greater average distances would be

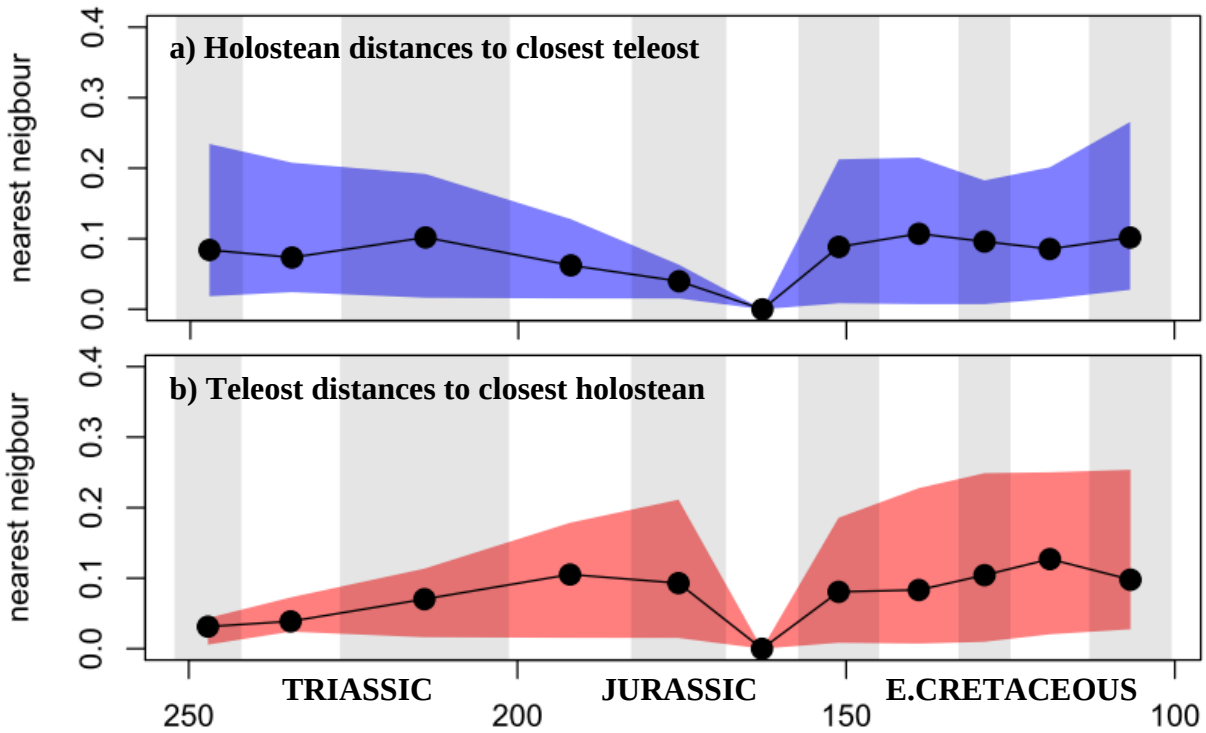

Fig. 3.19. The distribution of nearest neighbour distances in morphological space across eleven Mesozoic time bins between **a)** every holostean species to its closest teleost and **b)** every teleost species to its closest holostean. The mean distance and 95% confidence limits are presented for each bin.

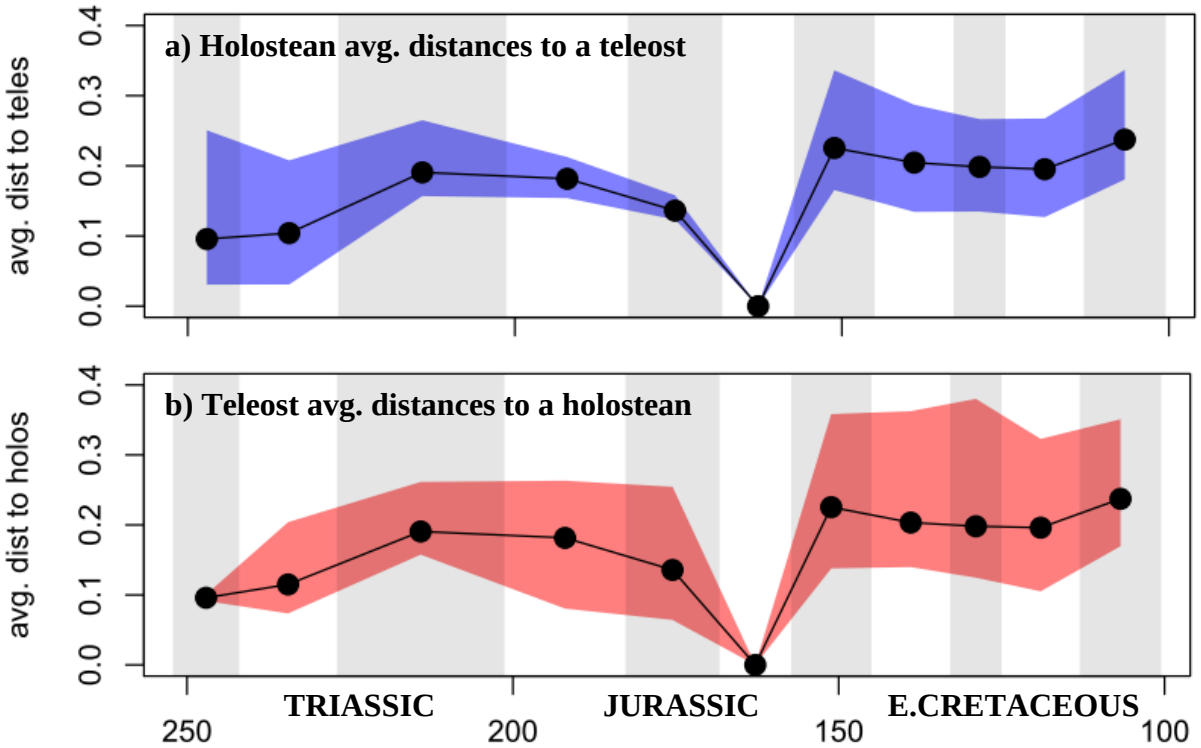

Fig. 3.20. Morphological space average distances between **a)** holosteans and all teleosts and **b)** teleosts and all holosteans.

expected as taxa are spread throughout a larger space. Furthermore, extreme regions of teleost morphospace, apparent from the Late Jurassic onwards (Q3 in Chapter 4), also appear to increase average distances, reflected in the larger upper confidence intervals of teleosts compared with holosteans from the Late Jurassic (**Fig. 3.20**). With expanded teleost extremes, nearest neighbour distances can be maintained at previous levels in three broad ways: 1) the concentration of non-extreme teleost taxa in holostean regions. 2) the occasional excursion of holostean taxa into teleost extreme regions. 3) a low density of teleost taxa at extremes. Examination of morphospace plots reveals that all three are relevant, sometimes in combination within the same bin (**Fig. 3.16**).

ii) Functional holostean and teleost distances

Nearest neighbour distances for holosteans (distance to closest teleost) are largest in the Early and Middle Triassic, before falling in the Late Triassic, and remaining relatively stable thereafter. However, even within that relative stability, the mean nearest neighbour distances from the Middle Jurassic onwards appear marginally lower than Late Triassic and Early Jurassic values (**Fig. 3.21a**). In addition, the lower confidence limits from the Late Jurassic onwards fall to their lowest point, indicating the presence of holosteans through this period that are closer to a teleost than any previous time. However, any signal for a decline appears incredibly weak given that these marginally smaller mean nearest neighbour values from the Late Jurassic onwards fall well inside the confidence intervals of previous time bins, therefore I cannot reject that nearest neighbour distances remain stable.

Nearest neighbour distances for teleosts (distance to closest holostean) echoes the holostean pattern, showing relative stability from the Late Triassic onwards (**Fig. 3.21b**). Yet again, the mean distances and lower confidence interval of Late Jurassic-Early Cretaceous appear

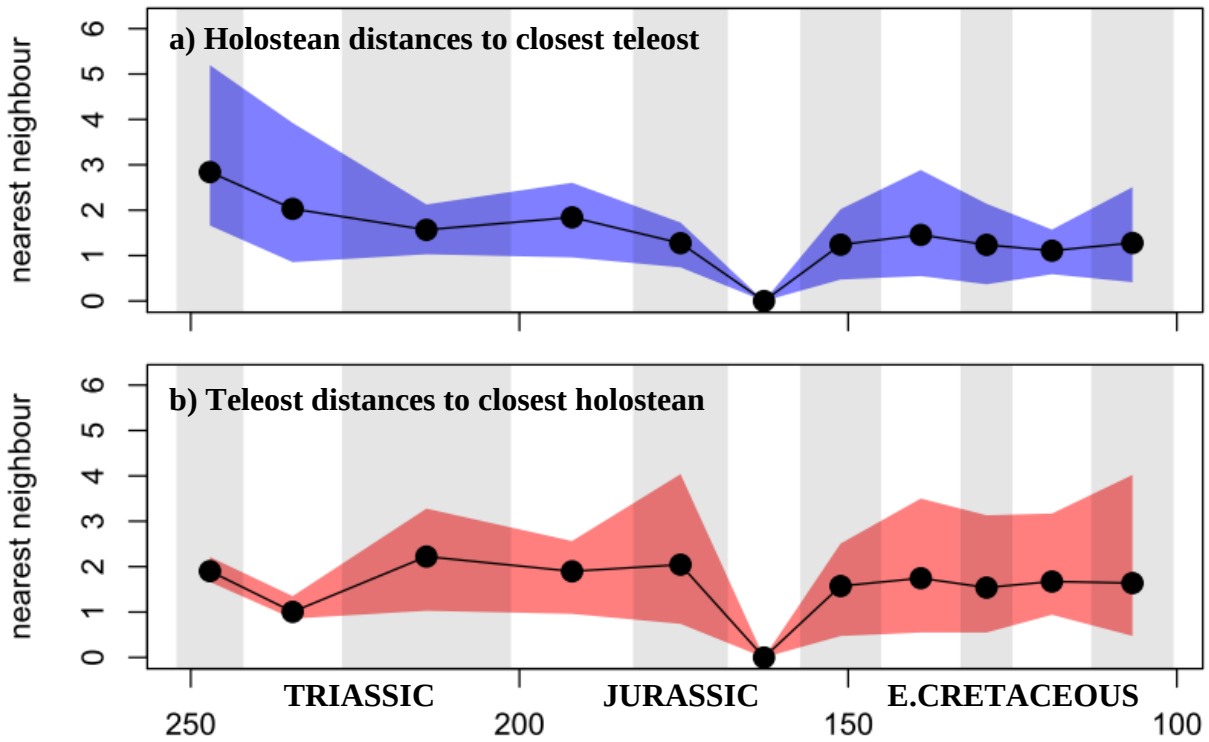

Fig. 3.21. Functional space nearest neighbour distances between **a)** holosteans to closest teleost and **b)** teleosts to closest holostean.

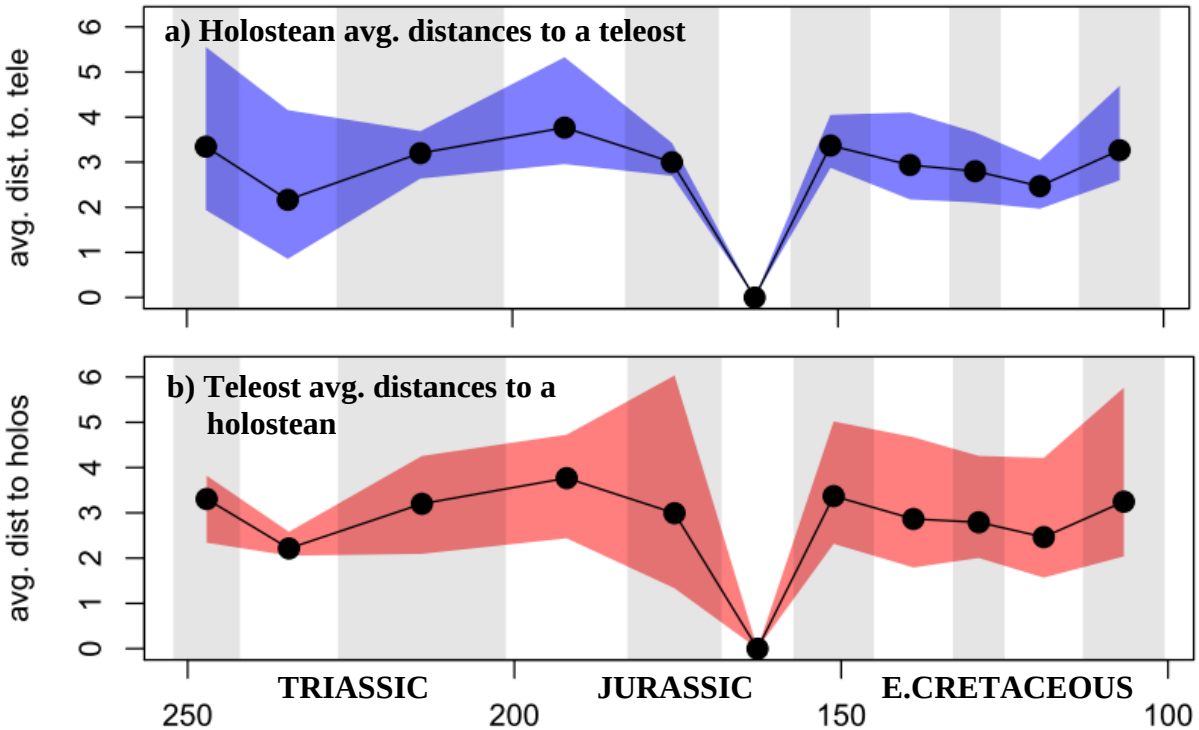

Fig. 3.22. Functional space average distances between **a)** holosteans and all teleosts and **b)** teleosts and all holosteans.

marginally lower than Late Triassic-Middle Jurassic distances. Once again these lowered values fall comfortably inside the confidence intervals of previous time bins, therefore stability cannot be rejected.

Average distances between holosteans and teleosts, regardless of the direction of comparison (**Fig. 3.22**), indicate relative stability from the Late Triassic onwards. Under these circumstances, additional explanations for why nearest neighbour distances also remain stable are not required (unlike for morphology, see points 1, 2 and 3 above). The stability in average distances between holosteans and teleosts reflects the lack of expansion in functionspace, as space occupancy remains comparable for much of the Mesozoic. Teleosts also fail to occupy extremes that are distant from holosteans, as they do in morphology, reflected in the absence of inflated upper confidence intervals from the Late Jurassic onwards (**Fig. 3.20b** *versus* **Fig. 3.22b**).

iii) Conclusions

The primary analysis of interest regarding the nearest neighbour distances of each holostean to its closest teleost in morphospace and functionspace reveals no fundamental change in this relationship through the Mesozoic (although subtle, non-significant trends for smaller distances through time are apparent in function). Thus, there is no clear signal supporting either the encroachment of teleosts upon holostean space, or the expansion of holosteans into remote, teleost free regions of space.

An unchanging relationship in nearest neighbour distances could imply highly contrasting scenarios regarding the nature of interactions between holosteans and teleosts. Under the assumption that morphospace and functional space are ecologically informative, it could

imply that holosteans were consistently in close contact with teleosts over the Mesozoic, with sustained potential for competitive interactions, or that holosteans were consistently distant from teleosts, relatively free from even the potential of competitive interactions. Visual inspection of the morphospace and functional spaces, and the values underlying them, would tentatively support the former interpretation, as many holostean taxa appear to have very close teleost analogues, but such observations are speculative, and do not account for geography, rock type, or the specific age of deposits within time bins, which could still be separated by millions of years. Whatever the case, the data presented here does not conform to the predictions of a competitive replacement of holosteans by teleosts.

There is, however, one facet of the competitive replacement that exploits the fragility of the relationship between morphology, function and ecology, which could render my results compatible with replacement. This facet concerns discussions of 'efficiency', the idea that teleosts did not simply crowd holostean phenotypic space, but were somehow more efficient, possessing adaptations that gave them a competitive advantage. Such adaptations may, for the same region of ecospace as a holostean, deliver new body forms, jaw mechanisms or body proportions, all of which would distance the teleosts concerned from holosteans in morphological and functional space. A clear example of this can be seen amongst living taxa, where competitive interactions can still occur between taxa of different sizes, where the smaller, invasive species has the advantage (Britton et al. 2007). Thus, a non-changing relationship between holosteans and teleosts in morphology and function space could easily be reconciled with competition. Therefore clearer information regarding how morphology and function relate to ecology is required.

Future work – Additional work examining the potential for competitive interactions between holosteans and teleosts, or indeed, between any other clades of organisms, should seek to develop further metrics to capture their proximities in ordination space, perhaps incorporating both the density and the distance of nearest neighbours. Geographical, temporal and environmental considerations could also be taken into account. However, the main advances will come from quantifying these metrics for living species in instances where the effects of competition are clear, such as for invasive species. These case studies will help identify the ecological correlates that are most important for competition, and will hopefully deliver the most appropriate morphological and functional proxies for these ecologies. Abundance is also an important factor in competition (Britton et al. 2007), and efforts could be made to incorporate abundance information into any search for potential ecological interactions in the fossil record. While we wait for a clearer picture to emerge, another avenue is to focus on fewer traits that may be more closely tied to resources (e.g. absolute jaw length). Competition need not be the only factor, as many of the Mesozoic neopterygians appear piscivorus, and so predation may play an important role. Either way, it will be difficult if not impossible to truly confirm biological interactions in the majority of fossil species, therefore even with better proxies, the methods will likely be most effective at rejecting the potential for interactions, rather than seeking to confirm them.

Chapter Summary

Q1. Axes of variation

1. Four axes of morphological shape variation explained more than 5% of the variance in the dataset, although the forth relative warp appeared to characterise post-mortem ventral-dorsal flexion, and was discarded. RW1 (42.53%) captures changes from slender bodied taxa to

deep-bodied taxa, RW2 (21.43%) captures the position of the dorsal fin relative to the anal fin, and RW3 (13.52%) captures variation in the length of the dorsal fin base.

2. Five axes of functional trait variation accounted for more than 5% of the variance in the dataset. Positive PC1 (50.37%) scores are associated with small aspect ratio bodies and jaws, with large jaw-closing and jaw-opening mechanical advantages and larger eyes relative to their body length. Negative PC1 scores are associated with the inverse of these traits. Positive PC2 (24.3%) scores reflect taxa with large eyes and jaws relative to their body length, and negative scores capture the opposite. Positive PC3 (9.37%) scores highlight taxa with large jaw-closing MAs but small jaw-opening MAs, and negative scores the opposite. Positive PC4 (7.7%) scores capture characterise taxa with small eyes yet long jaws, both relative to body length, and negative scores the opposite. Positive PC5 scores (5.3%) bear very weak correlations to traits, but should characterise taxa with some combination of the following traits: slender bodies, moderately large opening-MAs, and relatively large eyes. Negative scores show the opposite. Correlations between traits and axes are much weaker on lower axes, so the functional correlates outlined above are not perfectly captured along axes, but characterise a general trend, even if numerous taxa deviate from it.

Q2. To what extent does the morphospace reflect functional space?

1. Correlations were performed between morphological and functional axes. The main axis of morphological variation correlated well with the main axis of functional variation. This acts to establish the functional correlates of morphological change, where deep-bodied taxa possess heavier jaws with large jaw-closing and opening MAs, and to a lesser extent, relatively large eyes and short jaws compared with body length. RW2 showed little correspondence to any functional axis, suggesting that the position of the dorsal fin relative to the anal fin is not

associated with a suite of functional changes. By contrast, RW3, capturing the length of the dorsal fin base, showed some weak correlation to PC2, suggesting that taxa with large dorsal fin bases tend to possess somewhat larger eyes and jaws relative to their body length, whereas those with shorter dorsal fin bases have somewhat smaller eyes and jaws relative to body length.

2. There was no correspondence between distances between taxa in morphospace and functionspace based upon a mantel test. Thus minimally, morphological (body shape) diversity and multivariate functional diversity (specifically, the 6 traits selected here) should not be inferred from one another. Examination of the distances also reveals extreme instances of decoupling, where similar functional taxa can be morphologically divergent and vice versa. Furthermore, an asymmetry is apparent, where it is more common for functionally similar taxa to show large morphological differences than morphologically similar taxa to express vast functional differences. Beyond many-to-one mapping, the structure of morphospace and functionspace may contribute to this finding.

Q3. How similar are Mesozoic teleosts and holosteans morphologically and functionally?

1. Throughout the phenotypic spaces, there are many instances of similarity between holosteans and teleosts, and some particularly densely populated areas are highlighted. However, whereas for most holostean phenotypes there is an analogous teleost phenotype, the same cannot be said in reverse. This is because teleosts occupy far more unique regions than holosteans in phenotypic space. Additional avenues for research are suggested.

Q4. What is the pattern of ordination space occupation through time?

1. Holosteans show two extreme morphologies in the Induan-Anisian, in the form of an elongate parasemionotid and a deep-bodied ginglymodian. Although the latter represents a deep-bodied taxon with high jaw-closing MA from the Anisian, it is not until the Norian that these phenotypes are common among neopterygians. The Toarcian to Bathonian represents the first appearance of slender morphologies with longer jaws relative to their body length. Many extreme regions of morphological and functional spaces are recovered in the Late Jurassic, and are mostly retained thereafter. Holosteans and teleosts possess most of their historically extreme phenotypes simultaneously at the very end of the Early Cretaceous (Albian).

2. Teleosts are good at retaining extreme morphologies once they evolve, although this pattern is less apparent in function. Holosteans by contrast often gain and loose extreme regions of morphological space. Extreme regions of morphological space, often forming dense clusters, appear to contain greater functional variety. As such, morphological extremes do not correspond well to functional extremes, and functional extremes are often gained and lost, rather than retained after discovery like morphology.

Q5. Do holosteans become crowded out by teleosts in morphological or functional space?

1. Nearest neighbour distances were used to examine whether teleosts became closer to holosteans on average throughout the Mesozoic in morphology and function. No clear change in nearest neighbour distances between holosteans and teleosts were apparent, in either morphology or function, throughout the time series.

2. Although these findings could be taken to reject a competitive replacement, it hinges on the assumption that either morphology or function are ecologically relevant, an assumption that is

difficult to test until ecological correlates of morphological and functional capabilities are quantified in a broad range of taxa in the Recent. This is of particular relevance to notions of teleosts replacing holosteans, where teleosts innovations are proposed to have made them more 'efficient' than holosteans. Under this scenario, taxa in different regions of morphological and functional space may exhibit strong competition, reemphasising the need for ecological correlates to be established.

Chapter 4
Patterns of morphological and functional disparity in Mesozoic neopterygians

Introduction

Chapter 3 documented morphological and functional variety in neopterygians for the first 150 million years of their history. This chapter aims to use that information to quantify morphological and functional diversity (=disparity) through eleven Mesozoic time bins to reveal changing patterns over time, and use this information to address a series of evolutionary questions. Examination of disparity through time is commonplace in palaeontology (Foote 1997, Ruta et al. 2013, Gerber 2013, Hopkins 2014), providing an additional means to quantify biological variety beyond taxonomic richness. Furthermore, disparity offers some clear sampling advantages over species counts, since similar morphologies/functions are often shared by large numbers of species. However, disparity does not merely represent an alternative, comparable metric to richness, but instead allows researchers to ask different kinds of evolutionary questions that pertain specifically to the evolution of form, function and ecology. As such, disparity has been successfully employed to tackle a broad variety of questions (see Foote 1997 for a review), such as highlighting extinction selectivity (Churchill 1996, Friedman 2009), defining adaptive radiations (Sundberg 1996, Jernvall et al. 1996, Foote 1997), and revealing instances where clades rapidly fill recently vacated regions of morphological space (Friedman 2010). However, the vast majority of disparity studies to date focus upon morphological disparity, rather than a specific set of functional traits, yet the completeness of neopterygian material allows

collection of both, providing a rare opportunity to examine both form and function in a diverse clade over a long timescale.

The primary aim of this chapter is to use both morphological and functional disparity simply as measures of diversity. Neopterygian fishes exhibit huge morphological and functional variety in the Recent (see Chapter 1), and show a considerable variety of body shapes from the Late Cretaceous onwards (Friedman 2010). By quantifying disparity for the first 150 million years of the neopterygian radiation, I can document the pattern by which this disparity was assembled for the first 60% of the clade's history. Because numerous factors can influence patterns of disparity over time, I will interrogate this pattern with respect to uncertainty in taxonomy and fossil deposit ages and *Lagerstätten* effects. With the disparity trajectory for morphology and function in place for holosteans, teleosts and neopterygians as a whole, I then use this information to address the following five questions:

1) How do patterns of morphological and functional disparity compare?

The extent to which morphological and functional ordination axes covary, and whether distances between taxa in morphospace correspond to distances in functionspace, have already been discussed in Chapter 3. Here, I focus specifically upon whether patterns of disparity in form are similar to those of function. The justification for this comparison has, in part already been outlined in Chapter 3, where workers have tended to assume that morphological disparity may act as some proxy for ecological disparity. For this to be true, morphology would have to show good correspondence to function, because function acts as the intermediate link between a morphology and ecology (e.g. Collar and Wainwright 2006). Yet, where the relationship between form and function has been examined on individual faunas or living taxa, there is commonly disconnect between the two (e.g. Anderson 2009,

Hulsey and Wainwright 2002, Collar and Wainwright 2006, Wainwright 2007). However, studies that compare morphology and function over a long time series using fossil taxa are rare, and where this has been done (Stubbs et al. 2013) no quantitative comparison has been made. Therefore I ask: 1) Are patterns of morphological and functional disparity through time comparable? 2) What is the strength of the correlation between morphological and functional disparity?

2) Is there any evidence for early high disparity?

The attainment of high morphological disparity early in a clade's history is a widely discussed (Gould 1989, McShea 1998, Wills and Fortey 2000, Erwin 2007, Hughes et al. 2013) and commonly observed pattern throughout the Phanerozoic (Hughes et al. 2013), yet most of the clades tested for early high disparity are relatively small (Hughes et al. 2014:SI). The neopterygian dataset presented here represents the second largest fossil vertebrate dataset to quantify shape disparity after Friedman (2010), and therefore provides a rare opportunity to look for early high disparity in a large vertebrate clade. Furthermore, although early high disparity is usually discussed purely in the context of morphology, here I can also test for the phenomenon in functional diversity.

3) Was there a transition from a holostean dominated world to a teleost dominated world within the Mesozoic?

Textbook discussions of actinopterygian diversification describe three successive radiations of fishes. This pattern, most clearly articulated in Romer 1966 and Colbert 1969, was framed in a taxonomic context and suggested that three radiations of fishes proceeded sequentially, with each successive radiation becoming taxonomically dominant over its predecessor, causing the previous group to decline. They proposed that 'Chondrosteans' (which, to Romer and Colbert

consisted of palaeoniscoids, ropefish, sturgeons and paddlefish) represent the first fish fauna, dominating aquatic environments from the Devonian until the Triassic. 'Chondrosteans' then decline as they are replaced by holosteans, which dominate the Jurassic and Early Cretaceous, after which time they decline due to replacement by teleosts, who proceed to dominate from the Late Cretaceous until the present day.

These claims of the rise and fall of successive radiations are descriptions of diversity patterns combined with some theory of causation by replacement. Here, I only seek to address the former; discussions of replacement are examined in Chapter 3 (Q5). These diversity patterns have not been revisited in the light of recent phylogeny, nor have they ever been examined from a morphological and functional perspective. Here, I aim to interrogate these patterns by asking two main questions: 1) did holosteans ever dominate (defined here as 'show greater diversity than') over teleosts in richness and disparity between the Triassic and Early Cretaceous?, 2) did teleosts become dominant over holosteans in richness and disparity at any point between the Triassic and Early Cretaceous? After these questions have been addressed, I focus specifically on the disparity pattern to ask whether there is any evidence for a decline in holostean disparity over time coincident with a teleost rise over time, as claimed on the basis of richness in textbook accounts. I then ask whether any of the disparity findings are surprising given a null model of trait evolution, before examining whether crown teleosts play an important role in any potential transition from a holostean dominated, to a teleost dominated world.

4) Is there any evidence of changes over the Triassic – Jurassic extinction boundary?

Great uncertainty exists over the effects of the end-Triassic extinction on fishes, due in part to the paucity of relevant data available (Hallam 2002, Friedman and Sallan 2012). Current

understanding of the event derives purely from taxonomic 'range through' data (The Fossil Record 2: Gardiner 1993, Patterson 1993), which suggests that no osteichthyan family goes extinct across the boundary (Hallam 2002). Consequently, there is no evidence of any impact of the extinction event on fishes to date. To address this, I examine both disparity and phenotypic space occupancy of neopterygians on either side of the boundary, and discuss the potential impacts of the Triassic-Jurassic extinction on the neopterygian radiation.

5) Is there any evidence for a growing significance of durophagous taxa, consistent with claims of a Mesozoic Marine Revolution?

The Mesozoic Marine Revolution (MMR) is loosely defined and characterises a series of changes perceived to have occurred within the Mesozoic that signal a departure from the status quo established in the Paleozoic (Vermeij 1977). The most significant changes relate to aspects of community structure, such as a shift from Paleozoic and Early Mesozoic communities dominated by epifaunal species (Stanley 1972, 1977) to those with a larger proportion of infaunal species with greater potential depths of bioturbation (Bush and Bambach 2011:Fig.3b,e). However, since the very conception of MMR (Vermeij 1977) the main emphasis has focused upon a perceived increase in the predation abilities and overall predation intensity of taxa, citing the diversification of fishes, decapod crustaceans and carnivorous gastropods (Stanley 1977, Vermeij 1977). These two observations, have inspired a scenario of escalation (Vermeij 1987), an evolutionary arms race where durophagous groups diversify, increasing the predation pressure on a whole host of invertebrate prey and causing them to evolve armoured and ornamented forms, alter their modes of life to obtain greater protection, or decline altogether (Vermeij 1977).

A vast literature on the MMR has since accrued, mostly focusing upon evidence of predation, the degree of ornamentation, and the diversification dynamics of the prey (reviewed in Kelley and Hansen 2001, Harper 2003, Harper 2006, Jablonski 2007, Bush and Bambach 2011) yet comparatively little attention has been paid to the functional capabilities of specific groups of durophages (*but see* qualitative descriptions of durophagy in decapods (Schweitzer and Feldmann 2010) and neopterygians (Tintori 1998, Kriwet 2001, Lombardo and Tintori 2005). This is unfortunate, since the MMR provides a clear expectation that durophagous groups should not only become more diverse, but should show increasingly destructive morphologies in response to increasingly well armoured prey (Jablonski 2007:725). These expectations are explicit and testable, yet little attempt has been made to address the latter question from a biomechanical perspective.

The morphological and functional dataset presented in this chapter enable me to test the claims of the MMR that pertain to neopterygian fishes. Specifically, I test for Mesozoic increases in 1) the percentage of taxa with specialised crushing dentitions, 2) average jaw-closing mechanical advantage, and 3) the morphological and functional disparity of taxa with higher than average jaw-closing mechanical advantage. Together, I can evaluate the evidence for notions of growing significance among neopterygian durophages.

MATERIAL AND METHODS

(a) Morphological and functional dataset

The morphological and functional dataset, based upon ordinations of 356 species, is identical to that outlined in Chapter 3.

(b) Calculating and testing for differences in morphological and functional disparity

i) Time bin selection

The Triassic, Jurassic and Early Cretaceous were together divided into 11 time bins in identical fashion to Chapter 3. Time bins were as follows: 1) Induan-Anisian, (duration: 10.17 Ma); 2) Ladinian-Carnian (duration: 15 Ma); 3) Norian-Rhaetian (duration: 25.7 Ma); 4) Hettangian-Pliensbachian (duration:18.6 Ma); 5) Toarcian-Bajocian (duration: 14.4 Ma); 6) Bathonian-Oxfordian (duration:11 Ma); 7) Kimmeridgian-Tithonian (duration:12.3 Ma); 8) Berriasian-Valanginian (duration:12.1 Ma); 9) Hauterivian-Barremian (duration: 7.9 Ma); 10) Aptian (duration: 12 Ma); 11) Albian (duration: 12.5 Ma).

ii) Accounting for uncertainty in phylogeny and the ages of fossil deposits

Before disparity can be calculated for any given clade in any given time bin, taxa need to be assigned to clades and fossil deposits assigned to the appropriate time bin. However, both assignments are subject to uncertainty. The supertrees generated in Chapter 2 clearly highlight numerous neopterygian taxa that could be holosteans, teleosts, or stem neopterygians. Placement of fossils within time bins is uncertain where the deposit overlaps multiple time bins, and the specific age of the fossils within the deposit are not known. Instead of making arbitrary decisions as to where taxa and deposits should be placed to create a single version of events, I incorporate uncertainty by calculating Mesozoic disparity based upon 100 replicates (i.e. 100 versions of events), pooling the disparity values, and presenting mean and 95% confidence intervals from these values. Assignment of taxa to Holostei and Teleostei for each replicate correspond one to one with assignment of taxa in 100 randomly selected supertrees from the 10,500 generated in Chapter 2. To incorporate fossil age uncertainty, the ages of fossil deposits in each replicate were randomised between their minimum and maximum possible age interpretations. Fossils were then assigned to time bins based upon the outcome.

The end result was 100 replicates which contain slightly different compositions of taxa assigned to Holostei and Teleostei, with deposits occasionally falling within different composite time bins.

iii) Measuring morphological disparity and testing for differences in disparity

There are several ways to measure disparity (Ciampaglio et al. 2001). For this study, I use multivariate variance (aka. sum of variances, sum of univariate variances) as it appears relatively insensitive to changes in sample size, unlike range-based measures (Ciampaglio et al. 2001, Foth et al. 2012). Disparity was calculated upon axes which explain more than 5% of overall variance, as higher axes often summarise noise. This resulted in the examination of three ordination axes for morphology, and five ordination axes for function. To obtain the mean disparity and 95% CI for a given group in a given time bin (e.g. holosteans of the first time bin), the protocol was as follows: 1) For each of the 100 replicates, 1000 bootstrap values (calculation of disparity after resampling taxa with replacement) were obtained for the clade in the specific bin; 2) Disparity values were pooled, resulting in 10,000 values (100 replicates multiplied by 1000 bootstraps); 3) Mean and 95% CIs were derived from these 10,000 values. This distribution is then called upon for any statistical test between that specific clade in a specific bin to any other clade (including the same clade) in a specific bin. The process was repeated to obtain disparity measures for holosteans, teleosts, and all neopterygians in each time bin.

The distributions described above were drawn upon to test for differences in disparity between 1) holosteans and teleosts within each time bin, and 2) changes in holostean, teleost and neopterygian disparity (individually) between every time bin. A modified *t* test was used to perform these analyses under the method outlined in Zelditch et al. 2004 (p222).

Calculation of the *t* statistic requires the number of taxa sampled for a given clade in a given time bin (e.g. 10 teleosts in the Late Triassic) to be specified, a value that might vary across the replicates due to taxonomic and faunal uncertainty. To address this in a conservative manner, for a given clade in a given time bin, I took the lowest number of taxa observed in any of the 100 replicates as the sample size value required for the t test.

(c) Alternative disparity trajectories, summary trajectories and null model simulations

The procedure for disparity calculation outlined above, performed upon the full dataset of 356 species, will deliver a single pattern of disparity with associated uncertainty. However, there are additional considerations that may alter these trajectories, such as exceptional deposits (i.e. *Lagerstätten*), or additional phylogenetic uncertainty. I therefore derive a series of alternative trajectories, which, along with their associated statistical tests are presented in the Appendix. I discuss the basis for these alternative trajectories below.

i) Trajectories to illustrate the importance of Dapedidae

Chapter 2 revealed that neopterygian family Dapedidae was rendered Neoptergii *incertae sedis* in consensus trees. The family ranges from the Late Triassic to the Late Jurassic and consists of five deep-bodied genera: *Dapedium*, *Paradapedium*, *Dandya*, *Heterostrophus* and *Tetragonolepis*. Because of their deep body form, preliminary analyses highlighted their ability to greatly alter the overall pattern of disparity observed in the Late Triassic and Early-Middle Jurassic, depending upon whether they were assigned to holosteans or teleosts. As such, three versions of the full dataset (i.e. with no *Lagerstätten* removal) were produced: 1) a trajectory where Dapedidae are teleosts (in all 100 replicates), 2) a trajectory where Dapedidae are holosteans (in all 100 replicates), and 3) a trajectory where Dapedidae are teleosts in 50 replicates, and holosteans in 50 replicates. Examination of all three trajectories

makes clear the importance of Dapedidae on patterns of disparity. In other trajectories outlined below (*Lagerstätten* removal and genus range trajectory), Dapedidae are placed as teleosts, simply to avoid additional permutations. This is not problematic since all trajectories are considered together in discussions of pattern (see 'summary trajectories' outlined below).

ii) Robustness of pattern to Lagerstätten effects

Exceptional fossil deposits have the potential to distort patterns of richness through time. These influences have been referred to as *Lagerstätten* effects (Raup 1972) and their ability to inflate richness has been documented in several groups (e.g. Penney 2003, Labandeira 2005, Butler et al. 2009), yet they have been little discussed by authors employing subsampling approaches (Lloyd and Friedman 2013:14, *but see* Benson et al. 2009 for discussion in modelling approaches). There are numerous *Lagerstätten* throughout the Mesozoic that influence the diversity of marine tetrapods (Benson et al. 2009) and fishes specifically (Cavin and Forey 2007, Cavin 2010, Lloyd and Friedman 2013). Although these studies make it clear that *Lagerstätten* effects need to be taken into account, their influence on disparity estimates has rarely been examined, and where they have been removed in studies of disparity, they did not alter the results (Friedman 2010). I seek additional evidence regarding the influence of *Lagerstätten* on disparity by applying two *Lagerstätten* removal approaches, comparable to those applied in Friedman (2010). *Lagerstätten* removal approach 1 eliminated the single fossil deposit in each time bin with the highest number of sampled neopterygian species. Where there was a tie, a deposit was selected at random for that replicate. *Lagerstätten* removal approach 2 excluded any deposit with 10 or more sampled neopterygian species, and thus could result in the removal of multiple deposits, or no deposits, for any individual time bin. Disparity under these approaches was calculated in identical fashion to the full dataset, using the same 100 replicates outlined above that account for taxonomic and age uncertainty.

iii) Genus range pattern

Although the use of genus range data has been commonly employed in studies of taxonomic diversification (e.g. Sepkoski 1998, Cavin et al. 2007, Alroy et al. 2008), it is less commonly employed in studies of disparity (*but see* Anderson et al. 2011, Anderson et al. 2013). To derive a genus range disparity trajectory, I performed the following steps: 1) derive a single morphological shape (or functional entity) for each genus by averaging the traits of its constituent species. 2) Use these genus averaged morphologies (or functional measurements) as the basis for an ordination to derive axes of variation in identical fashion to the species ordination. 3) Genera are then assigned to all time bins that fall within the known range of that genus (rather than purely the time bins that recover an occurrence of the genus), and disparity is then calculated for clades and time bins based upon the scores from the genus ordination.

The rationale for employing a genus range trajectory was threefold. First, there were numerous instances where poorly preserved remains of genera were present in certain faunas, but could not be identified to the species level. Thus, the method ensures genus morphologies are sampled whenever material is available, no matter how incomplete. Second, the number of species within a given genus can be inflated for well-studied deposits relative to poorly studied deposits as a result of differing worker effort. Examination of a genus pattern may provide a way to make fairer comparisons between such sites. Third, it was thought that range data would provide useful insight where sampling or preservation was particularly poor, such as in the third bin in the Jurassic (Bathonian-Oxfordian), or where articulated specimens of clade are absent, such as the Early-Middle Jurassic for the deep-bodied teleost order Pycnodontiformes, only known from dentitions at this time.

iv) Summary trajectories

The trajectories derived from the full dataset and the alternative datasets add considerable complexity for interpretation. For each clade, there are six trajectories in total: 1) full dataset where Dapedidae is assigned to Teleostei; 2) full dataset where Dapedidae is assigned to Holostei; 3) full dataset where Dapedidae is assigned to Teleostei for 50 replicates, then Holostei for 50 replicates; 4) *Lagerstätten* removal approach one; 5) *Lagerstätten* removal approach two; 6) Genus range dataset.

To process this complexity, for the holosteans, teleosts, and neopterygians as a whole, I use information from all trajectories to derive a summary trajectory that attempts to capture the clearest overall pattern for each clade. The confidence intervals of these trajectories seek to exhibit a 'worst case scenario', with the upper and lower limits for each time bin derived from the largest and smallest disparity estimate from any of the six disparity trajectories presented for each clade. The mean disparity in the summary always derives from *Lagerstätten* removal approach two, deemed the most appropriate because the absolute numbers of taxa sampled from each time bin were more comparable than with any other trajectory, and as such, may offer a fairer means of comparison between time bins. There were three instances where the mean was not derived from *Lagerstätten* removal approach two: 1) the first Jurassic bin, where the mean is obtained from the full dataset since nearly all of the time bins diversity is contained within a single *Lagerstätten*. 2) the third Jurassic bin, where the pattern seen in the genus trajectory informs choice of a mean because holosteans are absent from the species pattern, and 3) the Late Triassic, where a highly non-normally distributed arrangement of taxa inflates the teleost mean, which is arbitrarily lowered to signify this. Important to note is that the summary trajectory itself is not used as the basis for any statistical test, it merely exists to

aid interpretation of the most significant findings from the six trajectories that underlie it, and to argue for a pattern that appears to be the most representative given the uncertainty.

v) Simulated disparity trajectories

I sought to establish simulated null models for morphological and functional evolution for comparison with the observed 'full dataset' trajectory. To achieve this, it was necessary to simulate the relative warp axes under a Brownian motion model of evolution using the same 100 supertrees that underlie the disparity replicates outlined above. In order to generate a null trajectory directly comparable to that of my observed data, I first fitted a Brownian-motion model to each of the relative warp axes in my observed dataset to obtain the Brownian variance parameter for each axis. I then used these parameters when simulating each relative warp axis individually.

Chapter 2 outlined the uncertainty regarding the neopterygian timescale, resulting in the creation of a purely fossil based timescale, and molecular based timescale, where fossils were included but molecular clock estimates informed the age of the neopterygian, holostean and teleost crown nodes. Null disparities were therefore derived from both the fossil based and molecular based time scaled trees.

Disparity was calculated using the same procedure as for observed data, but simply based upon the simulated relative warp axes for the taxa present in each time bin. Each replicate (the same 100 that were used to accommodate phylogenetic and deposit age uncertainty for the observed data) was based upon a separate simulation.

(d) Addressing Q1-5 based upon the established patterns of disparity

The majority of the questions outlined in the introduction can be examined with reference to the established patterns of disparity, and their associated t tests (outlined above). However Q1 regarding the relationship between morphological and functional disparity patterns, and Q5 regarding the Mesozoic Marine Revolution (MMR), require additional methods.

i) Additional methods for Q1 – Correlations (Spearman's *rho*) of mean neopterygian disparity, and the first differences of mean neopterygian disparity, were used to assess covariation between morphological and functional disparity trajectories.

ii) Addition methods for Q5 – Three analyses were performed to test the expectations of the Mesozoic Marine Revolution pertaining to neopterygians. The first sought to test whether clear durophages (those taxa with specialised crushing dentition) represent an ever increasing proportion of neopterygian diversity throughout the Mesozoic. This was achieved by identifying those taxa with batteries of flattened, peg-like teeth in the dataset, and calculating what percentage of all taxa, in each Mesozoic time bin, they represent. Due to uncertainty in faunal ages, the same 100 replicates used in disparity analysis were used for these calculations, which provided a confidence limit on percentages within time bins.

Second, I focused on a single mandibular trait, jaw-closing mechanical advantage (MA), to ask whether the average mechanical advantage of taxa increased through the Mesozoic. Jaw-closing MA, as outlined in the methods section of Chapter 3, represents the proportion of input muscle force that is applied at the dentition. Higher ratios imply greater bite forces, and greater bite forces are correlated with consumption of harder prey items (Wainwright 1988, Westneat 1994, Wainwright and Richard 1995, Bellwood et al. 2006), and thus, represent an ideal proxy for potential durophagy. Furthermore, moderate durophagy (i.e. crushing weak

thin-shelled gastropods and crustaceans) appears to be within the range of many species, not purely those with specialised dentitions (David Bellwood personal communication, although broad surveys describing this are lacking, *but see* the large disparity of taxa that feed on micro-crustacea in Bellwood et al. 2006). Taken together, jaw-closing MA appears to be the best available proxy for potential durophagy, and any shifts in the distribution of this measure through time could provide insights on the relative pressures exerted by durophages (or the prevalence of durophagy) on invertebrate prey.

Third, I sought to quantify the disparity of taxa with above-average mechanical advantages, in both morphology and function, to assess the disparity of potential durophages through time. If durophages represent a more varied threat throughout the Mesozoic, they would be expected to accumulate larger disparity throughout this time, which might translate into a greater variety of ecologies. However, this is the most assumption laden of all analyses, since it requires an arbitrary threshold for potential durophages (those with larger than average jaw-closing MA), and because the relationship between morphology, function and ecology are not well understood, and may become decoupled (e.g. Bellwood et al. 2006).

Results and Discussion

Establishing patterns of morphological disparity

i) Neopterygii

The Early and Middle Triassic[1], similar in overall disparity, mark the low point of Mesozoic neopterygian disparity in the full dataset (**Fig. 4.1a**) and all alternative trajectories (**Fig. A1.1**), as reflected in the summary trajectory (**Fig. 4.1b**). All trajectories then show a significant increase in disparity between the Middle and Late Triassic (**Table A1.1**); the only instance of a clear increase in disparity between two consecutive time bins within the entire time series. This is achieved by both the arrival of the most deep-bodied taxa and shallow-bodied taxa, and a greater spread of morphologies within central morphospace contrasting with the dense packing seen within the central region in the Middle Triassic (**Fig. 4.5**). Disparity then remains relatively stable at near Late Triassic levels for the remainder of the Jurassic until another increase occurs in the Late Jurassic (**Fig. 4.1b**). This second increase is difficult to characterise with the full dataset due to poor sampling (**Fig. 4.1a**). Insights are therefore drawn from the genus pattern (**Fig. A1.1d**), which suggests there is an increase (albeit not statistically significant p=0.27, **Table A1.1**). The Early Cretaceous shows an increase in disparity with time (**Fig. 4.1b**), an insight based mainly upon the second *Lagerstätten* procedure and the genus range trajectory (**Fig. A1.1c-d**). Considering the entire time series, the neopterygian disparity is punctuated by two, step-wise increases, resulting in a three tiered structure overall. The first tier was the Early – Middle Triassic, followed by a sharp increase to the Late Triassic – upper Middle Jurassic tier, and followed by another, milder increase to the Late Jurassic – Early Cretaceous tier. It is open to interpretation whether the final tier represents a plateau, or a steady increase in disparity with time.

[1] The terms Early, Middle and Late Triassic are commonly used throughout the text in reference to the three composite time bins that were created in the Triassic. However, this is simply for ease of discussion, since these composite bins do not precisely correspond to the Lower, Middle and Upper Triassic in the geological timescale.

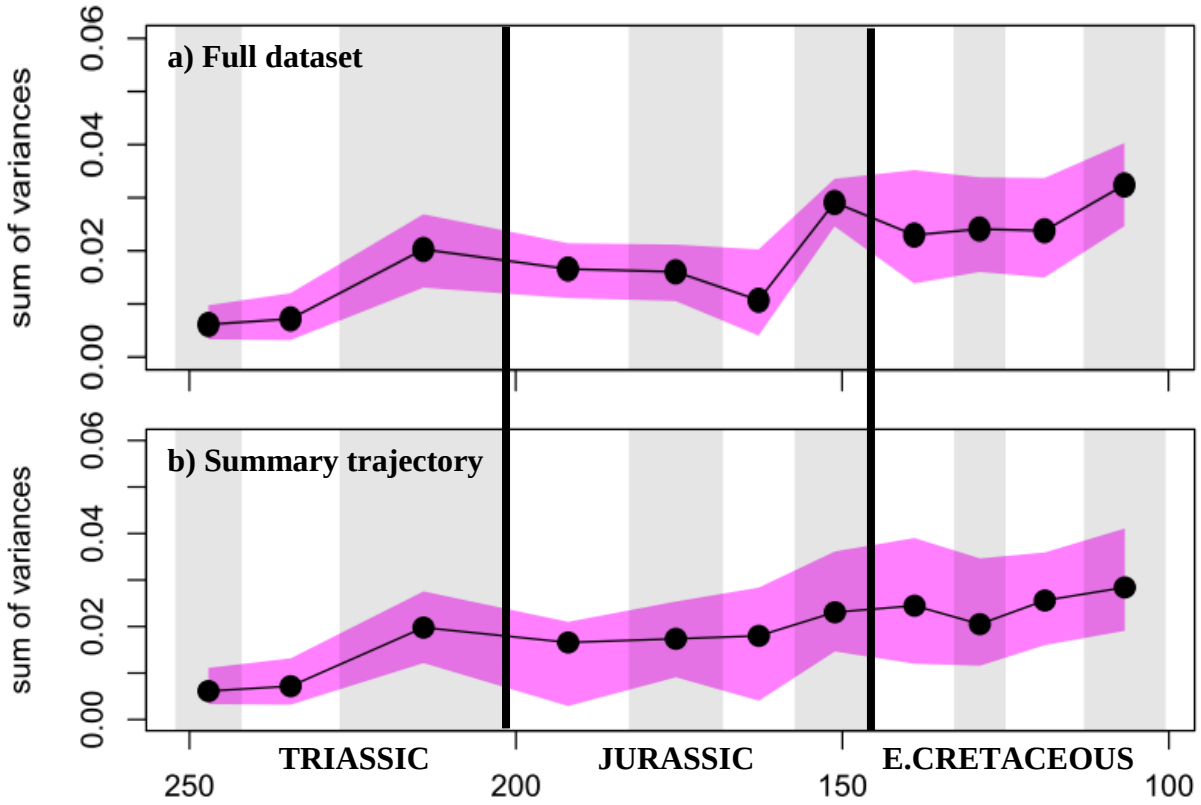

Fig. 4.1. Neopterygian morphological disparity through eleven Mesozoic time bins based upon a) the full dataset of 356 species, b) a summary aiming to capture the most reliable pattern of disparity by incorporating information from the full dataset and all the alternative trajectories (e.g. *Lagerstätten* removal) that are presented in the Appendix.

ii) Teleostei

The presence of just two teleosts of similar morphology in the first Triassic bin (species which derive from the Anisian) results in low disparity. The second Triassic bin also contains small sample sizes, yet generates large uncertainties due to the highly abnormal distribution of taxa in morphospace, but on average, disparity is low. The full dataset then suggests a sharp and significant increase in disparity between the Middle and Late Triassic (**Fig. 4.2a**). However, the highly non-normally distributed nature of Late Triassic teleosts in morphospace, which fall into two very distant morphological clusters of comparable taxon number (between the deep-bodied forms such as pycnodonts, and fusiform species such as *Pholidophorus*, **Fig. 4.5**), results in high disparity values. Due to this abnormal, highly split distribution, my disparity metric (multivariate variance) is likely highly inflated and should be read with caution. To highlight this, mean disparity is arbitrarily lowered in the summary trajectory (**Fig. 4.2b**).

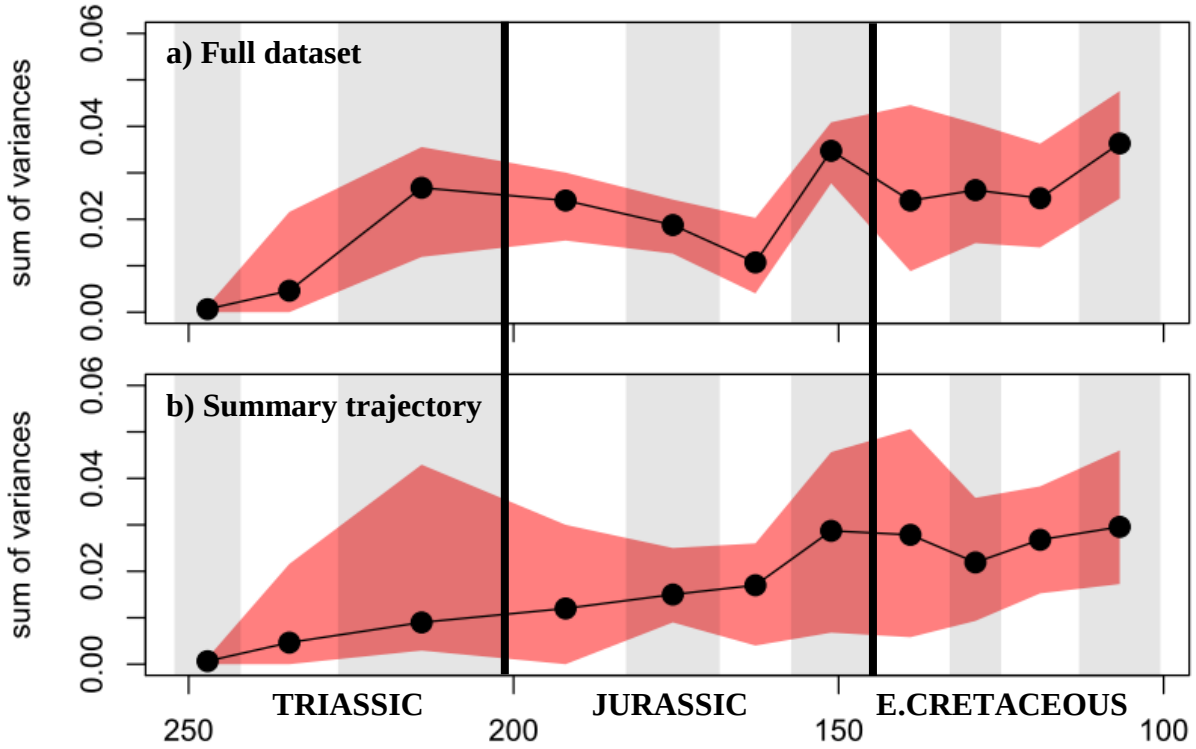

Fig. 4.2. Teleost morphological disparity through eleven Mesozoic time bins based upon a) the full dataset of 356 species, b) a summary aiming to capture the most reliable pattern of disparity by incorporating information from the full dataset and all the alternative trajectories (e.g. *Lagerstätten* removal) that are presented in the Appendix.

In the Jurassic, phylogenetic uncertainty and sampling have huge influence on teleost disparity, and determine whether, across the first three Jurassic time bins, they exhibit a shallow decline (**Fig. A1.2a**), relative stability (**Fig. A1.2c, f**), or some erratic pattern of increases and decreases (**Fig.1.2.d, e**). The correct scenario will become clear once the affinity of Dapedidae is resolved. Following this uncertain period is an unambiguous increase in disparity between the third and final Jurassic bin, an increase is apparent (often significantly) in every trajectory (**Fig. A1.2, Table A1.2**). However, poor sampling in the third Jurassic bin exaggerates the scale of this increase, since the genus trajectory (which improves sampling of this bin) reports a milder, non-significant increase in disparity (**Fig. A1.2f, Table A1.2**, $p = 0.18$). Nevertheless, some degree of increase appears to occur in the Late Jurassic. According to *Lagerstätten* removal and genus range trajectories, Late Jurassic mean disparity remains relatively stable throughout the Early Cretaceous (**Fig. A1.2e, f**), a pattern accepted in the summary trajectory (**Fig. 4.2b**).

In summary, teleost disparity increases throughout the Triassic, which is followed by a period of uncertainty until an increase occurs in the Late Jurassic and is maintained throughout the Early Cretaceous.

iii) Holostei

Holostean disparity is comparable in the Early and Middle Triassic, prior to a Late Triassic increase (**Fig. 4.3**). According to the full dataset, Late Triassic disparity is almost significantly different to Early Triassic disparity ($p = 0.054$) but not the Middle Triassic disparity ($p = 0.13$), findings echoed in all alternative trajectories (**Fig. A1.3, Table A1.3**). Jurassic disparity is heavily influenced by phylogenetic uncertainty and sampling. In trajectories where Dapedidae are teleosts (**Fig. A1.3a, c-f**), holostean disparity undergoes a significant decline

over the Triassic-Jurassic boundary (e.g. full dataset p = 0.018) and remains low into the second Jurassic bin. However, when Dapedidae are holosteans, Late Triassic levels of disparity are maintained throughout the first two Jurassic time bins (**Fig. A1.3b**). The absence of articulated holosteans in the third Jurassic bin prevents calculation of disparity, yet genus range data suggest disparity was comparable to Late Triassic levels (**Fig. A1.3f**). Late Jurassic disparity is influenced by *Lagerstätten* effects. The full dataset suggests Late Jurassic disparity is greater than any previous bin, yet the second *Lagerstätten* approach and genus range trajectories (**Fig. A1.3e-f**) suggests disparity is comparable to Late Triassic levels. I accept the latter on the basis that *Lagerstätten* removal from the Late Jurassic ensures its sampling is more comparable to surrounding time bins. Late Jurassic disparity, which is similar to Late Triassic levels, is then maintained throughout the Early Cretaceous according to both *Lagerstätten* approaches and the genus range pattern (**Fig. A1.3d-f**), trajectories that also remove the apparent Albian peak in disparity seen in the full dataset (**Fig. 4.3a**), rendering it another *Lagerstätten* effect.

The summary trajectory best captures the overall pattern (**Fig. 4.3b**), demonstrating a Triassic increase, a period of uncertainty representing either stability or decline, before a Late Jurassic increase in disparity marking a return to Late Triassic levels, a level maintained throughout the Early Cretaceous.

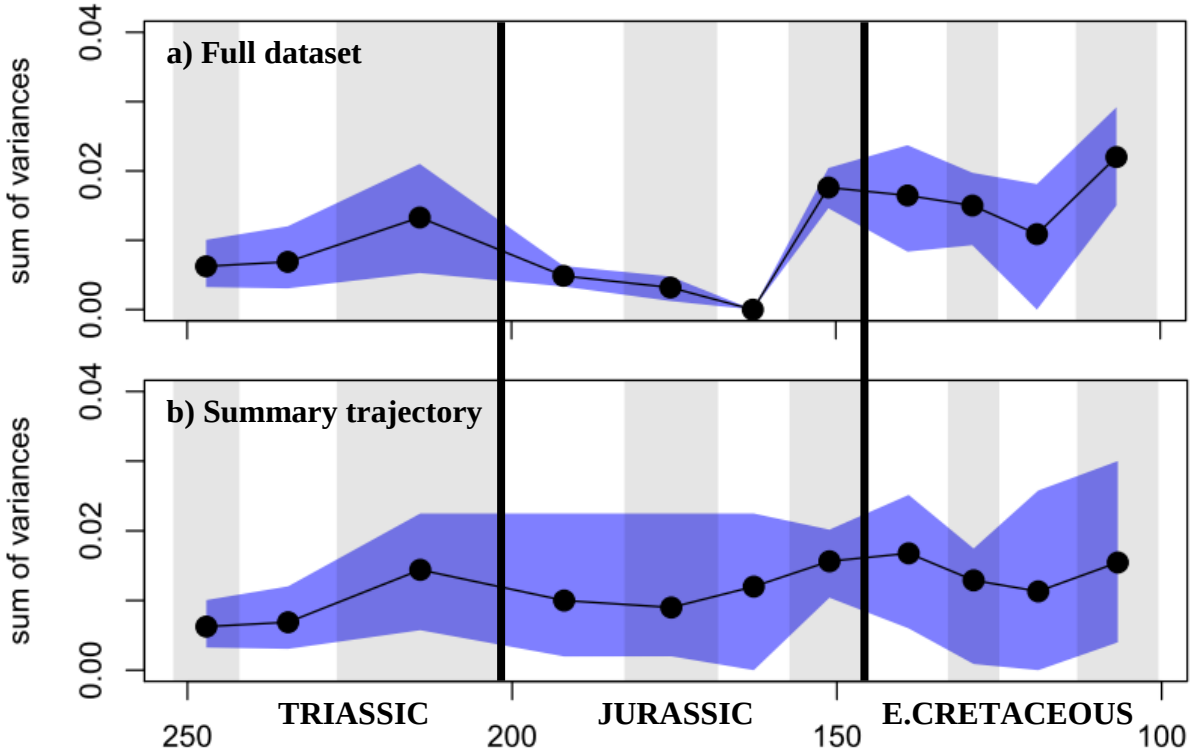

Fig. 4.3. Holostean morphological disparity through eleven Mesozoic time bins based upon a) the full dataset of 356 species, b) a summary aiming to capture the most reliable pattern of disparity by incorporating information from the full dataset and all the alternative trajectories (e.g. *Lagerstätten* removal) that are presented in the Appendix.

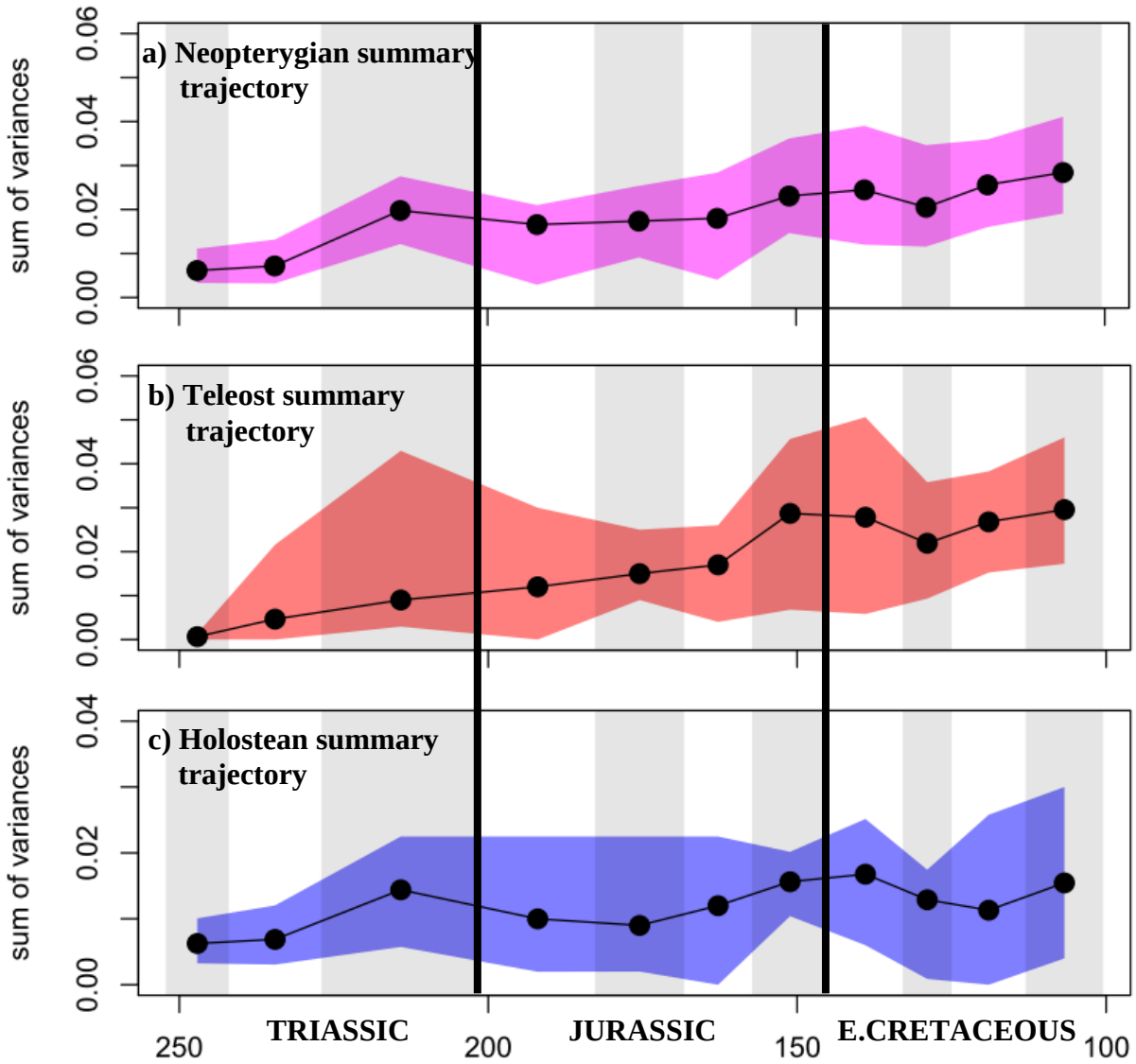

Fig. 4.4. Summaries aiming to capture the most reliable pattern of morphological disparity by incorporating information from the full dataset and all the alternative trajectories (e.g. Lagerstätten removal) that are presented in the Appendix for a) neopterygians, b) teleosts and c) holosteans.

iv) Conclusions

Although the three clades each express unique trajectories and uncertainties, within each Mesozoic period there are consistent trends directly observable in the summary trajectories for each clade (**Fig. 4.4**).

Triassic: A time of increasing disparity

All clades show a pattern of increasing disparity through the Triassic. For holosteans and Neopterygii this pattern is particularly clear, and Late Triassic disparity is often significantly different to Early Triassic disparity. Teleosts too clearly show an increase, yet large uncertainties obscure the pattern.

Jurassic: Uncertainty prior to a Late Jurassic disparity increase

The Jurassic pattern is the most variable, with suggestions of stability, a steady increase or a steady decline in disparity both across clades and between alternative trajectories of the same clade. What is clear across all clades is that disparity in the Late Jurassic is greater than any previous point in the Jurassic, even when Late Jurassic Lagerstätten effects (driven by Solnhofen and Cerin) are taken into account.

Early Cretaceous: A time of relative stability

All clades show relative stability across the Early Cretaceous when *Lagerstätten* effects (affecting the Late Jurassic and Albian) are considered, maintaining disparity at Late Jurassic levels. However, confidence intervals are sufficiently broad to accommodate alternative interpretations for individual clades (e.g. subtle increases or declines in disparity).

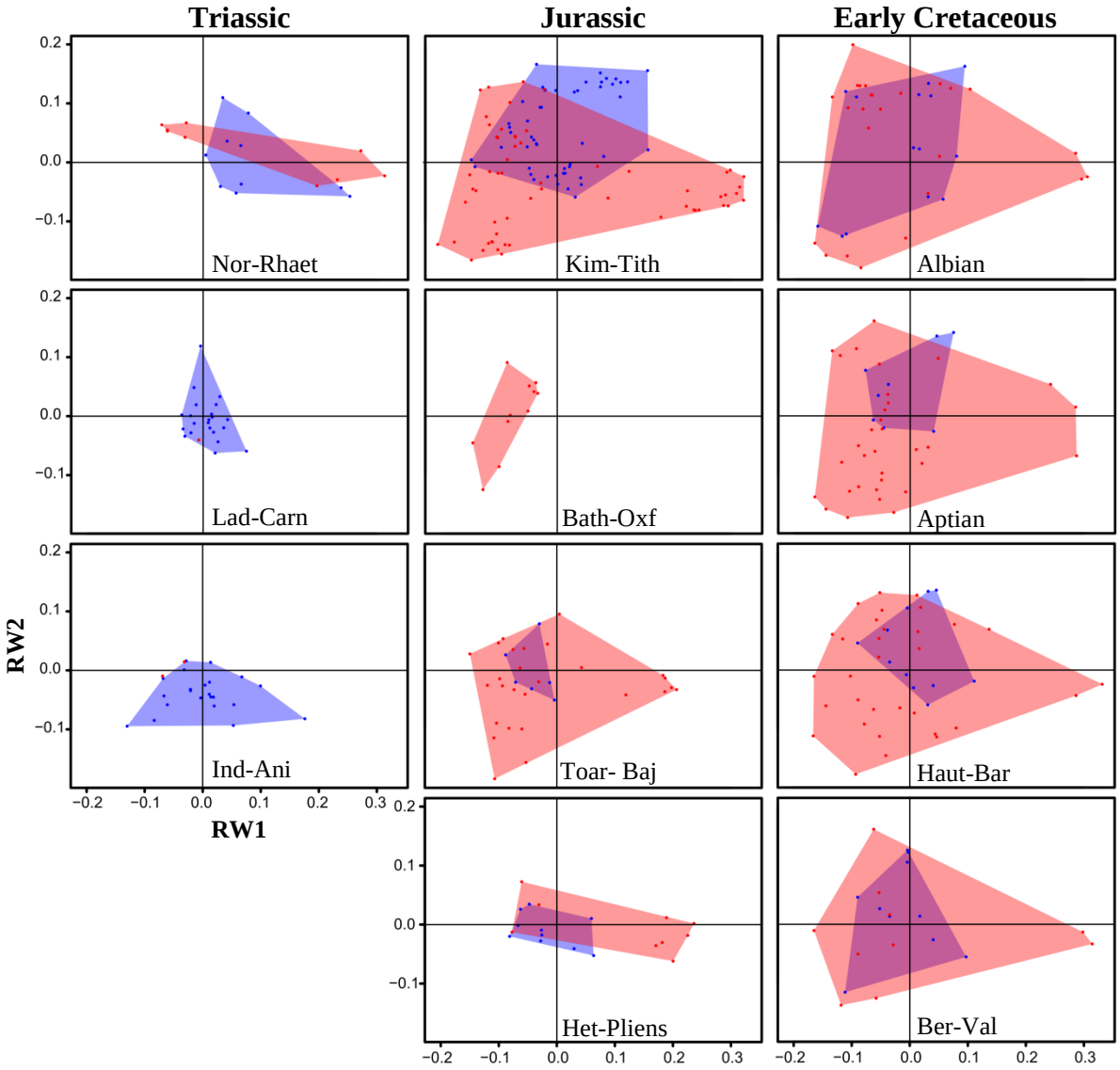

Fig. 4.5. Morphospace plots of relative warp axes 1 and 2 for the full dataset of 356 species divided over eleven Mesozoic time bins. Holosteans are denoted in blue, and teleosts in red, with convex hulls drawn for each.

Establishing patterns of functional disparity

i) Neopterygii

There is evidence for subtle, yet non-significant increases in neopterygian functional disparity between the Early and Middle Triassic in most trajectories (**Fig. A1.4**). Late Triassic disparity appears indistinguishable from Middle Triassic levels, especially under *Lagerstätten* removal approaches (**Fig. A1.4**). Ambiguity surrounds the Late Triassic to Early Jurassic transition, with the full dataset suggesting a non-significant increase in the disparity (**Fig. A1.4a**), and the *Lagerstätten* removal approaches suggesting a non-significant decline (**Fig. A1.4b-c**). Usually I would adopt the finding of the *Lagerstätten* removal approaches as the most insightful for time series comparison, however in this specific case, removal of the Blue Lias Formation + Charmouth Mudstone Formation (combined as one deposit due to fossil provenance uncertainties) leaves the Early Jurassic bin with considerably less diversity than surrounding time bins, making for a poor comparison. Thus, the Early Jurassic mean disparity from the full dataset is adopted for the summary trajectory (**Fig. 4.6b**), suggesting an increase (albeit non-significant) in disparity over the Triassic – Jurassic boundary (see Q4 in this chapter). Trajectories then report varying patterns for the rest of the Jurassic (**Fig. A1.4**), highlighting the sampling uncertainties present. I adopt the second *Lagerstätten* removal approach for the rest of the Jurassic, since this delivers comparable sampling between time bins. Functional disparity reaches its peak in the Early Jurassic and is followed by a shallow decline until the Late Jurassic (**Fig. 4.6b**). Disparity is then maintained at Late Jurassic levels for the Early Cretaceous, with the exception of the final bin (Albian) where disparity increases significantly in the full dataset (**Table A1.4,** p=0.05**)**. Signs of the Albian increase remain after *Lagerstätten* removal (**Fig. A1.4b-c**), albeit the increase is no longer statistically significant (**Table A1.4,** p=0.09).

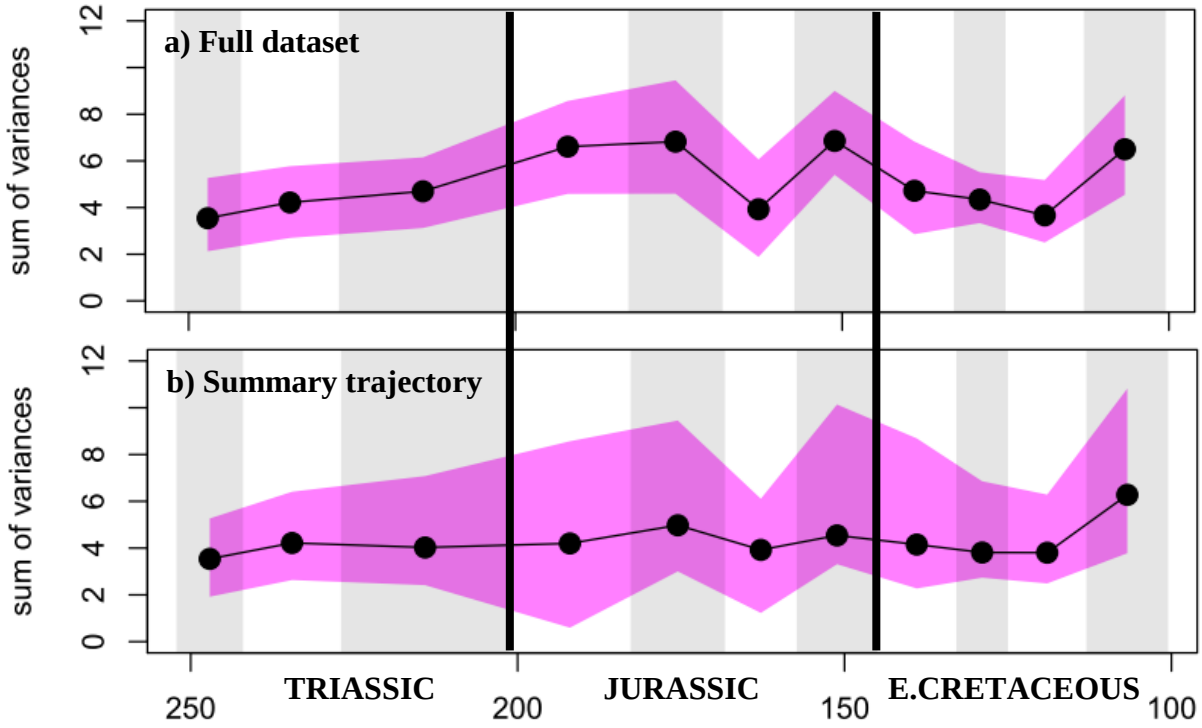

Fig. 4.6. Neopterygian functional disparity through eleven Mesozoic time bins based upon a) the full dataset of 356 species, b) a summary aiming to capture the most reliable pattern of disparity by incorporating information from the full dataset and all the alternative trajectories (e.g. *Lagerstätten* removal) that are presented in the Appendix.

ii) Teleostei

The functional disparity of teleosts in the Early and Middle Triassic is comparable, and represents the low point of the entire time series in all trajectories (**Fig. A1.5**). Disparity then increases between the Middle and Late Triassic, although it only ever nears significance (**Fig. A1.5, Table A1.5**). As with morphological disparity, the non-normally distributed nature of Late Triassic teleosts in ordination space inflates their disparity values. Therefore exact values should be read with caution. Nevertheless, some degree of increased disparity is clear.

Overlooking *Lagerstätten* removal approaches that eliminate the Blue Lias + Charmouth Mudstone (reasons previously articulated), teleost disparity in the Early Jurassic and second Jurassic bin is comparable to the Late Triassic (**Fig. 4.7b**). Some trajectories then detect a drop in disparity in the third, poorly sampled bin, yet the drop appears to be minor once *Lagerstätten* in surrounding time bins are pruned (**Fig. A1.5e**). Thus, under more comparable sampling, disparity in the Jurassic remains relatively stable at Late Triassic levels.

The Early Cretaceous represents a continuation of the Late Triassic – Jurassic disparity plateau, until a significant increase in disparity occurs in the final Early Cretaceous bin (**Fig. 4.7b**). An increase in disparity between the Aptian and Albian is apparent in all trajectories (**Fig. A1.5**), and is significant in all but the second *Lagerstätten* removal approach (**Table A1.5**). In summary, the overall pattern begins with low initial disparity followed by an increase in the Late Triassic, and maintenance of this disparity for most of the time series until

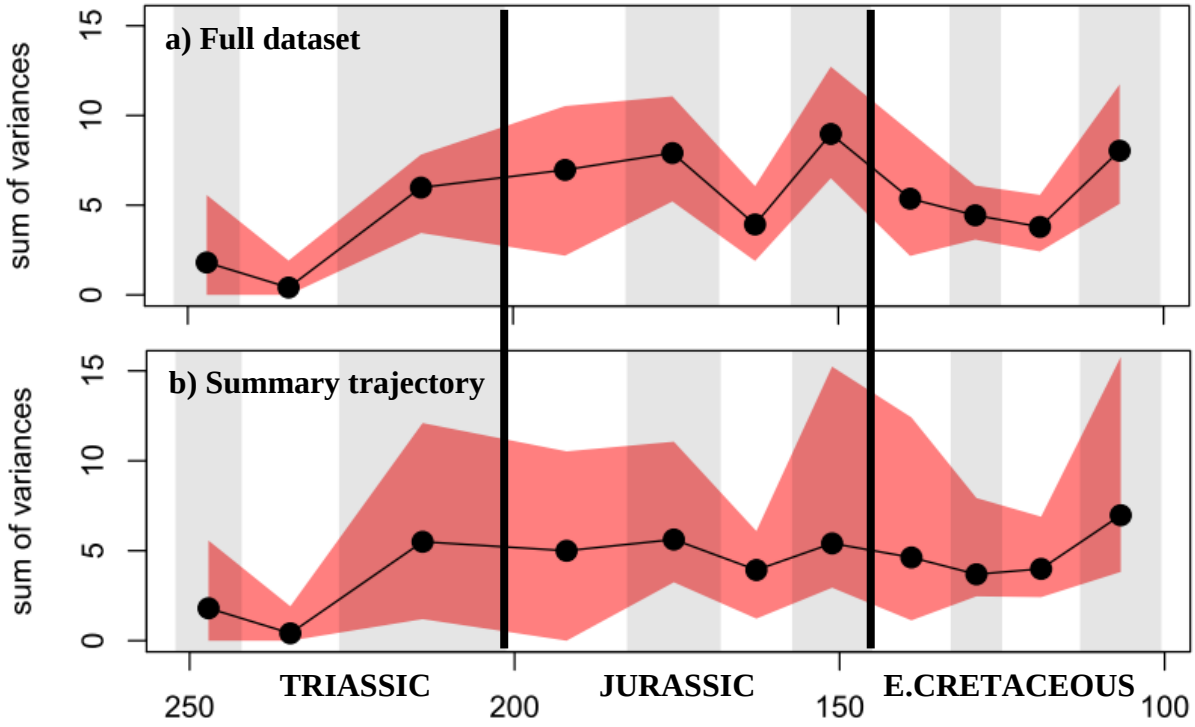

Fig. 4.7. Teleost functional disparity through eleven Mesozoic time bins based upon a) the full dataset of 356 species, b) a summary aiming to capture the most reliable pattern of disparity by incorporating information from the full dataset and all the alternative trajectories (e.g. *Lagerstätten* removal) that are presented in the Appendix.

a second increase occurs in the final bin of the Early Cretaceous. Therefore functionally,

teleost disparity is relatively stable for most of the Mesozoic with *Lagerstätten* removed.

iii) Holostei

Holostean functional disparity in the first Triassic bin typifies the average disparity seen across the entire time series (**Fig. 4.8b**).There is then an increase in disparity (albeit not significant), as the Middle Triassic displays the largest mean disparity value in the time series in most trajectories (**Fig. A1.6, Table A1.6**). There is then a sharp decline in disparity between the Middle and Late Triassic observable in all trajectories (**Fig. A1.6**).

Sampling and phylogenetic uncertainty greatly influence holostean functional disparity in the Jurassic. Disregarding Early Jurassic *Lagerstätten* removal (**Fig. A1.6d-e**), holostean disparity increases between the Late Triassic and Early Jurassic in all other trajectories (**Fig. A1.6**), and the extent of the increase depends upon the assignment of Dapedidae to Holostei. Without Dapedidae, the increase is near significant (**Fig. A1.6a, Table A1.6a,** p=0.06), yet with Dapedidae, the increase is significant and the Early Jurassic becomes the peak of Mesozoic holostean disparity (**Fig. A1.6b, Table A1.6b,** p=0.01). Inclusion of Dapedidae likewise increases disparity in the second Jurassic bin (**Fig. A1.6b**), which without Dapedidae expresses the lowest disparity of the time series (**Fig. A1.6a**). Given the uncertainty, I use the means derived from the analysis where Dapedium is used in 50% of the replicates (**Fig. A1.6c**) to inform the summary trajectory. There are no articulated holostean species to inform disparity in the third Jurassic bin, but from the Late Jurassic onwards, disparity appears relatively stable at levels comparable to the Early Triassic.

In summary, the overall time series displays relative stability, with the exception of a Middle Triassic peak (and potentially an Early Jurassic peak). However, given the large uncertainties throughout, the interpretation that disparity underwent a minor decline throughout the time series is also possible.

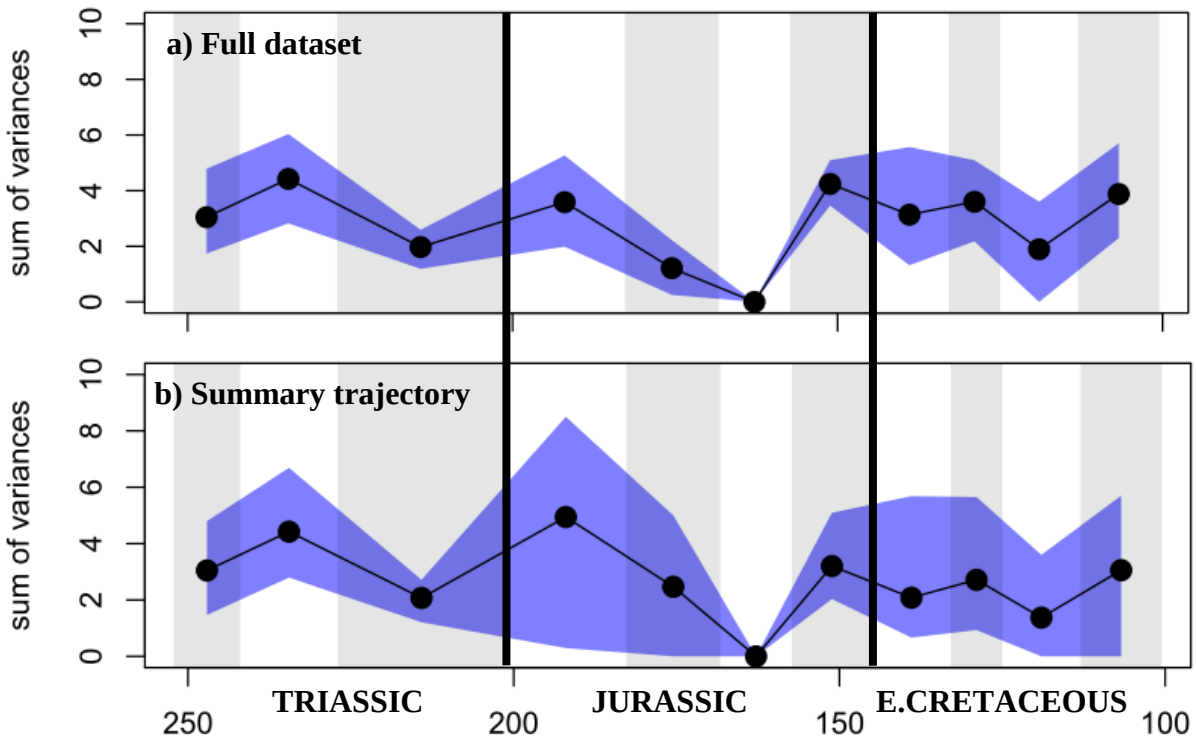

Fig. 4.8. Holostean functional disparity through eleven Mesozoic time bins based upon a) the full dataset of 356 species, b) a summary aiming to capture the most reliable pattern of disparity by incorporating information from the full dataset and all the alternative trajectories (e.g. *Lagerstätten* removal) that are presented in the Appendix.

iv) Conclusions

Generalities regarding patterns of functional disparity within each Mesozoic period, based upon the summary trajectories (**Fig. 4.9**), are as follows.

Triassic: A period of variable disparity

Each clade shows a different pattern of functional disparity across the Triassic, highlighting functional variability at this time. Interestingly, the teleost pattern is the inverse of the holostean pattern in each Triassic bin, whereas Neopterygii exhibit stability.

Jurassic: A time of relative stability

Despite large Jurassic confidence intervals driven by sampling and phylogenetic uncertainty, summary of alternative trajectories implies relative stability across the Jurassic. Interestingly, although the recovery of a Late Jurassic increase was apparent in the full dataset of all clade trajectories, all traces of this disappear under the second *Lagerstätten* removal approach, highlighting *Lagerstätten* effects caused by Solnhofen and Cerin in the Late Jurassic.

Early Cretaceous: Stability followed by an Albian peak

All clades show relative stability across the first three time bins of the Early Cretaceous. Even when exceptional sites are removed, the increase in disparity between the Aptian and the Albian is always present. Therefore although *Lagerstätten* effects were responsible for a rise in Albian morphological disparity, it is not responsible for a rise in functional disparity, which appears genuine.

Future work – Further studies are required to examine addition sources of influence on disparity patterns. For example, we currently know little about how the type of rock and palaeoenvironment may influence patterns of disparity (*but see* Rook et al. 2012 for

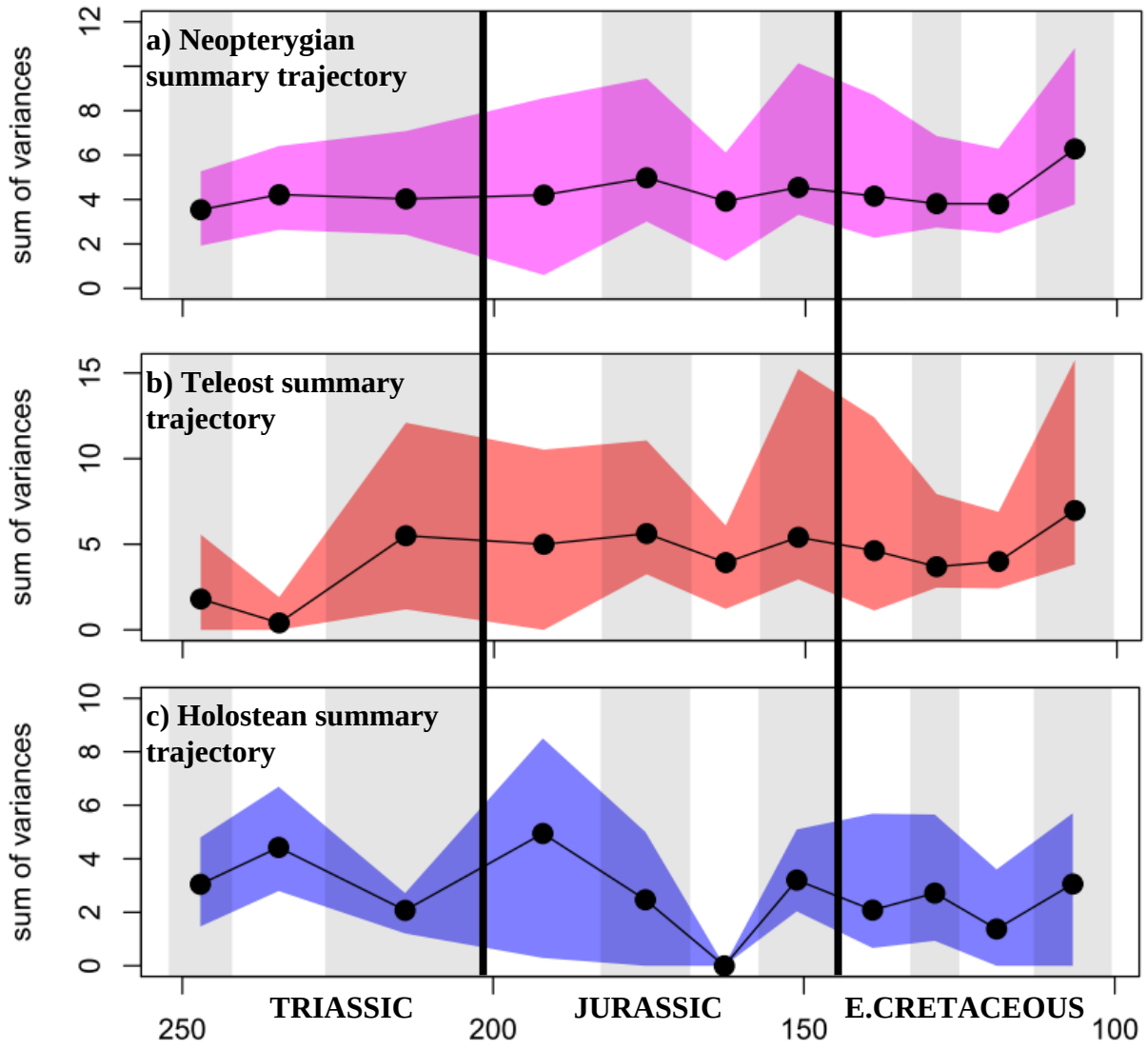

Fig. 4.9. Summaries aiming to capture the most reliable pattern of functional disparity by incorporating information from the full dataset and all the alternative trajectories (e.g. *Lagerstätten* removal) that are presented in the Appendix for a) neopterygians, b) teleosts and c) holosteans.

taxonomic, and Hopkins et al. 2014 for disparity). If clear relationships can be established between disparity and rock type, we may therefore expect to see changing disparity in a transition between say, a time bin dominated by shale deposits, and another time bin dominated by limestone deposits, and could seek to correct for this in any comparison. Many other influences may similarly influence disparity patterns, such as palaeolatitude, or the difference between marine and freshwater/terrestrial environments, and present ample opportunity for future work.

Q1. How do patterns of morphological and functional disparity compare?

First, I assess the extent to which the morphological pattern reflects the functional pattern based upon the full dataset. Although it is clear that various factors influence disparity patterns, these issues are irrelevant for this question, as the focus is solely upon how the same taxa might produce different morphological and functional patterns. I compare the morphological and functional patterns for Neopterygii, Holostei and Teleostei individually (**Fig. 4.10**).

i) Neopterygii

Spearman's rank correlation of mean disparity values from the full dataset yields a moderate positive, yet non-significant relationship between the morphological and functional trajectories (*rho* = 0.46, p = 0.15). First differences of these values imply a stronger positive and significant association (*rho* = 0.68, p= 0.035). Despite this association, the actual patterns of morphological and functional evolution differ markedly. The full dataset morphology pattern suggests stability in the Early and Middle Triassic followed by a sharp increase in the Late Triassic, while the function pattern suggests steady accumulation of disparity throughout the Triassic (**Fig. 4.10a,b**). Morphology then suggests a period of stasis throughout the

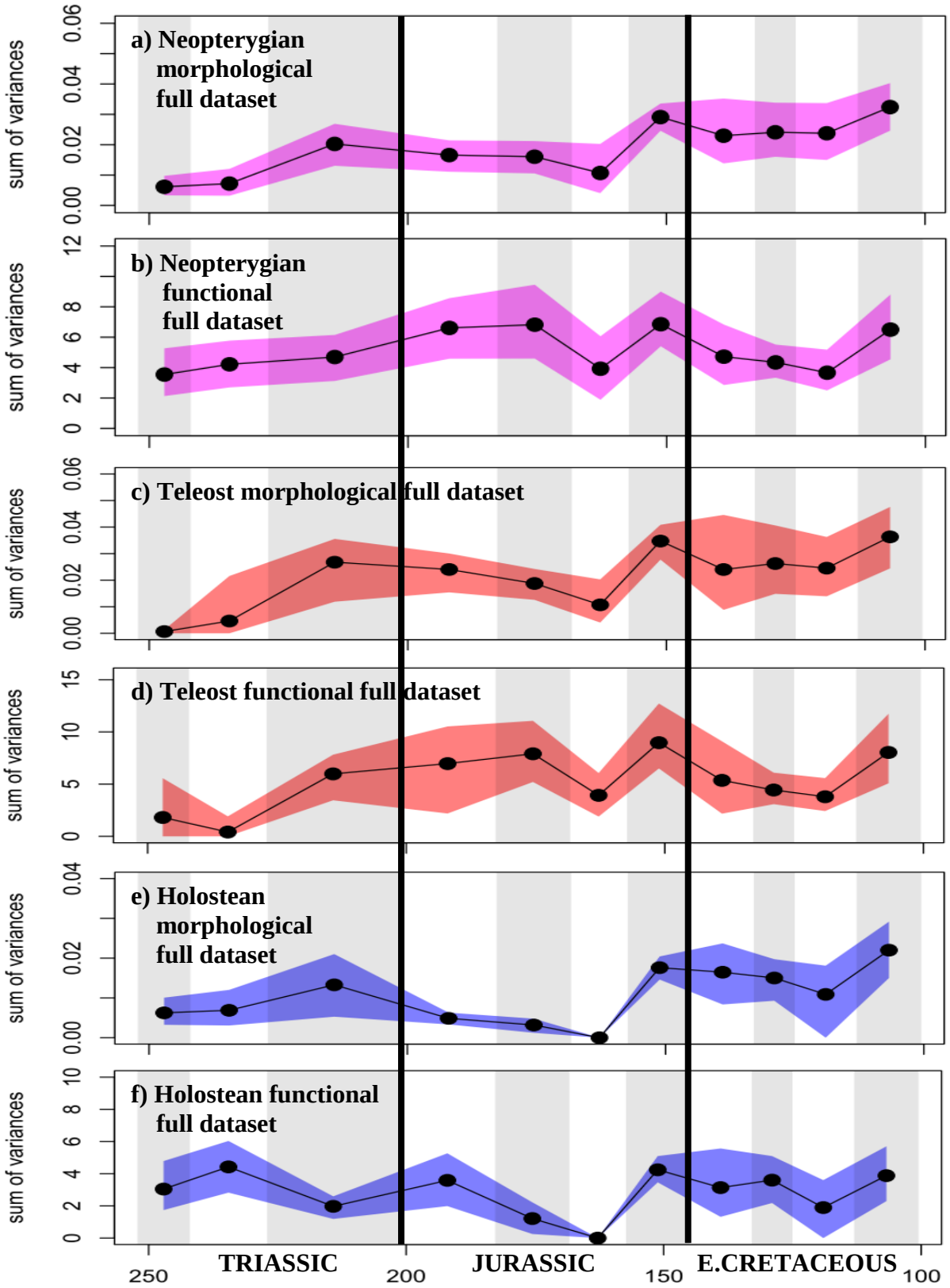

Fig. 4.10. Disparity through eleven Mesozoic time bins based upon the full dataset of 356 species for a) neopterygian morphology, b) neopterygian function, c) teleost morphology, d) teleost function, e) holostean morphology, f) holostean function.

Jurassic (with a minor drop due to poor sampling) prior to a Late Jurassic peak, whereas in function, the peak disparity for the time series is essentially achieved in the Early Jurassic and maintained (again with the presence of a sampling drop) until the Late Jurassic. In the Early Cretaceous, the morphological and functional patterns are at their most similar, showing some decline after the Late Jurassic and stability, followed by an Albian increase. The overall Mesozoic pattern is therefore highly discordant, with morphology suggesting a three tiered structure punctuated by rapid increases, and function suggesting a gradual increase leading to an Early Jurassic – Late Jurassic peak disparity plateau, followed by a decline to Triassic levels for most of the Early Cretaceous before an Albian return to Jurassic peak levels.

ii) Teleostei

Spearman's rank correlation calculated upon raw full dataset mean values and first differences yield correlation coefficients and *p* values of (*rho* = 0.71, p = 0.018) and (*rho* = 0.75, p = 0.018) respectively, suggesting a strong and significant correspondence between morphology and function. The patterns of disparity change also show moderate correspondence. Both datasets indicate low disparity in the Early – Middle Triassic, followed by a sharp increase to the Late Triassic, followed by a period of relative stability (aside from a poor sampling drop). However, patterns differ from the Late Jurassic onwards. Morphology suggests that disparity in the Late Jurassic and Early Cretaceous is greater than any previous point in the time series, whereas function indicates that disparity in the Late Jurassic – Early Cretaceous is no greater than earlier periods of the Jurassic. Thus, morphology shows an increase over the time series, whereas function shows stability or subtle signs of decline.

iii) Holostei

Although a correlation directly upon the raw means values yields a weak-moderate, non-significant correspondence between morphology and function (*rho* = 0.49, p = 0.15), first differences show even weaker correspondence (*rho* = 0.36, p = 0.33). Regarding pattern, morphology suggests there is stable Early and Middle Triassic disparity followed by a marked increase in the Late Triassic (**Fig. 4.10e**), whereas function suggests an increase between the Early and Middle Triassic (with the later representing the peak mean disparity of the entire Mesozoic) followed by a sharp decline in the Late Triassic (**Fig. 4.10f**). Whereas morphology then suggests a decline between the Late Triassic and Early Jurassic, function depicts an increase, although both datasets illustrate a decline in the second Jurassic bin. Both patterns then display relative stability from the Late Jurassic onwards, yet for morphology this plateau has greater disparity than any previous time, and for function the plateau is comparable in disparity to previous time bins. Thus, the overall pattern in morphology suggests disparity was mostly low until a dramatic increase in the Late Jurassic to a higher plateau, whereas the functional pattern suggests that maximum disparity was obtained early on and matched subsequently in the Early Jurassic, Late Jurassic, and occasionally in the Early Cretaceous.

iv) Conclusions

Moderate correlation commonly exists between morphological and function disparity, although holosteans deviate considerably from this by decoupling morphology and function more regularly and more dramatically than any other clade (e.g. there are instances where increases in morphological disparity correspond to decreases in functional disparity, and vice versa). Despite the presence of moderate correlation, the overall trajectories produced by morphology and function always differ, often with a common theme. For example, whereas all morphological trajectories display some increase in disparity with time, functional trajectories appear relatively flat. In this way, morphology better agrees with the predictions

of null models of diversification (**Fig. A1.7**), whereas functional disparity, showing stability, does not (**Fig. A1.8**). Indeed, long periods of functional stability have been observed in other time series (Anderson et al. 2011, Stubbs et al. 2013), and may prove to be a common feature of functional disparity. Nevertheless, these findings illustrate the ability of neopterygian clades to expand their range of morphologies even when functional disparity remains constant, and to attain considerable functional disparity even when morphological disparity is low.

Decoupling of morphology and function in Mesozoic neopterygians, also reported in Chapter 3, adds further weight to the growing body of evidence that function, and by extension ecological diversity, cannot be reliably inferred from morphological diversity (Bellwood et al. 2006). Corollary, functional disparity cannot predict morphological disparity. Therefore traits, be they morphological or functional, need to be carefully chosen for the question at hand, echoing the sentiments of other authors (e.g. Alfaro et al. 2004, Anderson 2009, Anderson and Friedman 2012). Where authors do wish to speculate beyond the remits of their dataset, they should state their assumptions outright, and not use this data as the basis for firm conclusions. My intention here was to use morphology and function simply as methods to quantify diversity in neopterygians, and elsewhere in the thesis where some correspondence between morphology and function to ecological variety is implied (Chapter 3 Q5, this chapter Q5) the caveat regarding the uncertainty in this relationship is clearly stated.

Future work – Although rates of speciation and morphological diversification have been explored (e.g. Rabosky et al. 2014), thus far there is very little information regarding the relationship between rates of morphological and functional evolution (*but see* Collar and Wainright 2006). This represents an obvious next step for the neopterygian dataset assembled

here, providing the duel benefit of new results bearing upon the poorly understood relationship between morphological and functional rates, while simultaneously overcoming the non-independence issues of phylogeny (Felsenstein 1985, Collar et al. 2005, O'Meara et al. 2006).

Q2. Is there evidence for early high disparity?

Numerous types of pattern have been incorporated under the umbrella of early high disparity. For example Hughes et al. (2013) cite both the bottom heaviness of clades as a form of early high disparity, and the finding that the disparity of arthropods was comparable in the Cambrian and the Recent, in the absence of any information regarding the top or bottom heavy nature of the clade. Based upon the variability, I define three forms of early high disparity that will aid interpretation of the neopterygian trajectories, and any other clade of organisms: **1) Bottom heavy early high disparity.** The majority of the disparity occurs in the first half of the time series. **2) Uniquely early maximum disparity.** The clade can be either bottom heavy, top heavy or largely symmetrical, yet the all-time peak in disparity uniquely occurs within the first half of the trajectory, and is never matched at any point in the second half of the time series. **3) Shared early maximum disparity.** The clade can be either bottom heavy, top heavy or largely symmetrical, yet an all-time peak in disparity occurs within the first half of the trajectory and *is* matched by another time period (or periods) in the second half of the time series. Thus, even a flat disparity trajectory can be included under this third definition. With these definitions, I aim to assess which, if any, are applicable to holosteans, teleosts and neopterygians as a whole, principally focusing upon the morphological and functional summary trajectories that best capture the uncertainties present.

i) Is early high disparity expected in neopterygian clades under a null model?

A crucial starting point is to consider whether we should expect to see any form of early high disparity under a null model. Under Brownian motion, the disparity of any given clade should increase linearly from time of origin (Felsenstein 1985), thus, early high disparity is unexpected. However, this information alone is insufficient to establish a null model for Mesozoic Neopterygii, since, if more derived fossils actually appear earlier stratigraphically, with early evolving species recovered later in the succession, we would expect early high disparity under a Brownian null. By deriving null models for both morphological and functional datasets across all three clades in exact accordance with the appearance of fossils in the observed data and performed under both fossil and molecular timescales, no form of early high disparity is present in any trajectory (**Fig. A1.7, A1.8**). Instead, disparity increases with time, although the rate of increase appears to slow or halt after the Late Jurassic within holosteans and teleosts, but not within Neopterygii as a whole. Nevertheless, no form of morphological or functional early high disparity is expected under a Brownian null model.

ii) Are any forms of early high disparity present in the observed trajectories?

The summary morphological and functional disparity trajectories for all three clades are presented in **Figure 4.11**, with the midpoint of the time series indicated. All morphological trajectories appear top heavy (**Fig. 4.11a,c,e**). In addition, there is little evidence for **shared early maximum disparity** in Neopterygii, since the Albian contains statistically greater disparity than any time in the first half of the time series in most trajectories (**Table A1.1**), and is only marginally non-significant with *Lagerstätten* are removed. However, holostean and teleost Late Triassic disparity can never be statistically distinguished from any bin in the second half of the time series (**Table A1.2, A1.3**), and so they exhibit **shared early maximum disparity**. However, as previously discussed, uncertainty regarding Late Triassic

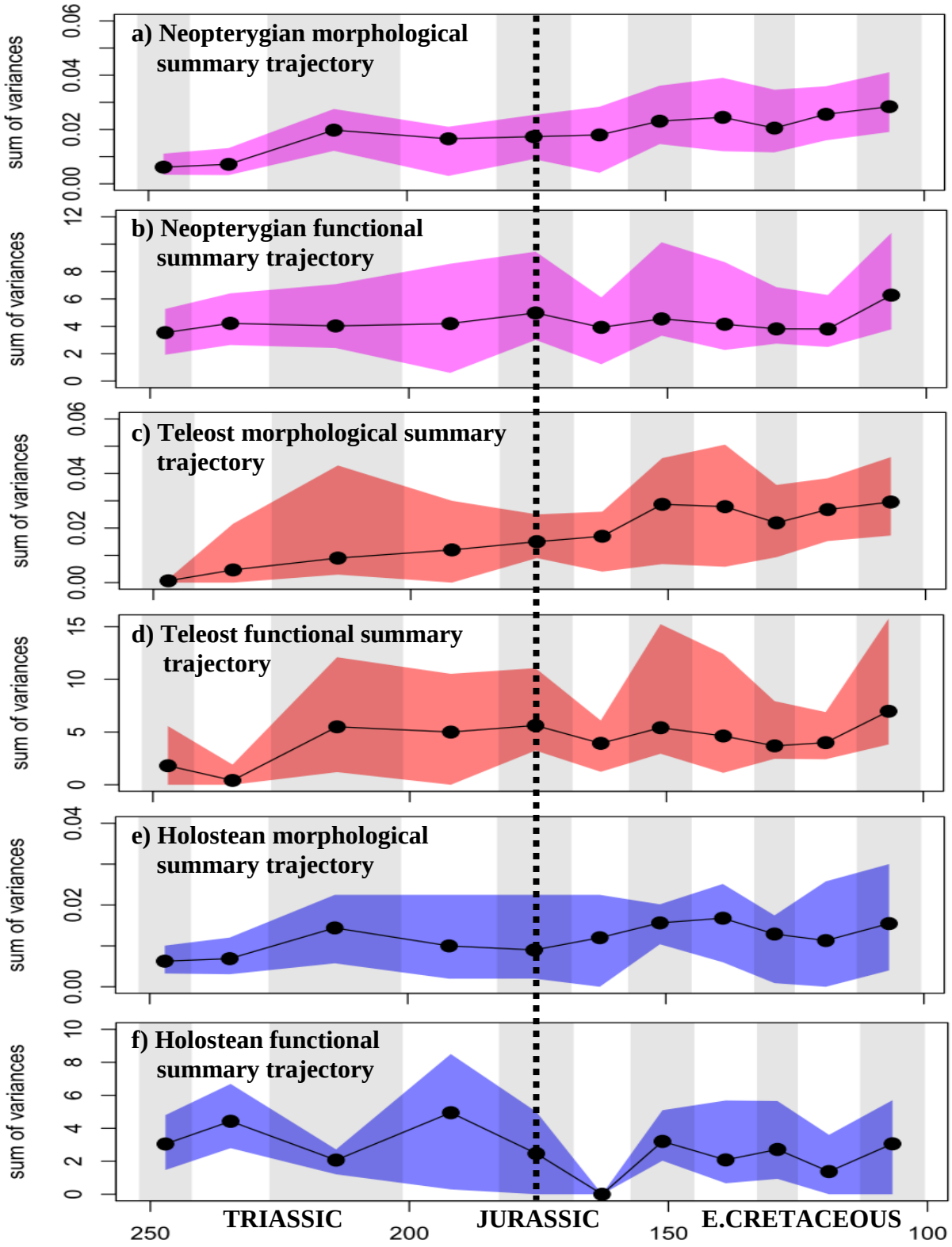

Fig. 4.11. Disparity through eleven Mesozoic time bins based upon the summary trajectories for a) neopterygian morphology, b) neopterygian function, c) teleost morphology, d) teleost function, e) holostean morphology, f) holostean function. Midpoint of time series indicated with a black dashed line.

teleosts suggested their disparity was artificially inflated, rendering **shared early maximum disparity** unlikely for teleosts.

Functional trajectories appear much more stable and symmetrical. As a consequence, all trajectories display **shared early maximum disparity**, as time bins with the greatest disparity in the first half of the time series are statistically indistinguishable from any bin within the second half (**Table A1.4, A1.5, A1.6)**. Furthermore, holosteans almost achieve **uniquely early high disparity**, since their mean disparity in the Middle Triassic (and potentially the Early Jurassic if Dapedidae are holosteans) is marginally larger than any bin in the second half of the trajectory, yet this is not statistically significant (**Table A1.6**). Furthermore, holosteans have the potential to show **bottom heavy early high disparity** if Dapedidae are holosteans and *Lagerstätten* are removed (with the exception of the Early Jurassic *Lagerstätte*, which should be retained). This scenario can be imagined by combining the Early Jurassic disparity from **Fig. A1.6b** with the MiddleJurassic onwards disparity of **Fig. A1.6d/e.**

iii) Conclusions.

Whereas morphological trajectories appear top heavy, with limited evidence for any form of early high disparity, all functional trajectories exhibit **shared early maximum disparity**.
Of the three clades examined, holosteans display the greatest capacity for early high disparity in both morphology and function, unequivocally expressing **shared early maximum disparity** in both trajectories, with some potential to show **uniquely early maximum disparity** and, perhaps, bottom heavy early disparity too if Dapedidae are holosteans.

The majority of clades with truncated morphological trajectories (either by mass extinction or the present day) display a top heavy disparity (Hughes et al. 2013). As such, it might be

expected that our trajectories, arbitrarily truncated at the end of the Early Cretaceous, might also appear top heavy. Morphological trajectories fit this expectation, adding further observational evidence to this general pattern. By contrast functional trajectories are not top heavy. Perhaps this discordance should not be unexpected; the link between truncation and top heaviness in Hughes et al. (2013) was based upon discrete morphological characters, characters which have been demonstrated to show only modest correspondence to functional disparity (Anderson and Friedman 2012). Additionally, other truncated clades that examine functional disparity similarly fail to capture a top heavy pattern, recovering heavy bottom early disparity combined with uniquely early maximum disparity (Anderson et al. 2011, Stubbs et al. 2013). Whether this tendency to attain maximum functional disparity early on is a common feature in the history of clades, a trait common to relatively large datasets, or is purely a coincidental finding resulting from the paucity of studies available for comparison, remains to be seen.

Future work – Beyond the quantification of disparity, further methods to quantify and detect for the three forms of early high disparity could be developed. Such methods exist for detection of top and bottom heavy clades (Hughes et al. 2013) but cannot be immediately applied to the neopterygian dataset without further modification, as it currently fails to account for taxonomic and deposit age uncertainty. It would also be beneficial to determine whether measurement based and cladistic based measures of morphology reveal substantially different results regarding early high disparity. Cladistic disparity may for instance, introduce a directional bias and lower the recorded instances of early high disparity, as workers seek to identify shared derived characters throughout the tree. This may lead to biases in worker effort, where instead of describing ever more characters for taxa that are clearly very different, more time is invested into groups which are similar, to find subtle differences to

resolve their relationships. Therefore unless efforts are made to down weight subtle differences relative to major differences, highly similar species may appear as disparate, purely on the number of characters defined, as highly dissimilar taxa. Further efforts to determine the prevalence of early high disparity in functional is required.

Q.3 Was there a transition from a holostean dominated world to a teleost dominated world within the Mesozoic, and if so, when did the transition occur, and which clades are responsible for its occurrence?

i) Did holosteans ever dominate?

Any Mesozoic transition from a holostean dominated world to one dominated by teleosts first requires that holosteans were substantially more diverse than teleosts early in the Mesozoic. Taxonomically, this is undoubtedly the case, as holosteans with 20+ species represent over 90% of neopterygian species in the Early and Middle Triassic (**Fig. 4.12a-b**). The picture from disparity is less clear (**Fig. 4.12c-d**), since small teleost sample sizes and broad confidence intervals hinder attempts to recover any statistically significant difference between holosteans and teleosts in Early and Middle Triassic in either morphology or function (**Table A1.7, A1.8**). Nonetheless, there are periods where there is no overlap between holostean and teleost confidence intervals, such as the Early Triassic for morphology (**Fig. 4.12c**), and the Middle Triassic for function (**Fig. 4.12d**). Holosteans also possess larger mean morphological and functional disparities than teleosts in the Early and Middle Triassic in every trajectory (**Fig. A1.9, A1.10.**). Furthermore, if Dapedidae are holosteans, their period of dominance could stretch into the first and second Jurassic time bins (**Fig. A1.9b, A1.10b**). Even so, evidence for a long, sustained period of unequivocal holostean dominance, as alluded to in previous accounts, is clearly lacking; their time as morphological and functional dominants is tentative and fleeting at best.

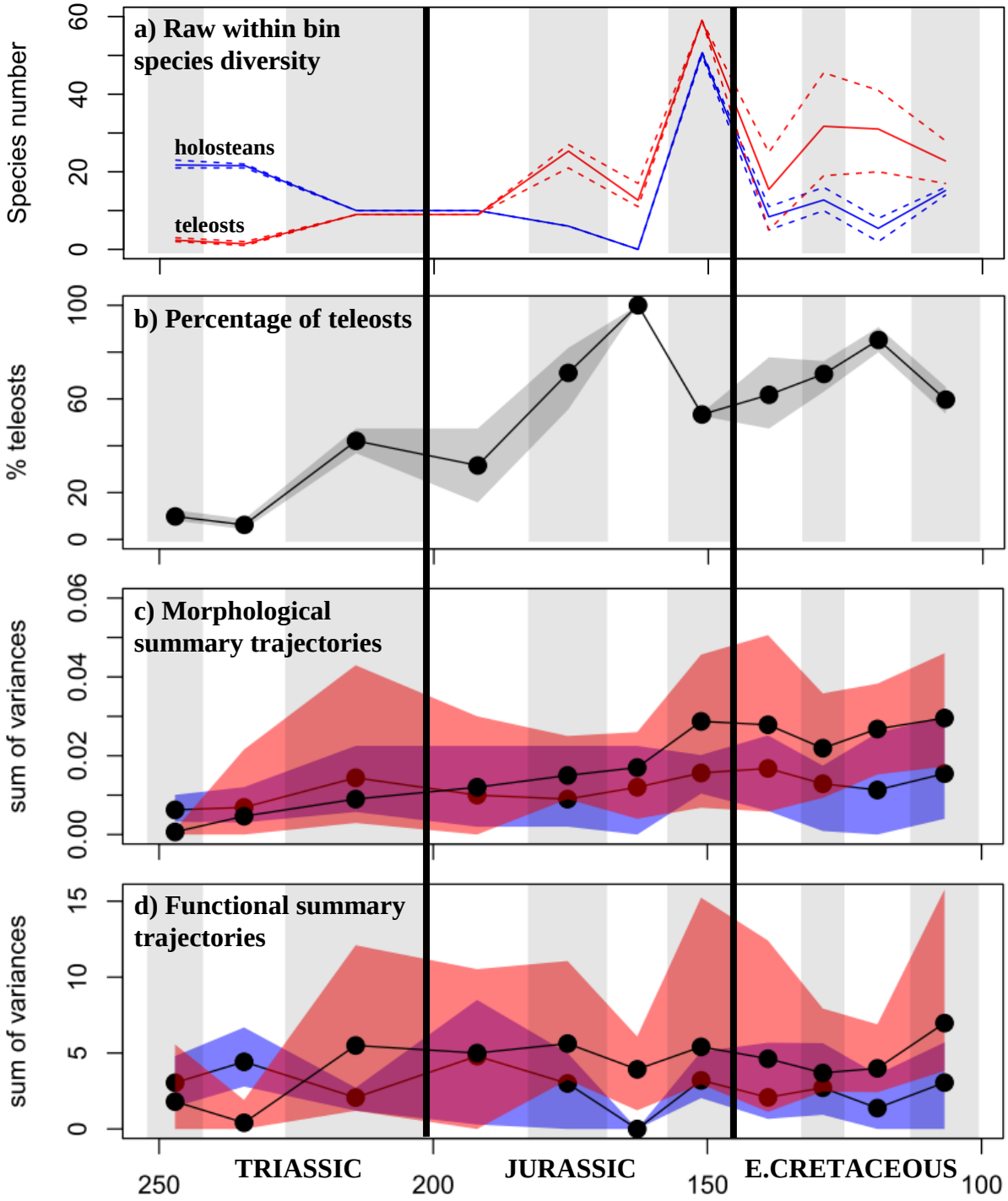

Fig. 4.12. A comparison of holostean and teleost species proportions and disparity across eleven Mesozoic time bins. a) The percentage of neopterygians that are teleosts. b) Summary trajectories for holosteans and teleosts plotted together for b) morphological disparity and c) functional disparity.

ii) Was there a transition to a teleost dominated world, and if so, when does this occur?

A brief examination of the Early Cretaceous in **Fig. 4.12** makes it clear that teleosts did dominate (i.e. show greater diversity) over holosteans taxonomically, morphologically and functionally within the time series I examine. For instance, it is common in the Early Cretaceous for teleosts to represent over 60% of neopterygian taxa (**Fig. 4.12b**), and Early Cretaceous mean teleost disparity is always greater than holostean disparity, in both morphology and function, in all underlying trajectories (**Fig. A1.9, A1.10**). Therefore there clearly is some transition from a world in which holosteans dominate taxonomically and tentatively possess higher disparity, to a world in which teleosts comprise a small majority of taxa and possess marginally higher disparity. The question that remains is when did the transition occur?

As discussed above, the holostean period of reliable (i.e. robust to sampling and taxonomic uncertainty) dominance was brief, restricted to the Early and Middle Triassic. Therefore the transition to a teleost dominated world must occur after this time. The taxonomic transition appears quite clear[2], the Late Triassic witnesses the expansion in the number of teleosts to around 50% of neopterygian species in these time bins, and teleosts proceed to form the majority of neopterygian taxa from the second Jurassic bin onwards (**Fig. 4.12a-b**).

Disparity patterns are less clear, and there is a protracted period of uncertainty, indicated by particularly broad confidence intervals, from the Late Triassic until the Late Jurassic (**Fig. 4.12c-d**). However, the uncertainty does not necessarily imply that holostean and teleost disparity was comparable throughout this period. On the contrary, many trajectories recover

[2] Simply because the pattern appears clear given the data, I do not consider it robust, future work utilising an occurrence database of fishes is required to properly interrogate taxonomic patterns.

significant differences between holostean and teleost disparity, purely driven by the phylogenetic placement of Dapedidae (**Fig. A1.9, A1.10; Table A1.7, A1.8)**. Two scenarios for transition are possible. If Dapedidae are teleosts, the transition occurs in the Early Jurassic, and teleosts maintain their advantage over the time series (**Fig. A1.9a, A1.10a**). However, if Dapedidae are holosteans, the transition does not occur until the Late Jurassic (**Fig. A1.9b, A1.10b**). Just as for the period of holostean dominance, in either scenario, the period of teleost dominance is rarely statistically significant (**Table A1.7, A1.8**), it is a simply a period in which the mean teleost disparity is consistently greater than that of holosteans in every bin, and these mean values are often out of reach of the upper holostean confidence interval.

iii) Is there evidence for a holostean decline over time coincident with a teleost rise, as reported on the basis of richness in textbook accounts?

Taxonomic diversity

My taxonomic pattern shows the greatest concordance with previous accounts given that there is a general increase in teleost diversity over the time period examined while holostean diversity undergoes some form of decline (**Fig. 4.12a**). However, this pattern still differs significantly from previous accounts where holostean disparity remained high throughout the entirety of the time period I examined, before waning suddenly in the Late Cretaceous. Instead, my data show that holosteans had their highest species diversity in the Early and Middle Triassic, before falling in diversity in the Late Triassic and maintaining this lowered diversity throughout my study period (with the exception of a Late Jurassic *Lagerstätten* driven spike in species numbers).

Morphological disparity

There is evidence for increasing teleost disparity with time, yet there is no corresponding decline in holostean morphological disparity, which attains a peak disparity plateau from the Late Jurassic onwards (**Fig. 4.12c**, and see 'Establishing patterns of morphological disparity' section above).

Functional disparity – Functional disparity trajectories for both holostean and teleosts exhibit relative stability (**Fig. 4.12d**, and see 'Establishing patterns of functional disparity' section above), and thus deviates from the waxing teleost, waning holostean pattern described. However, uncertainty may permit interpretations of a holostean decline (see discussion for the potential of a bottom heavy functional disparity in holosteans, Q3 above), but at present, the evidence is equivocal. Therefore for function, as with morphology, there is no clear signal for waxing teleost disparity corresponding to waning holostean disparity as reported in textbook richness accounts, within the time period examined here.

Holostean decline and teleost rise after the Early Cretaceous

Although the patterns described above differ from previous accounts in numerous features, my data pertain only to the first 60% of the neopterygian radiation. Therefore, it is worth considering the neopterygian record following my study period to further characterise the holostean decline and teleost rise. Regarding the taxonomic holostean decline, imagine I were to construct four additional Late Cretaceous time bins 1) Cenomanian (6.6 Ma), 2) Turonian-Santonian (10.3 Ma), 3) Campanian (11.5 Ma), 4) Maastrichtian (6.1 Ma). Based upon information in the appendix Cavin et al. 2007, there appears to be comparable number of holostean species in the Cenomanian (~ 12 species) as there was is the final bin of my dataset (Albian). Holostean species then roughly half in number for the remaining Late Cretaceous bins (Turonian-Santonian: 5 species, Campanian: 4 species, Maastrichtian: 7 species),

showing some resemblance to the sudden Late Cretaceous holostean decline in textbook accounts. The decline then appears to continue, as only 13 species are recovered from the ~40 million years of the Paleogene. According to Grande and Bemis (1998) and Grande (2010), there are then a small number of occurrences of 2 halecomorph genera and 4 ginglymodian genera across the 20 million years of the Eocene, yet none from the Oligocene and Miocene. Thus, regarding taxonomic measures of diversity, the holostean decline, continues after the period studied in this thesis. By contrast, teleosts are responsible for "the second age of fishes" in the Late Mesozoic and early Cenozoic when most of the lineages that make up living actinopterygian diversity arose. Given these observations, some pattern of holostean decline relative to a teleost rise is inevitable. Instead, the main insight from the Triassic, Jurassic and Early Cretaceous is that holosteans, although more diverse than teleosts in the Triassic, were never as diverse as accredited in previous accounts, and that the holostean decline is a long protracted process throughout the Mesozoic, often characterised by long periods of stasis, where species numbers remain relatively constant across numerous time bins. These observations combined appear to conflict with the notion of a sudden replacement from a holostean dominated fauna to a teleost dominated one. Instead, the clades show comparable diversity over long time periods, giving way to a much more subtle transition.

Regarding phenotypic diversity, the main observation from Triassic - Early Cretaceous dataset was the lack of a decline in holostean disparity. On the contrary, holosteans seem to express their highest or joint highest levels of morphological and functional disparity in the last time bin examined (Albian). This pattern of high phenotypic disparity might be expected to continue into the first half of the Late Cretaceous, where a number of holosteans with bizarre morphologies are recovered. For example, alongside morphologies analogous to the living bowfin and gar, there is a highly elongate, eel like morphology (*Aphanepygus*:

Macrosemiiformes), and forms that appear to be suited to deep water environments, with large eyes and fangs (*Tomognathus*:Amiiformes) or ventral-dorsally compressed bodies with multiple rows of sharp teeth (*Lophiostomus*:Amiiformes). Therefore it appears as if holosteans show high phenotypic disparity just before their taxonomic diversity drops in the latter part of the Late Cretaceous. The rest of the holostean record after the Turonian is essentially limited to forms that closely resemble living bowfins and gars. Although this would be assumed to represent low disparity, given multivariate variance was my measure of disparity, it would likely lead to a somewhat misleadingly high characterisation of holostean disparity, due to the non-normally distributed nature of these taxa. Much like the taxonomic patterns discussed, disparity does not show a dramatic peak and trough in holosteans coincident with a rapid teleost increase. Instead, the transition in more subtle, as holostean disparity either increases (morphologically) or remains stable (functionally) across the Mesozoic, even though they may contain greater disparity than teleosts for parts of the Triassic.

iv) How does the observed transition compare with null models of trait evolution?

It is possible that any shift from a world where holosteans show the larger mean disparity to a world where teleosts possess greater disparity would be expected, given my sampling, under a null model of trait evolution. The disparity of holosteans and teleosts under a Brownian motion model of trait evolution, based solely upon the full dataset, is presented for both morphology and function under both fossil based and molecular based timescales (**Fig. 4.13**). One should bear in mind that, because the null trajectories were based upon the full dataset, the trajectories are only directly comparable to that single dataset (where Dapedidae are teleosts and *Lagerstätten* have not been removed). This is justified, as the reliable finding of

greater teleost disparity from the Late Jurassic onwards is apparent in the full dataset, and this represents the main feature I want to examine with the null model.

Different time scaling procedures produce different outcomes as to which clade is more disparate in the Late Jurassic and Early Cretaceous. Under fossil based timescales, a higher disparity holostean world is predicted at this time, whereas under molecular based timescales, teleosts are expected to show greater disparity. This is not unexpected, since molecular based timescales disproportionally alter teleost history, making the crown teleost node over 150 million years older, whereas the holostean crown node remains essentially the same age (Chapter 2). This suggests that if molecular timescales are closer to the truth, the age of teleosts could provide either part, or a full explanation for their greater disparity. This observation can still be relevant even if morphological and functional traits evolve in a non-Brownian manner, so long as time to accumulate disparity is an important variable in alternative models of trait evolution. This is significant as there is evidence that morphology and function evolve in a non-Brownian fashion, both based upon differences in pattern (**Fig. 4.13**), functional disparity remains stable, rather than exhibiting increases in disparity predicted under Brownian motion) and magnitude (**Fig. 4.13**, simulated disparities are much larger than observed disparities).

v) *Are crown teleosts responsible for the relatively higher disparity in teleosts compared with holosteans from the Late Jurassic onwards?*

The arrival of crown group teleosts in the Late Jurassic coincides with a period where teleosts show higher disparity than holosteans, a situation maintained throughout the Early Cretaceous when crown teleosts continue to diversify. I seek to establish whether crown teleost taxa are responsible for producing this period of higher teleost disparity.

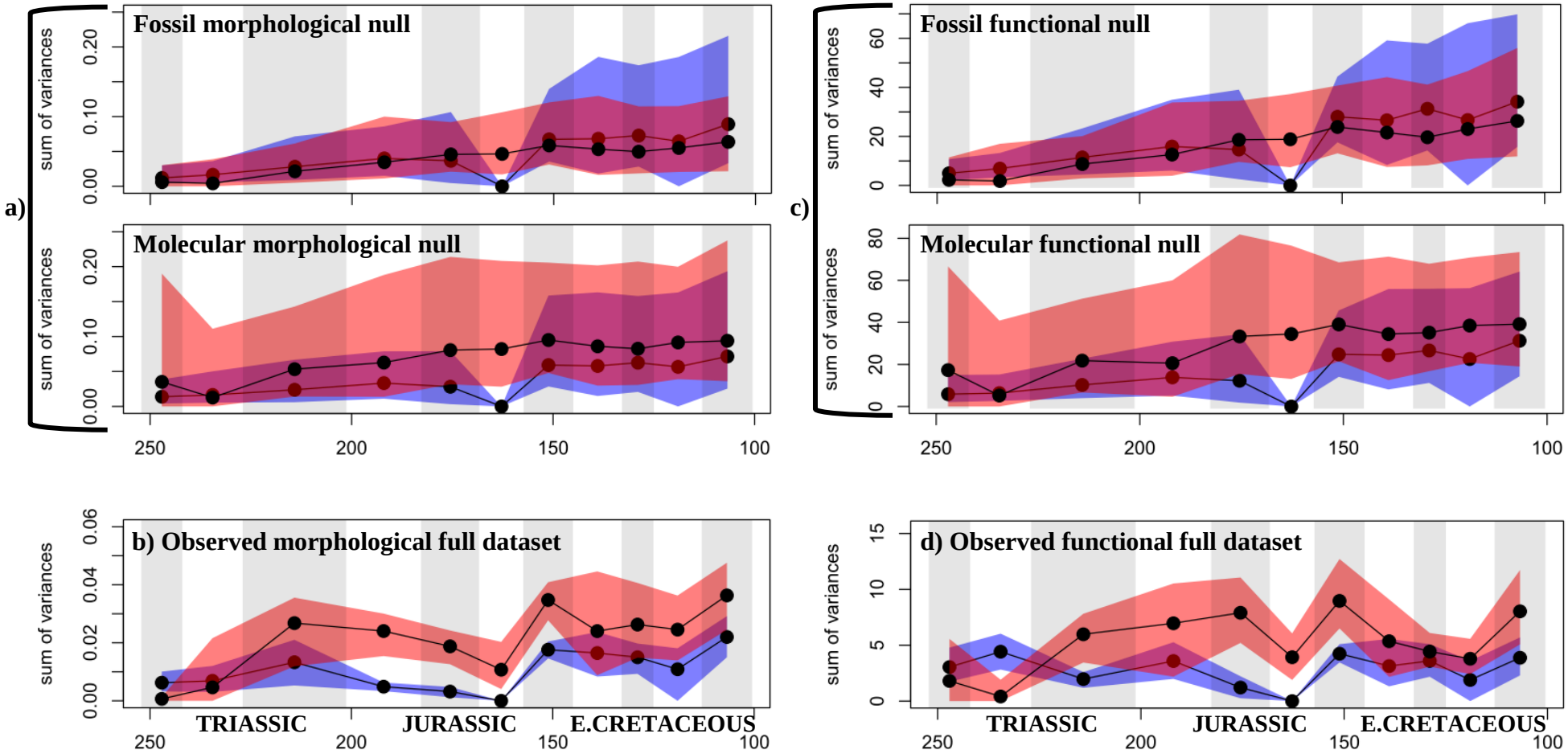

Fig. 4.13. Teleosts and holostean disparity plotted together through eleven Mesozoic time bins. a) Simulated morphological trajectory under Brownian motion applied to (top) fossil only time calibrated trees and (bottom) combined molecular and fossil time calibrated trees. b) Observed morphological disparity trajectories based upon the full dataset of 356 species. c) Simulated functional trajectory under Brownian motion applied to (top) fossil only time calibrated trees and (bottom) combined molecular and fossil time calibrated trees. d) Observed functional disparity trajectories based upon the full dataset of 356 species.

Figure 4.14a illustrates the period from the Late Jurassic onwards in which teleosts show higher disparity than holosteans. **Figure 4.14b** displays the underlying distribution of points in morphospace for each time bin, with stem teleosts plotted in orange and crown teleosts plotted in green. **Figure 4.14b** demonstrates that, at the time where teleosts are first unequivocally more disparate than holosteans (Late Jurassic), teleosts have established the three most extreme regions of their morphospace (top left, bottom left and far right) for the first time. Interestingly, it is the stem teleosts that populate the three extreme regions, particularly the early diverging (but relatively late appearing) lineages. The far right consists of only a single clade, the pycnodonts, whereas taxa in the lower left derive from numerous parts of the teleost stem, including Aspidorhychiformes, Pachycormiformes, Ichthyodectiformes and 'pholidophoriforms'. The upper left region is similarly populated by stem teleosts, deriving from the ' pholidophoriforms ', Crossognathiformes and Leptolepidae, yet it also represents the region to which the first fossil crown teleosts belong, represented by Elopomorpha and a few 'salmonid' euteleosts. Therefore it was not the appearance of crown teleosts in the Late Jurassic that rendered teleosts unambiguously more disparate than holosteans. Instead, the stem teleosts alone are sufficient to create this difference, further evidenced by comparing the disparity of stem teleosts with holosteans (**Fig. 4.14c**). Furthermore, it is clear that the three extremes remain populated by stem teleosts throughout the Early Cretaceous (**Figure 4.14b**, with the exception of the 2nd Early Cretaceous bin, where only a far left to far right occupation is present), maintaining the higher disparity of stem teleosts relative to holosteans. In fact, the difference between holostean and stem teleost disparity appears greater than when holosteans are compared to total group teleosts (**Fig. 4.14a vs c**). However, stem teleost disparity confidence intervals are fairly broad. What crown teleosts contribute, from the 2nd Early Cretaceous bin onwards, is to reduce the uncertainty in the pattern.

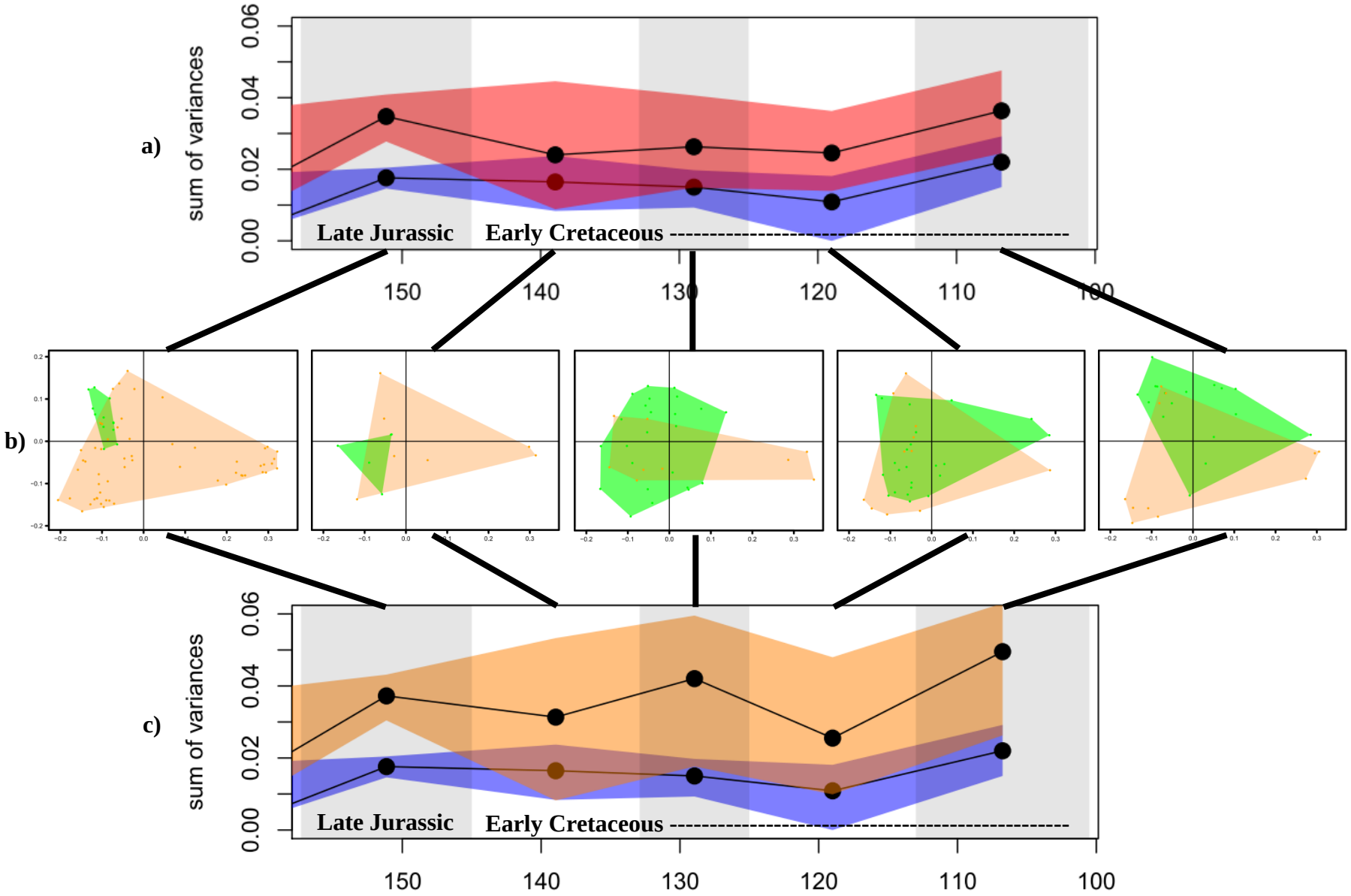

Fig. 4.14. The pattern of morphospace occupation underlying larger teleost disparity, compared with holosteans, from the Late Jurassic onwards. a) Full dataset disparity for teleosts (red) and holosteans (blue). b) Morphospace occupation in the full dataset, of stem teleosts (orange) and crown teleosts (green). c) Full dataset disparity for stem teleosts (orange) and holosteans (blue).

Near identical conclusions can be made for functional disparity, where stem teleosts alone are sufficient to maintain greater disparity in teleosts compared with holosteans in the Late Jurassic and Early Cretaceous (**Fig. 4.15**). Once again, the contribution of crown teleosts is to reduce uncertainty, and lower the mean disparity of teleosts slightly. Where functionspace occupation differs is that stem teleosts do not form easy definable extreme clusters. Instead, they form a general diagonal spread between the upper right quadrant of functionspace (positive PC1 and PC2 scores) and the lower left quadrant (negative PC1 and PC2 scores) (**Fig. 4.15**). The occupation seen in the Late Jurassic is exaggerated by *Lagerstätten,* and resembles more closely the first three Early Cretaceous time bins on removal. In contrast, the increase in disparity apparent in the Albian is robust to *Lagerstätten* removal, and is again driven by stem teleosts, which represent nearly every historical functional extreme simultaneously at this time, while crown teleosts cluster centrally (Fig. 4.15b).

vi) *Conclusions*

1. There was a transition from a world of higher holostean richness and disparity to a world of higher teleost richness and disparity within the Mesozoic. However, my pattern differs substantially from previous accounts (Romer 1966, Colbert 1969) in two main ways. First, the period of holostean dominance (as measured by disparity) is somewhat tentative and short lived in contrast to the protracted period of holostean dominance previously suggested to have spanned the Triassic, Jurassic and the Early Cretaceous (by taxonomic measures). Second, there is no clear evidence for the account of waning holostean diversity coincident with a waxing teleost diversity, as holostean disparity either remains stable (function) or shows some sign of increase with time, expressed as top heaviness (morphology).

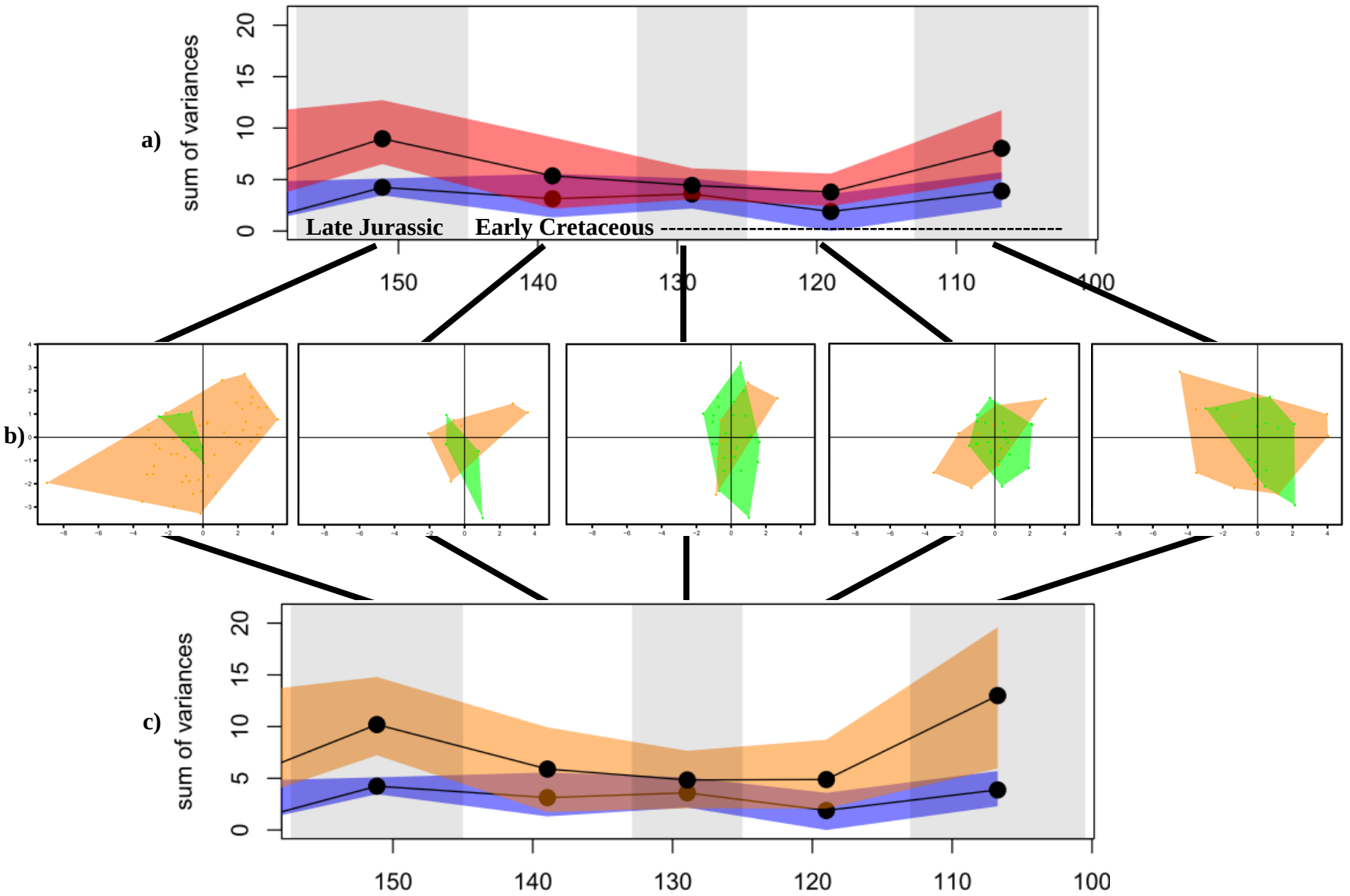

Fig. 4.15. The pattern of functionspace occupation underlying larger teleost disparity, compared with holosteans, from the Late Jurassic onwards. a) Full dataset disparity for teleosts (red) and holosteans (blue). b) Functionspace occupation in the full dataset, of stem teleosts (orange) and crown teleosts (green). c) Full dataset disparity for stem teleosts (orange) and holosteans (blue).

2. The principal reason that my account differs so drastically from previous accounts is not solely because I focus mainly upon disparity, rather than taxonomic patterns. Instead, it is the substantial change in the phylogenetic relationships of neopterygians between previous accounts and those summarised by the supertrees that likely account for the differences. All of the most morphologically extreme groups, now included within the teleost stem, were previously considered holosteans (Pycnodontiformes, Pachycormiformes, Aspidorhynchiformes and numerous 'pholidophoriforms'). Their inclusions within Holostei would have undoubtedly altered the trajectories to more closely approximate previous accounts, since holosteans would have appeared taxonomically, morphologically and functionally dominant throughout the Triassic, Jurassic and Early Cretaceous. Some authors still question the affinity of the early diverging stem teleost groups (e.g. Pachycormiformes: Arratia and Schultze 2013) and further work clarifying their placement should be a priority for Mesozoic neopterygian systematic research. Nevertheless, even with substantial changes in our phylogenetic understanding, holostean remain taxonomically dominant in the Triassic.

3. Null models indicate that, given my sampling, a pattern of higher teleost disparity throughout the Late Jurassic and Early Cretaceous is more likely under molecular time scales. However, discrepancies between the pattern and magnitude of observed and null disparity suggest that disparity evolves in a non-Brownian fashion.

4. The appearance of crown group teleosts does not underpin the period of higher teleost disparity from the Late Jurassic onwards. Instead, it is principally the early diverging (but relatively late appearing) lineages of stem teleosts that occupy extreme regions of morphospace that determine the overall pattern.

Q4. Is there any evidence of changes over the Triassic – Jurassic extinction boundary?

Differences in both disparity and phenotypic space occupation were examined over the Triassic-Jurassic (TJ) boundary for the Neopterygii. *Lagerstätten* removal approaches completely determine the outcome in terms of disparity changes (**Table 4.1**). I briefly outline the details below, before discussing changes over the boundary observed if the *Lagerstätte* in the Early Jurassic is retained.

The Late Triassic and Early Jurassic each possess a deposit with 10 and more crown neopterygian taxa for which fully articulated and complete body specimens are known. These are the Zorzino limestone (aka. Calcare di Zorzino, ZZ limestone) of northern Italy for the Late Triassic, and for the Early Jurassic, the various deposits in southern England, most commonly exposed at Lyme Regis, attributable to either the Blue Lias Formation or Charmouth Mudstone Formation, considered together here as a single deposit, as precise bed information is often lacking. Removal of these two *Lagerstätten* always results in a decline in both morphological and functional disparity over the TJ boundary in the Neopterygii. Furthermore, these declines are not brought about by the inflation of Late Triassic disparity (which declines when the Zorzino limestone is removed) but by a huge reduction in Early Jurassic disparity due to the disappearance of all deep-bodied taxa. The majority of taxa known from the Early Jurassic derive from southern England, and so removal of this deposit eliminates most of the diversity present. Under these circumstances, where *Lagerstätten* removal leaves considerably less taxa in a bin compared with surrounding time bins, it is arguably better to retain the site for fairer comparison, especially when sample sizes are already small. Therefore for this specific part of the time series (Early Jurassic) I recommend

retention of sites from southern England, and interpret disparity and morphospace occupation under these conditions.

Morphological changes (**Fig. 4.16a**) – Neopterygian morphological disparity remains relatively stable over the TJ boundary with *Lagerstätten* retained (**Table 4.1, Fig. A1.1a,d**). In terms of morphospace occupation, this situation arises because very little changes in terms of morphospace occupation (**Fig. 4.16a**), as in both the Late Triassic and Early Jurassic, there is a band of taxa ranging between taxa close to the origin and those with highly positive scores in RW1 (**Fig. 4.16**). There are, however, some changes that likely account for a slight lowering of the mean disparity over the TJ boundary. These include a greater density of taxa around the origin, the loss of taxa with the largest RW2 and smallest RW3 scores, and the positioning of deep-bodied taxa with slightly less positive RW1 scores. Furthermore, there is some taxonomic changeover. The loss of the most extreme RW1 values is due to the absence of Pycnodontiformes, but they are known from dentitions throughout the Jurassic, and articulated specimens in the Late Jurassic. The deep-bodied representatives in their place, with slightly less positive RW1scores, are all from the same genus, *Dapedium*. The absence of Macrosemiiformes accounts for the loss of highly positive RW2 and highly negative RW3 values. However, they are not extinct, since, as with Pycnodontiformes, articulated forms return in the Late Jurassic. The only other change of note is that the space originally occupied only by 'pholidophoriforms' on weakly negative RW1 scores, become invaded by numerous holosteans, from both the gar stem (Caturus:Amiiformes) and bowfin stem (Furo:Ionoscopiformes).

		Full dataset		*Lagerstätten* removal	
Neopterygians	Morphological	stable	0.378	decline	0.003
	Functional	stable/ non-sig. increase	0.124	decline	0.153

Table 4.1. The pattern of change in morphological and function disparity over the Triassic-Jurassic boundary under a range of analyses presented alongside t test p values.

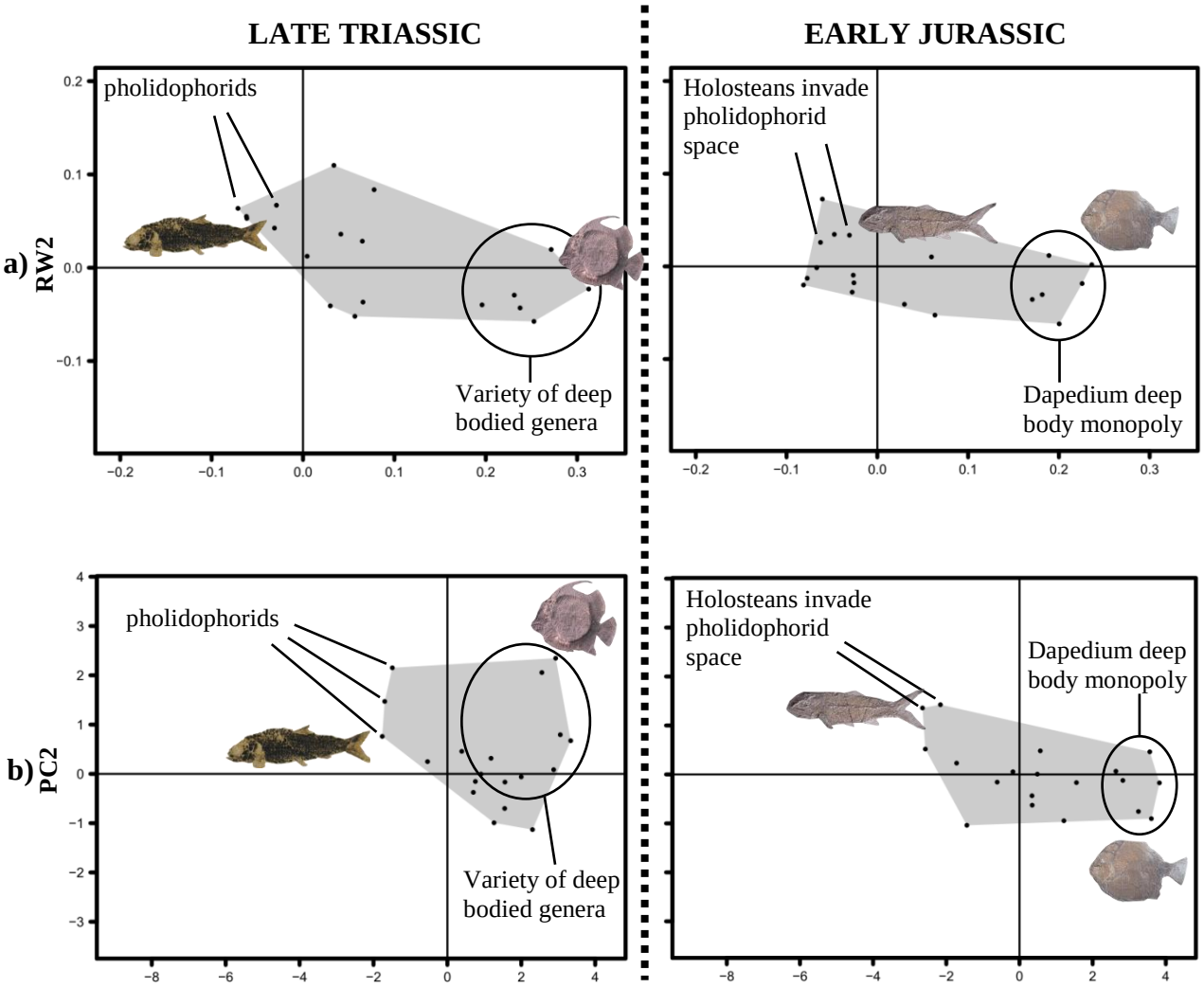

Fig. 4.16. Changes in ordination space occupation over the Triassic-Jurassic boundary according to a) morphology (RW1-2) and b) function (PC1-2). The Late Triassic represents the Norian-Rhaetian (25.7 Ma), and the Early Jurassic the Hettangian-Pliensbachian (18.6 Ma).

Functional changes (**Fig. 4.16b**) – Neopterygian function disparity remains relatively stable over the TJ boundary with *Lagerstätten* retained (**Table 4.1**, **Fig. A1.4a,d**). However, this stability is accompanied by some changes in functionspace occupation. As discussed above, the variety of deep-bodied forms in the Late Triassic give way to a *Dapedium* monopoly in the Early Jurassic. Whereas in morphology, this change only resulted in a slight lowering of RW1 scores, functionally the changes are more pronounced. This results in the complete disappearance on the upper right region of functionspace (strongly positive PC1 and PC2 scores, where Pycnodontiformes were present), and instead, deep-bodied holosteans have even more extreme PC1 scores, but PC2 scores around zero (**Fig. 4.16b**). This signals the difference between taxa with some of the lowest body aspect ratios (Pycnodontiformes), and *Dapedium* species with the largest jaw-opening mechanical advantages. As with morphology, holosteans also invade regions of functionspace previously only occupied by 'pholidophoriforms' (the upper left region of functionspace), forms with smaller jaw-closing mechanical advantages and longer jaws relative to their body length.

Conclusions

Neopterygians exhibit stability over the Triassic-Jurassic boundary in morphological and functional disparity. However, this is accompanied by some changes to ordination space occupation, and taxonomic composition. Three observations seem particularly noteworthy. First, holosteans, absent from negative RW1 and negative PC1 scores in the Late Triassic, occupy these regions in the Early Jurassic, essentially invading space that was unique to Late Triassic teleosts. However, there may be no real significance to this observation, since holosteans commonly occupied this space in the Early and Middle Triassic. Second, there are substantial changes associated with deep-bodied taxa over the boundary. The relatively diverse assemblage of such forms in the Late Triassic, which derive from six different genera,

both holosteans and teleosts, is replaced in the Early Jurassic solely by species of *Dapedium*, which appear functionally distinct from most Triassic deep-bodied forms. Third, if *Dapedium*, and Dapedidae more generally are teleosts instead of holosteans, the Triassic-Jurassic boundary marks the disappearance of deep-bodied holosteans. However, if Dapedidae are holosteans, deep-bodied holosteans remain until the Jurassic-Cretaceous boundary.

The above results and observations represent one of the very few pieces of evidence to bear on the potential impacts of the Triassic-Jurassic extinction in fishes beyond the observation by Hallam (2002) that no osteichthyan family goes extinct across the boundary (based upon range data presented The Fossil Record 2: Gardiner 1993, Patterson 1993). Comparable with these findings, disparity remains stable for the Neopterygii, and the pattern of phenotypic space occupation exhibits only subtle changes, comparable to the types of changes that occur between other successive time bins in the time series (Chapter 3 Q4). In fact, the similarities between Late Triassic and Early Jurassic phenotypic space occupation are strikingly similar, more so than is typical between successive Triassic or Jurassic time bins (Chapter 3 Q4). The only speculative signs of decline could cite the temporary absence of Macrosemiiformes and Pycnodontiformes, the dominance of *Dapedium* as some form of disaster taxon (also common during the Toarcian OAE that occurs within the Posidonia shales) and even more speculatively, the lack of Parasemionotiformes, which are also absent from the Late Triassic, on the chance they persisted in the Late Triassic unsampled, and instead disappeared at the end-Triassic.

These results agree more generally with Hallam's (2002) failure to find convincing evidence of a global disaster over the boundary, but contrasts with recent findings that indicate clear declines in disparity over the boundary in crurotarsans (Stubbs et al. 2013) and ichthyosaurs

(Thorne et al. 2011). However, the findings here, and those of numerous other analyses are vulnerable because much of the diversity in both the Late Triassic, but especially the Early Jurassic derive from two *Lagerstätten,* the Zorzino limestone and the combined Blue Lias + Charmouth Mudstone formations, respectively. As such, it is difficult to make broad generalisations based upon them.

Future work – This study, as well as numerous others (e.g. Friedman 2010, Thorne et al. 2011, Benson and Druckenmiller 2014) highlight the utility of disparity (based upon species occurrence data) in illuminating patterns of change over proposed extinction boundaries. Regarding the Triassic-Jurassic boundary, there is need for more work in this vein, especially to determine whether disparity changes in other groups of fishes are as subtle as those observed here for neopterygians.

Q5. Is there any evidence for a growing significance of durophagous taxa, consistent with claims of a Mesozoic Marine Revolution?

A growing significance (richness, disparity and increasing destructiveness) of durophagous neopterygian fishes, a key line of evidence supporting the notion of a MMR, is tested in three aspects of their diversification. First, I examine the percentage of neopterygians with specialised crushing dentitions (**Fig. 4.17a**). The percentage of distinguishable durophages (i.e. taxa that possess batteries of flattened, peg like teeth) is low in the first Triassic bin, but steadily increases throughout the Triassic and peaks between 30 and 40% of all taxa in the

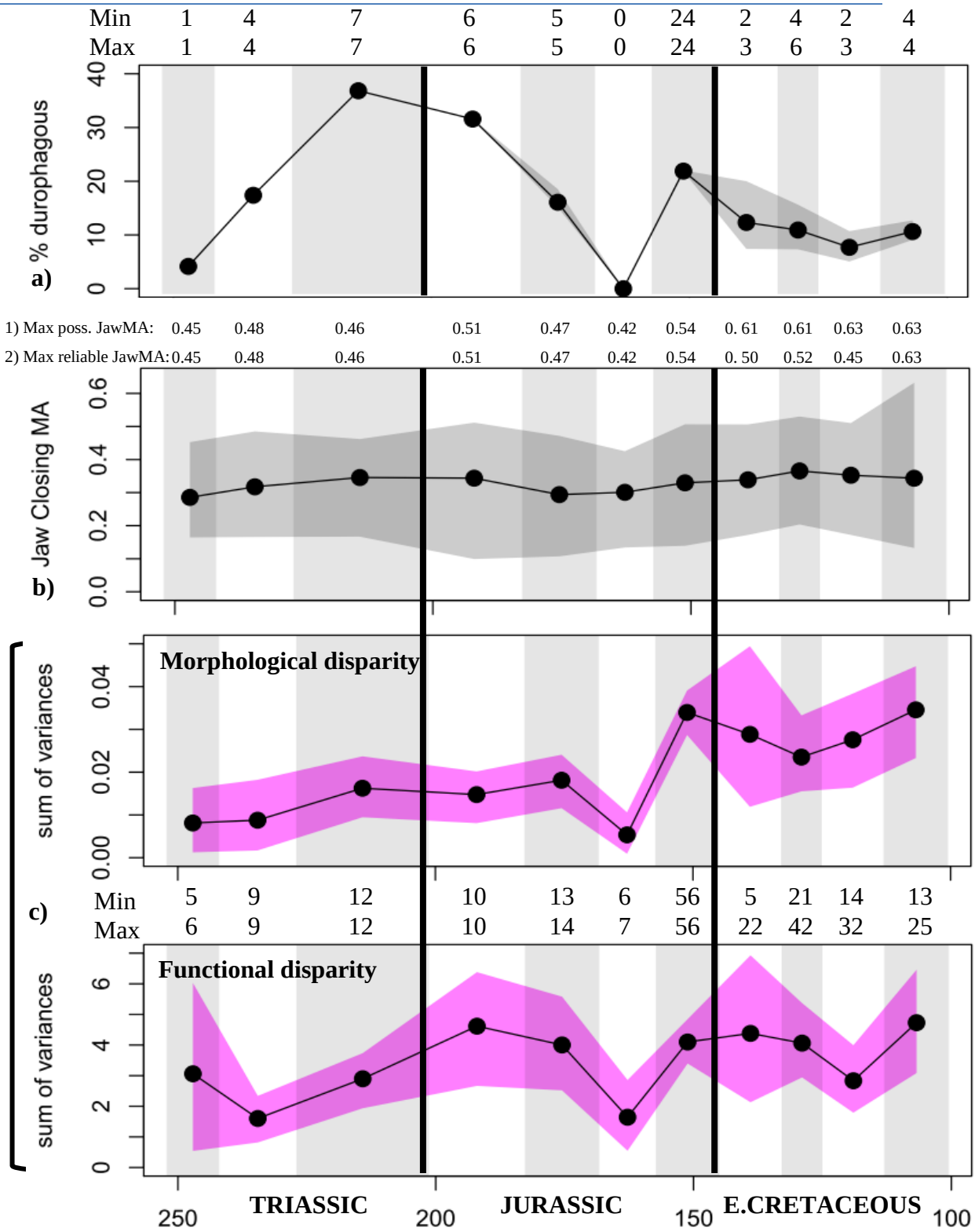

Fig. 4.17. Four patterns of diversification, through eleven time bins, that are pertinent to testing the predictions of the Mesozoic Marine Revolution. **a)** The percentage of neopterygians with specialised crushing dentitions, **b)** The distribution of mechanical advantages of jaw closing. **c)** The morphological (top) and functional (bottom) pattern of disparity for taxa with larger than average mechanical advantage of jaw closing. 95% confidence limits are presented for each based upon 100 replicates that account for stratigraphic and taxonomic uncertainty. 95% CI's in c) also incorporate bootstrapping. Maximum and minimum numbers of taxa (due age uncertainty preventing certain assignment of some taxa to a single time bin) that fall within each time bin (across 100 replicates) for the relevant analysis are provided (i.e. those with crushing dentitions in **a**, and taxa with higher than average jaw-closing MAs in **c**).

Late Triassic and Early Jurassic. This percentage falls to around 20% in the latter part of the Jurassic (with the exception of the 3rd Jurassic bin, which is poorly sampled and reports no clear durophages), and falls further to around 10% in the Early Cretaceous. Thus, there is no increasing proportion of clearly identifiable durophages throughout the Mesozoic. Furthermore, although the percentage drops, the absolute numbers of clear durophages remain comparable, indicating that it is the proliferation of neopterygians without specialised crushing dentitions that causes the percentage of clear durophages to fall.

Second, I examine the distribution of jaw-closing MAs to assess whether there is any tendency for average jaw-closing MA to increase (towards greater bite forces) throughout the Mesozoic, consistent with the expectation that taxa became more destructive in their feeding capabilities. There is no evidence for an increase in average jaw-closing mechanical advantage though time (**Fig. 4.17b**), and no two time bins approach any significant difference in jaw-closing MA (**Table 4.2a**). However, there is a trend for increasing maximum jaw-closing MA through the Mesozoic. Specifically, although the maximum appears drift between higher and lower values across three time slices of the Triassic, and the following three time slices of the Jurassic, from the Late Jurassic onwards jaw-closing MA's remain consistently high (**Fig. 4.17b**). Not only is this Late Jurassic increase in jaw-closing MA (and the maintenance of these higher values in the Early Cretaceous) apparent from the upper bound of the 95% CI presented in **Fig. 4.17b,** but it is also apparent in the raw maximum values (i.e. taxa that fall outside of the 95% confidence envelope) provided above the figure. Two rows of values are presented: 1) the largest possible individual maximum jaw-closing MA, which considers all taxa that might potentially be assigned to a given time bin (i.e. taxa whose ages are poorly constrained that may jump between different time bins when their ages are randomised in different replicates), and 2) the reliable individual maximum jaw-closing MA,

which considers only those taxa which are unequivocally assigned to that time bin (i.e. taxa whose ages are sufficiently well constrained that they can be assigned to a particular time bin with full confidence). Both sets of values indicate that taxa with jaw-closing MAs of 0.5 or larger likely persist in every time bin from the Late Jurassic onwards. Finally, according to the 95% Cis, there is a noticeable expansion in the range of forms with both very high jaw-closing MAs in the final time bin of the series (Albian), concurrent with an expansion in taxa with very small jaw-closing MAs (**Fig. 4.17b**).

Third, I examine whether the morphological and functional disparity of potential durophages (taxa with larger than average jaw-closing MAs) increases throughout the Mesozoic, consistent with the notion that durophages pose a more varied ecological threat with time (strictly under the assumption that morphology and function correlate loosely with ecology). The morphological disparity of high MA taxa increases throughout the Mesozoic (**Fig. 4.17c**), in a three tiered manner. Initially there is an Early-Middle Triassic low, increasing slightly to a Late Triassic-Middle Jurassic plateau, increasing dramatically to a Late Jurassic-Early Cretaceous plateau, although comparisons between tiers are not always statistically significant (**Table 4.2b**). Functional disparity appears more stable (Fig. 4.17c), yet average disparity from the Early Jurassic onwards appears to form a relatively stable plateau (with the exception of instances of poor sampling) that is higher than disparity levels in the Triassic, sometimes significantly so (Table 4.2c). Furthermore, Figure 4.17c also indicates a higher richness in the Late Jurassic and Early Cretaceous compared to earlier in the Mesozoic. Thus, not only do taxa with larger mechanical advantage appear to attain greater morphological disparity, but greater richness also.

a) Jaw-closing mechanical advantage

	AOI	CL	RN	PSH	BAT	OCB	TiKi	ValBer	BarHau	Apt	Alb
AOI	1	0.787117	0.572454	0.624286	0.951885	0.885211	0.844977	0.670319	0.572696	0.589617	0.702087
CL	0.787117	1	0.826208	0.851323	0.87618	0.89766	0.959401	0.878379	0.752035	0.795874	0.873768
RN	0.572454	0.826208	1	0.987052	0.736097	0.68356	0.950132	0.959828	0.901104	0.960311	0.98982
PSH	0.624286	0.851323	0.987052	1	0.756254	0.735721	0.956681	0.972945	0.89322	0.950298	0.999427
BAT	0.951885	0.87618	0.736097	0.756254	1	0.96495	0.86016	0.750066	0.610757	0.656938	0.747754
OCB	0.885211	0.89766	0.68356	0.735721	0.96495	1	0.915782	0.791308	0.699728	0.720626	0.810857
TiKi	0.844977	0.959401	0.950132	0.956681	0.86016	0.915782	1	0.962263	0.815636	0.890153	0.938146
ValBer	0.670319	0.878379	0.959828	0.972945	0.750066	0.791308	0.962263	1	0.83859	0.90986	0.973451
BarHau	0.572696	0.752035	0.901104	0.89322	0.610757	0.699728	0.815636	0.83859	1	0.913244	0.869669
Apt	0.589617	0.795874	0.960311	0.950298	0.656938	0.720626	0.890153	0.90986	0.913244	1	0.944885
Alb	0.702087	0.873768	0.98982	0.999427	0.747754	0.810857	0.938146	0.973451	0.869669	0.944885	1

b) Morphological disparity

	AOI	CL	RN	PSH	BAT	OCB	TiKi	ValBer	BarHau	Apt	Alb
AOI	1	0.916545	0.151549	0.168471	0.065947	0.548329	0.001982	0.260631	0.198771	0.128718	0.020481
CL	0.916545	1	0.182111	0.251267	0.079686	0.538122	0.000368	0.189517	0.138775	0.078684	0.007836
RN	0.151549	0.182111	1	0.740904	0.678381	0.03676	0.003269	0.339023	0.395948	0.216971	0.026366
PSH	0.168471	0.251267	0.740904	1	0.431522	0.031315	0.003019	0.324215	0.344925	0.19618	0.025063
BAT	0.065947	0.079686	0.678381	0.431522	1	0.011337	0.004438	0.379251	0.495478	0.265261	0.031031
OCB	0.548329	0.538122	0.03676	0.031315	0.011337	1	0.000255	0.170054	0.102445	0.062149	0.006304
TiKi	0.001982	0.000368	0.003269	0.003019	0.004438	0.000255	1	0.483889	0.0357	0.236704	0.906687
ValBer	0.260631	0.189517	0.339023	0.324215	0.379251	0.170054	0.483889	1	0.567077	0.901997	0.587961
BarHau	0.198771	0.138775	0.395948	0.344925	0.495478	0.102445	0.0357	0.567077	1	0.562941	0.122836
Apt	0.128718	0.078684	0.216971	0.19618	0.265261	0.062149	0.236704	0.901997	0.562941	1	0.367042
Alb	0.020481	0.007836	0.026366	0.025063	0.031031	0.006304	0.906687	0.587961	0.122836	0.367042	1

c) Functional disparity

	AOI	CL	RN	PSH	BAT	OCB	TiKi	ValBer	BarHau	Apt	Alb
AOI	1	0.241662	0.887984	0.320295	0.515828	0.337517	0.38882	0.57649	0.553434	0.871106	0.36302
CL	0.241662	1	0.036401	0.005414	0.018715	0.951257	0.007947	0.139201	0.066094	0.244333	0.030645
RN	0.887984	0.036401	1	0.071009	0.219545	0.103754	0.140558	0.363182	0.315886	0.944651	0.143226
PSH	0.320295	0.005414	0.071009	1	0.587485	0.018615	0.580135	0.897369	0.672685	0.108509	0.935995
BAT	0.515828	0.018715	0.219545	0.587485	1	0.046579	0.905051	0.811584	0.957598	0.228311	0.557243
OCB	0.337517	0.951257	0.103754	0.018615	0.046579	1	0.02199	0.199913	0.11225	0.327262	0.060637
TiKi	0.38882	0.007947	0.140558	0.580135	0.905051	0.02199	1	0.765855	0.956228	0.049162	0.419245
ValBer	0.57649	0.139201	0.363182	0.897369	0.811584	0.199913	0.765855	1	0.790963	0.194392	0.804868
BarHau	0.553434	0.066094	0.315886	0.672685	0.957598	0.11225	0.956228	0.790963	1	0.148997	0.511798
Apt	0.871106	0.244333	0.944651	0.108509	0.228311	0.327262	0.049162	0.194392	0.148997	1	0.053089
Alb	0.36302	0.030645	0.143226	0.935995	0.557243	0.060637	0.419245	0.804868	0.511798	0.053089	1

Table 4.2. P values derived from t tests comparing **a)** jaw-closing mechanical advantage between time bins, **b)** morphological disparity between time bins and **c)** functional disparity between time bins. Significant differences highlighted in red.

Conclusions

Evidence for a growing significance of neopterygian durophages could derive from a range of sources, including absolute numbers, abundances or proportions of taxa with specialised crushing dentitions, increases in average, maximum or minimum jaw-closing MAs, or data on the disparity of forms with large jaw-closing MAs. Absolute and relative numbers of taxa with specialised crushing dentitions remain stable and decrease respectively across the time series, and the average jaw-closing MA of neopterygian taxa also remains stable across all bins. Thus, these lines of evidence fail to support any increasing significance of durophagy. On the contrary, examination of the maximum jaw-closing MA and the morphological and functional disparity of potential durophages (i.e. those taxa with greater than average jaw-closing MAs) could be taken to indicate some growing significance of durophagy throughout the Mesozoic. Specifically, maximum jaw-closing MA and morphological disparity appear to increase in the Late Jurassic and remain high throughout the Early Cretaceous, while functional disparity peaks and remains high from the Early Jurassic onwards. The jaw-closing MA results suggest the arrival and survival of taxa with larger than ever before mechanical advantages, while the increased disparity of potential durophages could be taken to represent a more varied ecological threat from durophages in the Jurassic and Cretaceous.

Before placing elevated maximum jaw-closing MAs and greater disparity of potential durophages into context, it is worth reiterating the limitations of the potential durophage disparity results. First, these potential durophages were arbitrarily chosen as those taxa with greater than average jaw-closing MAs. There are currently no broad surveys of living taxa to establish whether this is true (David Bellwood, personal communication), making choice of a sensible cut off for potential durophages difficult. Instead, it was inspired by the observation that taxa with around the average abilities for crushing in Bellwood et al. (2006) and above

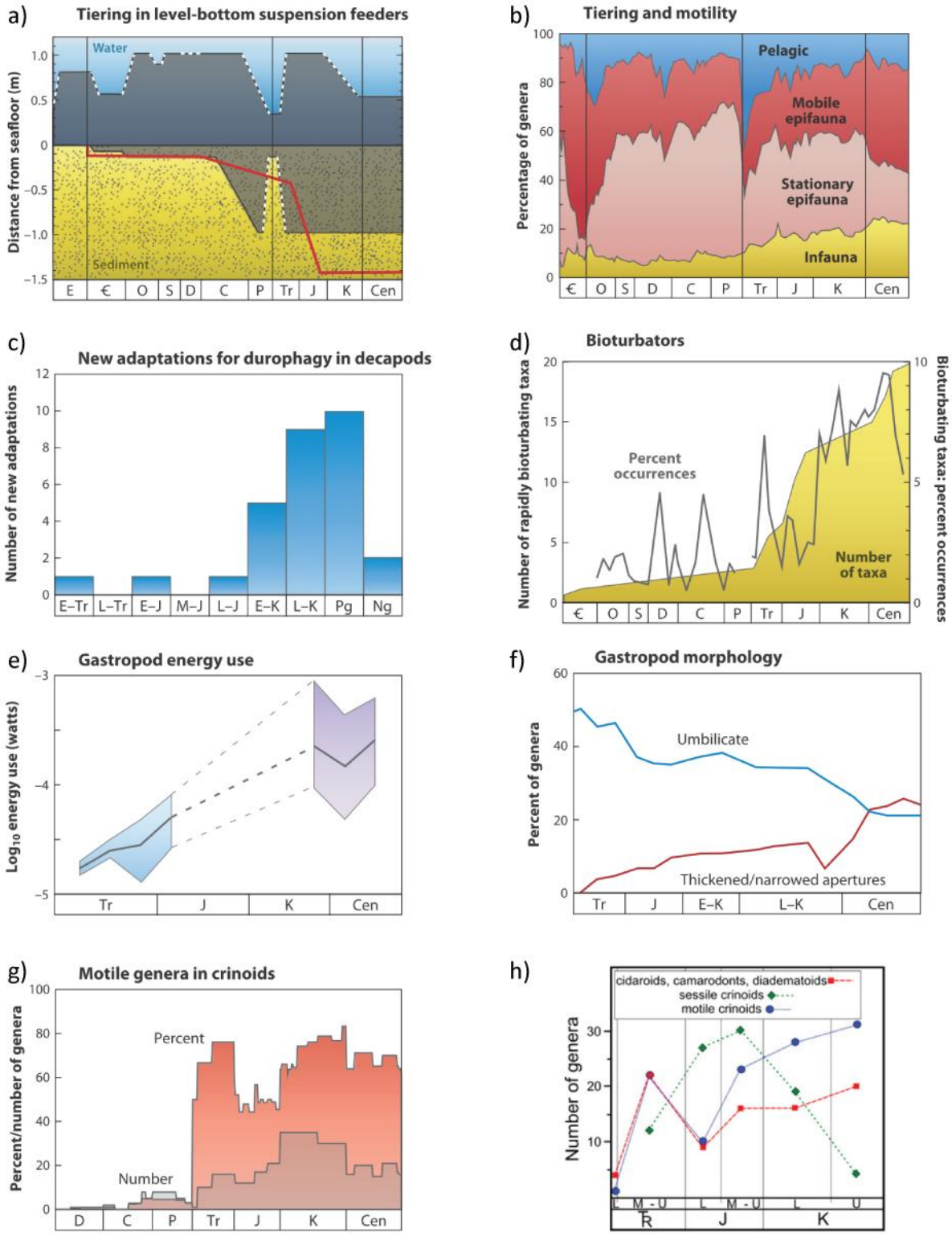

Fig. 4.18. Patterns in invertebrate groups pertinent to the Mesozoic Marine Revolution. **a)** Tiering, where the red line is the maximum average depth of bioturbation. **b)** Proportional diversity of different tiers and motility levels, based on Sepkoski's genus compendium. **c)** Percentage abundance and diversity of bioturbators. The grey line captures the % of bioturbating taxa in the PBDB, while the yellow field captures the absolute numbers of rapidly bioturbating taxa. **d)** Number of new durophagous adaptations per time bin in decapod crustaceans. **e)** Medians and 95% quantiles for gastropod energy use. **f)** Gastropod morphology trends, where predation-resistant morphologies increase and predation-susceptible morphologies decrease through time. **g)** Percentage and number of motile crinoid genera. **h)** Numbers of motile and sessile cronoids, and the number predatory sea urchin taxa across the Mesozoic. Figures **a-g** taken from Bush and Bambach (2011), while figure **h** is taken from Gorzelak et al. (2012).

can exhibit moderate durophagy. Second, as made clear in the introduction and methods, but also in Chapter 3 and Q1 of this chapter, the relationship between morphology, function and ecology is poorly constrained. Thus, whether the greater disparity observed for these potential durophages unequivocally translates into a greater range of ecologies is difficult to demonstrate without additional work on the morphological and functional correlates of ecology in living fishes. Thus, although there is some uncertainty in the disparity results, the disparity increase is interesting none the less, and will be discussed in relation to the MMR.

If increasing maximum jaw-closing MA and greater disparity of potential durophages are taken as proxies for an increased significance of durophages in neopterygians from the Jurassic onwards, there is considerable correspondence to be found in patterns of invertebrate evolution cited regarding the MMR (**Fig. 4.18.**). Many patterns cited in support of a MMR report some form of increasing predation pressure or perceived responses to this predation pressure by invertebrate prey throughout the Mesozoic. For instance, there is a general increase in the proportion of infauna (**Fig. 4.18b**), gastropod energy use (**Fig. 4.18e**), the proliferation of predation-resistant gastropod morphologies as predation-susceptible morphologies decrease (**Fig. 4.18f**) and an increase in the number of motile crinoids (**Fig. 4.18g**). Furthermore, there are patterns that more closely resemble those seen in neopterygian fishes, most notably, a sharp increase in predator or prey proxies in the Late Jurassic, which are either maintained or increase throughout the Early Cretaceous. Most pertinently, there is a sharp increase in the average depth of bioturbation in the Late Jurassic (**Fig. 4.18a**) coincident with a sharp increase in the number of rapidly bioturbating taxa (**Fig. 4.18d**) to levels that are maintained (or continue to increase) throughout the Early Cretaceous. Similarly, there is an increase in the number of motile crinoids in the Mid to Late Jurassic coincident is an increase in predatory sea urchins (**Fig. 4.18h**). The number of motile crinoids continues to increase in

the Early Cretaceous while numbers of predatory sea urchins remain stable, therefore the pattern in predatory sea urchins somewhat mirrors my proxies for neopterygian fish durophagy. Taken together, the data from neopterygian fishes presented in this chapter is consistent with a MMR, where proxies for neopterygian durophagy increase in the Jurassic, and are either maintained or continue to increase in the Early Cretaceous, in line with numerous other invertebrate proxies cited in support of an MMR.

There is one final consideration for the patterns recovered here regarding the nature of the rock record. Whereas the record of fishes in the Triassic and Jurassic are dominated by marine deposits, the Early Cretaceous is dominated by freshwater deposits. This complicates examination of durophagy in neopterygians and the MMR more generally, since freshwater invertebrates are expected to be less heavily biomineralised than marine taxa, reducing the need for as heavily specialised crushing dentitions. This might, for example, underlie the Early Cretaceous drop in the percentage of taxa with crushing dentitions (although the number of these taxa is comparable to when the record was mostly marine, **Fig. 4.17a**). Furthermore, there is no corresponding fall in the jaw-closing MA, suggesting that either powerful jaws are retained due to phylogeny, that sufficiently hard invertebrates still persist, or that they are primarily required for piscivory, and have little to do with durophagy. Further work is required to determine the effect of environment on durophagy in fishes, and what implications these variations in the rock record have for the MMR more generally.

Future work – As an immediate extension of the work presented here, greater attention could be placed simply upon those relatively few taxa identified to show durophagous features to determine whether the jaw-closing MAs of these species change throughout the time series. However, due to a focus on few species, measurements from greater numbers of specimens of

each species would be necessary. More generally, the conclusions highlighted the need for broad ranging surveys in living taxa relating morphology, function and ecology. Although this is an active area of enquiry, much of the research has been biased towards coral reef fishes, yet we ultimately require broader coverage of a wide range of taxa and environments. Specifically, we require more information on the prevalence of moderate durophagy, and the morphological and functional correlates of such behaviour. I also highlighted the need for a better understanding of marine and freshwater durophagy, and what implications this might have for our interpretation of the proposed MMR. Beyond these things, serious efforts need to be made to biomechanically quantify the capabilities of durophages and the adaptations of their prey over vast timescales, including the Palaeozoic and the Cenozoic. Fishes provide a good candidate to examine changes in functionality, and possess structures that can be quantified throughout much of the Phanerozoic. However, the many other predatory groups touted as evidence of the MMR require similar attention.

Chapter Summary

The pattern of disparity

1. Disparity (sum of variances in multivariate space) through eleven Mesozoic time bins was quantified on the basis of geometric morphometric body landmarks for morphology, and a selection of six biomechanical traits for function.

2. Morphological disparity trajectories were all top heavy, showing some general pattern of increasing disparity with time as the Late Jurassic and Cretaceous possessed higher disparity than the Early and Middle Triassic in Neoptergii, Holostei and Teleostei. By contrast, functional disparity was relatively stable throughout the time series, meaning that disparity in the Triassic is comparable to that seen the Jurassic and Early Cretaceous (although this may

not be true of teleosts, which are rare early in the Triassic). One exception is the final time bin of the series (Albian) in which functional disparity increases across all clades, although is marginally non-significant under *Lagerstätten* removal.

3. *Lagerstätten* effects are responsible for Late Jurassic and Albian highs in morphological disparity. Although strictly true of functional disparity also, the Albian increase in functional disparity is easily observed and near significant after *Lagerstätten* removal, providing some evidence for a legitimate increase.

Q1. Morphological and functional axes and distances

1. Correlation of first differences (i.e. the change between successive values) of mean disparity in morphology and function suggests a moderate correlation between the two in Neopterygii and Teleostei, but poorly in Holostei. Despite this correlation, fundamental features of individual morphological and functional trajectories differ, and overall morphological disparity tends to increase while functional disparity remains relatively stable throughout the time series.

Q2. Early high disparity

1. I define three forms of early high disparity to aid interpretation of neopterygian trajectories: 1) Bottom heavy early high disparity, 2) Uniquely early maximum disparity, and 3) Shared early maximum disparity. I establish that, for my data, in both morphology and function, no form of early high disparity is expected under a Brownian null model.

2. All morphological trajectories appear top heavy. For Neopterygii, there is no clear evidence for any form of early high disparity, but holosteans and teleosts may show shared early maximum disparity.

3. All functional trajectories appear relatively symmetrical and show shared early maximum disparity. Holosteans may also demonstrate uniquely early high disparity, depending upon the placement of Dapedidae.

Q3. Transition from holostean world to teleost world

1. There is evidence for a higher proportion of holostean taxa showing higher disparity compared with teleosts in the Early and Middle Triassic, signalling the holostean dominated fauna. There is also evidence for a teleost dominated fauna, as they represent the taxonomic majority and slightly higher disparity than holosteans from the Late Jurassic onwards. The question that remained was the timing of the transition between the holostean dominated and teleost dominated faunas, falling sometime between the Middle Triassic and the Late Jurassic.

2. Two scenarios for transition are possible, and they depend upon the assignment of Dapedidae. If Dapedidae are holosteans, holosteans show greater phenotypic disparity than teleosts across the entire Triassic and most of the Jurassic, only giving way to teleosts in the latest Jurassic (Kimmeridgian – Tithonian), after which teleosts possess marginally higher disparity in all remaining time bins. If Dapedidae are teleosts, the holostean period of dominance is brief, restricted only to the Early and Middle Triassic, after which, in the Late Triassic potentially, but Early Jurassic definitively, teleosts obtain greater phenotypic disparity and maintain this for the rest of the time series.

3. These findings differ from previous accounts in two ways. First, the holostean period of dominance, even under the second scenario stated above, is brief compared with previous accounts. Second, there is no sign within my time series of waning holostean disparity coincident with waxing teleost disparity. Both differences are likely accounted for by changing phylogeny.

4. Under a molecular constrained timescale, a transition from a holostean to a teleost dominated world is expected. Under fossil only timescales, holostean and teleost disparity are comparable until the Late Jurassic, after which holosteans are marginally more desperate.

5. Crown teleosts are not responsible for generating or maintaining higher disparity in teleosts over holosteans from the Late Jurassic onwards.

Q4. Triassic-Jurassic extinction

1. The Neopterygii show comparable levels of morphological and functional disparity before and after the Triassic-Jurassic boundary. Ordination space occupation is also highly comparable, although this is not simply driven by a taxonomic stasis; there are instances where new, distantly related species happen to possess similar morphological and functional traits to Late Triassic forms.

2. The most notable changes were the temporary disappearance of Pycnodontiformes and Macrosemiiformes; the drop in generic diversity of deep-bodied forms from six to one (*Dapedium*); the expansion of holosteans into 'pholidophoriform' space; the possibility that the Triassic-Jurassic boundary may mark the end of deep-bodied holosteans and the highly speculative notion that Parasemionotiformes may have gone extinct at the boundary.

However all insights are essentially derived from a single exceptional site in both the Late Triassic and Early Jurassic, questioning the generality of the findings. Huge uncertainties and a decline in disparity occur if *Lagerstätten* are removed.

Q5. Mesozoic Marine Revolution

1. A commonly cited line of evidence for the occurrence of a Mesozoic Marine Revolution is a growing significance (e.g. diversity, disparity, destructiveness) of durophagous and grazing taxa in the Mesozoic compared with any previous time. Neopterygian fishes are commonly cited as evidence, yet their diversity, disparity and biomechanical capabilities through the Mesozoic have not been examined.

2. Clearly identifiable durophages fall as a percentage, but remain similar in overall number throughout the Mesozoic. The average jaw-closing MA of neopterygians, used as a measure of destructiveness, remains constant throughout the Mesozoic, although there are signs of an expansion in capabilities during the final time bin of the series (Albian), as taxa with the absolute largest and smallest jaw-losing MAs appear. Maximum jaw-closing MA does increases in the Late Jurassic and remains high during the Early Cretaceous. The morphological and functional disparity of potential durophages also shows some increase through the Mesozoic.

3. There is no strong signal for a growing significance of 'clear' durophages in proportion or number, nor any evidence that neopterygians were attaining ever more destructive feeding modes on average. However, and increase in the maximum jaw-closing MA, and the higher disparity of potential durophages provide some support for an escalated and more varied durophagous threat. The timing of the maximum jaw-closing MA and disparity data agree

well with proxies derived from invertebrates that are cited in support of a Mesozoic Marine Revolution. Thus, the data from neopterygians seems consistent with the notion of a Late Jurassic through Early Cretaceous increase in durophagy, and responses to durophagy. Concerns regarding disparity as an ecological proxy, the identification of potential durophages, the importance of freshwater and marine sediments and the utility of abundance data are discussed.

Chapter 5
The tempo and mode of morphological evolution in Mesozoic neopterygians

INTRODUCTION

Numbering approximately 29,000 species, teleost fishes account for half of modern vertebrate richness, assume a bewildering array of morphologies, and have come to occupy nearly every aquatic environment. In dramatic contrast, their holostean sister group contains a mere eight species, considered 'living fossils', which are restricted to freshwaters of eastern North America. This pattern of extreme dissimilarity, gleaned from living taxa alone, has provided the basis for assertions of teleost superiority and fuelled a series of evolutionary scenarios.

Classic explanations for the spectacular diversity of teleosts have centred on key innovations in feeding (e.g. protrusible jaws, pharyngeal jaws, Pough et al. 1996) and reproduction (Callazo 1994, Callazo 1996). The most fashionable hypothesis at present invokes the duplicate genomes of teleosts relative to those of all other jawed vertebrates, and claims a causal relationship between genome duplication and teleost success (Amores et al. 1998, Taylor et al 2001, Postlethwait et al. 2004, Volff 2005). Specifically, it has been suggested that genome duplication might explain the morphological diversity of teleosts (Meyer and Peer 2005, Hoegg et al. 2004, Van de Peer 2004, Wittbrodt et al. 1998), reflecting more general hypotheses that increased morphological diversification is an expected consequence of genome duplication (Freeling and Thomas 2006, Van de Peer et al., 2009).

Despite wide interest, arguments for elevated rates of diversification and phenotypic change in clades with duplicated genomes have typically been asserted rather than demonstrated empirically. Existing quantitative comparisons have been made exclusively on the basis of living species (Alfaro et al. 2009, Santini et al. 2009, Mayrose et al. 2011, Rabosky et al. 2013, Zhan et al. 2014), even though it is clear that inclusion of even small quantities of fossil data can significantly alter the outcome of comparative analyses (e.g. Finarelli and Flynn 2006, Slater et al. 2012).

A convincing test of the relationship between genome duplication and morphological diversification requires: 1) the ability to survey morphological change in deep time, owing to the fact that genome duplication occurred in the teleost ancestor at least 150 million years ago (indicated by the oldest fossils of crown teleosts, Arratia 2000); and 2) placement of teleost morphological diversification within a comparative framework with clades that have not undergone genome duplication. Palaeontological data satisfy both criteria. Here I examine size and shape directly from fossil taxa flanking the genome duplication to test the prediction that taxa with duplicate genomes demonstrate greater capacity for morphological diversification.

MATERIALS AND METHODS

(a) Morphological dataset

i) Taxa

The dataset spans over 160 Ma from the late Permian (base of the Wuchiapingian, 259.9 Ma) to the end of the Early Cretaceous (Albian, 100.5 Ma). Morphological data derive both from original photographs of museum specimens and published images and measurements

available in the literature. The resulting dataset consists of 1138 specimens of crown Neopterygii (the clade composed of Holostei and Teleostei) assigned to 471 species. Subsets of individuals were used for the relevant body size and shape analyses.

ii) Shape analysis

All protocols for quantification of shape and relative warp analysis are identical the Chapter 3. The only difference here is that I apply these protocols to a slightly larger sample size, 799 individuals assigned to 398 species (as opposed to 356 species in Chapter 3, where complete functional measurements were required for all taxa). Four axes explain >5% of the variation and the anatomical correlates of these four axes are identical to those presented in Chapter 3. Once again, RW4 looked to characterise subtle ventral-dorsal flexion commonly exhibited by fish after death. Therefore I did not seek to analyse this axis, but instead used RW1-3 as the basis for all rate and innovation analyses.

iii) Standard length

Standard length (SL) is measured here from the anterior tip of the snout to the base of the caudal fin (last vertebral centra). This measurement permits fair comparison between all individuals, regardless of whether they have highly specialized, damaged, or missing caudal fins. Standard length was obtained for 954 specimens assigned to 471 species. A majority of these lengths where derived from photographs and images accompanied with scale bars, although some where obtained directly from SL reported in the literature.

iv) Centroid size

Centroid size (CS) provides an alternative measure of body size to SL, and is measured as the square root of the sum of squared distances of a set of landmarks from their centroid. CS is

beneficial because it should, under most circumstances, provide a measure of size independent of shape (Bookstein 1986). To measure CS, I required fully landmarked specimens from the shape dataset (described above) plus a means of scaling the image. However, some individuals lacked a scaled bar, either because they were missing in images gifted to the authors, or, more commonly, were presented in the literature without one, intentionally in the case of many reconstructions. In these instances, if a representative (adult or an averaged value) standard length had already been calculated for the species, I used this measurement to set the scale for the landmarked individual. This resulted in 385 fully landmarked species with associated scales from which centroid size was calculated in TPSDIG2 (Rohlf 2013). Where species were represented by multiple specimens, the average CS was obtained.

b) Accounting for uncertainty in phylogeny and timescale.

Comparative analysis of evolutionary tempo and mode requires a hypothesis of phylogeny scaled to time. However, results may not be robust to variations in either the interrelationships of species or the implied timescale. This presents a particular challenge in palaeobiology, where ambiguity surrounding phylogeny and time scale is commonplace. Chapter 2 summarised the current uncertainty present in Mesozoic neopterygian relationships, highlighting the lack of a consensus regarding the interrelationships of many extinct clades, and the large number of forms that have never been included in a formal analysis. Chapter 2 also illustrated considerable disagreement between molecular-constraint and fossil based estimates regarding the timescale of neopterygian evolution, generating a mismatch for some nodes exceeding 100 million years (e.g., crown teleosts, the 'teleost gap', Near et al. 2012). Because of uncertainty present in both phylogeny and timescale, it is imperative that I perform all analyses over a wide array of topologies and two fundamentally different

timescales to determine whether the results are robust to this variation. Regarding phylogeny, I apply all analyses to 100 randomly selected supertrees from the 10,500 derived in Chapter 2. These are the same 100 trees used in generating null models in Chapter 4. Regarding timescale, I run all analyses on the two timescales presented in Chapter 2, which represent a timescales informed exclusively by fossils and by both fossils and molecular data.

c) Exploring evolutionary rates and mode of change

i) Groups for comparison

Testing the predictions of genome duplication requires that I specify clades for comparison *a priori*. In all, five comparisons were made: **1) Between the teleost crown group and all other neopterygian taxa** (holosteans + stem teleosts, referred to here as 'background'), acting to compare taxa known to have duplicate genomes to everything else. **2) Between the teleost crown group and the holostean total group**. This provides a controlled comparison between taxa with and without duplicate genomes, unlike the first comparison, where there is a chance that some stem teleosts (included in background) also have duplicate genomes. **3) Between the teleost total group** (which underwent genome duplication at an unspecified time) **and the holostean total group** (that lack duplicated genomes). **4) Between stem teleosts and the holostean total group**, to examine whether holosteans, when compared to closely related taxa for which key innovations have not been proposed (i.e. stem teleosts), still appear to evolve at slower rates with less innovation, consistent with their characterisation as 'living fossils'. **5) Between stem teleosts and crown teleosts**, to clarify whether teleosts as a whole represent a clade evolving and innovating morphology in a similar manner, or whether over the course of time there have been changes in their evolutionary regime. All five sets of group comparisons were conducted for all analyses of evolutionary rates and mode across 100 supertrees under both molecular-constraint and fossil-only timescales.

ii) Testing for differences in tempo and mode of shape evolution

1) Rate

Numerous methods of evolutionary rate exist, but in a comparative phylogenetic framework, the most commonly used metric is Brownian variance (σ^2). In phylogenetic methods, if one wishes to statistically examine trends across a phylogeny, one must first specify an evolutionary model detailing the evolutionary process responsible for generating the data. Brownian motion (BM: Edwards and Cavalli-Sforza 1964, Felsenstein 1973, Felsenstein 1981, Felsenstein 1985, Felsenstein 2004) is the most commonly used model, where phenotypic changes are assumed to be independent from time step to time step, the mean displacement is zero, and the variance (σ^2) is proportional to time (Felsenstein 1973, Felsenstein 2004). Therefore for a set of taxa given a phylogeny, the net change in the phenotypic trait is expected to be zero, while the expected variance among taxa increases linearly with time. Thus, the reason that σ^2 (i.e. the Brownian variance) is commonly used as a rate metric, to the extent that it is often referred to directly as the evolutionary rate parameter (Martins 1994, Garland and Ives 2000, O'Meara 2012), is because σ^2 describes the rate at which phenotypic variation accumulates per unit time (Felsenstein 1985). Three of the rate methods employed in this chapter utilise Brownian variance as a measure of rate, whereas the method developed by Sidlauskas (2008) uses a different measure (= the total amount of morphological change along the branches of a phylogeny a group of interest divided by the total duration, in millions of years, of those branches), and thus is referred to throughout the methods section as 'rate'.

Bayesian rate estimation and clade comparison - rate

The third approach was that of Eastman et al. (2011). This approach is only designed for univariate traits, and was applied to both measures of body size and the two main shape axes

derived from the relative warp analysis, using the auteur package in R. The method employs reversible-jump Markov chain Monte Carlo to assess the fit of multiple models of differing complexity and samples them in proportion to their posterior probability, delivering distributions of relative rates for every branch in the tree. I implemented the method over 1,000,000 generations, discarding the first 250,000 generations as burn-in. I then conducted randomization tests across the five sets of clade comparisons to determine the significance of rate differences.

Q-mode rate estimation and simulations - rate

The first approach, developed by Adams (2014), permits estimation of evolutionary rate within a multivariate dataset. By utilizing the statistical equivalency (given Euclidean data) of R-mode approaches (employing a covariance matrix) and Q-mode approaches (employing a distance matrix), Adams (2014) derived an evolutionary rate parameter from multivariate data analogous to that derived from univariate traits. Simulation of evolution under a null model of equal rates is used to generate a null distribution of the difference in the estimated rate parameter between the two focal clades, against which the observed difference in estimated rates can be compared.

MEDUSA model implemented in the R package MOTMOT

I estimated the phylogenetic position and magnitude of changes in the rate of evolution of body shape using the trait MEDUSA method of Thomas and Freckleton (2012). Specifically, I used the function transformPhylo.ML with the tm1 algorithm in MOTMOT R package (Thomas and Freckleton 2012) to fit the trait MEDUSA model the multivariate shape axes 1 to 3. Unlike the two other methods of rate estimation outlined above, it is a truly multivariate approach that can analyse all axes of shape variation simultaneously. I allowed up to 20

possible rate shifts and set the minimum clade size to 5 to avoid searching for shifts in small clades. The intention here is to implement this approach in a purely exploratory manner to examine whether the gross patterns of rate change on a single MPT appear consistent the results from other shape analyses.

Phylomorphospace simulations – 'rate'

The second approach similar to that outlined in Sidlauskas (2008), is comparable to the first approach in that it evaluates the significance of differences between clades in reference to simulations under a null model. However, the phylomorphospace component of the method, and the highly customisable nature of the technique allows me to explore tempo and mode in both univarite and multivariate traits. The basic principle of this approach is to consider all relevant body shape axes in multivariate space and to plot the phylogeny within this space. Once ancestral states have been estimated for all internal nodes, the Euclidean distance between the start and end points of a branch in morphospace provides a value of morphological change. Combined with branch duration in millions of years, 'rates' of change for any collection of branches (i.e., clades) can be obtained (the sum total of all morphological branch lengths within the clade divided by the sum total of all branch durations for the clade). The 'rate' measurement of the Sidlauskas (2008) approach is not to be confused with the Brownian variance parameter, a more commonly accepted measure of rate, and will continue to be denoted in quotes to highlight the distinction. The 'rate' information of the Sidlauskas (2008) approach alone is insufficient to directly compare the 'rate' of one clade to another and determine which exhibits higher 'rates'. Reasons for this are twofold.

First, direct measures and comparisons of 'rate' are uninformative because this measure is not purely a function of Brownian variance, but Brownian variance combined with the

distribution of branch lengths within a clade. This disconnect occurs because expected change is not proportional to the length of time between observations (branch duration in this scenario); we observe proportionally less change on longer branches than on shorter branches (Gingerich 2001). This is significant; one clade may show higher 'rates' than another simply because it has shorter branches on average than another other clade. Comparison with simulations is therefore essential to determine whether observed 'rates' fall within a distribution of 'rates' obtainable by Brownian motion alone. Second, even if 'rates' obtained from the data were meaningful (i.e., if the distribution of branch lengths for two clades were identical), it would still not be possible to determine whether differences between clades occur as differing outcomes of the same underlying evolutionary process, or if the difference require alternative processes. This is because even a Brownian null model can produce clades with substantially different 'rates'. Therefore I must determine whether the magnitude of the difference I observe is sufficiently rare in simulations before I can invoke departures from the null model.

Simulations were based upon parameters estimated from the observed data. These included the tree topologies, branch durations, and the Brownian variance parameter (σ) for the three relative warp axes of interest, obtained using the fitContinuous function of the R package geiger. Simulations of Brownian-motion trait evolution were then performed using the fastBM function of the R package phytools (Revell 2012). Each of the 100 supertree MPTs was treated as a separate trial. In a single trial, the ratio of the 'rate' calculated for one clade (sum of the morphological change on all branches of the clade divided by summed durations of all that clade's branches) to a second clade was obtained from the observed morphometric data on a single MPT. This ratio was then compared with 100 ratios from the same clade comparison derived from 100 simulations of trait evolution on the same topology. This differs

from the approach of Sidlauskas (2008), where a single observed ratio from a single phylogeny was compared to a pooled distribution of null models derived from different topologies. I feel it is preferable to avoiding comparisons between null models and observed data generated on the basis of different underlying phylogenies, and so my approach only compares observed and simulated data from the same topology, treating each topology as a separate trial. The percentile in which the observed ratio (from a single MPT) falls relative to simulated ratios (for the same MPT) therefore gives the probability of obtaining the observed ratio by 'chance' (i.e. under a Brownian motion null model) given that topology. For example, if the observed ratio falls close to the 50^{th} percentile, the result is easily obtainable under the null model that both clades evolve at equal 'rates', whereas the closer it falls to either tail of the distribution, the null model would be an increasingly poor explanation for the observed data, to the point that below the 5^{th} or above the 95^{th} percentile, the null model of equal 'rates' could be justifiably rejected (in a one-way framework, outlined below). Depending upon how the ratios were obtained (i.e., which clade's 'rate' was divided by another clade's 'rate'), I can determine which clade is likely to be evolving faster directly from the percentiles. The same process is repeated across all 100 MPTs, generating a distribution of 100 percentiles. Further details are outlined in a worked example in the section below.

Phylomorphospace simulations – 'rate': A worked example

In this example, I wish to ask whether 'rates' of morphological evolution in holosteans are different to those in teleosts, and I also wish to know which clade shows the higher 'rate'. For a single MPT, I then calculate 'rate' for holosteans (total amount of change across all holosteans branches divided by total duration across all holosteans branches) and for teleosts, and divide the holostean 'rate' by the teleost 'rate' to obtain my observed ratio. I then perform 100 Brownian motion simulations of morphological evolution on that same MPT, calculate

holostean and teleost "rates" for each, and derive 100 simulated holostean/teleost ratios. Now I have specified precisely how the ratio was obtained i.e. which clade's 'rate' was divided by another clade's 'rate' (holostean 'rate' / teleost 'rate' in this case), it becomes clear how the percentile can determine which clade shows higher 'rates'. If my ratio is in the 2nd percentile, not only does it inform me that the result was very unlikely under the null model, but that the holostean to teleost 'rate' ratio is far smaller than the vast majority of simulations, necessitating that teleosts display higher 'rates' of change than holosteans. However if the observed ratio fell within the 98th percentile, it would mean that the holostean to teleost 'rate' ratio is far larger than expected under a null model, necessitating that holosteans are evolving at faster 'rates'. In this framework, it is clear that any value below the 50th percentile implies that teleosts are evolving faster than the majority of the null models for a given MPT, and any value above the 50th percentile implies that holosteans are evolving faster than the majority of null models for a given MPT. Through examination of the percentiles in which the observed data fell from all 100 MPTs, I can then more clearly assess where the balance of evidence lies. For example, given the holostean and teleost example, if all 100 observed 'rate' values fell within the 1st percentile of their respective simulation distributions, we could be in no doubt that all trees support higher 'rates' in teleosts, and that all of the individual differences were significant. However, there may be a situation where, across 100 MPTs, observed ratios fall across many percentiles in their respective simulations, but with a heavy skew so that 80 of the trees report values that lie between the 5th and 15th percentile. Under conventional statistical approaches, this result would be ignored entirely, yet clearly the bulk of evidence still suggests that teleosts show higher 'rates'.

To expand upon and formalise this approach further, percentiles are directly equivalent to one-way *p-values* (and can easily be converted into two-way p-values). Given the

holostean:teleost 'rate' example outline above, a observed value in the 2nd percentile of the simulated ratios is directly equivalent to a one-way p value of 0.02 that teleosts evolve at faster 'rates' than holosteans (p = 0.02 means we can reject the null hypothesis that the holosteans 'rate' ≥the teleost 'rate', accepting the alternate hypothesis that the teleost 'rate' > the holostean 'rate'). By the same logic, the 98th percentile is a one-way p value of 0.98, meaning we cannot reject the null that holostean 'rate' ≥the teleost 'rate'. However, the 98th percentile is *also* equivalent to the one-way p value that holosteans possess higher 'rates' at p = 0.02, this time rejecting the null that the teleost 'rate' ≥the holostean 'rate', accepting the alternate hypothesis that the holostean 'rate' > the teleost 'rate'. Thus, for any given percentile, two separate one-way p-values can be derived with different null and alternative hypotheses. Two-way p-values (which ask if the 'rate' in two clades is different regardless of the direction of effect) are easily calculated by doubling the value of the lowest of the two possible one-way p-values obtainable from the percentile. Calculation of p-values from percentiles is only relevant to the size and shape methods where I employ the modified method of Sidlauskas's approach, since the Q mode approach and Bayesian approaches return one-way p-values by default.

2) Mode/innovation (lineage density)

Phylomorphospace simulations

Mode of evolution was examined using the same simulations outlined above, gathering density information instead of 'rate' information. The only difference is the way in which the results are presented. With 'rates' of evolution, I illustrate which clade shows higher 'rates' through one-way p-values (e.g. **Fig. 5.3**) and a heatmap (**Fig. 5.1**) – thus focusing on which has the greater 'rate'. It would be confusing if I did the same for density, as focusing on the clade with the greatest density actually means focusing upon the least innovative clade,

complicating comparison with 'rates' in the heatmap. Therefore I flip the interpretation of the *p*-values to ask which clade shows greater innovation (i.e. lower density) instead. Density was calculated for shape data using the same two measures outlined in Sidlauskas (2008), although I focus on his 'density 1' ('density 2' provided very similar results). Both require a measure of total morphological change for a clade, divided by a measure of volume in morphospace occupied by a clade. When applied to univariate data, a multidimensional measure of volume is not required, and so the range was used as a measure of occupation. The calculation of density was therefore the total amount of body shape change divided by the mathematical range of a given clade's body size.

RESULTS

Tempo and mode of morphological change

Crown teleosts vs background – Teleosts with duplicate genomes (crown group teleosts) show significantly higher rates of shape and size change relative to other neopterygian taxa (background) in the majority of supertrees across all measures of shape and size in every analysis under both molecular-constraint and fossil-only timescales (**Fig. 5.1 a, a' - Rates**). Crown teleosts also display greater shape innovation (i.e. lower lineage density) but not in body size, where background taxa are better innovators (**Fig. 5.1 a, a' –Mode, Fig. 5.8**). These inferences are robust to time scaling procedure (**Fig. 5.1 a, a', Fig. 5.8**).

Crown teleosts vs holosteans – Under fossil-only timescales, crown teleosts show higher rates of evolution, and a greater capacity to innovate, in all measures of shape and size (**Fig. 5.1b, Fig. 5.4**). Phylomorphospace plots clearly illustrate how holosteans and crown teleosts differ in their ability to innovate shape (**Fig. 5.1d-e**). Although the total space occupied by each appears similar, if fossil-only timescales are correct, the crown teleost space was populated in

just 60 million years, just one third of the time it took holosteans to generate a similarly sized space. In addition, crown teleost taxa appear overdispersed in morphospace, whereas holostean taxa are tightly clustered, especially around the origin (0,0). However, under molecular-constraint timescales, the crown teleost space becomes the product of over 200 million years of evolution. Under this revised timescale, supertrees weakly favour holosteans as better shape innovators (i.e. with lower lineage densities) than crown teleosts (**Fig. 5.1b' Mode, Fig. 5.9**). Surprisingly, even under molecular-constraint timescales, a small majority of supertrees indicate that crown teleosts show higher rates of shape and size evolution, and greater size innovation, compared with holosteans (**Fig. 5.1b', Fig. 5.4, Fig. 5.9**).

Holosteans vs Teleosts – A comparison of rates and mode in holosteans versus total group teleosts (**Fig 5.1c, c'**) suggests that holosteans evolve at comparable rates to teleosts under fossil-only timescales, but only in shape, as teleosts exhibit higher rates of body size evolution, and greater innovation in both size and shape (**Fig. 5.1c**). However, under molecular-constraint timescales, holosteans show higher rates of size and shape evolution, and greater innovation in shape than teleosts (**Fig. 5.1c', Fig. 5.10**).

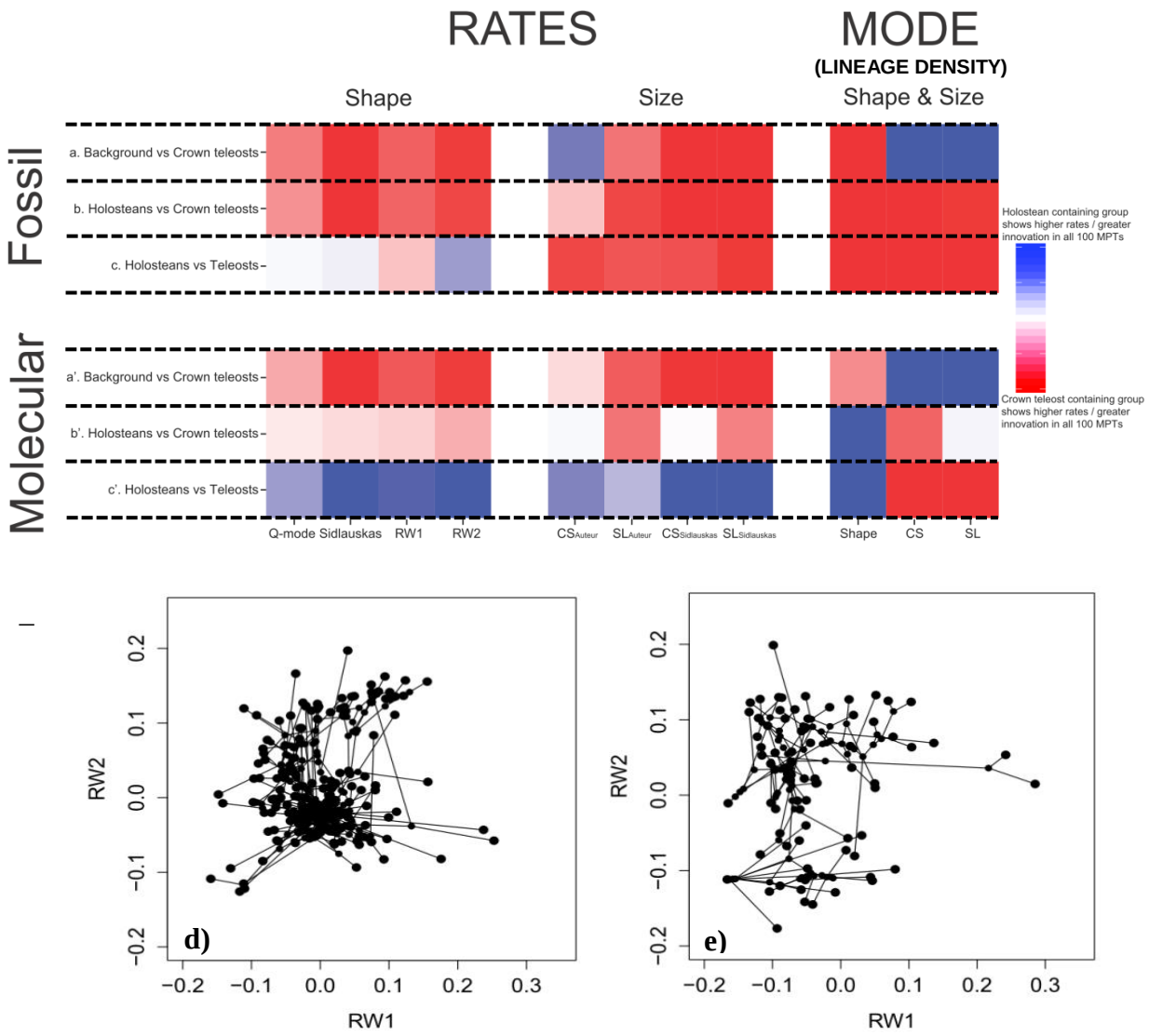

Fig. 5.1. Heatmap indicating whether the majority of supertrees support higher rates / greater innovation within a group containing at least some taxa with duplicate genomes (red), or a group containing holosteans (blue). Shading represents the size of that majority, where the darkest shades for either colour represent a complete majority (100 supertrees in support) and lightest shade only a slight majority (e.g. 51 supertrees in support). Groups under comparison are labelled to the left of the heatmap, each with its own letter (**a-c**), and the results from both fossil based and molecular based timescales are compared. Additional information regarding the composition and rationale for group choice is outlined in the text. Support for higher rates / greater innovation was determined in reference to one-way p-values, which are equivalent to percentiles in reference to simulated outcomes, as detailed in the text. Projection of the phylogeny in shape space (=phylomorphospace) shown for **d)** holosteans and **e)** crown teleosts.

Stem teleosts vs holosteans and stem teleosts vs crown teleosts – The stark contrast in the results when holosteans were compared with total-group teleosts (**Fig. 5.1c, c'**) as opposed to when they were compared to crown teleosts alone (**Fig. 5.1c b,b'**), especially clear on molecular-constraint timescales (**Fig. 5.1c c' *versus* Fig. 5.1c b'**), suggests that the stem teleosts possess lower rates and innovation. This was tested by comparing rates and innovation in stem teleosts to both holosteans and crown teleosts separately (**Fig. 5.6 and 5.7 for rates, 5.11 and 5.12 for mode**). Stem teleosts exhibit low rates of shape change and are poor shape innovators compared to both holosteans and crown teleosts, particularly on fossil-only timescales. However, stem teleosts are exceptional size innovators, showing greater innovation than both holosteans and crown teleosts regardless of timescale (**Fig. 5.11, 5.12**), and higher rates of size evolution than holosteans on fossil-only timescales (**Fig. 5.7**). Given the low rates of shape evolution in stem teleosts, it is not surprising that rates of shape evolution appear indistinguishable between holosteans and teleosts under fossil-only timescales (**Fig. 5.1c**), a consequence of high crown teleost rates becoming diluted by low rates in stem teleosts. This dilution is large enough that, on molecular-constraint timescales, holosteans actually evolve faster than teleosts in shape and size, and show greater shape innovation (**Fig. 5.1c'**). Only innovation in size appears to be the preserve of total group teleosts regardless of timescale (**Fig. 5.1c, c'**, driven by stem teleosts).

The clearest patterns to emerge from rate comparisons are summarised in **Fig. 5.2**, which displays and handpicked (yet representative) relative warp 1 rate analysis output from Auteur. This RW1 analysis happens to match the outcome of statistical tests between clades across the numerous methods applied above, including the Sidlauskas (2008), Eastman et al. (2011) and Adams (2014) approaches. Crown teleosts display elevated rates of morphological change,

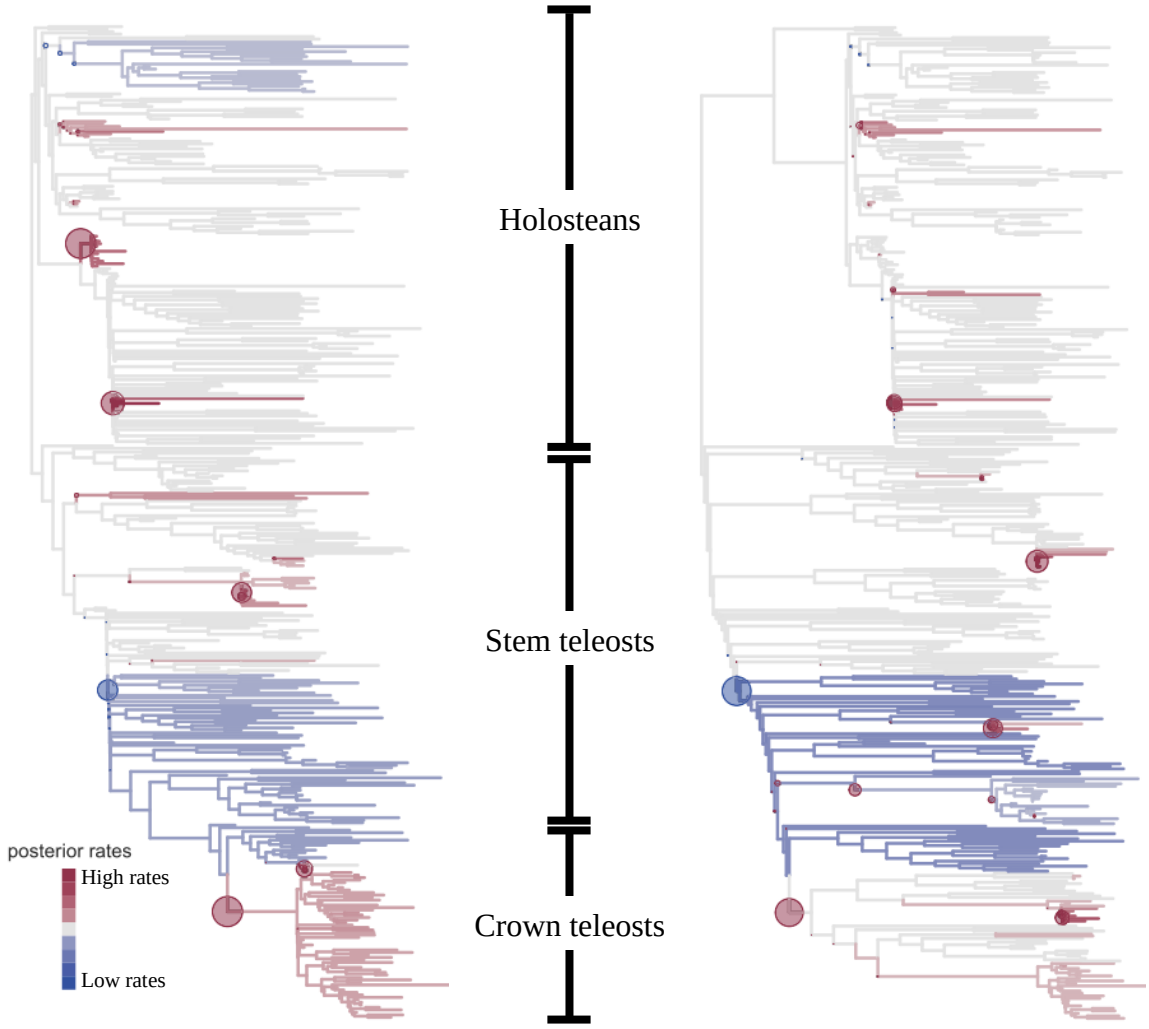

Fig. 5.2. Rates of shape evolution in RW1 for a single (but representative) supertree scaled to **a)** fossil and **b)** molecular timescales. Branches coloured according to posterior model-averaged rates of evolution in Relative Warp 1. Circles indicate rate shifts, where larger circles correspond to larger posterior probabilities. This supertree summarises the main findings from all group comparisons of rate. Crown teleosts show higher rates of evolutionary change, whereas stem teleosts typically show lower rates than the average and holosteans tend not to deviate from the median rate. Under molecular timescales, rates of morphological evolution in the both stem and crown teleosts decrease whereas holosteans are largely unaffected.

Fossil based timescale		Molecular based timescale	
Shift position	**Frequency**	**Shift position**	**Frequency**
Upper teleost stem	2	Upper teleost stem	0
Teleost crown	6	Teleost crown	20
Within teleost crown	92	Within teleost crown	80

Table. 5.1. Positions of the teleost rate shift increase across 100 supertrees when scaled to fossil and molecular timescales.

stem teleosts exhibit decelerated rates, and holosteans tend not to deviate from the median neopterygian rate. However, molecular-constraint timescales disproportionally affect teleosts, lowering both stem and crown teleost rates (**Fig. 5.2b**), whereas holostean rates are essentially unaffected, and thus, come closer to expressing comparable or higher rates of evolution than teleosts on molecular-constraint timescales (**Fig. 5.1b', c'**).

Beyond an *a priori,* clade definition and comparison approach, it is possible with some of the methods applied (Auteur and MOTMOT) to examine rates, and shifts in rate, across a phylogenetic tree in an exploratory fashion. Thus, it may be possible to identify the precise node where, for instance, higher rates in crown group teleosts come about, rather than always considering them as a homogenous group in statistical analysis. Since the rate increase in teleosts, as predicted by numerous explanations of teleost success, is of primary interest here, I will consider the evidence for the position of this shift.

Fig. 5.2 illustrates a representative tree for the major axis of body shape variation, RW1. Interestingly, it actually indicates that the rate shift increase occurs within the teleost crown, at the node named Osteoglossocephala (Near et al. 2012), which represents the divergence between Osteoglossomorpha and Clupeocephala. This means that the earliest diverging lineage of teleosts, the Elopomorpha, appear to possess rates more typical of the teleost stem than the teleost crown. To determine whether this shift position really was representative, I examined the position of the shift across all 100 MPTs on both fossil and molecular timescales with RW1 (**Table. 5.1**). This revealed that by far the most common pattern was a rate shift within crown teleosts (sometimes in varying positions, but most often at node Osteoglossocephala), rather than immediately preceding the entire teleost crown group,

although the likelihood that the crown teleost node is the correct position of the rate shift increases on molecular timescales (**Table. 5.1**). Examination of other RW axes reveals a different pattern. Representative RW2 trees tend to report a rate shift at the teleost crown node (**Fig. 5.13**), whereas RW3 indicates no rate shift within, at or considerably before the teleost crown node (**Fig. 5.14)**. Furthermore, the output from MOTMOT on a single MPT, which considers all three RW axes simultaneously, suggests that a weak rate increase encapsulates the entire teleost crown group on fossil timescales, or a stronger rate increase limited to small and independent subsets of the crown on molecular timescales (**Fig. 5.15**). Therefore, there is some disagreement between methods and axes as to precisely where rates increase in relation to the teleost crown. While the Osteoglossocephala are particularly good at varying their body depth profiles (RW1; from a spectrum of deep and rounded to shallow and elongate) to the exclusion of the Elopomorpha, all crown teleosts are relevant to increased rates of evolution in fin position (RW2), and none in relation to variation in relative dorsal fin base length (RW3). Further investigations into the positives and negatives of examining multivariate data in a univariate fashion, potential methods to summarise multiple MOTMOT output, and whether newly developed multivariate approaches agree with the output of MOTMOT will be beneficial to clarify the position of the teleost rate shift increase.

DISCUSSION

Elevated rates and greater innovation in crown teleosts

There is evidence for elevated rates of morphological evolution and greater morphological innovation in fossil teleosts with duplicate genomes, consistent with the predictions of genome duplication enhanced morphological diversification. This discovery runs contrary to previous assertions about rates of phenotypic change based solely upon the observation that

fossilised stem teleosts exist (Donoghue and Purnell 2005). Placed into context, these findings represent the third piece of evidence consistent with a genome duplication enhanced diversification in teleosts more generally, beyond 1) the observation that teleosts are highly diverse today and 2) the identification of a shift in diversification rate at the origin of teleosts (Santini et al. 2009). However, all three lines of evidence are entirely correlational, meaning we still lack direct evidence for a causal link between genome duplication and accelerated morphological diversification. The advantage of the evidence presented here is that it limits the range of explanations to only those acting upon on the earliest crown teleost representatives, rather than the entirety of teleost evolution.

Nevertheless, there are a host of competing explanations, including reproductive and developmental innovations (Soin 1981, Callazo 1994, Callazo 1996); trends for increased jaw mobility, reduction of armour, homocercal tail development (Romer 1966, Pough et al 1996); influences from the break-up of supercontinent Pangaea (Cavin et al. 2008); and the role of freshwater radiations (Cavin et al. 2007) given that crown teleosts exhibit higher rates and greater innovation in the Early Cretaceous where the record is dominated by freshwater deposits. Before preference can be shown towards any theory, explicit demonstrations of causation are required. For genome duplication, this would mean demonstrating its involvement across a suite of specific morphological traits responsible for elevated rates and apparent innovation. Yet to date as there is very little information regarding the role of genome duplication in the evolution of any morphological traits, let alone the traits responsible for the pattern observed in the Mesozoic. A rare example is the independent evolution of electric organs in both the African elephantfish and the South American knifefish via neofunctionalization of the scn4aa paralog (Arnegard et al. 2010). Other more significant traits, such as the staggering diversity and complexity of colour pigmentation seen in teleosts,

have been suggested to have evolved due to the preferential retention of duplicated pigmentation genes (Braasch et al. 2008, Braasch et al. 2009, Braasch and Postlethwait 2012), yet direct evidence linking quantity of genes to greater pigmentation diversity is lacking. Workers have also mused as to whether the alternative morphological explanations for teleost diversification (e.g. jaw modifications), and even the synapomorphies that define teleosts (reviewed in de Pinna 1996) might themselves have evolved as a consequence of genome duplication (Braasch and Postlethwait 2012). Once again, evidence for these claims is lacking, and where studies have actively searched for a link between genome duplications and 'key innovations' earlier in vertebrate history, they found that vertebrate innovations such as neural crest, placodes and the development of a large brain originated in a precursory form *prior* to any duplications (Cañestro 2012). Therefore we are some distance from understanding the role of genome duplication in morphological diversification, a distance that can only be scaled with broader genomic sampling of living taxa and a sustained collaboration between morphologists and molecular biologists to reveal the genetic underpinnings of specific morphological novelties.

Implications for holosteans as 'living fossils'

The results presented here also act to test the two predictions of holosteans as 'living fossils', namely, that they should exhibit low rates of morphological change and possess little capacity for phenotypic innovation. Timescale has an important influence on the results, and can paint two quite extreme pictures of holosteans. Under molecular-constraint timescales, holosteans exhibit near comparable rates of shape and size evolution to crown teleosts, and even obtain greater innovation in shape (**Fig. 5.1b'**), yet under fossil-only timescales, crown teleosts comfortably exceed holosteans in every aspect of morphological diversification (**Fig. 5.1b**). Nevertheless, one finding is clear: holosteans show higher rates of shape change than stem

teleosts, regardless of timescale (**Fig. 5.2**). Thus, holosteans cannot be considered to exhibit abnormally low rates of phenotypic change, rejecting the first prediction of the 'living fossil' model. However, some support can be found for the second prediction, that holosteans are poor phenotypic innovators. This support derives from examination of size, where regardless of timescale across all comparisons with teleosts, holosteans are the poorest size innovators (**Fig. 5.9, 5.10, 5.12**). Although this could be seen to tally with results from neontological work that found low rates of body size evolution in holosteans (Rabosky et al. 2013), holostean rates of size evolution in the Mesozoic are not particularly low (**Fig. 5.4, 5.5, 5.7**). In conclusion, holosteans cannot be easily characterised as 'living fossils'. Instead, the picture is more nuanced, with each group examined here (holosteans, stem teleosts and crown teleosts) expressing differing capabilities for rates and innovation in different traits. Nevertheless, holosteans do appear conservative in size evolution; when all their living and fossil ancestors are considered, they differ by a maximum of one order of magnitude, whereas Mesozoic teleosts alone span numerous orders of magnitude, and when living representatives are included, they span more.

The mosaic capabilities of Mesozoic neopterygians

The findings suggest a mosaic of capabilities within Mesozoic neopterygians. For example, crown teleosts may tend to have higher rates and greater innovation than holosteans, but holosteans have higher rates of shape evolution than stem teleosts, yet stem teleosts are the best size innovators of any group, even though they possess lower rates of size evolution than crown teleosts, and comparable rates to holosteans. This mosaic contrasts with the more structured pattern apparent in dinosaurs (Benson et al. 2014a), where body mass showed high rates at the origin of dinosaurs, as all of the major lineages became established, only for rates to slow in most of these lineages, with the exception of maniraptoran dinosaurs where high

rates were sustained. This inspired the idea that one possible mechanism for the unevenness of biodiversity may be maintenance of high rates (a proxy for evolutionary potential, aka. evolvability) over long timescales in certain lineages (Benson et al. 2014a). Given that teleost fishes contribute greatly to the unevenness of biological diversity in the Recent, showing considerably greater richness and phenotypic variety compared with clades of comparable age or older (e.g. holosteans, chondrosteans, polypterids) the maintenance of evolvability in deep time would be an appealing candidate to explain their apparent success. A cursory examination of their record would also appear to support this, given that the early diverging stem teleost lineages are highly morphologically divergent (Pycnodontiformes, Aspidorhynchiformes, Pachycormiformes). However, the data show that, not only are many of these early diverging lineages relatively late appearing, allowing them sufficient time to acquire their varied morphologies, but more importantly, a vast swathe of the teleost stem is characterised by exceptionally low rates of size and shape evolution (blue regions, **Fig. 5.2**), driven entirely by the large paraphyletic assemblage of taxa referred to as 'pholidophorids'. If this vast grade of stem teleosts is not merely an artefact of systematic ignorance (Chapter 2), teleosts as a whole clearly illustrate how high rates of phenotypic change (within the crown group) can return to lineages that appear, by all other measurable respects, to be evolutionary dead-ends. This would suggest that evolvability need not always be maintained, but can return, even to those lineages that appear the least likely to evolve at high rates in future, so long as they can avoid extinction. Why then have high rates seemingly never returned to the numerous 'living fossil' clades that appear to be champions of warding off extinction (Stanley 1984)? This suggests it may not merely be a matter of time, but opportunity that brings about the return of evolvability. Clearly more work is required to reveal the opportunities that drive high rates of evolutionary change, and if many clades

respond similarly to the same opportunity, or whether some clades are fundamentally constrained in ways that prevent them from attaining high rates.

The importance of timescale

A broader message to emerge from this work is the importance of timescale selection. For example, under fossil-only timescales, there is little doubt that crown teleosts show higher rates and greater innovation in most analyses compared to background, and to holosteans. However, under molecular-constraint timescales, support for these conclusions is considerably weakened, and in specific analyses they are overturned completely, such as when holosteans show greater shape innovation than crown teleosts (**Fig. 5.1 b'**). Therefore it is clear that molecular-constraint timescales, and thus, molecular timescales in general have the potential to deliver drastically different conclusions regarding tempo and mode compared with purely palaeontological trees. The implications of this for palaeontology are huge since the vast majority of phylogenetic comparative analyses conducted on extinct taxa exclusively use palaeontological timescales (e.g. Lloyd et al. 2012, Anderson et al. 2013, Benson and Choiniere 2013, Benson et al. 2014a). The need to account for timescale uncertainty is therefore essential, especially in cases where a large mismatch exists between molecular and fossil ages, other major examples of which include arthropods (Edgecombe and Legg 2014) and land plants (Clarke et al. 2011). The way forward for palaeontologists exploring tempo and mode is to employ numerous timescales so they can define the temporal limits of their conclusions and ensure their results remain interpretable in the light of future revisions to the timescale.

Given my specific scenario, the influence of molecular timescales weakens, yet does not entirely revise the finding that crown teleosts possess higher rates and greater innovation in

phenotype compared with all other neopterygians sampled and holosteans. However, as discussed in Chapter 2, the molecular constraint ages implemented here, taken from Near et al. 2012, appear to be in need of revision. For example, the constraint on the age of crown teleosts in this study (307Ma, Near et al. 2012) is amongst the oldest ever recovered, and introduces some 150 million year gap between this estimate and the estimate derived from palaeontological timescales. In contrast, recent clock analyses are creeping towards ever younger ages for the teleost crown (179Ma Chen 2012, 284Ma Broughton et al. 2013, 283Ma Betancur-R. et al. 2013, 269Ma Faircloth et al. 2013, 244 Ma Dornburg et al. 2014). Furthermore, the age for holosteans appears to be stable around the age applied here (271Ma) and is perhaps older (296Ma Faircloth et al. 2013), while crown neopterygian estimates (361Ma here) tend to be getting younger (323Ma Broughton et al. 2013, 328Ma Betancur-R. et al. 2013, 311Ma Dornburg et al. 2014). Based upon these changes, the likelihood is that the presence of higher rates and greater innovation in crown teleost phenotypes compared with those of other Mesozoic neopterygians will retain good-moderate support. Regarding holosteans, clearly the robust findings here will remain intact (higher rates of shape change than stem teleosts, poor size innovators overall), yet any sign that holosteans might show greater shape innovation than crown teleosts or stem teleosts (relatively weakly supported under the oldest molecular timescales **Fig. 5.11, 5.12**) will likely disappear. This will essentially rule out the notion that holosteans ever possessed the greatest capacity for phenotypic diversification among their Mesozoic counterparts, despite their considerable diversity at this time.

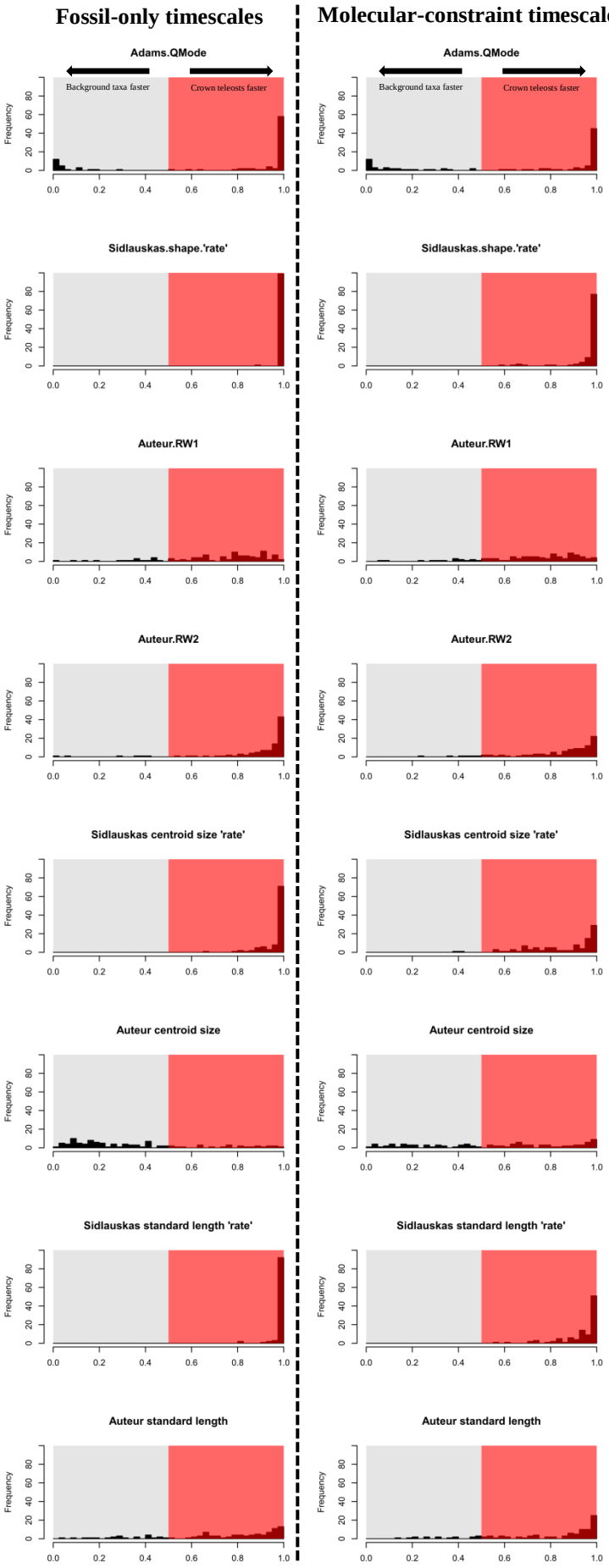

Fig. 5.3. Levels of support for higher rates of evolution in background (grey) compared with crown teleosts (red) according to 100 one-way p-values (where each p-value derives from analysis of a single MPT). *p*-values below 0.5 suggest (to varying degrees of significance) that the group on the left, denoted by shading, evolved at higher rates than the group on the right, whereas above 0.5 they support higher rates in the group on the right compared to the group on the left (again, to varying degrees of significance).

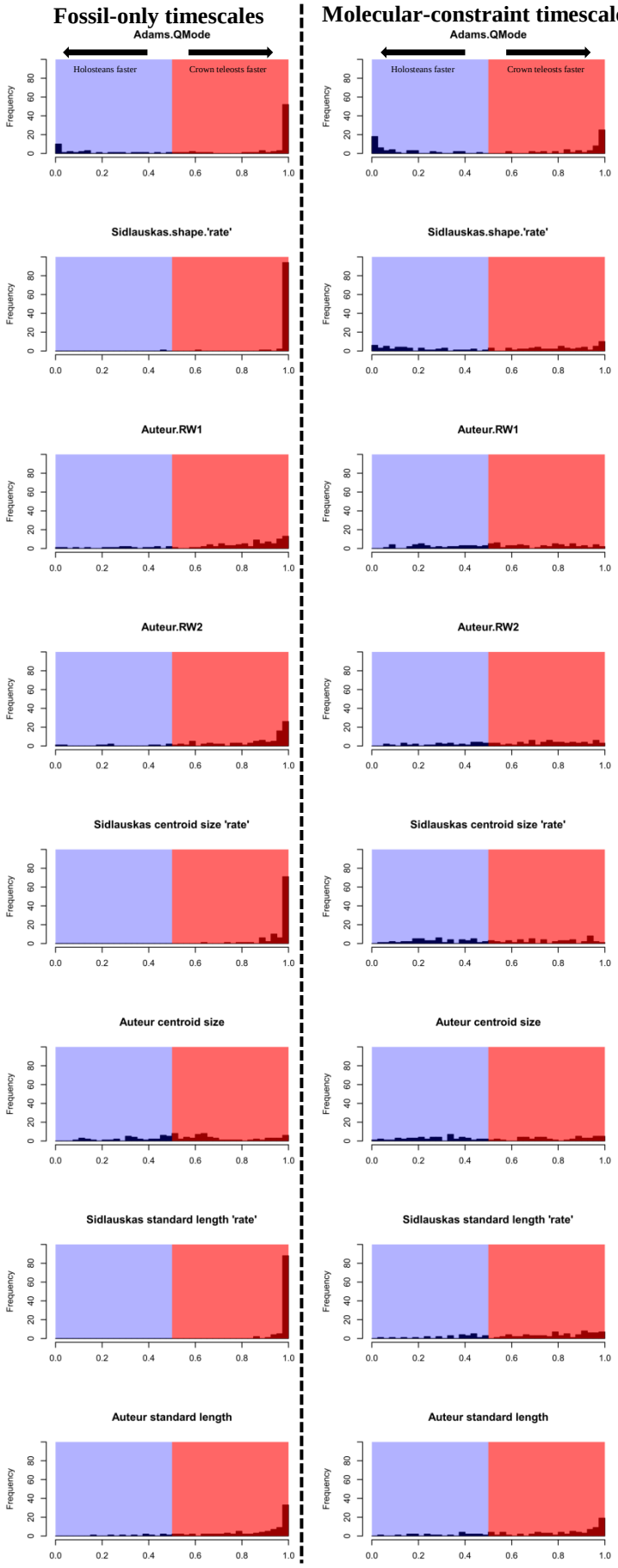

Fig. 5.4. Levels of support for higher rates of evolution in holosteans (blue) compared with crown teleosts (red) according to 100 one-way p-values (where each p-value derives from analysis of a single MPT). *p*-values below 0.5 suggest (to varying degrees of significance) that the group on the left, denoted by shading, evolved at higher rates than the group on the right, whereas above 0.5 they support higher rates in the group on the right compared to the group on the left (again, to varying degrees of significance).

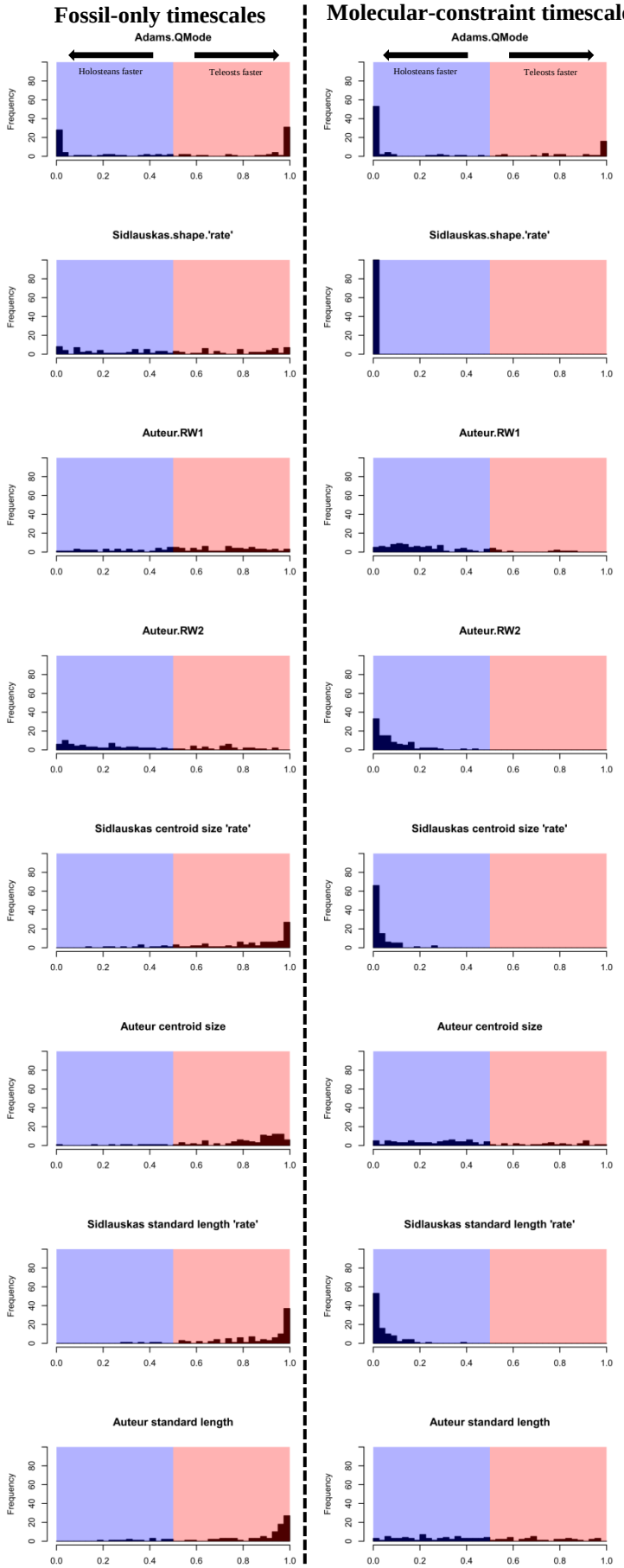

Fig. 5.5. Levels of support for higher rates of evolution in holosteans (blue) compared with teleosts (red) according to 100 one-way p-values (where each p-value derives from analysis of a single MPT). *p*-values below 0.5 suggest (to varying degrees of significance) that the group on the left, denoted by shading, evolved at higher rates than the group on the right, whereas above 0.5 they support higher rates in the group on the right compared to the group on the left (again, to varying degrees of significance).

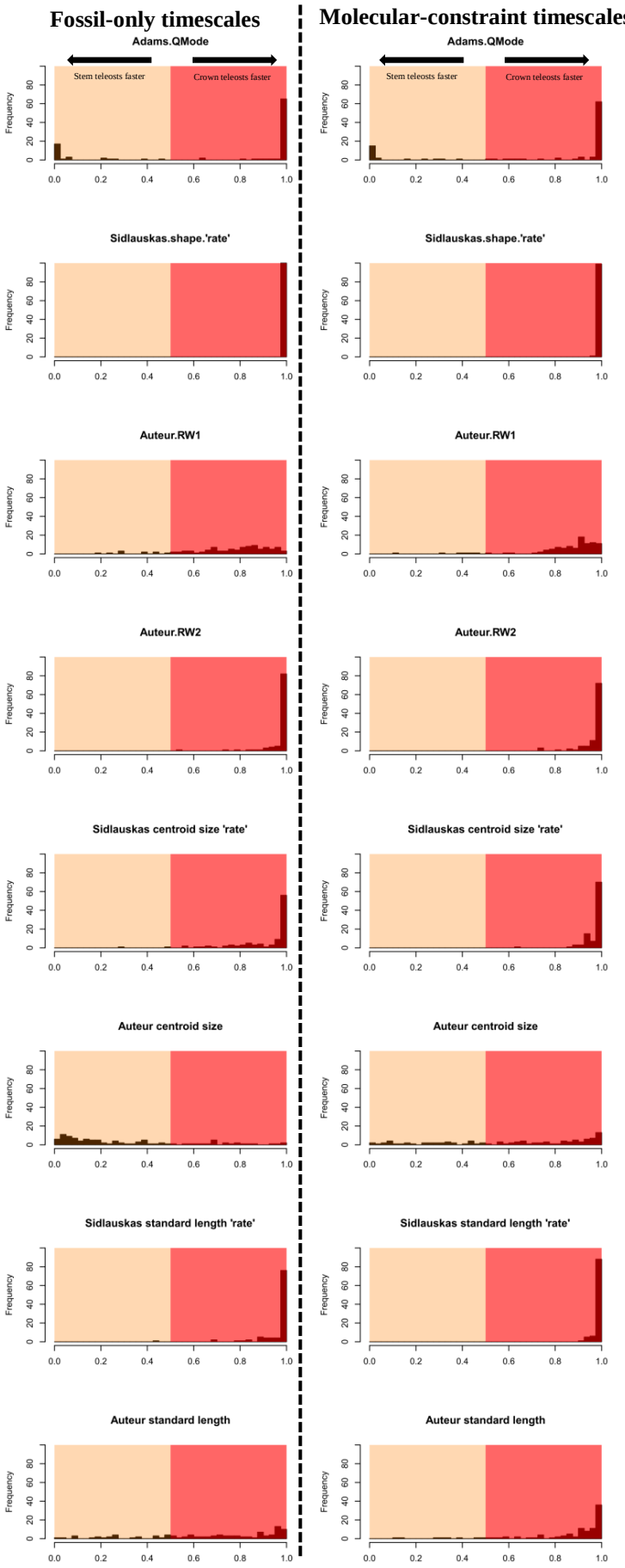

Fig. 5.6. Levels of support for higher rates of evolution in stem teleosts (orange) compared with crown teleosts (red) according to 100 one-way p-values (where each p-value derives from analysis of a single MPT). *p*-values below 0.5 suggest (to varying degrees of significance) that the group on the left, denoted by shading, evolved at higher rates than the group on the right, whereas above 0.5 they support higher rates in the group on the right compared to the group on the left (again, to varying degrees of significance).

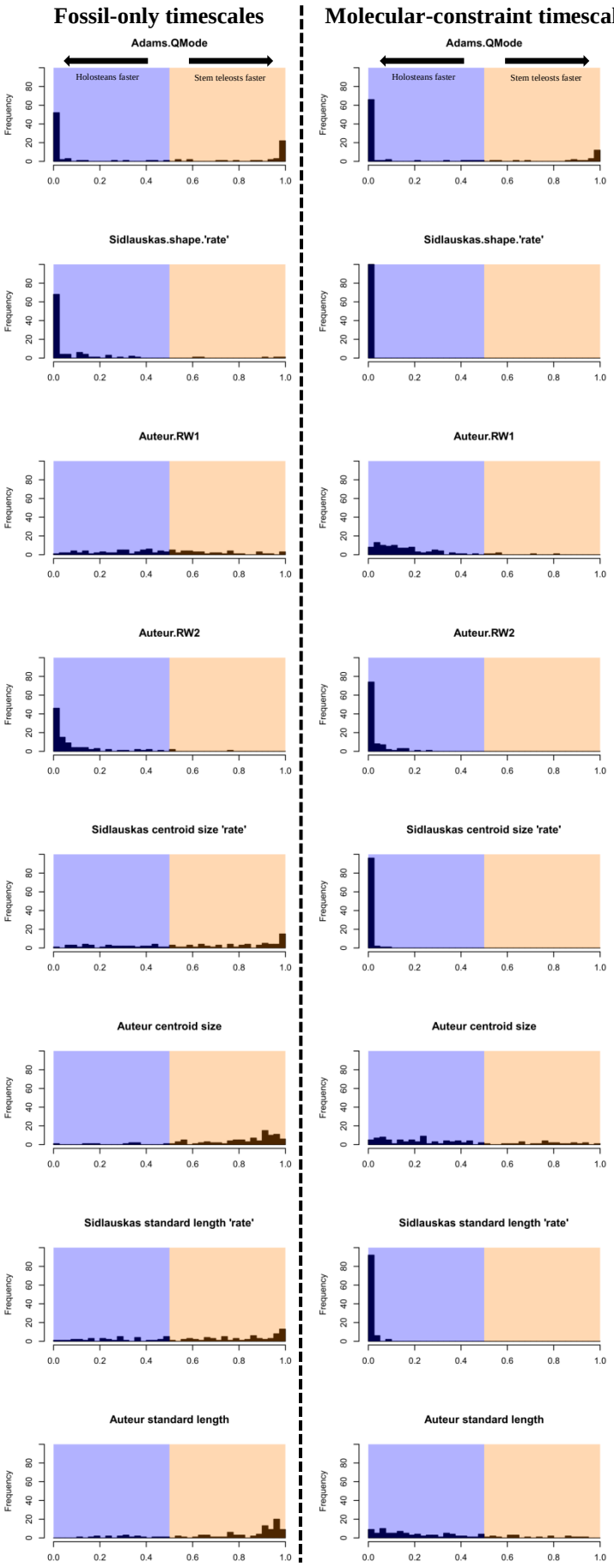

Fig. 5.7. Levels of support for higher rates of evolution in holosteans (blue) compared with stem teleosts (orange) according to 100 one-way p-values (where each p-value derives from analysis of a single MPT). *p*-values below 0.5 suggest (to varying degrees of significance) that the group on the left, denoted by shading, evolved at higher rates than the group on the right, whereas above 0.5 they support higher rates in the group on the right compared to the group on the left (again, to varying degrees of significance).

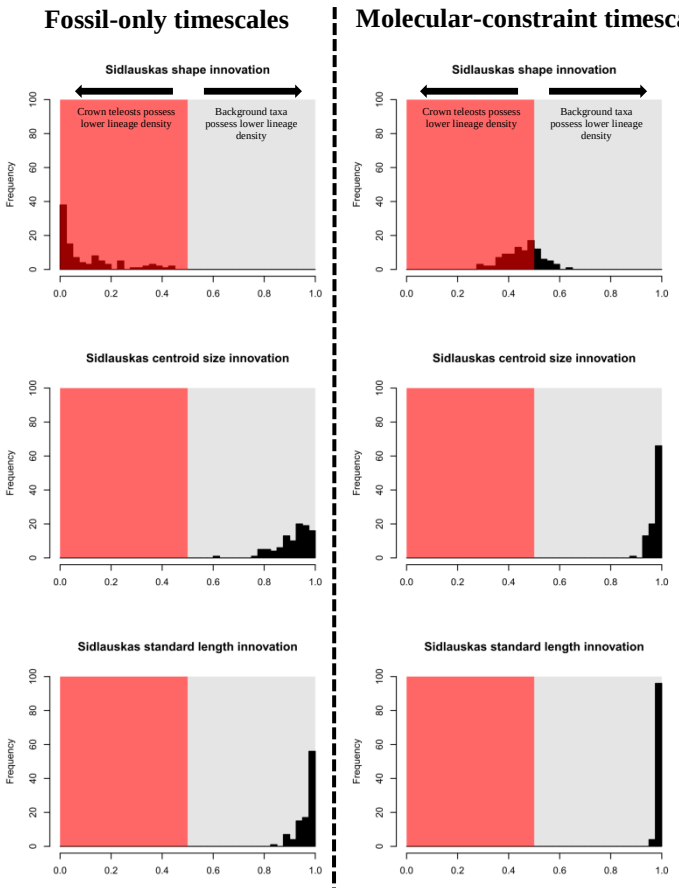

Fig. 5.8. Levels of support for greater innovation in crown teleosts (red) compared with background (grey) according to 100 one-way p-values (where each p-value derives from analysis of a single MPT). *p*-values below 0.5 suggest (to varying degrees of significance) that the group on the left, denoted by shading, shows greater innovation than the group on the right, whereas above 0.5 they support greater innovation in the group on the right compared to the group on the left (again, to varying degrees of significance).

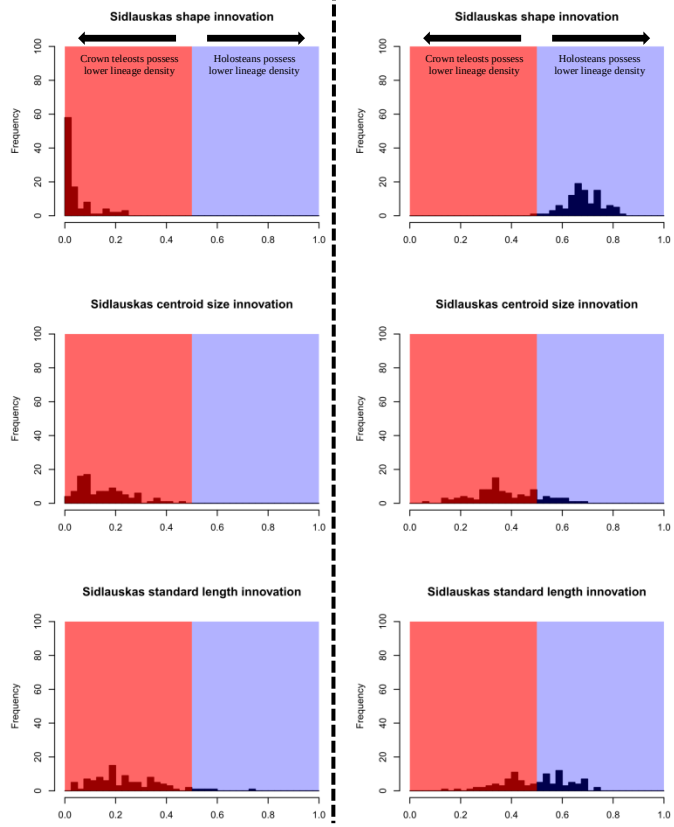

Fig. 5.9. Levels of support for greater innovation in crown teleosts (red) compared with holosteans (blue) according to 100 one-way p-values (where each p-value derives from analysis of a single MPT). *p*-values below 0.5 suggest (to varying degrees of significance) that the group on the left, denoted by shading, shows greater innovation than the group on the right, whereas above 0.5 they support greater innovation in the group on the right compared to the group on the left (again, to varying degrees of significance).

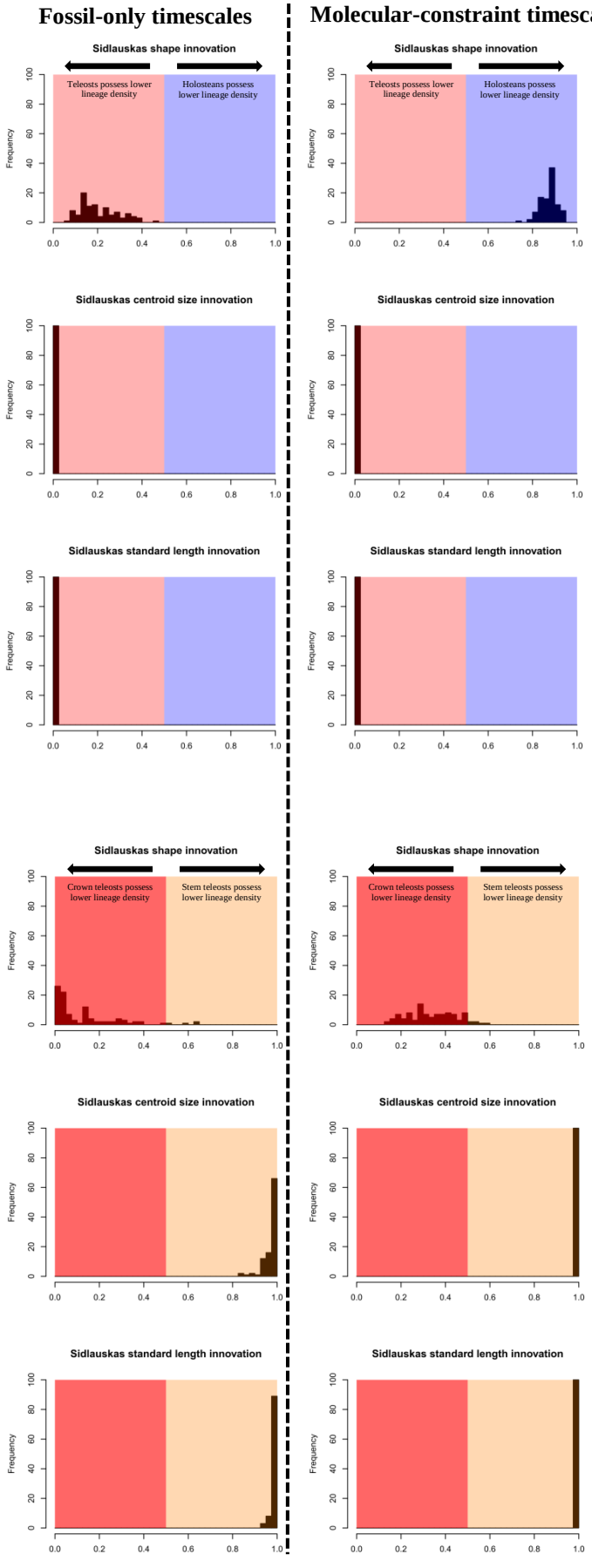

Fig. 5.10. Levels of support for greater innovation (i.e. lower lineage density) in total group teleosts (light red) compared with holosteans (blue) according to 100 one-way p-values (where each p-value derives from analysis of a single MPT). *p*-values below 0.5 suggest (to varying degrees of significance) that the group on the left, denoted by shading, shows greater innovation than the group on the right, whereas above 0.5 they support greater innovation in the group on the right compared to the group on the left (again, to varying degrees of significance).

Fig. 5.11. Levels of support for greater innovation (i.e. lower lineage density) in crown teleosts (red) compared with stem teleosts (orange) according to 100 one-way p-values (where each p-value derives from analysis of a single MPT). *p*-values below 0.5 suggest (to varying degrees of significance) that the group on the left, denoted by shading, shows greater innovation than the group on the right, whereas above 0.5 they support greater innovation in the group on the right compared to the group on the left (again, to varying degrees of significance).

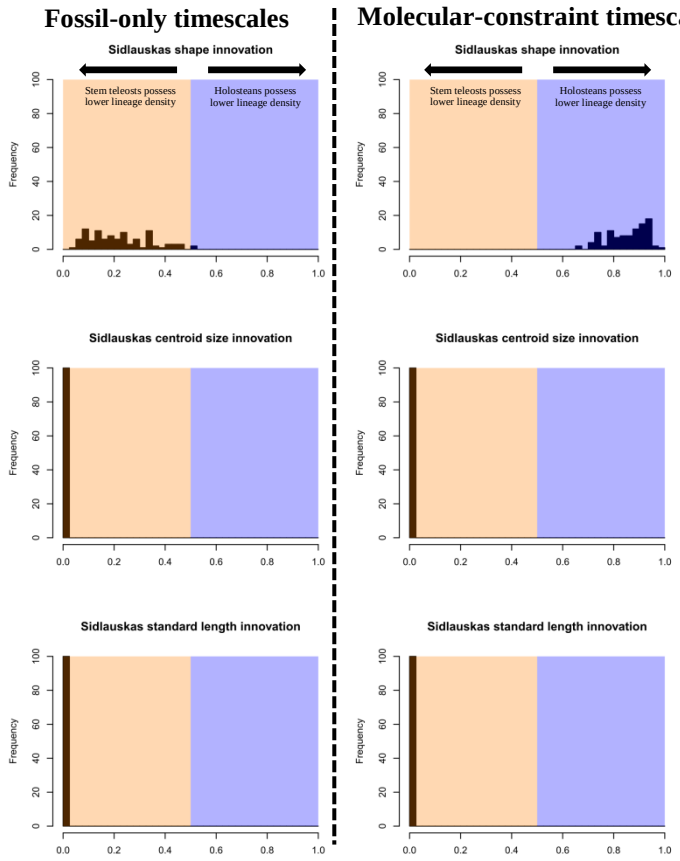

Fig. 5.12. Levels of support for greater innovation (i.e. lower lineage density) in stem teleosts (orange) compared with holosteans (blue) according to 100 one-way p-values (where each p-value derives from analysis of a single MPT). *p*-values below 0.5 suggest (to varying degrees of significance) that the group on the left, denoted by shading, shows greater innovation than the group on the right, whereas above 0.5 they support greater innovation in the group on the right compared to the group on the left (again, to varying degrees of significance).

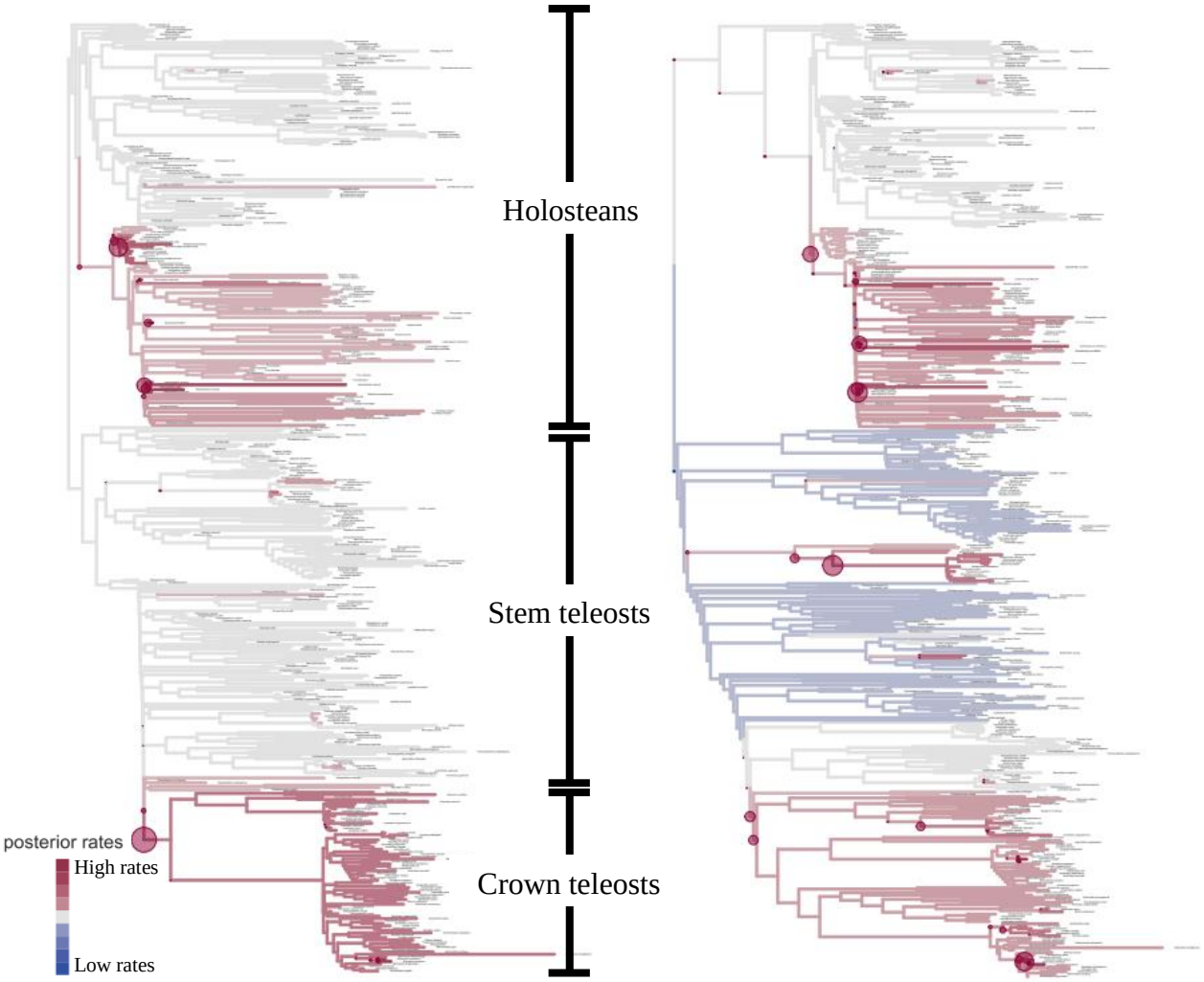

Fig. 5.13. Rates of shape evolution in RW2 for a single (but representative) supertree scaled to **a)** fossil and **b)** molecular timescales. Branches coloured according to posterior model-averaged rates of evolution in Relative Warp 2. Circles indicate rate shifts, where larger circles correspond to larger posterior probabilities. Crown teleosts and halecomorphs show higher rates of evolutionary change, whereas stem teleosts typically show average or (on molecular timesscales) lower rates than the average, and ginglymodians do not to deviate from the median rate.

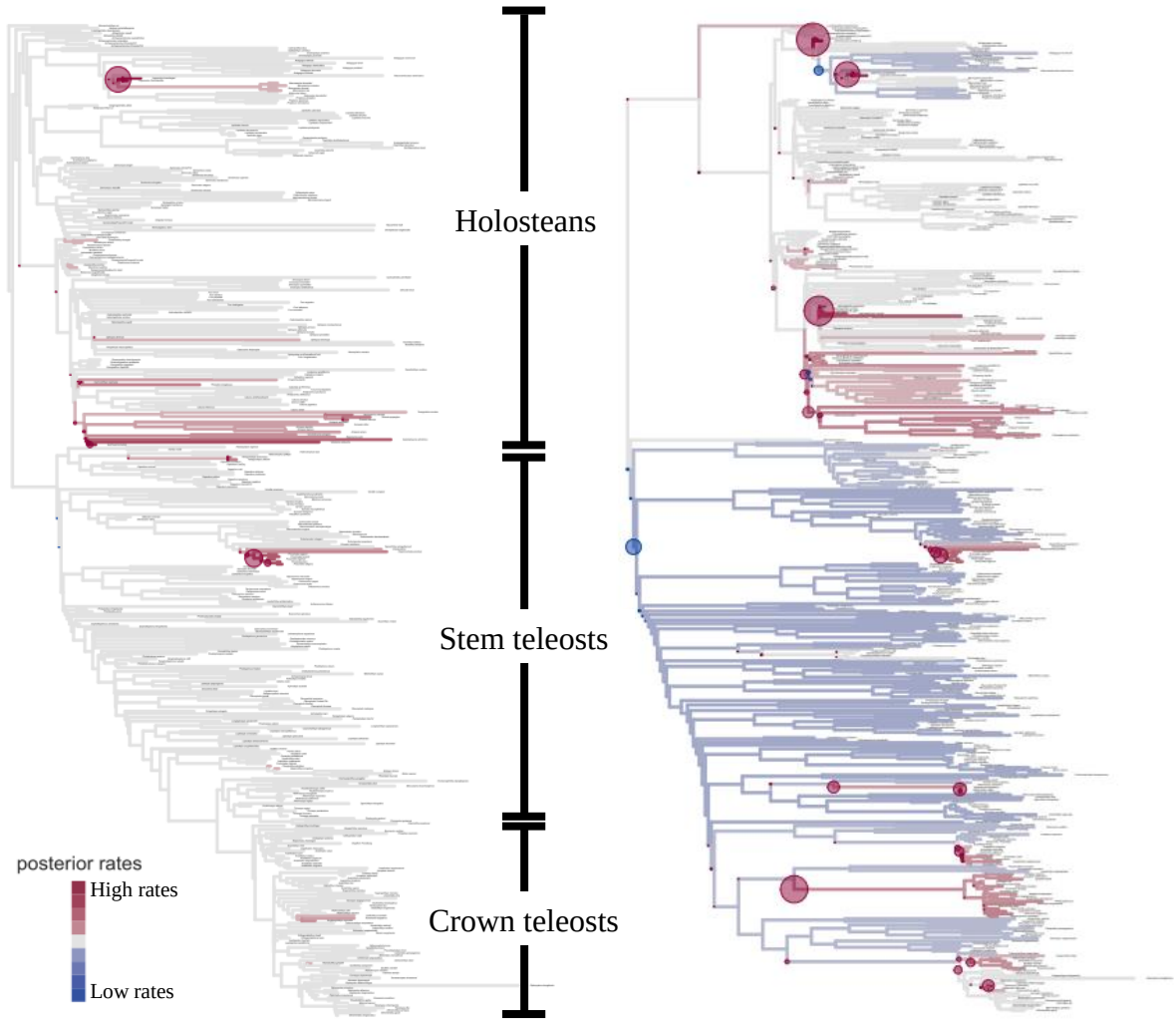

a. Fossil based timescale **b. Molecular based timescale**

Fig. 5.14. Rates of shape evolution in RW3 for a single (but representative) supertree scaled to **a)** fossil and **b)** molecular timescales. Branches coloured according to posterior model-averaged rates of evolution in Relative Warp 3. Circles indicate rate shifts, where larger circles correspond to larger posterior probabilities. Some halecomorphs show high rates of evolutionary change regardless of timescale, whereas teleosts typically show lower rates than the average under molecular timescales.

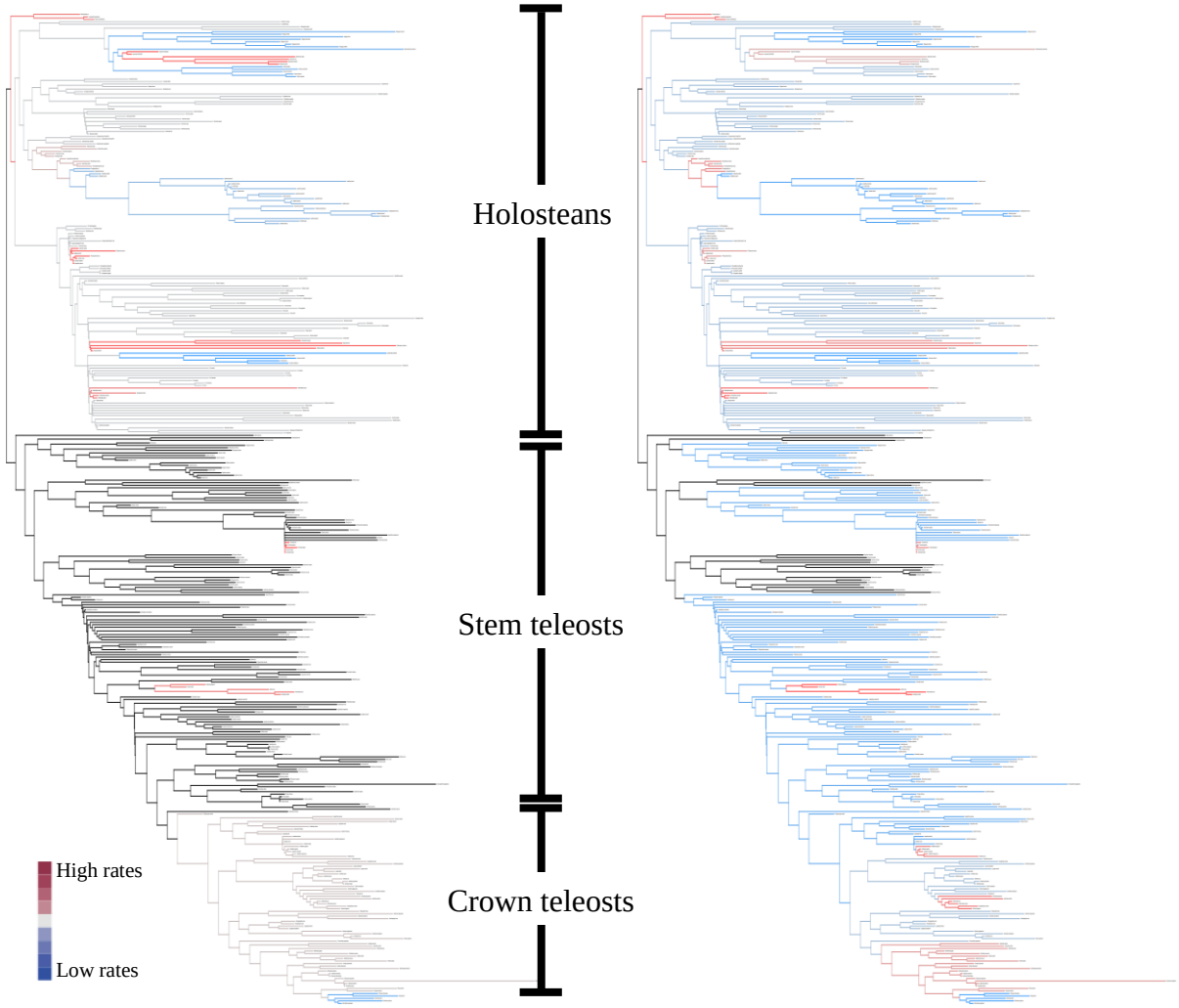

Fig. 5.15. Rates of shape evolution across RW 1-3 according to MOTMOT for a single supertree scaled to **a)** fossil and **b)** molecular timescales. Branches coloured according to rates of evolution. Crown teleosts show higher rates of shape change on fossil timescales, a result weakened considerably on molecular timescales. Some halecomorphs also show high rates of evolutionary change. Ginglymodi and stem teleosts show average rates of change on fossil timescales, but low rates on molecular timescales.

Chapter 6: Thesis summary

This thesis has examined a wide variety of themes relating to the morphological and functional diversification of neopterygian fishes. Specifically, it has focused upon the first 150 million years of this radiation, utilising information from over 600 fossil species recovered from freshwater and marine sites all over the globe. These fossils were placed into a framework with living species to provide the first representation of many Mesozoic taxa within a phylogenetic tree (Chapter 2). These supertrees opened the door to numerous questions that could not have been addressed in the absence of such a framework. Each major theme addressed in the thesis is summarised below.

The assembly of neopterygian diversity: the first 150 million years

A principal aim of this dissertation was to document morphological and functional variety for 60% of neopterygian history. This was examined for the Neopterygii as a whole by means of disparity and patterns of phenotypic ordination-space occupation. The main results are summarised below.

Disparity – The pattern of morphological disparity for neopterygians as a whole from the beginning of the Triassic until the end of the Early Cretaceous increases with time in a two-step fashion (Chapter 4). A low disparity plateau in the Early and Middle Triassic is followed by an increase to a second plateau spanning the Late Triassic to Oxfordian. A final increase then occurs between the second plateau and a Late Jurassic (Kimmeridgian – Tithonian) through Lower Cretaceous plateau. In contrast, the functional disparity of neopterygians is relatively stable for most of this time period, except for the final time bin (Albian) where an increase is observed.

These findings deliver unique insights about the assembly of neopterygian form and function that could not be inferred from studying extant species alone. Specifically, the findings imply very different scenarios for how the morphological and functional diversity of neopterygians was assembled. Morphological disparity appeared to accumulate through time, and an examination of the disparity trajectory in Friedman (2010) suggests that it is likely, following the K-Pg mass extinction, that neopterygian disparity would have increased again to a fourth plateau. Functional disparity remained largely constant throughout the Mesozoic, which either implies that high functional disparity was acquired early on, or that the functional disparity of neopterygians was relatively low for 150 million years, before increasing rapidly in the past 100 million years to deliver the variety present in the Recent. To some extent the latter is known to be true; the vast majority of neopterygians found in the Recent are acanthomorphs and these do not appear in the fossil record until the Late Cretaceous (Patterson 1993). However, this does not preclude the existence of functional analogues before this time. Indeed, authors have previously highlighted examples where clades attain much of their functional variety early in their histories, (Anderson 2009, Anderson et al. 2011). Until the same functional traits are quantified in Late Cretaceous, Cenozoic and living taxa, it will not be possible to confidently determine whether most functional variety was established early, or if a substantial increase occurred later on. Furthermore, the measure of disparity used in this and other studies (sum of variances) is merely one way to examine the pattern, and may address whether the most densely populated major regions of functional space are occupied early on. However, if additional functional variety is continually added but these forms are rare, they may have little influence on overall levels of disparity.

Form and functionspace occupation – Discussions of general patterns in ordination space are difficult, as the distributions of taxa in space can vary considerably through time, which itself

suggests that few phenotypes are impervious to variability in rock record sampling. Nevertheless, the pattern becomes more stable from the Late Jurassic onwards, as regions of phenotypic space occupation remain comparable between bins. An examination of the final 100 million years of neopterygian history – albeit specific to the acanthomorph teleost radiation (Friedman 2010) – also appears to exhibit stable patterns of morphospace occupation, although there is a change from pre K-Pg period of stability to a post K-Pg period of stability.

Noteworthy changes in neopterygian phenotypic space occupation are as follows. The first appearance of a deep-bodied form with high jaw-closing and opening mechanical advantage occurs in the Anisian. Such forms temporarily disappear, before reappearing in the Late Triassic with considerably greater generic diversity. If Dapedidae are teleosts, the end-Triassic then marks the end of deep-bodied holosteans, and the Early Jurassic deep-bodied taxa known from articulated specimens are dominated by a single genus, *Dapedium*. Another first is the arrival of slender bodied taxa with larger relative jaw length in the Toarcian to Bathonian. After this time, most remaining morphological and functional extremes appear in the Late Jurassic, and many of these phenotypes are retained from this point onwards.

Finally, it appears that the extremes of Mesozoic neopterygian morphospace were uncovered gradually, rather than quickly early on. For morphology, many of these extreme regions are retained once they are discovered, as these regions become densely populated with taxa. Functionspace, by contrast, does not possess high densities of taxa at its extremes, and so they are more frequently gained and lost.

The contrasting histories of holosteans and teleosts

The living diversity of Neoptergii, as outlined in Chapter 1, has inspired many evolutionary scenarios pertaining to the success of teleosts and the apparent failure of holosteans to emulate their closest living relatives. Based upon these scenarios, the literature had painted two clear stereotypes for these two clades, with holosteans as 'living fossils', and teleosts as 'advanced' in most respects, stereotypes that suggest the differences we see in the Recent were predictable, or even inevitable. An examination of the fossil history of these clades offered the opportunity to challenge these views.

Uniqueness – One aspect of their history examined was the degree of uniqueness and convergence (Chapter 3 Q3) exhibited by the two clades. This revealed that, although there were some regions of morphological and functional space unique to holosteans, there were far more regions unique to teleosts in the Mesozoic. Therefore, for a given holostean phenotype there was almost always an analogous teleost phenotype, but the same cannot be said in reverse. Thus, although holosteans undoubtedly possessed greater phenotypic variety in the Mesozoic compared with the Recent, they still fail to occupy as many unique regions as teleosts.

Disparity – Greater uniqueness need not imply a greater overall spread of phenotypes throughout ordination space. This spread, quantified as the variance of points in the multivariate space, was used to compare phenotypic disparity in holosteans and teleosts throughout the Mesozoic. Two potential scenarios emerge (Chapter 4 Q3), and choosing the correct scenario depends entirely upon the placement of an enigmatic family of deep-bodied fishes, Dapedidae. If Dapedidae are holosteans, holosteans show greater phenotypic disparity than teleosts throughout the Triassic and most of the Jurassic, only giving way to teleosts in

the latest Jurassic (Kimmeridgian – Tithonian), after which teleosts possess marginally higher disparity in all remaining time bins. If Dapedidae are teleosts, the holostean period of dominance is brief, restricted to the Early and Middle Triassic. After this time, in the Late Triassic potentially, but Early Jurassic definitively, teleosts obtain greater phenotypic disparity and maintain this for the rest of the time series. Regardless of which scenario is true, holosteans were clearly a significant part of aquatic ecosystems for more than 60% of neopterygian history, and far from exhibiting a decline in phenotypic disparity throughout the Mesozoic, their phenotypic disparity towards the end of the Early Cretaceous is either comparable, or greater than any previous time in their history, and only marginally lower than that of teleosts. Pertinently, none of these insights could have been inferred from living holostean diversity alone. Furthermore, greater teleost disparity from the Late Jurassic onwards is expected under a Brownian-motion model of evolution on molecular-constraint timescales. Therefore, it is entirely possible that there is no fundamental difference in phenotypic diversification in holosteans and teleosts. To examine this further, rates of evolution and innovation where quantified across Mesozoic neopterygian phylogeny.

Rates and innovation in a comparative framework – To further interrogate the contrasting histories of holosteans and teleosts, evolutionary rates and morphological innovation were quantified within a phylogenetic comparative framework (Chapter 5). These approaches allowed the specific predictions surrounding holosteans as 'living fossils', and the notion of a genome-duplication enhanced teleost diversification to be tested directly. Regarding teleosts and genome duplication, results showed that teleost fishes guaranteed to possess duplicate genomes (i.e., the crown group) exhibit higher rates and greater innovation in most measures of morphological evolution compared with stem teleosts, holosteans, or both of these groups combined. These results were well-supported using fossil timescales (comparable those

commonly created and used for rate analyses in other fossil clades), and weakly supported under molecular-constraint timescales, and the outcome of some analyses reversed completely. This highlights both the relative stability of the crown teleost results, and the ability for timescale choice to alter, sometimes drastically, the outcome of comparative analysis. This has significant implications for all analyses that employ fossil timescales in isolation, and suggests practitioners of such methods on extinct organisms should perform their analyses over a variety of timescales to establish the limits of their conclusions. Regarding the role of genome duplication in teleost evolution, the results provide only correlational support for a link between the duplication and enhanced phenotypic diversification, since many other candidate explanations could equally be invoked, such as reproductive innovations unique to crown teleosts.

Beyond the results concerning crown teleosts, analysis of rates and innovation reveal novel insights into holosteans and stem teleosts. If holosteans are 'living fossils' they should exhibit especially low rates of morphological change and innovation. Clearly holosteans express lower rates and innovation compared to crown group teleosts in most analyses (except in shape innovation under molecular-constraint timescales), but this is also true for stem teleosts. Therefore, the clearest insight into holostean capabilities lay in comparison with the teleost stem group; if holosteans truly are 'living fossils', they should perform poorly in this comparison. In one measure this is undoubtedly true; stem teleosts are exceptional size innovators, to the extent that they show greater innovation in centroid size and standard length compared with holosteans and crown teleosts regardless of timescale choice. However, in other measures this is not true; holosteans show higher rates in all measures of shape evolution compared with stem teleosts regardless of timescale, and some evidence for greater shape innovation compared with teleosts under molecular timescales (in comparison to total

group, stem and crown group teleosts). In this light, Mesozoic holosteans poorly fit their living fossil stereotype in all but one respect: they are the worst innovators of size amongst Mesozoic neopterygians.

These results illustrate that the evolutionary capabilities of Mesozoic neopterygians vary considerably, and are far more nuanced than the classic evolutionary scenarios suggest. Furthermore rates and innovation may become decoupled, where a clade with the greatest size innovation need not show the highest rates of size evolution. The differing capabilities of the groups examined here, in terms of rates and innovation, suggest a mosaic view of phenotypic diversification over large timescales. This contrasts with the more structured pattern of rate evolution seen within dinosaurs (Benson et al. 2014a), which inspired the notion that the maintenance of high evolutionary rates (a proxy for evolutionary potential, aka. evolvability) over long timescales may help to explain the unevenness of biological diversity. Pertinently, the living radiation of teleosts did not emerge from a sustained period of high evolutionary rates within stem teleosts. Instead, stem teleosts exhibit extended periods of exceptionally low rates in both size and shape evolution, mainly through the paraphyletic assemblage of taxa referred to as 'pholodophorids'. If this pattern is not an artefact of inadequate phylogenetic resolution, it suggests that evolvability can arise in lineages that appear in all other measurable respects to be highly conservative evolutionary dead-ends.

The relationship between morphology and function

Morphology and function were compared in numerous ways throughout the thesis. First, the anatomical correlates of morphospace axes and the functional correlates of functionspace axes were established, and the appearance of both spaces examined. Morphospace appeared to possess greater structure than functionspace, with dense clusters of taxa in extreme regions,

whereas other regions connecting these clusters had very few taxa. By contrast, functionspace appeared far more symmetrical in all directions, and fairly evenly spread.

Second, correlations were performed between these axes, which revealed a good correspondence between the first axis of morphospace and functionspace. This acted to quantify associations workers might have suspected, such as a relationship between deep bodied taxa possessing powerful jaws, and perhaps more surprisingly, larger eyes. Another correlation recovered an association between dorsal fin base length and relative jaw and eye size, where taxa with long dorsal fin bases possess large relative jaw and eye sizes.

Third, a correlation of distance matrices revealed no association between morphological distances and functional distances, meaning there is a broad scale decoupling of these features. Indeed, extreme instances of decoupling were observed, as taxa close in functional space could be far apart in morphological space, and vice versa. However, an asymmetry was discovered, which demonstrated that it is easier for morphologically divergent taxa to be functionally convergent, than it is for morphologically convergent taxa to be functionally divergent.

Fourth, correlations of first differences in mean disparity through eleven Mesozoic time bins demonstrated a moderate correlation between morphological and functional measures in Neopterygii and Teleostei, but poor correlation in Holostei. Nevertheless, the actual disparity trajectories between morphology and function differed in numerous important features, most notably in that morphological disparity tended to increase with time, whereas functional disparity tended to remain stable.

All of the findings regarding morphology and function presented here corroborate the findings of numerous previous studies, all of which suggest significant potential for the two measures to become decoupled. This decoupling can occur as a result of trait choice, many-to-one-mapping and as suggested here, fundamental differences in the structure of morphospace and functionspace. These findings make clear that morphological (specifically body shape) diversity and functional (specifically the traits measured here) diversity cannot simply be inferred from one another, and as a consequence, traits should be carefully selected for the question at hand. At the very least, authors should state their assumptions clearly, and not place significant weight on any conclusions that require inference of one measure of disparity from another.

Fossil fishes as a powerful evolutionary toolkit

The findings summarised above outline the utility of fossil fishes principally in areas of diversification, including the assembly of neopterygian disparity, the dynamics of holostean and teleost diversification, and the contrasting outcomes of morphological and functional diversification. Yet fossil fishes allow for many types of question to be addressed, providing a toolkit for examining a wide range of evolutionary questions. For instance, throughout the thesis, fossil neopterygians were used to investigate notions of wholescale clade replacement, the effect of purported mass extinctions, and evidence for a Mesozoic Marine Revolution. The details of these investigations are summarised below.

First, the issue of clade replacement was examined. Although this has traditionally been discussed from a taxonomic standpoint, a clear scenario of ecological replacement has been presented for neopterygian fishes: teleosts are expected to have 'swamped' holosteans ecologically to bring about their decline. Under the assumption that either morphological or

functional ordination spaces may loosely correlate with ecology, the distance of each holostean species to its closest teleost was examined through eleven Mesozoic time bins to assess whether teleosts moved closer or further away from holostean species on average over time. The analysis revealed an unchanged relationship in nearest neighbour distances through the Mesozoic, meaning there is no evidence that holosteans had become increasingly 'swamped' by teleosts in phenotypic space. Neither was there evidence that holosteans had circumvented teleost encroachment by retreating to phenotypic refugia (with the exception of the Late Jurassic proliferation of Macrosemiiformes), far away from the reach of teleosts. The relatively stable relationship regarding nearest-neighbour distances could still imply many differing scenarios. Future directions were also suggested, especially regarding the ecological relevance of morphology and function. The potential for such methods to reject associations between clades in deep time, rather than demonstrate them, was emphasised.

Second, changes in disparity and ordination space occupation over the Triassic-Jurassic boundary were documented, revealing relatively little change in levels of neopterygian disparity, and largely similar patterns of phenotypic space occupation over the boundary, albeit with some new taxonomic actors in previous roles. The most notable change was a shift from a taxonomically diverse assemblage of deep-bodied taxa to a deep-bodied assemblage consisting entirely of *Dapedium* species. However, the limitations of generalisations based upon findings derived principally from two *Lagerstätten*, one before and after the boundary, was highlighted. Removal of these *Lagerstätten* leads to a decline in disparity due to a loss of all deep-bodied taxa.

Third, a growing significance (richness, disparity and increasing destructiveness) of durophagous neopterygian fishes forms a key line of evidence supporting the notion of a

Mesozoic Marine Revolution, yet these three attributes have not been quantified in neopterygian fishes. The proportion of neopterygian taxa with clearly identifiable crushing dentitions peaked in the Late Triassic, falling to a consistent low in the Early Cretaceous, while absolute numbers of these species remained comparable throughout the Triassic, Jurassic and Lower Cretaceous. Mean jaw-closing mechanical advantage, quantified for all neopterygians to assess whether taxa on average became more destructive in their feeding capabilities through time, remained stable throughout the Mesozoic (although a general expansion in the capabilities of taxa was observed in the Albian, when taxa with the largest and smallest recorded jaw-closing mechanical advantages appear). The maximum jaw-closing MA of neopterygians increases in the Late Jurassic and remains high throughout the Early Cretaceous. Finally, an analysis into the disparity of potential durophages revealed higher levels of disparity late in the Mesozoic compared with the Early and Middle Triassic, illustrating that durophages may have presented a more varied threat later in the Mesozoic. Taken together, the findings from maximum jaw-closing MA and disparity provide some support for a neopterygian contribution to the Mesozoic Marine Revolution, consistent with other proxies cited in support of this event within invertebrates. Concerns regarding disparity as an ecological proxy, the identification of potential durophages, the importance of freshwater and marine sediments and the utility of abundance data are discussed.

The introduction to the thesis outlined the recent surge of interest in living fishes as a model for large scale diversification studies. I then outlined the reasons why this should be extended to the record of fossil fishes due to the vast number of articulated specimens and relatively well constrained phylogenetic framework. In a series of case studies throughout the thesis, I have sought to illustrate the broad utility of this resource for a multitude of evolutionary questions, and there are many more questions that could be addressed with the dataset

presented here. Many ideas for extensions of the case studies have been described in various 'future work' sections, such as the suggestion to investigate the effect of depositional environment on patterns of disparity. Further ideas include investigations as to whether within species phenotypic differences are reflected between species, or whether changes in size influence rates of shape innovation.

The dataset compiled here is of comparable duration to a range of other studies using fossils, yet a key advantage of fossil fishes is that they provide a system that can be examined over vastly longer timescales. A wide suite of traits, from comparable phenotypic structures can be sampled continuously from deep in the Palaeozoic through to the Cenozoic. Even more pertinently, these traits can be quantified for living species where ecology is known, providing the potential to establish the morphological and functional correlates of particular ecologies, and to look for these correlates in the fossil record.. Altogether, fishes represent an unparalleled system for the long term study of ecological changes, biomechanical capabilities, evolutionary rates and patterns of morphological evolution all within a phylogenetic framework. This thesis contributes to a growing momentum in macroevolutionary studies of fishes, and I fully expect the momentum to continue, as palaeontologists interested in large scale patterns of diversification, along with systematists who seek to resolve the major remaining controversies within the vertebrate tree of life, turn to fishes – a major frontier of vertebrate palaeontological research.

APPENDIX

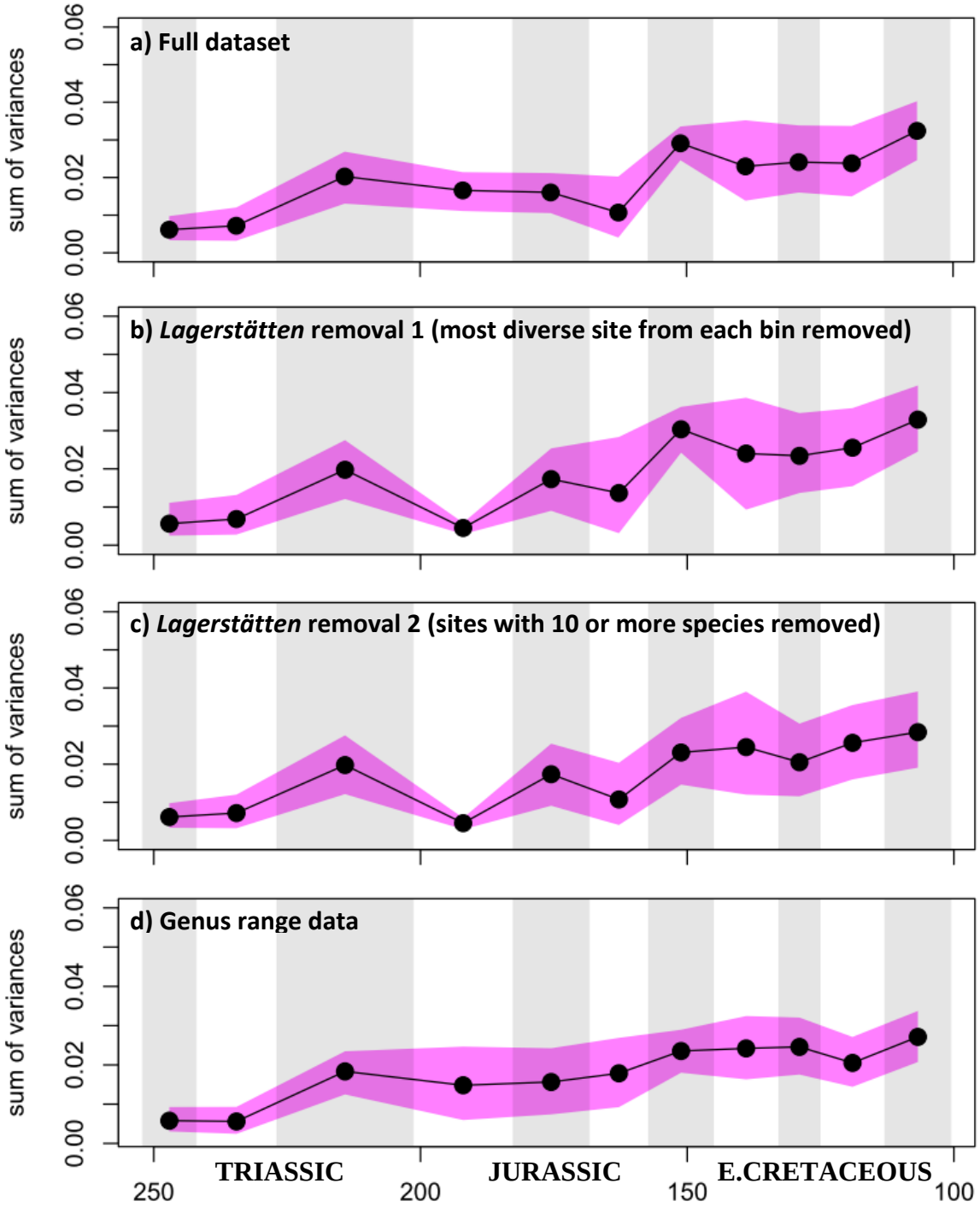

Fig. A1.1. Neopterygian morphological disparity through eleven Mesozoic time bins based upon a) the full dataset of 356 species, b) *Lagerstätten* removal 1 (most diverse site from each bin removed), c) *Lagerstätten* removal 2 (sites with 10 or more species removed), d) genus range data.

a) Full dataset

	AOI	CL	RN	PSH	BAT	OCB	TiKi	ValBer	BarHau	Apt	Alb
AOI	1	0.709839	0.000239	0.001364	0.00315	0.233784	2.61E-05	0.000345	0.000781	0.00032	4.73E-07
CL	0.709839	1	0.001623	0.007751	0.013913	0.412826	4.81E-05	0.002101	0.001821	0.001149	1.15E-06
RN	0.000239	0.001623	1	0.377687	0.320074	0.079614	0.142322	0.647817	0.520993	0.538391	0.030094
PSH	0.001364	0.007751	0.377687	1	0.880862	0.209935	0.015865	0.218712	0.151029	0.150162	0.001257
BAT	0.00315	0.013913	0.320074	0.880862	1	0.26606	0.010688	0.191625	0.123306	0.124949	0.00077
OCB	0.233784	0.412826	0.079614	0.209935	0.26606	1	0.009869	0.06894	0.059673	0.050186	0.001267
TiKi	2.61E-05	4.81E-05	0.142322	0.015865	0.010688	0.009869	1	0.429586	0.358325	0.391562	0.34094
ValBer	0.000345	0.002101	0.647817	0.218712	0.191625	0.06894	0.429586	1	0.876285	0.907967	0.182343
BarHau	0.000781	0.001821	0.520993	0.151029	0.123306	0.059673	0.358325	0.876285	1	0.955595	0.112483
Apt	0.00032	0.001149	0.538391	0.150162	0.124949	0.050186	0.391562	0.907967	0.955595	1	0.136007
Alb	4.73E-07	1.15E-06	0.030094	0.001257	0.00077	0.001267	0.34094	0.182343	0.112483	0.136007	1

b) *Lagerstätten removal 1* (most diverse site from each bin removed)

	AOI	CL	RN	PSH	BAT	OCB	TiKi	ValBer	BarHau	Apt	Alb
AOI	1	0.733249	0.001794	0.705693	0.009148	0.160073	4.35E-05	0.002769	0.003035	0.000803	6.12E-06
CL	0.733249	1	0.00729	0.541159	0.030634	0.271076	7.92E-05	0.008702	0.006555	0.001956	1.69E-05
RN	0.001794	0.00729	1	0.002598	0.650636	0.392666	0.10061	0.54666	0.579249	0.37052	0.037327
PSH	0.705693	0.541159	0.002598	1	0.008632	0.144308	0.000937	0.004605	0.010322	0.003751	0.000129
BAT	0.009148	0.030634	0.650636	0.008632	1	0.615662	0.058964	0.357887	0.379702	0.226768	0.020094
OCB	0.160073	0.271076	0.392666	0.144308	0.615662	1	0.059433	0.282368	0.279941	0.179955	0.026566
TiKi	4.35E-05	7.92E-05	0.10061	0.000937	0.058964	0.059433	1	0.468733	0.268937	0.439004	0.647401
ValBer	0.002769	0.008702	0.54666	0.004605	0.357887	0.282368	0.468733	1	0.945745	0.860819	0.289591
BarHau	0.003035	0.006555	0.579249	0.010322	0.379702	0.279941	0.268937	0.945745	1	0.766816	0.158608
Apt	0.000803	0.001956	0.37052	0.003751	0.226768	0.179955	0.439004	0.860819	0.766816	1	0.264548
Alb	6.12E-06	1.69E-05	0.037327	0.000129	0.020094	0.026566	0.647401	0.289591	0.158608	0.264548	1

c) *Lagerstätten* removal 2 (sites with 10 or more species removed)

	AOI	CL	RN	PSH	BAT	OCB	TiKi	ValBer	BarHau	Apt	Alb
AOI	1	0.70843	0.000479	0.523713	0.003515	0.233792	0.000764	0.001263	0.002424	0.000158	4.68E-06
CL	0.70843	1	0.003627	0.45721	0.019434	0.412976	0.002095	0.004003	0.007598	0.000553	5.03E-05
RN	0.000479	0.003627	1	0.002621	0.655115	0.112947	0.602887	0.518901	0.904147	0.364469	0.155978
PSH	0.523713	0.45721	0.002621	1	0.008287	0.216574	0.010444	0.011756	0.016055	0.003848	0.000228
BAT	0.003515	0.019434	0.655115	0.008287	1	0.252763	0.393982	0.351297	0.623969	0.224294	0.081805
OCB	0.233792	0.412976	0.112947	0.216574	0.252763	1	0.068132	0.081115	0.136891	0.032193	0.009002
TiKi	0.000764	0.002095	0.602887	0.010444	0.393982	0.068132	1	0.856965	0.694564	0.696404	0.44433
ValBer	0.001263	0.004003	0.518901	0.011756	0.351297	0.081115	0.856965	1	0.616613	0.888438	0.627409
BarHau	0.002424	0.007598	0.904147	0.016055	0.623969	0.136891	0.694564	0.616613	1	0.450527	0.253151
Apt	0.000158	0.000553	0.364469	0.003848	0.224294	0.032193	0.696404	0.888438	0.450527	1	0.691628
Alb	4.68E-06	5.03E-05	0.155978	0.000228	0.081805	0.009002	0.44433	0.627409	0.253151	0.691628	1

d) Genus range data

	AOI	CL	RN	PSH	BAT	OCB	TiKi	ValBer	BarHau	Apt	Alb
AOI	1	0.934465	0.00017	0.041555	0.018922	0.016552	0.00034	0.000219	0.000289	0.000621	1.55E-05
CL	0.934465	1	0.00034	0.051569	0.025192	0.023056	0.000725	0.000476	0.00062	0.00119	4.49E-05
RN	0.00017	0.00034	1	0.486707	0.571509	0.927777	0.303968	0.253449	0.238395	0.631362	0.077875
PSH	0.041555	0.051569	0.486707	1	0.893376	0.649395	0.155888	0.14593	0.134812	0.31583	0.046045
BAT	0.018922	0.025192	0.571509	0.893376	1	0.725162	0.171705	0.158213	0.14524	0.361846	0.047625
OCB	0.016552	0.023056	0.927777	0.649395	0.725162	1	0.275002	0.285398	0.241404	0.615543	0.088583
TiKi	0.00034	0.000725	0.303968	0.155888	0.171705	0.275002	1	0.892698	0.817789	0.496782	0.404568
ValBer	0.000219	0.000476	0.253449	0.14593	0.158213	0.285398	0.892698	1	0.945213	0.462557	0.569782
BarHau	0.000289	0.00062	0.238395	0.134812	0.14524	0.241404	0.817789	0.945213	1	0.404847	0.599052
Apt	0.000621	0.00119	0.631362	0.31583	0.361846	0.615543	0.496782	0.462557	0.404847	1	0.152578
Alb	1.55E-05	4.49E-05	0.077875	0.046045	0.047625	0.088583	0.404568	0.569782	0.599052	0.152578	1

Table A1.1. P values derived from t tests comparing the disparity of neopterygians between all Mesozoic time bins for a) the full dataset of 356 species, b) *Lagerstätten* removal 1 (most diverse site from each bin removed), c) *Lagerstätte* removal 2 (sites with 10 or more species removed), d) genus range data.
Stratigraphic interval abbreviations: AOI, Induan-Anisian; CL, Ladinian-Carnian; RN, Norian-Rhaetian; PSH, Hettangian-Pliensbachian; BAT, Toarcian-Bajocian; OCB, Bathonian-Oxfordian; TiKi, Kimmeridgian-Tithonian; ValBer, Berriasian-Valanginian; BarHau, Hauterivian-Barremian; Apt, Aptian; Alb, Albian.

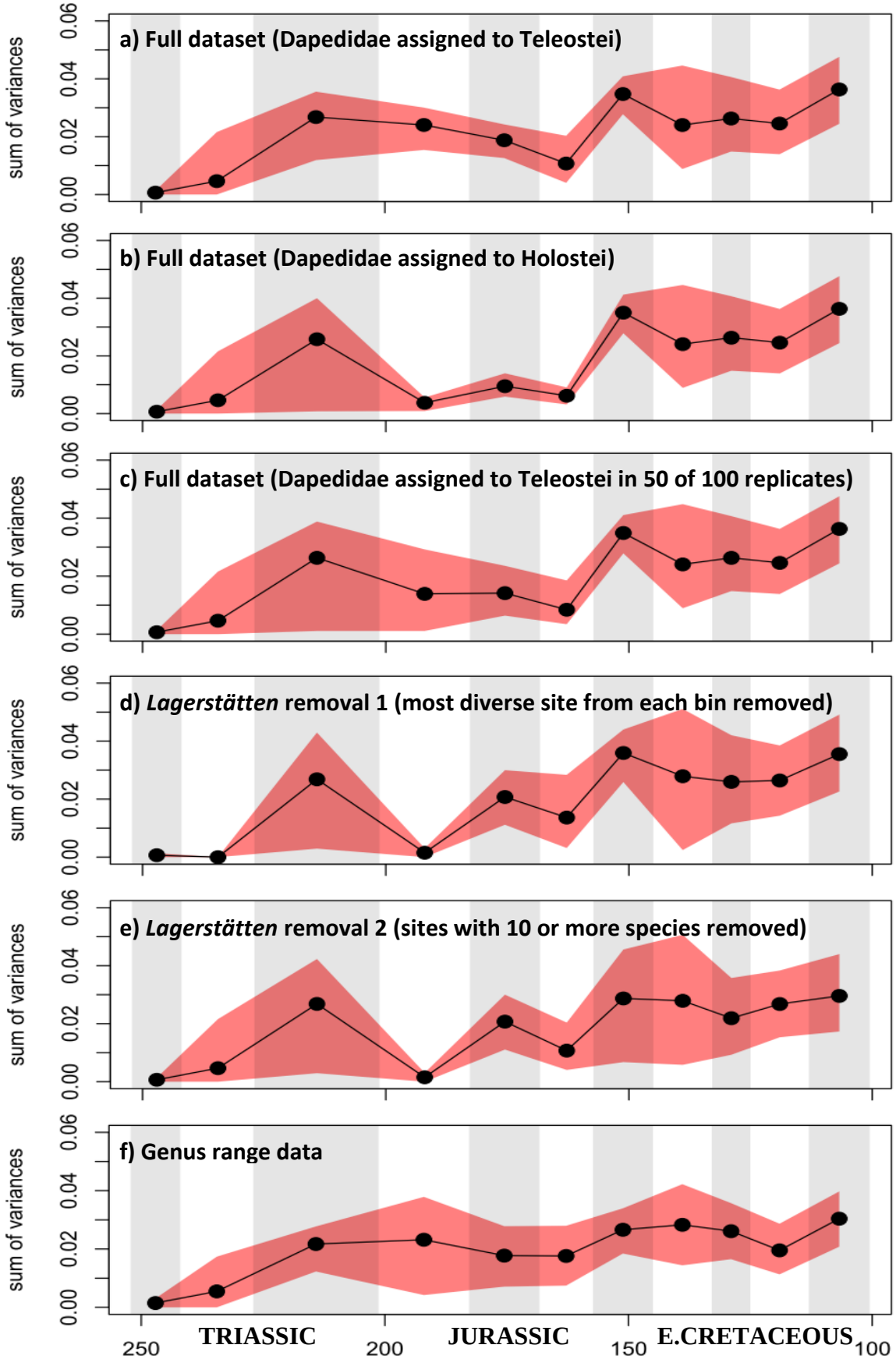

Fig. A1.2. Teleost morphological disparity through eleven Mesozoic time bins based upon a) the full dataset of 356 species, b) full dataset with Dapedidae assigned to Holostei, c) full dataset with Dapedidae assigned to Holostei in 50 of 100 replicates, d) *Lagerstätten* removal 1 (most diverse site from each bin removed), e) *Lagerstätten* removal 2 (sites with 10 or more species removed), f) genus range data.

a) Full dataset (Dapedidae assigned to Teleostei)

	T_AOI	T_CL	T_RN	T_PSH	T_BAT	T_OCB	T_TiKi	T_ValBer	T_BarHau	T_Apt	T_Alb
T_AOI	1	0.074719	0.034653	0.014787	0.062036	0.359722	0.083165	0.123973	0.191697	0.148703	0.054391
T_CL	0.074719	NA	0.171375	0.123597	0.289156	0.690517	0.275835	0.335688	0.428078	0.384948	0.213591
T_RN	0.034653	0.171375	1	0.644985	0.156075	0.023363	0.397122	0.763044	0.959088	0.79189	0.298954
T_PSH	0.014787	0.123597	0.644985	1	0.248032	0.019866	0.171679	0.998486	0.78228	0.942548	0.109383
T_BAT	0.062036	0.289156	0.156075	0.248032	1	0.105462	0.010083	0.448273	0.259946	0.32501	0.006624
T_OCB	0.359722	0.690517	0.023363	0.019866	0.105462	1	0.002154	0.11948	0.063714	0.060865	0.00184
T_TiKi	0.083165	0.275835	0.397122	0.171679	0.010083	0.002154	1	0.352929	0.238062	0.151513	0.817397
T_ValBer	0.123973	0.335688	0.763044	0.998486	0.448273	0.11948	0.352929	1	0.851511	0.960467	0.277555
T_BarHau	0.191697	0.428078	0.959088	0.78228	0.259946	0.063714	0.238062	0.851511	1	0.835429	0.239158
T_Apt	0.148703	0.384948	0.79189	0.942548	0.32501	0.060865	0.151513	0.960467	0.835429	1	0.140762
T_Alb	0.054391	0.213591	0.298954	0.109383	0.006624	0.00184	0.817397	0.277555	0.239158	0.140762	1

b) Full dataset (Dapedidae assigned to Holostei)

	T_AOI	T_CL	T_RN	T_PSH	T_BAT	T_OCB	T_TiKi	T_ValBer	T_BarHau	T_Apt	T_Alb
T_AOI	1	0.074764	0.178605	0.119904	0.117539	0.130877	0.085534	0.12291	0.190504	0.148218	0.054293
T_CL	0.074764	NA	0.402652	0.722497	0.527435	0.752473	0.278994	0.333898	0.426677	0.384106	0.213353
T_RN	0.178605	0.402652	1	0.050301	0.028618	0.013868	0.404024	0.893073	0.96482	0.91035	0.345366
T_PSH	0.119904	0.722497	0.050301	1	0.08504	0.265982	0.007565	0.027119	0.051778	0.034231	0.003754
T_BAT	0.117539	0.527435	0.028618	0.08504	1	0.190772	0.000501	0.021291	0.022595	0.016949	0.000226
T_OCB	0.130877	0.752473	0.013868	0.265982	0.190772	1	0.000376	0.006689	0.012879	0.007659	0.000162
T_TiKi	0.085534	0.278994	0.404024	0.007565	0.000501	0.000376	1	0.351166	0.231487	0.149181	0.847808
T_ValBer	0.12291	0.333898	0.893073	0.027119	0.021291	0.006689	0.351166	1	0.853466	0.960912	0.279302
T_BarHau	0.190504	0.426677	0.96482	0.051778	0.022595	0.012879	0.231487	0.853466	1	0.837958	0.239391
T_Apt	0.148218	0.384106	0.91035	0.034231	0.016949	0.007659	0.149181	0.960912	0.837958	1	0.142325
T_Alb	0.054293	0.213353	0.345366	0.003754	0.000226	0.000162	0.847808	0.279302	0.239391	0.142325	1

c) Full dataset (Dapedidae assigned to Teleostei in 50 of 100 replicates)

	T_AOI	T_CL	T_RN	T_PSH	T_BAT	T_OCB	T_TiKi	T_ValBer	T_BarHau	T_Apt	T_Alb
T_AOI	1	0.074607	0.098218	0.407585	0.346384	0.410523	0.082512	0.123823	0.191145	0.151034	0.054678
T_CL	0.074607	NA	0.292996	0.673795	0.634474	0.773407	0.274607	0.335532	0.427565	0.387793	0.21431
T_RN	0.098218	0.292996	1	0.303059	0.19316	0.027235	0.425019	0.838269	0.999388	0.861764	0.347938
T_PSH	0.407585	0.673795	0.303059	1	0.979316	0.51246	0.073543	0.410234	0.317896	0.32839	0.059694
T_BAT	0.346384	0.634474	0.19316	0.979316	1	0.384108	0.005732	0.309102	0.149127	0.171285	0.007074
T_OCB	0.410523	0.773407	0.027235	0.51246	0.384108	1	0.001086	0.056153	0.035659	0.030208	0.000861
T_TiKi	0.082512	0.274607	0.425019	0.073543	0.005732	0.001086	1	0.348839	0.232892	0.148911	0.837396
T_ValBer	0.123823	0.335532	0.838269	0.410234	0.309102	0.056153	0.348839	1	0.851787	0.960062	0.27997
T_BarHau	0.191145	0.427565	0.999388	0.317896	0.149127	0.035659	0.232892	0.851787	1	0.837125	0.241559
T_Apt	0.151034	0.387793	0.861764	0.32839	0.171285	0.030208	0.148911	0.960062	0.837125	1	0.144284
T_Alb	0.054678	0.21431	0.347938	0.059694	0.007074	0.000861	0.837396	0.27997	0.241559	0.144284	1

d) *Lagerstätten* removal 1 (most diverse site from each bin removed)

	T_AOI	T_CL	T_RN	T_PSH	T_BAT	T_OCB	T_TiKi	T_ValBer	T_BarHau	T_Apt	T_Alb
T_AOI	1	0.408109	0.089369	0.469512	0.055805	0.337234	0.055357	0.089573	0.188628	0.129434	0.043317
T_CL	0.408109	NA	0.195131	0.420132	0.145903	0.468421	0.161483	0.204249	0.331693	0.262748	0.131103
T_RN	0.089369	0.195131	1	0.09771	0.480474	0.235076	0.444889	0.936391	0.945206	0.971394	0.450947
T_PSH	0.469512	0.420132	0.09771	1	0.065308	0.368292	0.06117	0.096352	0.203005	0.141712	0.047934
T_BAT	0.055805	0.145903	0.480474	0.065308	1	0.36341	0.076125	0.460002	0.574497	0.487879	0.080284
T_OCB	0.337234	0.468421	0.235076	0.368292	0.36341	1	0.024751	0.267264	0.261692	0.189011	0.032467
T_TiKi	0.055357	0.161483	0.444889	0.06117	0.076125	0.024751	1	0.591922	0.244907	0.216014	0.96199
T_ValBer	0.089573	0.204249	0.936391	0.096352	0.460002	0.267264	0.591922	1	0.903106	0.917304	0.584315
T_BarHau	0.188628	0.331693	0.945206	0.203005	0.574497	0.261692	0.244907	0.903106	1	0.958972	0.33034
T_Apt	0.129434	0.262748	0.971394	0.141712	0.487879	0.189011	0.216014	0.917304	0.958972	1	0.29827
T_Alb	0.043317	0.131103	0.450947	0.047934	0.080284	0.032467	0.96199	0.584315	0.33034	0.29827	1

e) *Lagerstätten* removal 2 (sites with 10 or more species removed)

	T_AOI	T_CL	T_RN	T_PSH	T_BAT	T_OCB	T_TiKi	T_ValBer	T_BarHau	T_Apt	T_Alb
T_AOI	1	0.073922	0.088107	0.4603	0.056833	0.360678	0.196358	0.163659	0.206445	0.127679	0.047765
T_CL	0.073922	NA	0.266681	0.228979	0.251324	0.693137	0.420257	0.376335	0.45843	0.351319	0.197404
T_RN	0.088107	0.266681	1	0.096494	0.479848	0.073989	0.896503	0.937961	0.672925	0.997752	0.791317
T_PSH	0.4603	0.228979	0.096494	1	0.066597	0.402288	0.209378	0.175447	0.224415	0.139958	0.053499
T_BAT	0.056833	0.251324	0.479848	0.066597	1	0.1139	0.446243	0.474542	0.887236	0.459603	0.245968
T_OCB	0.360678	0.693137	0.073989	0.402288	0.1139	1	0.066235	0.081147	0.15017	0.03493	0.015097
T_TiKi	0.196358	0.420257	0.896503	0.209378	0.446243	0.066235	1	0.95542	0.541877	0.852122	0.940273
T_ValBer	0.163659	0.376335	0.937961	0.175447	0.474542	0.081147	0.95542	1	0.616553	0.923091	0.883511
T_BarHau	0.206445	0.45843	0.672925	0.224415	0.887236	0.15017	0.541877	0.616553	1	0.570426	0.415337
T_Apt	0.127679	0.351319	0.997752	0.139958	0.459603	0.03493	0.852122	0.923091	0.570426	1	0.757913
T_Alb	0.047765	0.197404	0.791317	0.053499	0.245968	0.015097	0.940273	0.883511	0.415337	0.757913	1

f) Genus range data

	T_AOI	T_CL	T_RN	T_PSH	T_BAT	T_OCB	T_TiKi	T_ValBer	T_BarHau	T_Apt	T_Alb
T_AOI	1	0.456296	0.021031	0.162303	0.19071	0.300163	0.153682	0.125362	0.155816	0.205014	0.080899
T_CL	0.456296	1	0.029205	0.170229	0.234297	0.34311	0.143264	0.114577	0.147784	0.230258	0.067882
T_RN	0.021031	0.029205	1	0.850032	0.528904	0.579715	0.540544	0.422422	0.580752	0.746988	0.255042
T_PSH	0.162303	0.170229	0.850032	1	0.540676	0.562471	0.729158	0.634113	0.770431	0.678282	0.455797
T_BAT	0.19071	0.234297	0.528904	0.540676	1	0.987535	0.247729	0.216728	0.285246	0.791932	0.097344
T_OCB	0.300163	0.34311	0.579715	0.562471	0.987535	1	0.179177	0.200035	0.232436	0.769858	0.070224
T_TiKi	0.153682	0.143264	0.540544	0.729158	0.247729	0.179177	1	0.828822	0.935649	0.251898	0.541203
T_ValBer	0.125362	0.114577	0.422422	0.634113	0.216728	0.200035	0.828822	1	0.790048	0.251098	0.793821
T_BarHau	0.155816	0.147784	0.580752	0.770431	0.285246	0.232436	0.935649	0.790048	1	0.315016	0.522811
T_Apt	0.205014	0.230258	0.746988	0.678282	0.791932	0.769858	0.251898	0.251098	0.315016	1	0.093588
T_Alb	0.080899	0.067882	0.255042	0.455797	0.097344	0.070224	0.541203	0.793821	0.522811	0.093588	1

Table A1.2. P values derived from t tests comparing the disparity of teleosts between all Mesozoic time bins for a) the full dataset of 356 species, b) full dataset with Dapedidae assigned to Holostei, c) full dataset Dapedidae assigned to Holostei in 50% of the time, d) *Lagerstätten* removal 1 (most diverse site from each bin removed), e) *Lagerstätten* removal 2 (sites with 10 or more species removed), f) genus range data.
Stratigraphic interval abbreviations: AOI, Induan-Anisian; CL, Ladinian-Carnian; RN, Norian-Rhaetian; PSH, Hettangian-Pliensbachian; BAT, Toarcian-Bajocian; OCB, Bathonian-Oxfordian; TiKi, Kimmeridgian-Tithonian; ValBer, Berriasian-Valanginian; BarHau, Hauterivian-Barremian; Apt, Aptian; Alb, Albian.

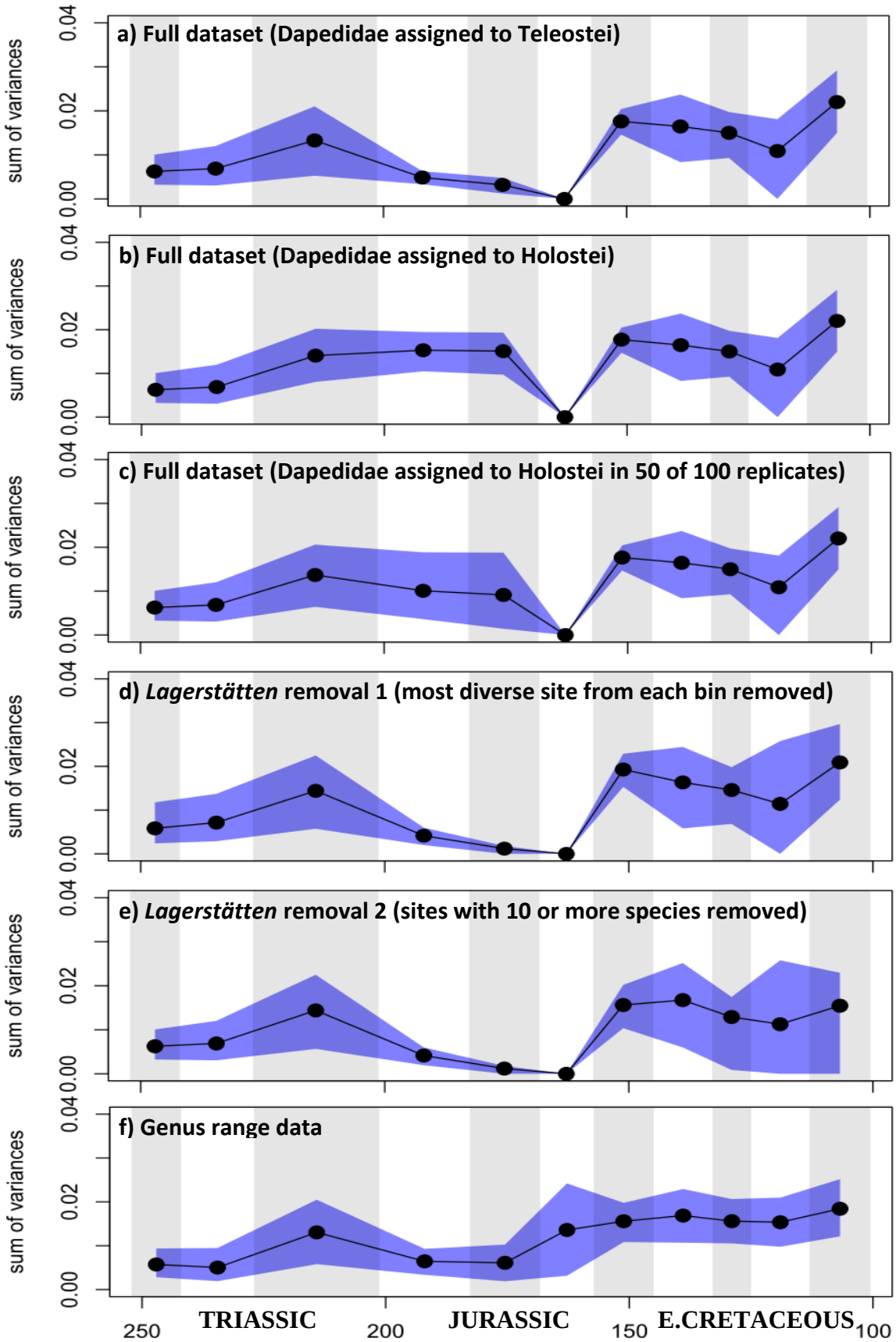

Fig. A1.3. Holostean morphological disparity through eleven Mesozoic time bins based upon a) the full dataset of 356 species, b) full dataset with Dapedidae assigned to Holostei, c) full dataset with Dapedidae assigned to Holostei in 50 of 100 replicates, d) *Lagerstätten* removal 1 (most diverse site from each bin removed), e) *Lagerstätten* removal 2 (sites with 10 or more species removed), f) genus range data.

a) Full dataset (Dapedidae assigned to Teleostei)

	H_AOI	H_CL	H_RN	H_PSH	H_BAT	H_OCB	H_TiKi	H_ValBer	H_BarHau	H_Apt	H_Alb
H_AOI	1	0.826457	0.055328	0.533097	0.352793	1	2.66E-05	0.010194	0.006278	0.416841	6.66E-05
H_CL	0.826457	1	0.138456	0.508757	0.420902	1	0.000168	0.058586	0.043218	0.614181	0.000545
H_RN	0.055328	0.138456	1	0.019201	0.057727	1	0.240932	0.572032	0.702729	0.78091	0.096776
H_PSH	0.533097	0.508757	0.019201	1	0.172124	1	4.11E-05	0.000195	0.00013	0.01493	5.28E-05
H_BAT	0.352793	0.420902	0.057727	0.172124	1	1	0.001758	0.003132	0.001926	0.012572	0.002203
H_OCB	1	1	1	1	1	NA	1	1	1	NA	1
H_TiKi	2.66E-05	0.000168	0.240932	4.11E-05	0.001758	1	1	0.801457	0.468488	0.382116	0.188586
H_ValBer	0.010194	0.058586	0.572032	0.000195	0.003132	1	0.801457	1	0.723995	0.377841	0.345147
H_BarHau	0.006278	0.043218	0.702729	0.00013	0.001926	1	0.468488	0.723995	1	0.459452	0.139834
H_Apt	0.416841	0.614181	0.78091	0.01493	0.012572	NA	0.382116	0.377841	0.459452	1	0.243302
H_Alb	6.66E-05	0.000545	0.096776	5.28E-05	0.002203	1	0.188586	0.345147	0.139834	0.243302	1

b) Full dataset (Dapedidae assigned to Holostei)

	H_AOI	H_CL	H_RN	H_PSH	H_BAT	H_OCB	H_TiKi	H_ValBer	H_BarHau	H_Apt	H_Alb
H_AOI	1	0.830302	0.01771	0.002005	0.003815	0.431987	2.27E-05	0.010213	0.00637	0.417962	6.53E-05
H_CL	0.830302	1	0.065455	0.011861	0.029156	0.536934	0.00014	0.058069	0.043052	0.613412	0.000532
H_RN	0.01771	0.065455	1	0.733271	0.784502	0.187789	0.274447	0.622488	0.81136	0.668198	0.090434
H_PSH	0.002005	0.011861	0.733271	1	0.95107	0.132034	0.374688	0.792697	0.935807	0.533844	0.090279
H_BAT	0.003815	0.029156	0.784502	0.95107	1	0.070531	0.427938	0.732109	0.980416	0.459928	0.118343
H_OCB	0.431987	0.536934	0.187789	0.132034	0.070531	NA	0.105653	0.088128	0.06931	0.207885	0.106381
H_TiKi	2.27E-05	0.00014	0.274447	0.374688	0.427938	0.105653	1	0.785154	0.450572	0.375356	0.198813
H_ValBer	0.010213	0.058069	0.622488	0.792697	0.732109	0.088128	0.785154	1	0.722119	0.376693	0.344681
H_BarHau	0.00637	0.043052	0.81136	0.935807	0.980416	0.06931	0.450572	0.722119	1	0.460022	0.138865
H_Apt	0.417962	0.613412	0.668198	0.533844	0.459928	0.207885	0.375356	0.376693	0.460022	1	0.241698
H_Alb	6.53E-05	0.000532	0.090434	0.090279	0.118343	0.106381	0.198813	0.344681	0.138865	0.241698	1

c) Full dataset (Dapedidae assigned to Holostei in 50 of 100 replicates)

	H_AOI	H_CL	H_RN	H_PSH	H_BAT	H_OCB	H_TiKi	H_ValBer	H_BarHau	H_Apt	H_Alb
H_AOI	1	0.83323	0.034172	0.413131	0.509448	1	2.24E-05	0.010271	0.006336	0.418369	6.52E-05
H_CL	0.83323	1	0.103425	0.524608	0.67306	1	0.000142	0.058154	0.042764	0.612887	0.000526
H_RN	0.034172	0.103425	1	0.581639	0.455495	1	0.266913	0.592245	0.751388	0.720317	0.098451
H_PSH	0.413131	0.524608	0.581639	1	0.912564	1	0.054113	0.437125	0.44548	0.952528	0.058947
H_BAT	0.509448	0.67306	0.455495	0.912564	1	1	0.076552	0.267936	0.273548	0.852471	0.055204
H_OCB	1	1	1	1	1	NA	1	1	1	NA	1
H_TiKi	2.24E-05	0.000142	0.266913	0.054113	0.076552	1	1	0.789343	0.455343	0.374347	0.190094
H_ValBer	0.010271	0.058154	0.592245	0.437125	0.267936	1	0.789343	1	0.72402	0.376577	0.342183
H_BarHau	0.006336	0.042764	0.751388	0.44548	0.273548	1	0.455343	0.72402	1	0.458625	0.138093
H_Apt	0.418369	0.612887	0.720317	0.952528	0.852471	NA	0.374347	0.376577	0.458625	1	0.241586
H_Alb	6.52E-05	0.000526	0.098451	0.058947	0.055204	1	0.190094	0.342183	0.138093	0.241586	1

d) *Lagerstätten* removal 1 (most diverse site from each bin removed)

	H_AOI	H_CL	H_RN	H_PSH	H_BAT	H_OCB	H_TiKi	H_ValBer	H_BarHau	H_Apt	H_Alb
H_AOI	1	0.826545	0.032281	0.464156	0.272802	1	0.002031	0.012164	0.104806	0.38383	0.069071
H_CL	0.826545	1	0.095281	0.494184	0.379298	1	0.01579	0.059853	0.2639	0.584084	0.205766
H_RN	0.032281	0.095281	1	0.031905	0.080736	1	0.776319	0.696339	0.805565	0.721546	0.886707
H_PSH	0.464156	0.494184	0.031905	1	0.070505	1	0.001876	0.005283	0.017541	0.025462	0.005461
H_BAT	0.272802	0.379298	0.080736	0.070505	1	1	0.012123	0.02794	0.043805	0.042195	0.02879
H_OCB	1	1	1	1	1	NA	1	1	1	NA	1
H_TiKi	0.002031	0.01579	0.776319	0.001876	0.012123	1	1	0.806798	0.555238	0.506399	0.977566
H_ValBer	0.012164	0.059853	0.696339	0.005283	0.02794	1	0.806798	1	0.505894	0.473056	0.848869
H_BarHau	0.104806	0.2639	0.805565	0.017541	0.043805	1	0.555238	0.505894	1	0.797645	0.669001
H_Apt	0.38383	0.584084	0.721546	0.025462	0.042195	NA	0.506399	0.473056	0.797645	1	0.526004
H_Alb	0.069071	0.205766	0.886707	0.005461	0.02879	1	0.977566	0.848869	0.669001	0.526004	1

e) *Lagerstätten* removal 2 (sites with 10 or more species removed)

	H_AOI	H_CL	H_RN	H_PSH	H_BAT	H_OCB	H_TiKi	H_ValBer	H_BarHau	H_Apt	H_Alb
H_AOI	1	0.730697	0.055848	0.623162	0.398901	1	7.41E-05	0.038707	0.064302	0.419192	0.00206
H_CL	0.730697	1	0.14069	0.492645	0.398202	1	0.000551	0.124821	0.194097	0.622025	0.00881
H_RN	0.055848	0.14069	1	0.030964	0.07922	1	0.220893	0.754493	0.975337	0.734871	0.256062
H_PSH	0.623162	0.492645	0.030964	1	0.070136	1	0.000165	0.003289	0.001296	0.032451	0.001899
H_BAT	0.398901	0.398202	0.07922	0.070136	1	1	0.003931	0.019993	0.007785	0.056964	0.018316
H_OCB	1	1	1	1	1	NA	1	1	1	NA	1
H_TiKi	7.41E-05	0.000551	0.220893	0.000165	0.003931	1	1	0.542306	0.320315	0.284396	0.686023
H_ValBer	0.038707	0.124821	0.754493	0.003289	0.019993	1	0.542306	1	0.718205	0.4791	0.474923
H_BarHau	0.064302	0.194097	0.975337	0.001296	0.007785	1	0.320315	0.718205	1	0.549646	0.30397
H_Apt	0.419192	0.622025	0.734871	0.032451	0.056964	NA	0.284396	0.4791	0.549646	1	0.312326
H_Alb	0.00206	0.00881	0.256062	0.001899	0.018316	1	0.686023	0.474923	0.30397	0.312326	1

f) Genus range data

	H_AOI	H_CL	H_RN	H_PSH	H_BAT	H_OCB	H_TiKi	H_ValBer	H_BarHau	H_Apt	H_Alb
H_AOI	1	0.780081	0.040056	0.792209	0.910752	0.07071	0.000933	0.00102	0.001289	0.002563	0.000582
H_CL	0.780081	1	0.042434	0.616442	0.757478	0.07298	0.001541	0.001692	0.001679	0.003186	0.0012
H_RN	0.040056	0.042434	1	0.139133	0.21001	0.930562	0.526338	0.401923	0.546303	0.603528	0.27053
H_PSH	0.792209	0.616442	0.139133	1	0.887666	0.164672	0.020405	0.014736	0.008585	0.014307	0.014557
H_BAT	0.910752	0.757478	0.21001	0.887666	1	0.238288	0.052644	0.040836	0.025538	0.037553	0.041962
H_OCB	0.07071	0.07298	0.930562	0.164672	0.238288	1	0.694207	0.561997	0.693069	0.741797	0.432867
H_TiKi	0.000933	0.001541	0.526338	0.020405	0.052644	0.694207	1	0.71845	0.994814	0.948862	0.445659
H_ValBer	0.00102	0.001692	0.401923	0.014736	0.040836	0.561997	0.71845	1	0.740324	0.703984	0.72103
H_BarHau	0.001289	0.001679	0.546303	0.008585	0.025538	0.693069	0.994814	0.740324	1	0.942779	0.503942
H_Apt	0.002563	0.003186	0.603528	0.014307	0.037553	0.741797	0.948862	0.703984	0.942779	1	0.486291
H_Alb	0.000582	0.0012	0.27053	0.014557	0.041962	0.432867	0.445659	0.72103	0.503942	0.486291	1

Table A1.3. P values derived from t tests comparing the disparity of holosteans between all Mesozoic time bins for a) the full dataset of 356 species, b) full dataset Dapedidae assigned to Holostei, c) full dataset with Dapedidae assigned to Holostei in 50% of the time, d) *Lagerstätten* removal 1 (most diverse site from each bin removed), e) *Lagerstätten* removal 2 (sites with 10 or more species removed), f) genus range data.
Stratigraphic interval abbreviations: AOI, Induan-Anisian; CL, Ladinian-Carnian; RN, Norian-Rhaetian; PSH, Hettangian-Pliensbachian; BAT, Toarcian-Bajocian; OCB, Bathonian-Oxfordian; TiKi, Kimmeridgian-Tithonian; ValBer, Berriasian-Valanginian; BarHau, Hauterivian-Barremian; Apt, Aptian; Alb, Albian.

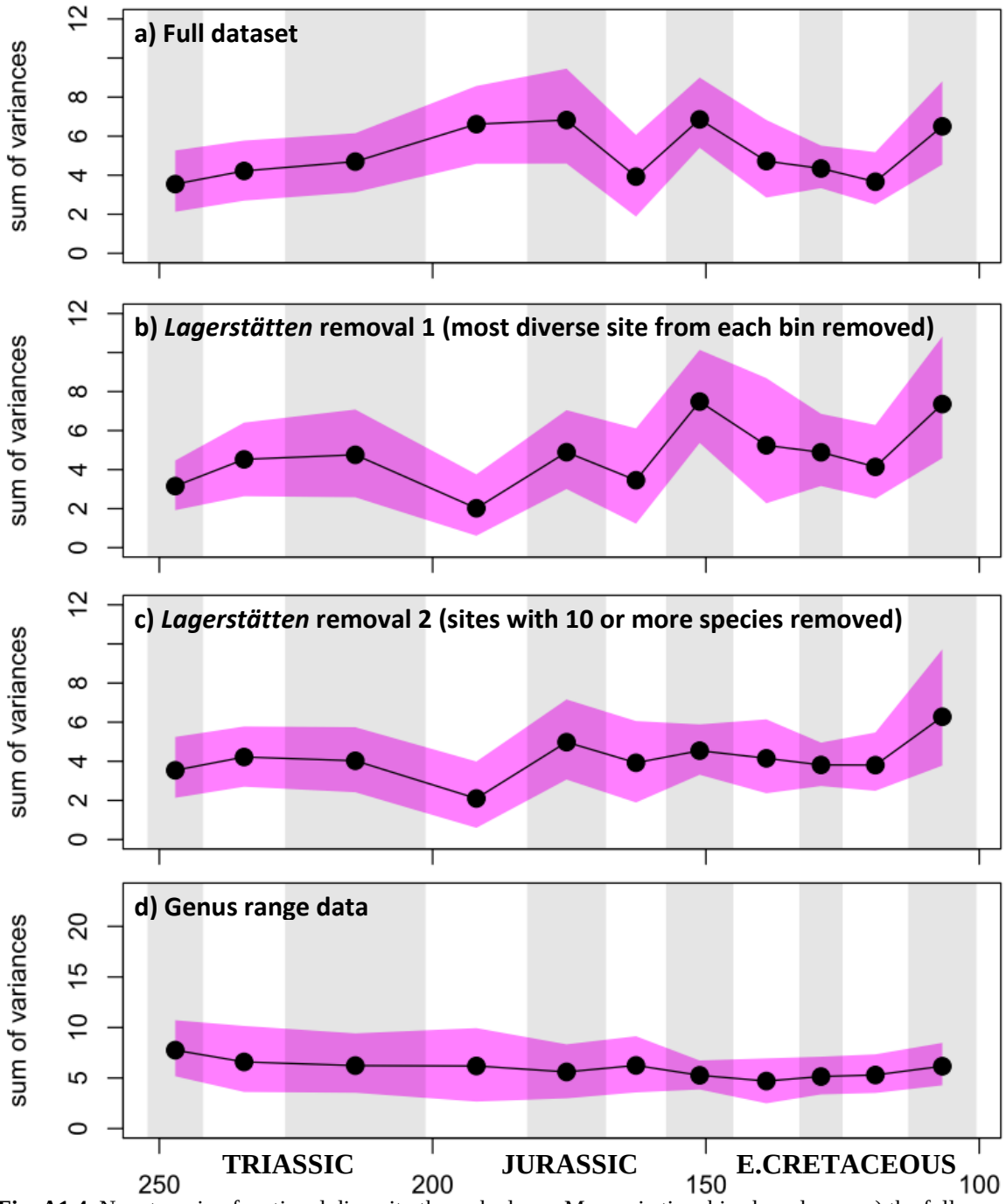

Fig. A1.4. Neopterygian functional disparity through eleven Mesozoic time bins based upon a) the full dataset of 356 species, b) *Lagerstätten* removal 1 (most diverse site from each bin removed), c) *Lagerstätten* removal 2 (sites with 10 or more species removed), d) genus range data.

a) Full dataset

	AOI	CL	RN	PSH	BAT	OCB	TiKi	ValBer	BarHau	Apt	Alb
AOI	1	0.538299	0.296491	0.016886	0.031357	0.772254	0.11197	0.380059	0.389946	0.906768	0.038964
CL	0.538299	1	0.656807	0.055107	0.082212	0.82211	0.204259	0.698997	0.889611	0.589415	0.105484
RN	0.296491	0.656807	1	0.124341	0.176239	0.533784	0.341613	0.983666	0.694798	0.30201	0.223267
PSH	0.016886	0.055107	0.124341	1	0.897144	0.078572	0.914654	0.21306	0.033098	0.015372	0.94352
BAT	0.031357	0.082212	0.176239	0.897144	1	0.148281	0.987118	0.305991	0.060532	0.040133	0.839615
OCB	0.772254	0.82211	0.533784	0.078572	0.148281	1	0.324681	0.559507	0.694161	0.820748	0.173113
TiKi	0.11197	0.204259	0.341613	0.914654	0.987118	0.324681	1	0.492393	0.180847	0.150105	0.847847
ValBer	0.380059	0.698997	0.983666	0.21306	0.305991	0.559507	0.492393	1	0.721153	0.356357	0.358715
BarHau	0.389946	0.889611	0.694798	0.033098	0.060532	0.694161	0.180847	0.721153	1	0.424632	0.082685
Apt	0.906768	0.589415	0.30201	0.015372	0.040133	0.820748	0.150105	0.356357	0.424632	1	0.05023
Alb	0.038964	0.105484	0.223267	0.94352	0.839615	0.173113	0.847847	0.358715	0.082685	0.05023	1

b) *Lagerstätten removal 1* (most diverse site from each bin removed)

	AOI	CL	RN	PSH	BAT	OCB	TiKi	ValBer	BarHau	Apt	Alb
AOI	1	0.187876	0.347079	0.367857	0.089338	0.647822	0.014915	0.286175	0.167696	0.466673	0.024884
CL	0.187876	1	0.687048	0.120007	0.742391	0.602221	0.290137	0.906833	0.836744	0.546393	0.206502
RN	0.347079	0.687048	1	0.150053	0.454954	0.798036	0.158709	0.81639	0.78475	0.847469	0.138256
PSH	0.367857	0.120007	0.150053	1	0.060448	0.285363	0.030533	0.119028	0.063255	0.214929	0.061476
BAT	0.089338	0.742391	0.454954	0.060448	1	0.41982	0.534513	0.682492	0.547254	0.347239	0.356594
OCB	0.647822	0.602221	0.798036	0.285363	0.41982	1	0.243256	0.660095	0.612133	0.918315	0.244533
TiKi	0.014915	0.290137	0.158709	0.030533	0.534513	0.243256	1	0.396029	0.177711	0.081817	0.462685
ValBer	0.286175	0.906833	0.81639	0.119028	0.682492	0.660095	0.396029	1	0.971987	0.702792	0.33119
BarHau	0.167696	0.836744	0.78475	0.063255	0.547254	0.612133	0.177711	0.971987	1	0.620682	0.131364
Apt	0.466673	0.546393	0.847469	0.214929	0.347239	0.918315	0.081817	0.702792	0.620682	1	0.080003
Alb	0.024884	0.206502	0.138256	0.061476	0.356594	0.244533	0.462685	0.33119	0.131364	0.080003	1

c) *Lagerstätten* removal 2 (sites with 10 or more species removed)

	AOI	CL	RN	PSH	BAT	OCB	TiKi	ValBer	BarHau	Apt	Alb
AOI	1	0.538451	0.68893	0.335329	0.267078	0.773273	0.335951	0.654812	0.794832	0.811365	0.074837
CL	0.538451	1	0.867147	0.150562	0.546797	0.820765	0.750895	0.954499	0.676021	0.696427	0.168187
RN	0.68893	0.867147	1	0.152872	0.457271	0.939143	0.615185	0.923342	0.820817	0.843656	0.164494
PSH	0.335329	0.150562	0.152872	1	0.061206	0.20462	0.045895	0.136919	0.103752	0.206774	0.044562
BAT	0.267078	0.546797	0.457271	0.061206	1	0.454629	0.694679	0.549331	0.270197	0.333546	0.445394
OCB	0.773273	0.820765	0.939143	0.20462	0.454629	1	0.585596	0.872755	0.908853	0.920505	0.189237
TiKi	0.335951	0.750895	0.615185	0.045895	0.694679	0.585596	1	0.722773	0.386472	0.448459	0.210204
ValBer	0.654812	0.954499	0.923342	0.136919	0.549331	0.872755	0.722773	1	0.738654	0.781378	0.236431
BarHau	0.794832	0.676021	0.820817	0.103752	0.270197	0.908853	0.386472	0.738654	1	0.996889	0.073186
Apt	0.811365	0.696427	0.843656	0.206774	0.333546	0.920505	0.448459	0.781378	0.996889	1	0.096119
Alb	0.074837	0.168187	0.164494	0.044562	0.445394	0.189237	0.210204	0.236431	0.073186	0.096119	1

d) Genus range data

	AOI	CL	RN	PSH	BAT	OCB	TiKi	ValBer	BarHau	Apt	Alb
AOI	1	0.582844	0.444985	0.487893	0.270213	0.437962	0.089795	0.083425	0.107446	0.131028	0.360212
CL	0.582844	1	0.867918	0.873144	0.647322	0.870027	0.395204	0.324516	0.407029	0.46299	0.819503
RN	0.444985	0.867918	1	0.987346	0.75162	0.993277	0.523374	0.393626	0.512788	0.575179	0.972473
PSH	0.487893	0.873144	0.987346	1	0.781068	0.981244	0.603161	0.454276	0.58108	0.634194	0.990359
BAT	0.270213	0.647322	0.75162	0.781068	1	0.742011	0.829044	0.599665	0.780928	0.852138	0.754059
OCB	0.437962	0.870027	0.993277	0.981244	0.742011	1	0.498935	0.377638	0.492883	0.557578	0.963651
TiKi	0.089795	0.395204	0.523374	0.603161	0.829044	0.498935	1	0.668956	0.916663	0.979444	0.46753
ValBer	0.083425	0.324516	0.393626	0.454276	0.599665	0.377638	0.668956	1	0.759193	0.679395	0.351961
BarHau	0.107446	0.407029	0.512788	0.58108	0.780928	0.492883	0.916663	0.759193	1	0.907786	0.468901
Apt	0.131028	0.46299	0.575179	0.634194	0.852138	0.557578	0.979444	0.679395	0.907786	1	0.544987
Alb	0.360212	0.819503	0.972473	0.990359	0.754059	0.963651	0.46753	0.351961	0.468901	0.544987	1

Table A1.4. P values derived from t tests comparing the disparity of neopterygians between all Mesozoic time bins for a) the full dataset of 356 species, b) *Lagerstätten* removal 1 (most diverse site from each bin removed), c) *Lagerstätten* removal 2 (sites with 10 or more species removed), d) genus range data.
Stratigraphic interval abbreviations: AOI, Induan-Anisian; CL, Ladinian-Carnian; RN, Norian-Rhaetian; PSH, Hettangian-Pliensbachian; BAT, Toarcian-Bajocian; OCB, Bathonian-Oxfordian; TiKi, Kimmeridgian-Tithonian; ValBer, Berriasian-Valanginian; BarHau, Hauterivian-Barremian; Apt, Aptian; Alb, Albian.

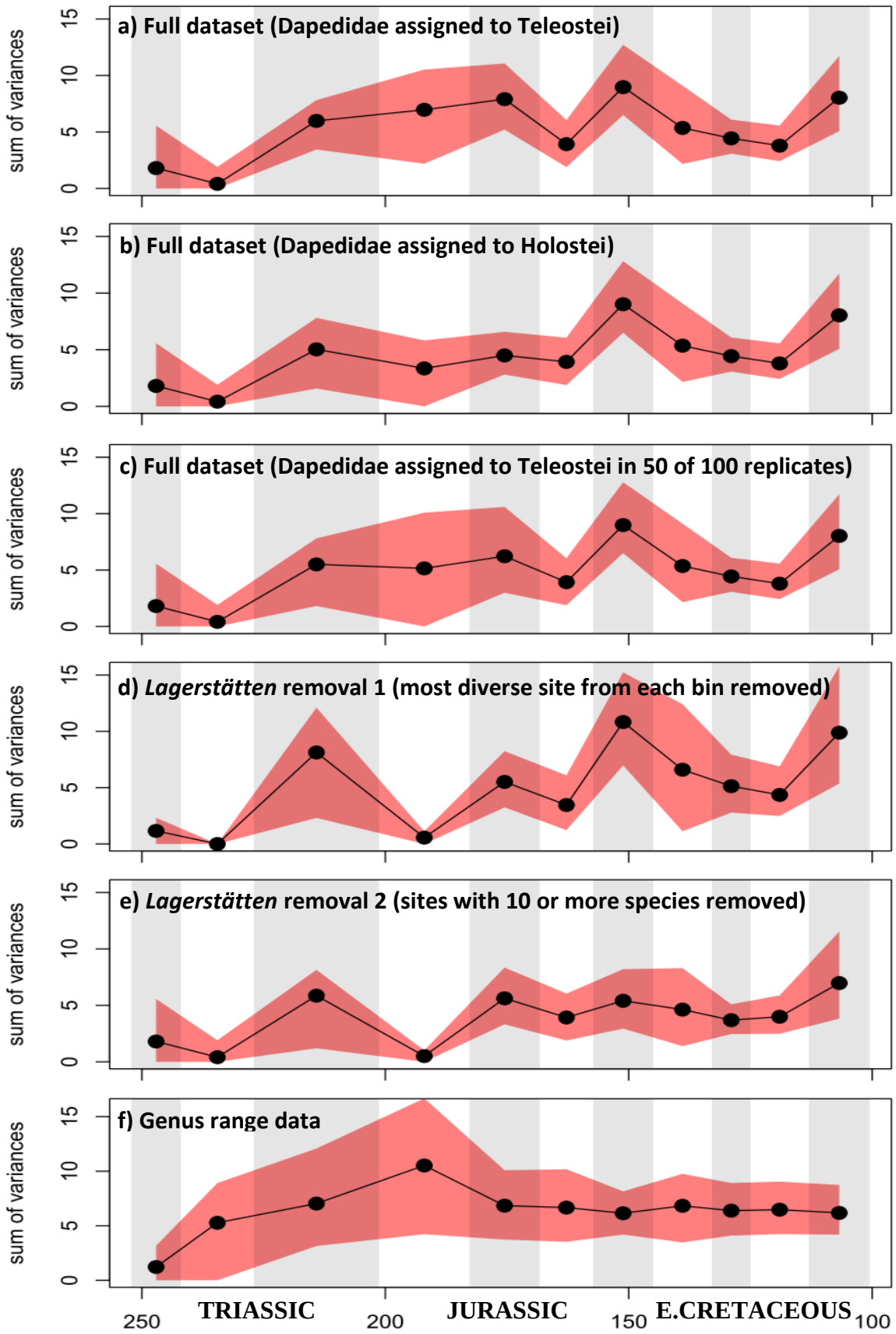

Fig. A1.5. Teleost functional disparity through eleven Mesozoic time bins based upon a) the full dataset of 356 species, b) full dataset with Dapedidae assigned to Holostei, c) full dataset with Dapedidae assigned to Holostei in 50 of 100 replicates, d) *Lagerstätten* removal 1 (most diverse site from each bin removed), e) *Lagerstätten* removal 2 (sites with 10 or more species removed), f) genus range data.

a) Full dataset (Dapedidae assigned to Teleostei)

	T_AOI	T_CL	T_RN	T_PSH	T_BAT	T_OCB	T_TiKi	T_ValBer	T_BarHau	T_Apt	T_Alb
T_AOI	1	0.487169	0.080977	0.223727	0.193104	0.36947	0.4148	0.173349	0.242104	0.395636	0.192572
T_CL	0.487169	NA	0.089701	0.26665	0.254025	0.284758	0.490205	0.169881	0.19967	0.300976	0.254389
T_RN	0.080977	0.089701	1	0.653221	0.400054	0.160255	0.472553	0.721509	0.227373	0.102117	0.381685
T_PSH	0.223727	0.26665	0.653221	1	0.709117	0.152242	0.633728	0.568118	0.150877	0.079721	0.683703
T_BAT	0.193104	0.254025	0.400054	0.709117	1	0.064794	0.708493	0.39861	0.045284	0.019738	0.952122
T_OCB	0.36947	0.284758	0.160255	0.152242	0.064794	1	0.183181	0.417932	0.674773	0.913449	0.06486
T_TiKi	0.4148	0.490205	0.472553	0.633728	0.708493	0.183181	1	0.516878	0.127826	0.082964	0.765837
T_ValBer	0.173349	0.169881	0.721509	0.568118	0.39861	0.417932	0.516878	1	0.560897	0.344929	0.385958
T_BarHau	0.242104	0.19967	0.227373	0.150877	0.045284	0.674773	0.127826	0.560897	1	0.544987	0.045192
T_Apt	0.395636	0.300976	0.102117	0.079721	0.019738	0.913449	0.082964	0.344929	0.544987	1	0.020624
T_Alb	0.192572	0.254389	0.381685	0.683703	0.952122	0.06486	0.765837	0.385958	0.045192	0.020624	1

b) Full dataset (Dapedidae assigned to Holostei)

	T_AOI	T_CL	T_RN	T_PSH	T_BAT	T_OCB	T_TiKi	T_ValBer	T_BarHau	T_Apt	T_Alb
T_AOI	1	0.48755	0.252869	0.502703	0.298931	0.371702	0.415682	0.173668	0.240796	0.394968	0.192826
T_CL	0.48755	NA	0.238272	0.365872	0.25976	0.288457	0.491824	0.170789	0.199197	0.301577	0.255116
T_RN	0.252869	0.238272	1	0.492842	0.749546	0.515846	0.402984	0.874257	0.686571	0.419353	0.26653
T_PSH	0.502703	0.365872	0.492842	1	0.602984	0.780413	0.434117	0.388526	0.571154	0.82513	0.235235
T_BAT	0.298931	0.25976	0.749546	0.602984	1	0.68134	0.169311	0.63417	0.958414	0.55762	0.07404
T_OCB	0.371702	0.288457	0.515846	0.780413	0.68134	1	0.183279	0.421956	0.677676	0.912657	0.065478
T_TiKi	0.415682	0.491824	0.402984	0.434117	0.169311	0.183279	1	0.514944	0.127177	0.082994	0.756879
T_ValBer	0.173668	0.170789	0.874257	0.388526	0.63417	0.421956	0.514944	1	0.56053	0.346057	0.386005
T_BarHau	0.240796	0.199197	0.686571	0.571154	0.958414	0.677676	0.127177	0.56053	1	0.546014	0.045156
T_Apt	0.394968	0.301577	0.419353	0.82513	0.55762	0.912657	0.082994	0.346057	0.546014	1	0.020738
T_Alb	0.192826	0.255116	0.26653	0.235235	0.07404	0.065478	0.756879	0.386005	0.045156	0.020738	1

c) Full dataset (Dapedidae assigned to Teleostei in 50 of 100 replicates)

	T_AOI	T_CL	T_RN	T_PSH	T_BAT	T_OCB	T_TiKi	T_ValBer	T_BarHau	T_Apt	T_Alb
T_AOI	1	0.487386	0.162624	0.279551	0.42974	0.372071	0.415025	0.173958	0.242886	0.394887	0.193548
T_CL	0.487386	NA	0.163035	0.283877	0.459553	0.286484	0.490418	0.170058	0.199851	0.299571	0.255136
T_RN	0.162624	0.163035	1	0.883116	0.816062	0.333658	0.461289	0.941032	0.456661	0.251853	0.34345
T_PSH	0.279551	0.283877	0.883116	1	0.815765	0.577975	0.593669	0.932514	0.721001	0.514512	0.464982
T_BAT	0.42974	0.459553	0.816062	0.815765	1	0.36653	0.415069	0.810278	0.38199	0.240626	0.486582
T_OCB	0.372071	0.286484	0.333658	0.577975	0.36653	1	0.1826	0.418602	0.674161	0.91579	0.065369
T_TiKi	0.415025	0.490418	0.461289	0.593669	0.415069	0.1826	1	0.51564	0.127294	0.082814	0.760423
T_ValBer	0.173958	0.170058	0.941032	0.932514	0.810278	0.418602	0.51564	1	0.561294	0.344816	0.387129
T_BarHau	0.242886	0.199851	0.456661	0.721001	0.38199	0.674161	0.127294	0.561294	1	0.545726	0.045639
T_Apt	0.394887	0.299571	0.251853	0.514512	0.240626	0.91579	0.082814	0.344816	0.545726	1	0.020843
T_Alb	0.193548	0.255136	0.34345	0.464982	0.486582	0.065369	0.760423	0.387129	0.045639	0.020843	1

d) *Lagerstätten* removal 1 (most diverse site from each bin removed)

	T_AOI	T_CL	T_RN	T_PSH	T_BAT	T_OCB	T_TiKi	T_ValBer	T_BarHau	T_Apt	T_Alb
T_AOI	1	0.419398	0.091434	0.489208	0.102178	0.235679	0.064672	0.15477	0.151043	0.253886	0.129214
T_CL	0.419398	NA	0.133081	0.419879	0.143374	0.225803	0.123196	0.204425	0.170099	0.262495	0.212251
T_RN	0.091434	0.133081	1	0.063504	0.907592	0.256927	0.426648	0.673404	0.380357	0.303348	0.357743
T_PSH	0.489208	0.419879	0.063504	1	0.068084	0.150344	0.045164	0.109729	0.093158	0.171962	0.105078
T_BAT	0.102178	0.143374	0.907592	0.068084	1	0.267825	0.233661	0.739233	0.378276	0.263697	0.195004
T_OCB	0.235679	0.225803	0.256927	0.150344	0.267825	1	0.058551	0.55573	0.630946	0.832247	0.091119
T_TiKi	0.064672	0.123196	0.426648	0.045164	0.233661	0.058551	1	0.330496	0.030684	0.011458	0.542565
T_ValBer	0.15477	0.204425	0.673404	0.109729	0.739233	0.55573	0.330496	1	0.80227	0.686992	0.331341
T_BarHau	0.151043	0.170099	0.380357	0.093158	0.378276	0.630946	0.030684	0.80227	1	0.762091	0.044727
T_Apt	0.253886	0.262495	0.303348	0.171962	0.263697	0.832247	0.011458	0.686992	0.762091	1	0.023131
T_Alb	0.129214	0.212251	0.357743	0.105078	0.195004	0.091119	0.542565	0.331341	0.044727	0.023131	1

e) *Lagerstätten* removal 2 (sites with 10 or more species removed)

	T_AOI	T_CL	T_RN	T_PSH	T_BAT	T_OCB	T_TiKi	T_ValBer	T_BarHau	T_Apt	T_Alb
T_AOI	1	0.487345	0.143484	0.339059	0.16549	0.372165	0.190617	0.318786	0.264898	0.386004	0.170218
T_CL	0.487345	NA	0.154073	0.846074	0.172167	0.288138	0.190423	0.284258	0.159944	0.310788	0.209126
T_RN	0.143484	0.154073	1	0.062833	0.906716	0.29059	0.822277	0.58893	0.133942	0.297815	0.656659
T_PSH	0.339059	0.846074	0.062833	1	0.068474	0.154021	0.081025	0.155681	0.06224	0.169221	0.092923
T_BAT	0.16549	0.172167	0.906716	0.068474	1	0.273212	0.897771	0.62528	0.134236	0.255158	0.511118
T_OCB	0.372165	0.288138	0.29059	0.154021	0.273212	1	0.349495	0.704817	0.836487	0.961675	0.123588
T_TiKi	0.190617	0.190423	0.822277	0.081025	0.897771	0.349495	1	0.707269	0.189261	0.338256	0.46115
T_ValBer	0.318786	0.284258	0.58893	0.155681	0.62528	0.704817	0.707269	1	0.523185	0.723955	0.373692
T_BarHau	0.264898	0.159944	0.133942	0.06224	0.134236	0.836487	0.189261	0.523185	1	0.788896	0.053593
T_Apt	0.386004	0.310788	0.297815	0.169221	0.255158	0.961675	0.338256	0.723955	0.788896	1	0.092752
T_Alb	0.170218	0.209126	0.656659	0.092923	0.511118	0.123588	0.46115	0.373692	0.053593	0.092752	1

f) Genus range data

	T_AOI	T_CL	T_RN	T_PSH	T_BAT	T_OCB	T_TiKi	T_ValBer	T_BarHau	T_Apt	T_Alb
T_AOI	1	0.201793	0.237757	0.089703	0.14003	0.267221	0.248607	0.13889	0.23219	0.192801	0.186518
T_CL	0.201793	1	0.666434	0.2384	0.622128	0.730976	0.803483	0.623453	0.755553	0.719128	0.771342
T_RN	0.237757	0.666434	1	0.331828	0.940621	0.892077	0.68924	0.93623	0.781538	0.806483	0.696866
T_PSH	0.089703	0.2384	0.331828	1	0.218402	0.242898	0.112164	0.215486	0.150566	0.145057	0.102035
T_BAT	0.14003	0.622128	0.940621	0.218402	1	0.939818	0.720139	0.994841	0.821024	0.850529	0.722342
T_OCB	0.267221	0.730976	0.892077	0.242898	0.939818	1	0.775994	0.944395	0.88607	0.921765	0.797818
T_TiKi	0.248607	0.803483	0.68924	0.112164	0.720139	0.775994	1	0.725133	0.879258	0.835212	0.983866
T_ValBer	0.13889	0.623453	0.93623	0.215486	0.994841	0.944395	0.725133	1	0.826028	0.855762	0.727331
T_BarHau	0.23219	0.755553	0.781538	0.150566	0.821024	0.88607	0.879258	0.826028	1	0.957422	0.900483
T_Apt	0.192801	0.719128	0.806483	0.145057	0.850529	0.921765	0.835212	0.855762	0.957422	1	0.854952
T_Alb	0.186518	0.771342	0.696866	0.102035	0.722342	0.797818	0.983866	0.727331	0.900483	0.854952	1

Table A1.5. P values derived from t tests comparing the disparity of teleosts between all Mesozoic time bins for a) the full dataset of 356 species, b) full dataset Dapedidae assigned to Holostei, c) full dataset Dapedidae assigned to Holostei in 50% of the time, d) *Lagerstätten* removal 1 (most diverse site from each bin removed), e) *Lagerstätten* removal 2 (sites with 10 or more species removed), f) genus range data. Stratigraphic interval abbreviations: AOI, Induan-Anisian; CL, Ladinian-Carnian; RN, Norian-Rhaetian; PSH, Hettangian-Pliensbachian; BAT, Toarcian-Bajocian; OCB, Bathonian-Oxfordian; TiKi, Kimmeridgian-Tithonian; ValBer, Berriasian-Valanginian; BarHau, Hauterivian-Barremian; Apt, Aptian; Alb, Albian.

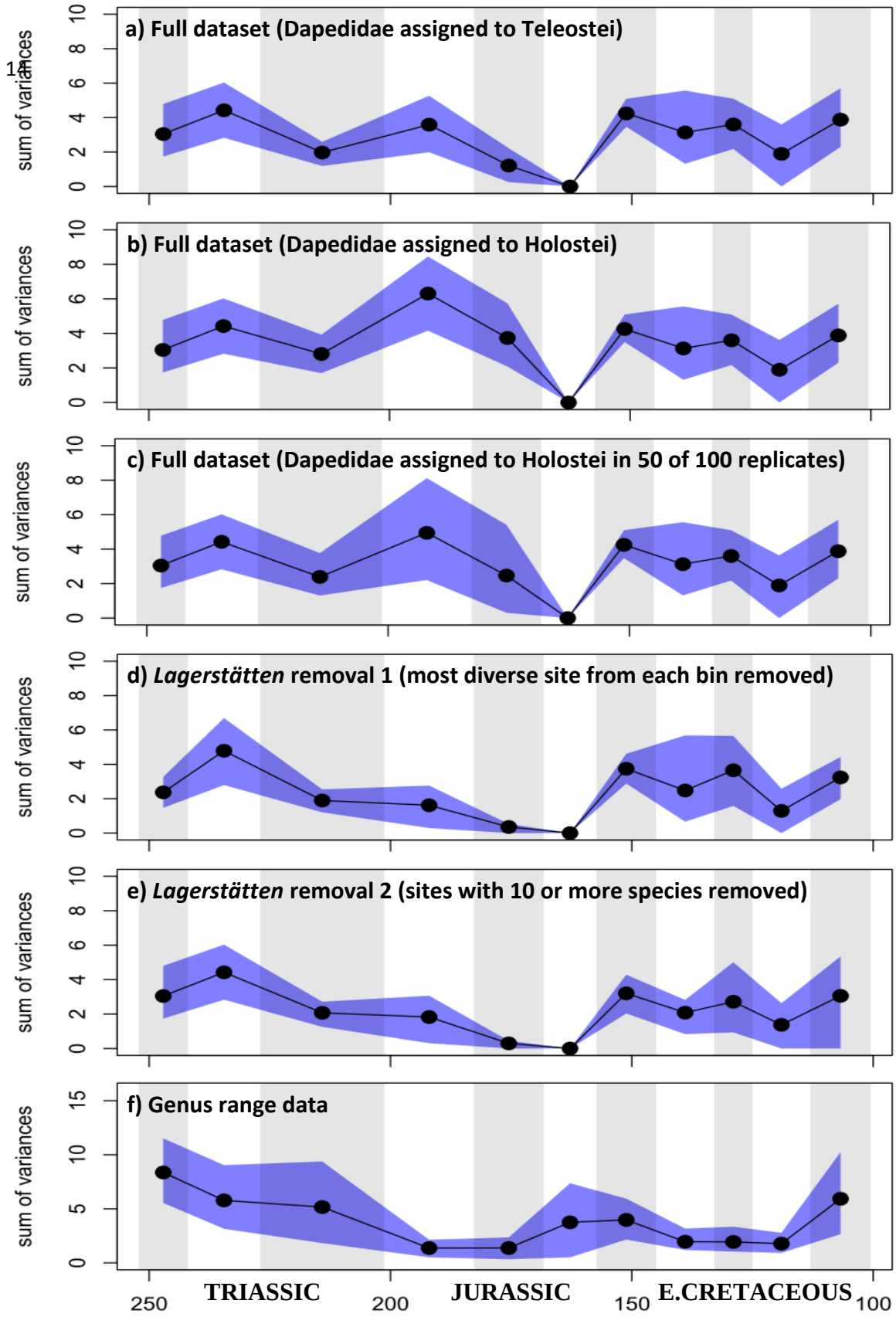

Fig. A1.6. Holostean functional disparity through eleven Mesozoic time bins based upon a) the full dataset of 356 species, b) full dataset with Dapedidae assigned to Holostei, c) full dataset with Dapedidae assigned to Holostei in 50 of 100 replicates, d) *Lagerstätten* removal 1 (most diverse site from each bin removed), e) *Lagerstätten* removal 2 (sites with 10 or more species removed), f) genus range data.

a) Full dataset (Dapedidae assigned to Teleostei)

0	H_AOI	H_CL	H_RN	H_PSH	H_BAT	H_OCB	H_TiKi	H_ValBer	H_BarHau	H_Apt	H_Alb
H_AOI	1	0.216723	0.350035	0.663985	0.218825	1	0.141744	0.956382	0.648216	0.64413	0.474752
H_CL	0.216723	1	0.041298	0.50747	0.03922	1	0.823557	0.442674	0.505282	0.322412	0.644329
H_RN	0.350035	0.041298	1	0.069438	0.218999	1	0.01659	0.172149	0.043147	0.920197	0.069585
H_PSH	0.663985	0.50747	0.069438	1	0.0431	1	0.503596	0.726562	0.988981	0.340122	0.802859
H_BAT	0.218825	0.03922	0.218999	0.0431	1	1	0.013544	0.091332	0.025479	0.493075	0.051947
H_OCB	1	1	1	1	1	NA	1	1	1	NA	1
H_TiKi	0.141744	0.823557	0.01659	0.503596	0.013544	1	1	0.405193	0.506256	0.252564	0.683883
H_ValBer	0.956382	0.442674	0.172149	0.726562	0.091332	1	0.405193	1	0.692371	0.425948	0.616702
H_BarHau	0.648216	0.505282	0.043147	0.988981	0.025479	1	0.506256	0.692371	1	0.276586	0.805022
H_Apt	0.64413	0.322412	0.920197	0.340122	0.493075	NA	0.252564	0.425948	0.276586	1	0.364596
H_Alb	0.474752	0.644329	0.069585	0.802859	0.051947	1	0.683883	0.616702	0.805022	0.364596	1

b) Full dataset (Dapedidae assigned to Holostei)

	H_AOI	H_CL	H_RN	H_PSH	H_BAT	H_OCB	H_TiKi	H_ValBer	H_BarHau	H_Apt	H_Alb
H_AOI	1	0.215584	0.831737	0.014164	0.573007	1	0.132253	0.957645	0.645212	0.644233	0.471521
H_CL	0.215584	1	0.155058	0.148567	0.57946	1	0.833287	0.440572	0.506178	0.321851	0.645844
H_RN	0.831737	0.155058	1	0.011171	0.379721	1	0.098363	0.75825	0.363447	0.497031	0.299008
H_PSH	0.014164	0.148567	0.011171	1	0.081199	1	0.02968	0.111202	0.066848	0.143732	0.082231
H_BAT	0.573007	0.57946	0.379721	0.081199	1	1	0.577954	0.687636	0.908788	0.400489	0.903131
H_OCB	1	1	1	1	1	NA	1	1	1	NA	1
H_TiKi	0.132253	0.833287	0.098363	0.02968	0.577954	1	1	0.391746	0.494144	0.24367	0.672352
H_ValBer	0.957645	0.440572	0.75825	0.111202	0.687636	1	0.391746	1	0.687699	0.427212	0.612555
H_BarHau	0.645212	0.506178	0.363447	0.066848	0.908788	1	0.494144	0.687699	1	0.275617	0.804384
H_Apt	0.644233	0.321851	0.497031	0.143732	0.400489	NA	0.24367	0.427212	0.275617	1	0.363107
H_Alb	0.471521	0.645844	0.299008	0.082231	0.903131	1	0.672352	0.612555	0.804384	0.363107	1

c) Full dataset (Dapedidae assigned to Holostei in 50 of 100 replicates)

	H_AOI	H_CL	H_RN	H_PSH	H_BAT	H_OCB	H_TiKi	H_ValBer	H_BarHau	H_Apt	H_Alb
H_AOI	1	0.214924	0.580862	0.225697	0.718437	1	0.137563	0.96014	0.646785	0.642858	0.474231
H_CL	0.214924	1	0.098493	0.739588	0.233825	1	0.826453	0.437878	0.504225	0.320137	0.641973
H_RN	0.580862	0.098493	1	0.133082	0.950013	1	0.052495	0.493138	0.190316	0.709031	0.1812
H_PSH	0.225697	0.739588	0.133082	1	0.274776	1	0.544056	0.426877	0.429466	0.377159	0.515016
H_BAT	0.718437	0.233825	0.950013	0.274776	1	1	0.160376	0.692177	0.404494	0.797496	0.358013
H_OCB	1	1	1	1	1	NA	1	1	1	NA	1
H_TiKi	0.137563	0.826453	0.052495	0.544056	0.160376	1	1	0.395729	0.500472	0.247156	0.676521
H_ValBer	0.96014	0.437878	0.493138	0.426877	0.692177	1	0.395729	1	0.686835	0.427568	0.612743
H_BarHau	0.646785	0.504225	0.190316	0.429466	0.404494	1	0.500472	0.686835	1	0.27681	0.806506
H_Apt	0.642858	0.320137	0.709031	0.377159	0.797496	NA	0.247156	0.427568	0.27681	1	0.36352
H_Alb	0.474231	0.641973	0.1812	0.515016	0.358013	1	0.676521	0.612743	0.806506	0.36352	1

d) *Lagerstätten* removal 1 (most diverse site from each bin removed)

	H_AOI	H_CL	H_RN	H_PSH	H_BAT	H_OCB	H_TiKi	H_ValBer	H_BarHau	H_Apt	H_Alb
H_AOI	1	0.023181	0.654835	0.543633	0.043909	1	0.057366	0.865574	0.213954	0.355513	0.264319
H_CL	0.023181	1	0.041628	0.096601	0.048313	1	0.173182	0.242214	0.441517	0.188792	0.202126
H_RN	0.654835	0.041628	1	0.731576	0.010897	1	0.045321	0.58223	0.084983	0.279241	0.13541
H_PSH	0.543633	0.096601	0.731576	1	0.147758	1	0.085714	0.557217	0.161398	0.63151	0.191731
H_BAT	0.043909	0.048313	0.010897	0.147758	1	1	0.009469	0.071198	0.017667	0.080198	0.017864
H_OCB	1	1	1	1	1	NA	1	1	1	NA	1
H_TiKi	0.057366	0.173182	0.045321	0.085714	0.009469	1	1	0.344019	0.932256	0.118849	0.596441
H_ValBer	0.865574	0.242214	0.58223	0.557217	0.071198	1	0.344019	1	0.436376	0.350525	0.557685
H_BarHau	0.213954	0.441517	0.084983	0.161398	0.017667	1	0.932256	0.436376	1	0.125836	0.754709
H_Apt	0.355513	0.188792	0.279241	0.63151	0.080198	NA	0.118849	0.350525	0.125836	1	0.162846
H_Alb	0.264319	0.202126	0.13541	0.191731	0.017864	1	0.596441	0.557685	0.754709	0.162846	1

e) *Lagerstätten* removal 2 (sites with 10 or more species removed)

	H_AOI	H_CL	H_RN	H_PSH	H_BAT	H_OCB	H_TiKi	H_ValBer	H_BarHau	H_Apt	H_Alb
H_AOI	1	0.215111	0.423481	0.456801	0.185983	1	0.889534	0.548578	0.839131	0.506313	0.994434
H_CL	0.215111	1	0.060614	0.122113	0.054315	1	0.290326	0.154276	0.305219	0.233858	0.514098
H_RN	0.423481	0.060614	1	0.732766	0.010568	1	0.102647	0.989503	0.437948	0.355496	0.239386
H_PSH	0.456801	0.122113	0.732766	1	0.147654	1	0.15805	0.770044	0.455516	0.709121	0.329711
H_BAT	0.185983	0.054315	0.010568	0.147654	1	1	0.01236	0.017369	0.068755	0.055149	0.036331
H_OCB	1	1	1	1	1	NA	1	1	1	NA	1
H_TiKi	0.889534	0.290326	0.102647	0.15805	0.01236	1	1	0.197066	0.62208	0.162104	0.898719
H_ValBer	0.548578	0.154276	0.989503	0.770044	0.017369	1	0.197066	1	0.532127	0.364745	0.316586
H_BarHau	0.839131	0.305219	0.437948	0.455516	0.068755	1	0.62208	0.532127	1	0.365558	0.797648
H_Apt	0.506313	0.233858	0.355496	0.709121	0.055149	NA	0.162104	0.364745	0.365558	1	0.227027
H_Alb	0.994434	0.514098	0.239386	0.329711	0.036331	1	0.898719	0.316586	0.797648	0.227027	1

f) Genus range data

	H_AOI	H_CL	H_RN	H_PSH	H_BAT	H_OCB	H_TiKi	H_ValBer	H_BarHau	H_Apt	H_Alb
H_AOI	1	0.222295	0.190114	0.009899	0.026857	0.118941	0.012178	0.001305	0.002663	0.002872	0.3085
H_CL	0.222295	1	0.791783	0.071166	0.123671	0.45906	0.282984	0.032431	0.04589	0.043364	0.949851
H_RN	0.190114	0.791783	1	0.10694	0.168302	0.606778	0.525381	0.066448	0.086587	0.077729	0.778534
H_PSH	0.009899	0.071166	0.10694	1	0.996728	0.168513	0.159248	0.423631	0.473856	0.524711	0.123181
H_BAT	0.026857	0.123671	0.168302	0.996728	1	0.238305	0.232037	0.495935	0.542159	0.587202	0.189033
H_OCB	0.118941	0.45906	0.606778	0.168513	0.238305	1	0.916619	0.196137	0.22631	0.17601	0.507111
H_TiKi	0.012178	0.282984	0.525381	0.159248	0.232037	0.916619	1	0.135276	0.162444	0.141813	0.312125
H_ValBer	0.001305	0.032431	0.066448	0.423631	0.495935	0.196137	0.135276	1	0.980768	0.783715	0.064668
H_BarHau	0.002663	0.04589	0.086587	0.473856	0.542159	0.22631	0.162444	0.980768	1	0.818988	0.084813
H_Apt	0.002872	0.043364	0.077729	0.524711	0.587202	0.17601	0.141813	0.783715	0.818988	1	0.082505
H_Alb	0.3085	0.949851	0.778534	0.123181	0.189033	0.507111	0.312125	0.064668	0.084813	0.082505	1

Table A1.6. P values derived from t tests comparing the disparity of holosteans between all Mesozoic time bins for a) the full dataset of 356 species, b) full dataset Dapedidae assigned to Holostei, c) full dataset with Dapedidae assigned to Holostei in 50% of the time, d) *Lagerstätten* removal 1 (most diverse site from each bin removed), e) *Lagerstätten* removal 2 (sites with 10 or more species removed), f) genus range data.
Stratigraphic interval abbreviations: AOI, Induan-Anisian; CL, Ladinian-Carnian; RN, Norian-Rhaetian; PSH, Hettangian-Pliensbachian; BAT, Toarcian-Bajocian; OCB, Bathonian-Oxfordian; TiKi, Kimmeridgian-Tithonian; ValBer, Berriasian-Valanginian; BarHau, Hauterivian-Barremian; Apt, Aptian; Alb, Albian.

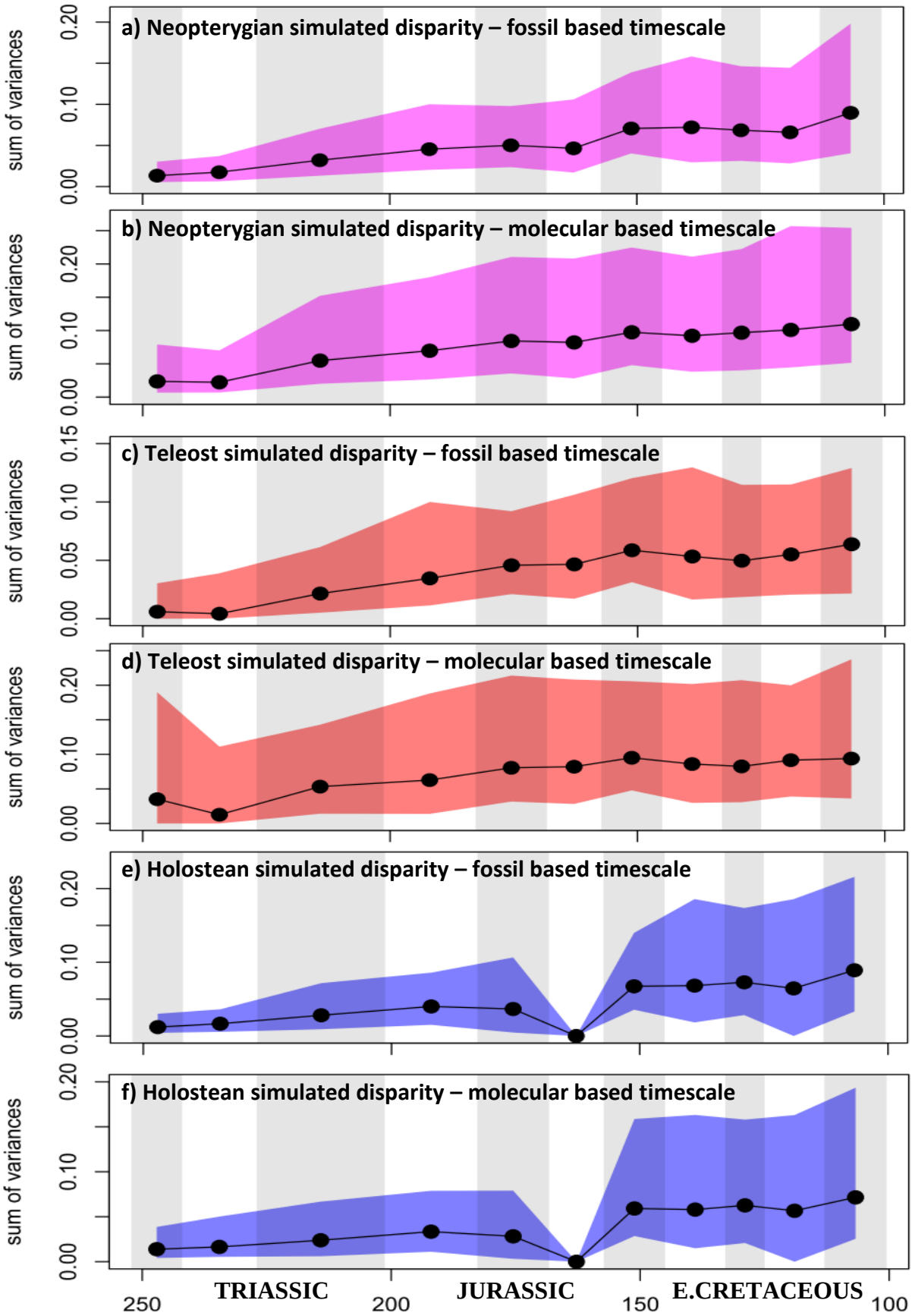

Fig. A1.7. Simulated morphological disparity through eleven Mesozoic time bins under fossil only (a, c, e) and fossil + molecular constraint (b, d, f) time calibration procedures. a, b) neopterygian simulations. c, d) teleost simulations. e, f) holostean simulations.

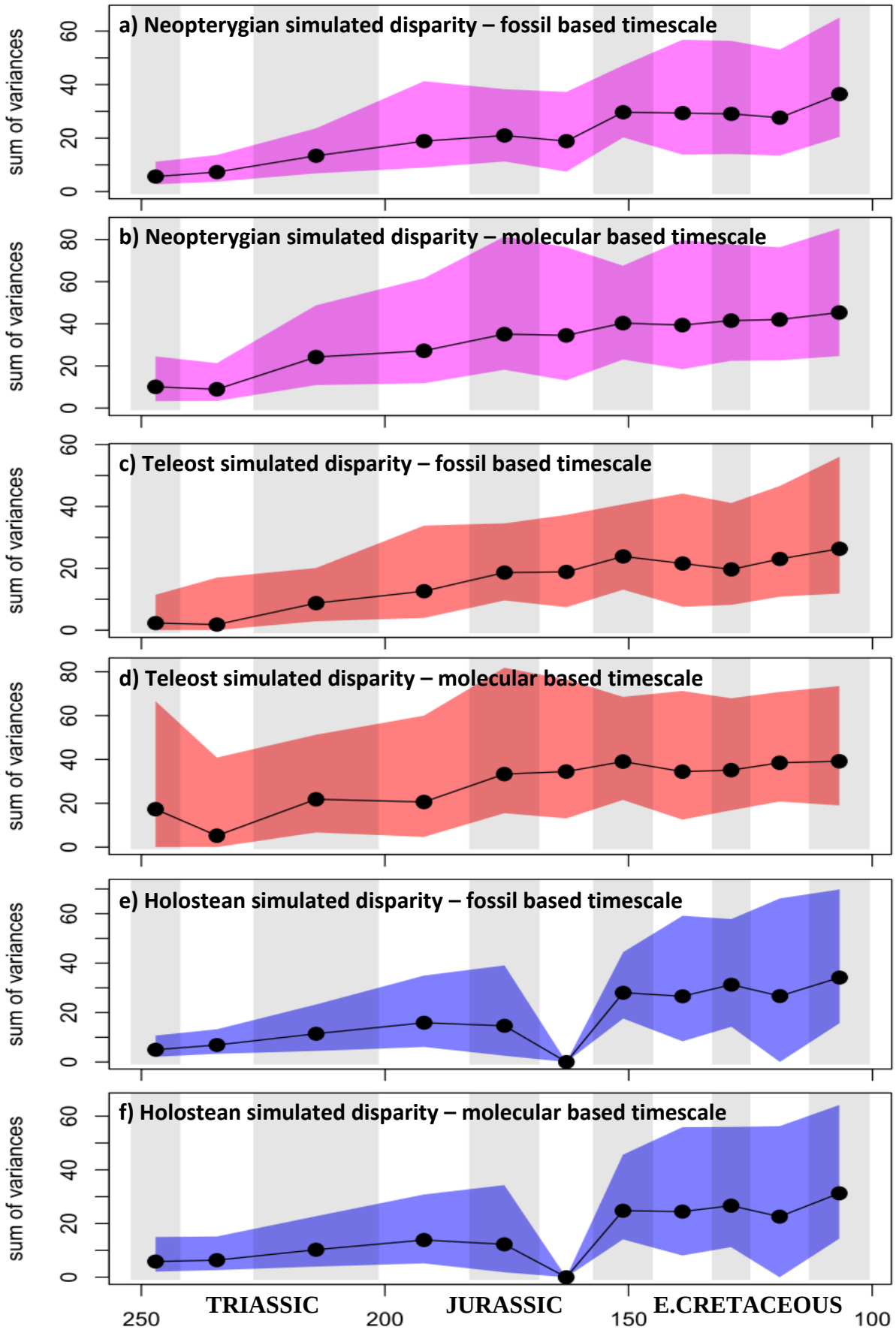

Fig. A1.8. Simulated functional disparity through eleven Mesozoic time bins under fossil only (a, c, e) and fossil + molecular constraint (b, d, f) time calibration procedures. a, b) neopterygian simulations. c, d) teleost simulations. e, f) holostean simulations.

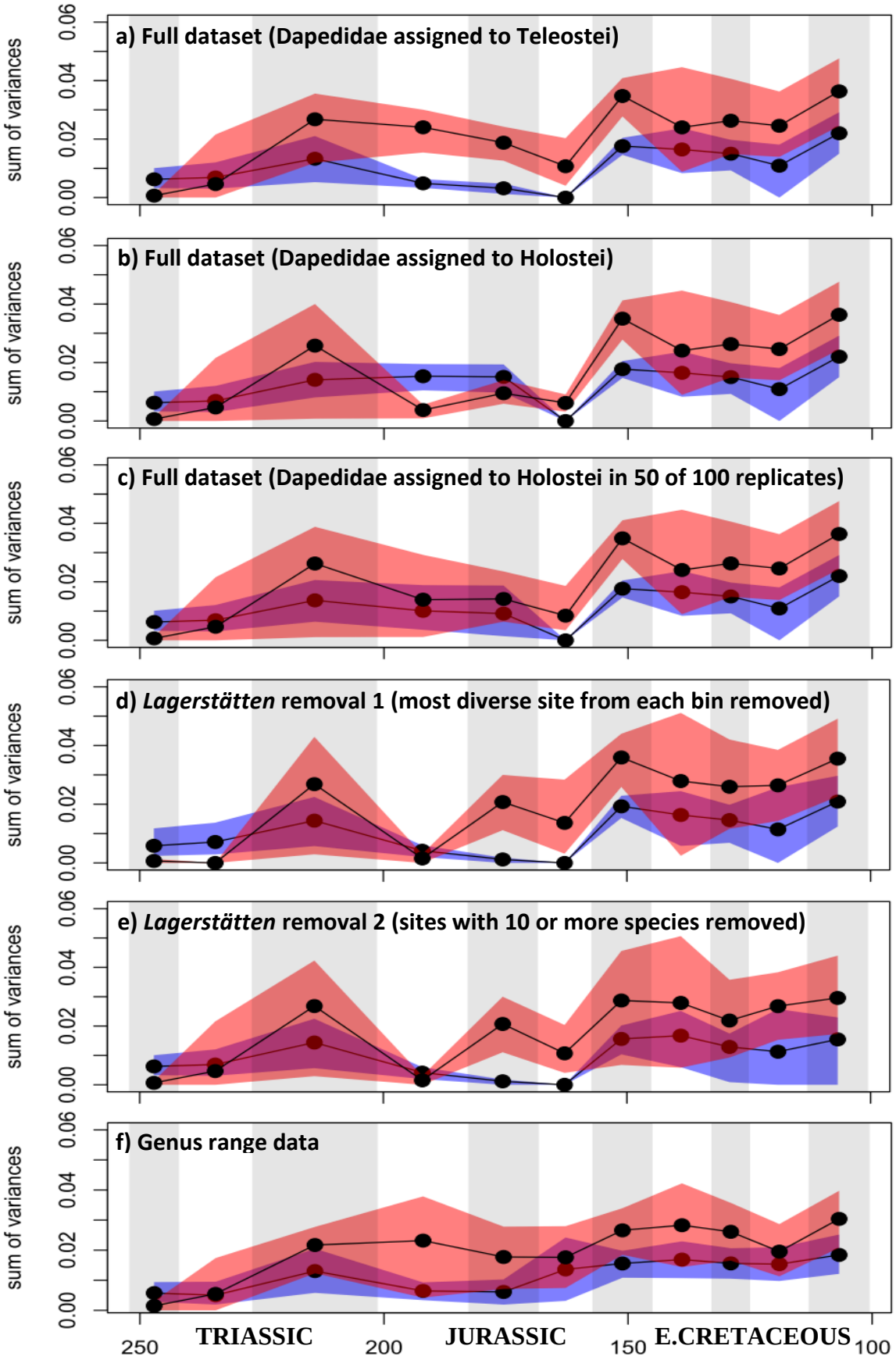

Fig. A1.9. Holostean and teleost morphological disparity through eleven Mesozoic time bins based upon a) the full dataset of 356 species, b) full dataset with Dapedidae assigned to Holostei, c) full dataset with Dapedidae assigned to Holostei in 50 of 100 replicates, d) *Lagerstätten* removal 1 (most diverse site from each bin removed), e) *Lagerstätten* removal 2 (sites with 10 or more species removed), f) genus range data.

a) Full dataset (Dapedidae assigned to Teleostei)

	T_AOI	T_CL	T_RN	T_PSH	T_BAT	T_OCB	T_TiKi	T_ValBer	T_BarHau	T_Apt	T_Alb
H_AOI	0.323168	0.837856	4.00E-05	9.25E-06	0.000461	0.261721	6.37E-06	0.002556	0.002191	0.00121	4.26E-06
H_CL	0.431385	0.838976	0.000346	0.000139	0.002212	0.388184	8.24E-06	0.009499	0.003522	0.002465	9.20E-06
H_RN	0.157356	0.476289	0.041248	0.040927	0.257826	0.65462	0.0127	0.180743	0.144027	0.141269	0.007499
H_PSH	0.036073	0.927091	3.92E-05	4.91E-06	0.000439	0.172339	0.00011	0.002194	0.006215	0.003108	5.01E-05
H_BAT	0.110652	0.471099	0.002256	0.00053	0.007393	0.241547	0.00622	0.024072	0.047149	0.03023	0.00328
H_OCB	NA	NA	1	1	1	1	1	1	1	1	1
H_TiKi	0.029918	0.232597	0.031634	0.06413	0.692661	0.057804	2.45E-05	0.219174	0.055038	0.087806	2.58E-05
H_ValBer	0.030216	0.189591	0.152066	0.1781	0.68642	0.396371	0.108412	0.393925	0.388575	0.400246	0.066082
H_BarHau	0.019766	0.187227	0.045922	0.050068	0.407185	0.423287	0.026634	0.210456	0.208344	0.208647	0.013408
H_Apt	0.066332	0.339314	0.168169	0.141996	0.403895	0.988253	0.222842	0.357254	0.426684	0.40059	0.161074
H_Alb	0.032876	0.196115	0.42773	0.67492	0.468794	0.042832	0.083613	0.786374	0.580262	0.705541	0.052298

b) Full dataset (Dapedidae assigned to Holostei)

	T_AOI	T_CL	T_RN	T_PSH	T_BAT	T_OCB	T_TiKi	T_ValBer	T_BarHau	T_Apt	T_Alb
H_AOI	0.323238	0.836912	0.003881	0.447843	0.217606	0.975873	7.28E-06	0.002502	0.002147	0.001195	4.27E-06
H_CL	0.431937	0.839147	0.009195	0.495643	0.422132	0.830857	9.23E-06	0.009273	0.003439	0.002416	9.13E-06
H_RN	0.08365	0.366999	0.158844	0.026191	0.184979	0.020811	0.009233	0.163497	0.132073	0.131782	0.004797
H_PSH	0.046097	0.286368	0.128577	0.008536	0.060999	0.004127	0.002099	0.150439	0.092719	0.10106	0.001026
H_BAT	0.019578	0.192479	0.187734	0.002813	0.069381	0.002226	0.016318	0.183833	0.173462	0.175137	0.007672
H_OCB	0.389653	NA	0.314544	0.17179	0.226159	0.223204	0.2128	0.242924	0.336694	0.286394	0.156421
H_TiKi	0.029166	0.229404	0.136077	0.002433	0.005864	0.000359	2.41E-05	0.223557	0.056227	0.089902	2.60E-05
H_ValBer	0.030074	0.188863	0.393035	0.004463	0.07811	0.003765	0.1093	0.391556	0.387756	0.399067	0.066242
H_BarHau	0.019903	0.187593	0.217222	0.003026	0.086112	0.002894	0.027071	0.208127	0.207125	0.207232	0.013415
H_Apt	0.066237	0.338846	0.407108	0.025571	0.801285	0.217632	0.225064	0.355148	0.42538	0.39954	0.160998
H_Alb	0.032326	0.194439	0.64891	0.002778	0.002819	0.000345	0.082405	0.781686	0.578829	0.701609	0.052279

c) Full dataset (Dapedidae assigned to Holostei in 50 of 100 replicates)

	T_AOI	T_CL	T_RN	T_PSH	T_BAT	T_OCB	T_TiKi	T_ValBer	T_BarHau	T_Apt	T_Alb
H_AOI	0.322806	0.837836	0.000721	0.199883	0.104494	0.550928	6.13E-06	0.002549	0.002171	0.001273	4.39E-06
H_CL	0.43247	0.840609	0.002892	0.292443	0.157843	0.711193	7.80E-06	0.009347	0.00345	0.002527	9.31E-06
H_RN	0.110538	0.41125	0.101583	0.979609	0.944351	0.304501	0.013677	0.178932	0.151304	0.150834	0.007929
H_PSH	0.486877	0.774173	0.085155	0.70066	0.575941	0.796488	0.001893	0.151504	0.065521	0.066721	0.002415
H_BAT	0.374373	0.729733	0.094301	0.655129	0.573586	0.913363	0.026172	0.144645	0.146414	0.129383	0.016922
H_OCB	NA	NA	1	1	1	1	1	1	1	1	1
H_TiKi	0.028222	0.227326	0.082396	0.482761	0.361014	0.009781	2.32E-05	0.218764	0.055322	0.08917	2.68E-05
H_ValBer	0.029829	0.188583	0.274506	0.792326	0.785789	0.185135	0.106291	0.391867	0.386942	0.40108	0.066456
H_BarHau	0.019602	0.186827	0.121845	0.885667	0.897446	0.172524	0.025877	0.209105	0.207151	0.209966	0.013544
H_Apt	0.066481	0.340037	0.292253	0.847314	0.817817	0.793273	0.220938	0.356525	0.425736	0.402751	0.161679
H_Alb	0.032431	0.194972	0.554774	0.312906	0.209782	0.011348	0.081231	0.784825	0.579247	0.704664	0.05298

d) *Lagerstätten* removal 1 (most diverse site from each bin removed)

	T_AOI	T_CL	T_RN	T_PSH	T_BAT	T_OCB	T_TiKi	T_ValBer	T_BarHau	T_Apt	T_Alb
H_AOI	0.441999	0.536555	0.003617	0.519938	0.003063	0.189791	3.32E-05	0.005366	0.008861	0.002661	5.86E-05
H_CL	0.451592	0.554783	0.010348	0.512569	0.011361	0.301947	3.81E-05	0.018161	0.012992	0.004324	0.000103
H_RN	0.129715	0.248706	0.143007	0.152823	0.284364	0.918062	0.012921	0.150019	0.212719	0.142742	0.013932
H_PSH	0.080372	0.129436	0.005851	0.18094	0.003348	0.173602	0.001002	0.00383	0.029999	0.012433	0.000866
H_BAT	0.402519	0.179987	0.047232	0.730335	0.026249	0.264271	0.022328	0.04404	0.119553	0.072715	0.017584
H_OCB	NA	NA	1	NA	1	1	1	1	1	1	1
H_TiKi	0.01365	0.064435	0.196089	0.018139	0.722169	0.267275	0.00142	0.205272	0.244147	0.158625	0.002473
H_ValBer	0.043056	0.112698	0.27575	0.052053	0.513213	0.765047	0.093141	0.236146	0.430365	0.348182	0.079228
H_BarHau	0.019676	0.06283	0.19094	0.025483	0.344045	0.913694	0.067208	0.151733	0.348572	0.26825	0.054548
H_Apt	0.114956	0.278339	0.280195	0.135823	0.349728	0.867705	0.17756	0.24738	0.441877	0.368004	0.14811
H_Alb	0.041856	0.120282	0.477752	0.049639	0.978557	0.341078	0.077566	0.450643	0.582113	0.495168	0.079382

e) *Lagerstätten* removal 2 (sites with 10 or more species removed)

	T_AOI	T_CL	T_RN	T_PSH	T_BAT	T_OCB	T_TiKi	T_ValBer	T_BarHau	T_Apt	T_Alb
H_AOI	0.320718	0.840081	0.000773	0.399808	0.00075	0.263788	0.002704	0.002413	0.007058	0.000487	3.65E-05
H_CL	0.431309	0.841184	0.004232	0.497021	0.004758	0.391247	0.004817	0.006349	0.013781	0.001015	0.000217
H_RN	0.131403	0.428806	0.14314	0.154976	0.287951	0.53567	0.173391	0.175991	0.362239	0.131949	0.047502
H_PSH	0.079828	0.839056	0.005703	0.181465	0.003501	0.242377	0.031414	0.022051	0.04239	0.011671	0.00147
H_BAT	0.382034	0.027571	0.046465	0.729964	0.02693	0.291942	0.126349	0.101588	0.136015	0.071115	0.021011
H_OCB	NA	NA	1	NA	1	1	1	1	1	1	1
H_TiKi	0.0297	0.232451	0.09214	0.039077	0.272833	0.301332	0.123902	0.123688	0.343293	0.093264	0.022026
H_ValBer	0.056136	0.259199	0.274586	0.06733	0.54129	0.386877	0.348298	0.335864	0.604187	0.317581	0.140072
H_BarHau	0.078544	0.345229	0.15533	0.096813	0.253086	0.764188	0.254612	0.230214	0.402701	0.204317	0.075707
H_Apt	0.092744	0.390156	0.27173	0.11205	0.342555	0.959785	0.411168	0.373693	0.51938	0.357	0.185085
H_Alb	0.062202	0.260436	0.333383	0.072994	0.527799	0.604573	0.447722	0.420261	0.635741	0.412944	0.216703

f) Genus range data

	T_AOI	T_CL	T_RN	T_PSH	T_BAT	T_OCB	T_TiKi	T_ValBer	T_BarHau	T_Apt	T_Alb
H_AOI	0.407407	0.953846	4.87E-05	0.003475	0.01001	0.027013	0.000452	0.000417	0.000691	0.005506	3.27E-05
H_CL	0.497503	0.924397	0.000131	0.006941	0.015594	0.039869	0.001502	0.001339	0.002069	0.010371	0.000167
H_RN	0.175739	0.294024	0.093224	0.200213	0.452905	0.523952	0.081629	0.064534	0.094756	0.323248	0.022402
H_PSH	0.109829	0.779261	0.001496	0.040701	0.079912	0.159495	0.024732	0.017525	0.027486	0.072669	0.00563
H_BAT	0.177138	0.876188	0.007533	0.091198	0.146843	0.247457	0.068365	0.05114	0.072385	0.140904	0.023475
H_OCB	0.214066	0.328696	0.195721	0.337755	0.60383	0.669637	0.209244	0.168839	0.225368	0.49085	0.090866
H_TiKi	0.062516	0.109753	0.133227	0.20466	0.6477	0.694921	0.044959	0.034115	0.05886	0.404948	0.006636
H_ValBer	0.056432	0.093453	0.288869	0.368484	0.877768	0.907638	0.157286	0.115991	0.180978	0.647698	0.0433
H_BarHau	0.028206	0.067816	0.147733	0.274497	0.700278	0.761231	0.133075	0.091845	0.149386	0.515288	0.035612
H_Apt	0.039639	0.088822	0.150317	0.280002	0.68011	0.743099	0.141096	0.09964	0.157359	0.507334	0.040578
H_Alb	0.069179	0.095985	0.500269	0.505394	0.902364	0.896303	0.210703	0.163907	0.245391	0.844944	0.062594

Table A1.7. P values derived from t tests comparing the disparity of holosteans and teleosts within and between each Mesozoic time bin for a) the full dataset of 356 species, b) full dataset with Dapedidae assigned to Holostei, c) full dataset with Dapedidae assigned to Holostei in 50 of 100 replicates, d) *Lagerstätten* removal 1 (most diverse site from each bin removed), e) *Lagerstätten* removal 2 (sites with 10 or more species removed), f) genus range data. Stratigraphic interval abbreviations: AOI, Induan-Anisian; CL, Ladinian-Carnian; RN, Norian-Rhaetian; PSH, Hettangian-Pliensbachian; BAT, Toarcian-Bajocian; OCB, Bathonian-Oxfordian; TiKi, Kimmeridgian-Tithonian; ValBer, Berriasian-Valanginian; BarHau, Hauterivian-Barremian; Apt, Aptian; Alb, Albian. H=Holostei, T= Teleostei

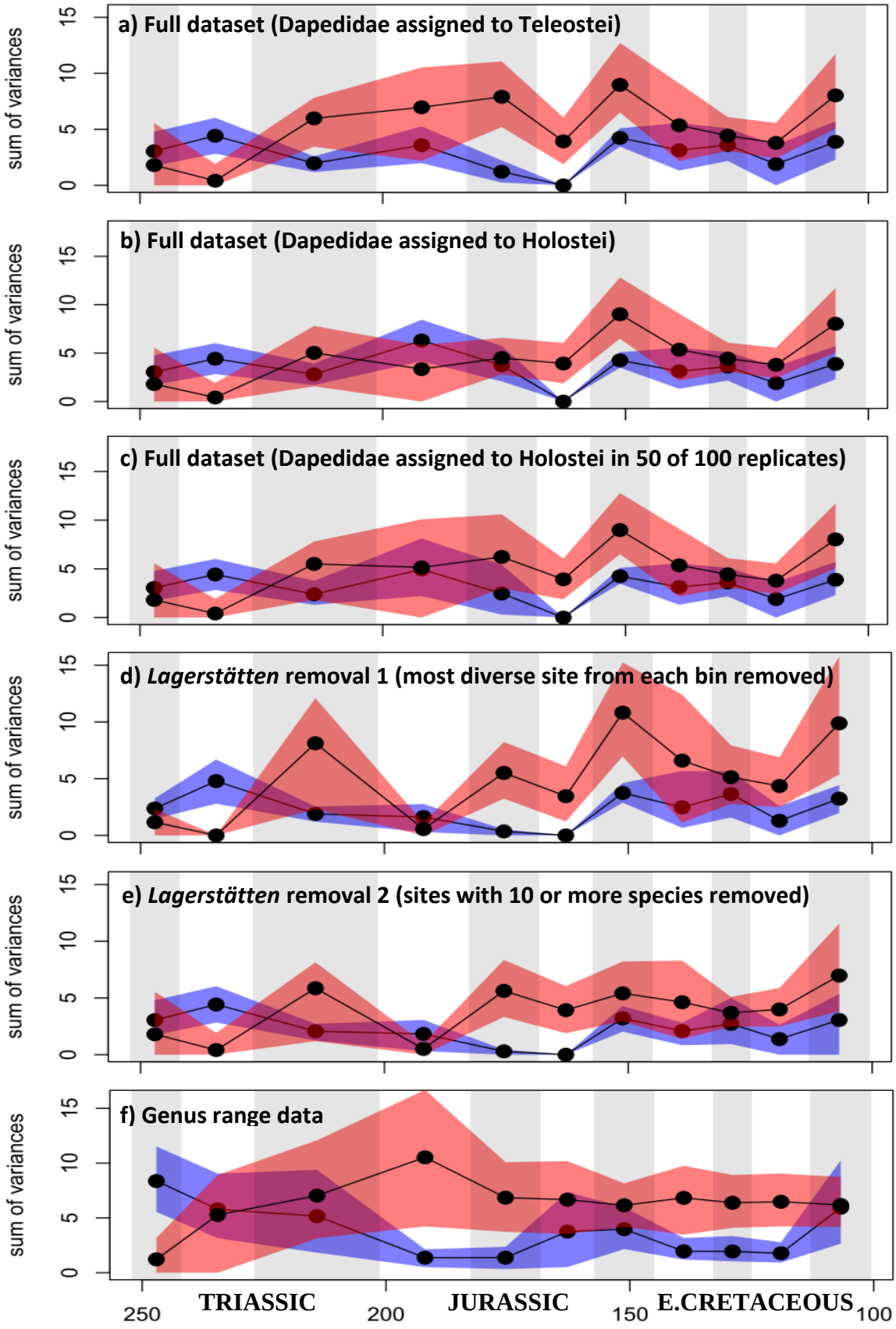

Fig. A1.10. Holostean and teleost morphological disparity through eleven Mesozoic time bins based upon a) the full dataset of 356 species, b) full dataset with Dapedidae assigned to Holostei, c) full dataset with Dapedidae assigned to Holostei in 50 of 100 replicates, d) *Lagerstätten* removal 1 (most diverse site from each bin removed), e) *Lagerstätten* removal 2 (sites with 10 or more species removed), f) genus range data.

a) Full dataset (Dapedidae assigned to Teleostei)

	T_AOI	T_CL	T_RN	T_PSH	T_BAT	T_OCB	T_TiKi	T_ValBer	T_BarHau	T_Apt	T_Alb
H_AOI	0.622243	0.454867	0.03738	0.030872	0.004541	0.494094	0.033692	0.189318	0.201584	0.498742	0.005249
H_CL	0.310186	0.266914	0.261549	0.154506	0.037907	0.702813	0.101257	0.59415	0.99012	0.569906	0.038999
H_RN	0.854312	0.152017	0.001001	0.014798	0.007287	0.081404	0.077908	0.009396	0.020639	0.094197	0.007642
H_PSH	0.332376	0.209142	0.072014	0.106333	0.050084	0.788453	0.174175	0.250731	0.458289	0.862229	0.049817
H_BAT	0.60404	0.542983	0.002672	0.029176	0.017962	0.064046	0.128937	0.016251	0.019884	0.068258	0.018897
H_OCB	NA	NA	1	1	1	1	1	1	1	1	1
H_TiKi	0.238067	0.186838	0.103948	0.036371	0.001698	0.750167	0.009724	0.416445	0.810537	0.58533	0.001972
H_ValBer	0.431369	0.231966	0.081206	0.168043	0.114267	0.618088	0.295098	0.2187	0.380114	0.669591	0.113071
H_BarHau	0.273495	0.154841	0.060768	0.10132	0.049149	0.788628	0.174959	0.225053	0.451585	0.867914	0.048594
H_Apt	0.944505	0.261503	0.080091	0.228021	0.198234	0.380528	0.420361	0.169045	0.251788	0.411152	0.197323
H_Alb	0.352024	0.263734	0.119727	0.109024	0.037558	0.970354	0.13067	0.367832	0.614792	0.937971	0.037993

b) Full dataset (Dapedidae assigned to Holostei)

	T_AOI	T_CL	T_RN	T_PSH	T_BAT	T_OCB	T_TiKi	T_ValBer	T_BarHau	T_Apt	T_Alb
H_AOI	0.622354	0.456059	0.213382	0.884691	0.233596	0.492508	0.0338	0.189272	0.200702	0.496669	0.005254
H_CL	0.30963	0.267349	0.703482	0.620839	0.952751	0.70455	0.100863	0.595307	0.991675	0.570083	0.039149
H_RN	0.478066	0.213646	0.10284	0.694005	0.14972	0.317028	0.089787	0.058627	0.111464	0.348669	0.012543
H_PSH	0.139335	0.165226	0.489883	0.245904	0.204096	0.122605	0.394807	0.641566	0.142549	0.056435	0.377482
H_BAT	0.387684	0.285653	0.42182	0.844563	0.56257	0.883691	0.14939	0.337064	0.545493	0.961829	0.044544
H_OCB	NA	NA	1	1	1	1	1	1	1	1	1
H_TiKi	0.229399	0.180442	0.520537	0.594948	0.787507	0.739808	0.009151	0.417033	0.82197	0.571048	0.001834
H_ValBer	0.432227	0.233501	0.318275	0.900181	0.42269	0.616836	0.295043	0.218534	0.37767	0.666708	0.113018
H_BarHau	0.2724	0.155287	0.331824	0.870901	0.482393	0.789638	0.175219	0.226596	0.452779	0.868942	0.048895
H_Apt	0.944468	0.263222	0.255931	0.497906	0.309156	0.382884	0.421192	0.169517	0.250471	0.41048	0.197583
H_Alb	0.350545	0.263704	0.460008	0.783091	0.624228	0.97087	0.130806	0.369564	0.617197	0.936334	0.03826

c) Full dataset (Dapedidae assigned to Holostei in 50 of 100 replicates)

	T_AOI	T_CL	T_RN	T_PSH	T_BAT	T_OCB	T_TiKi	T_ValBer	T_BarHau	T_Apt	T_Alb
H_AOI	0.622511	0.454185	0.117385	0.342667	0.111459	0.495497	0.033677	0.189191	0.201618	0.497427	0.005313
H_CL	0.308971	0.265338	0.488724	0.745112	0.363003	0.699379	0.101066	0.595165	0.992943	0.567765	0.039456
H_RN	0.681344	0.295531	0.027407	0.106567	0.140468	0.201392	0.09729	0.03982	0.065428	0.21555	0.013601
H_PSH	0.369166	0.35287	0.793084	0.94606	0.647514	0.571375	0.312154	0.86241	0.737054	0.458277	0.208094
H_BAT	0.776773	0.517983	0.120087	0.280184	0.264635	0.381342	0.203147	0.159381	0.190722	0.389217	0.058209
H_OCB	NA	NA	1	1	1	1	1	1	1	1	1
H_TiKi	0.233869	0.182793	0.294201	0.605502	0.14744	0.74154	0.009747	0.416973	0.817131	0.578209	0.001999
H_ValBer	0.43488	0.232899	0.186799	0.344982	0.387882	0.616779	0.294253	0.217605	0.377783	0.664736	0.113247
H_BarHau	0.275149	0.155834	0.175683	0.378161	0.310443	0.792395	0.174861	0.226789	0.453722	0.868554	0.049205
H_Apt	0.94806	0.261982	0.161752	0.271781	0.437108	0.381939	0.420217	0.169027	0.251588	0.409053	0.197933
H_Alb	0.352257	0.263276	0.28056	0.535143	0.304114	0.97216	0.130381	0.368144	0.6154	0.938485	0.038374

d) *Lagerstätten* removal 1 (most diverse site from each bin removed)

	T_AOI	T_CL	T_RN	T_PSH	T_BAT	T_OCB	T_TiKi	T_ValBer	T_BarHau	T_Apt	T_Alb
H_AOI	0.303201	0.167745	0.005792	0.130984	0.004874	0.20135	0.000129	0.053811	0.033458	0.102444	0.001303
H_CL	0.173114	0.207398	0.572756	0.116682	0.579791	0.498614	0.047974	0.977175	0.742582	0.533249	0.057721
H_RN	0.233236	0.064091	0.008568	0.053877	0.01132	0.148196	0.001569	0.034694	0.042785	0.121588	0.008529
H_PSH	0.565367	0.300191	0.039141	0.294307	0.042182	0.226122	0.012028	0.102612	0.095826	0.19397	0.037699
H_BAT	0.24215	0.219448	0.024285	0.503135	0.024833	0.069786	0.013208	0.04686	0.034924	0.081097	0.047491
H_OCB	NA	NA	1	NA	1	1	1	1	1	1	1
H_TiKi	0.099913	0.089016	0.050476	0.042537	0.039955	0.914708	0.00026	0.322642	0.329411	0.608467	0.001289
H_ValBer	0.32206	0.2147	0.104829	0.165337	0.121373	0.481304	0.043017	0.228123	0.261958	0.418774	0.085078
H_BarHau	0.117573	0.100979	0.184753	0.056042	0.22253	0.895634	0.063361	0.415888	0.536823	0.744844	0.099335
H_Apt	0.861343	0.261645	0.096619	0.279595	0.110922	0.255513	0.070277	0.160164	0.166945	0.276592	0.135473
H_Alb	0.141967	0.105561	0.06267	0.061795	0.069031	0.669966	0.006794	0.242974	0.276415	0.487231	0.019003

e) *Lagerstätten* removal 2 (sites with 10 or more species removed)

	T_AOI	T_CL	T_RN	T_PSH	T_BAT	T_OCB	T_TiKi	T_ValBer	T_BarHau	T_Apt	T_Alb
H_AOI	0.624438	0.457289	0.117368	0.315005	0.06984	0.492483	0.10696	0.377022	0.555174	0.405677	0.024877
H_CL	0.308628	0.265651	0.420327	0.130001	0.391465	0.70428	0.497067	0.907847	0.51358	0.707518	0.136216
H_RN	0.764802	0.122082	0.008369	0.052965	0.011406	0.114334	0.017222	0.07389	0.055893	0.117497	0.010973
H_PSH	0.988369	0.409599	0.038773	0.294523	0.042543	0.186703	0.056055	0.150829	0.108386	0.189393	0.043602
H_BAT	0.175027	0.566612	0.023923	0.500405	0.024993	0.070482	0.031544	0.07757	0.018581	0.078651	0.040147
H_OCB	NA	NA	1	NA	1	1	1	1	1	1	1
H_TiKi	0.305564	0.129907	0.056105	0.048027	0.06343	0.517861	0.092463	0.309716	0.558987	0.488216	0.03241
H_ValBer	0.783197	0.140143	0.038268	0.070147	0.049363	0.225855	0.064391	0.164385	0.137485	0.235146	0.048771
H_BarHau	0.568813	0.275868	0.100412	0.158346	0.114065	0.443082	0.144423	0.322476	0.398693	0.43569	0.088965
H_Apt	0.727371	0.317406	0.103079	0.218685	0.121305	0.278143	0.140898	0.245378	0.162689	0.296714	0.137432
H_Alb	0.424289	0.208773	0.206977	0.100878	0.250474	0.652849	0.292301	0.492198	0.644893	0.648959	0.200756

f) Genus range data

	T_AOI	T_CL	T_RN	T_PSH	T_BAT	T_OCB	T_TiKi	T_ValBer	T_BarHau	T_Apt	T_Alb
H_AOI	0.139644	0.435979	0.609748	0.492526	0.500587	0.440042	0.201136	0.496139	0.293509	0.315061	0.232512
H_CL	0.30327	0.889845	0.624359	0.127308	0.62773	0.687876	0.835165	0.631558	0.750494	0.711469	0.82591
H_RN	0.35079	0.975494	0.504389	0.108684	0.472953	0.550199	0.633456	0.475414	0.5752	0.535477	0.614629
H_PSH	0.853403	0.033106	0.041739	0.004624	0.012175	0.051219	0.040367	0.011961	0.035091	0.022597	0.021111
H_BAT	0.867715	0.067276	0.080511	0.014214	0.030694	0.095823	0.081158	0.030267	0.072224	0.05119	0.048555
H_OCB	0.405902	0.599023	0.295582	0.061271	0.217159	0.33241	0.349679	0.217269	0.316958	0.27428	0.298936
H_TiKi	0.417625	0.650817	0.138903	0.009863	0.103074	0.13354	0.13029	0.104	0.118127	0.099979	0.130604
H_ValBer	0.564496	0.035529	0.013726	0.000407	0.002873	0.017606	0.012911	0.002824	0.010645	0.005934	0.005903
H_BarHau	0.6036	0.050379	0.021451	0.000971	0.005347	0.026748	0.020391	0.005264	0.017136	0.010186	0.010125
H_Apt	0.601196	0.028521	0.02063	0.000998	0.004757	0.026455	0.020075	0.004669	0.016794	0.009816	0.009459
H_Alb	0.381761	0.882297	0.709572	0.205541	0.722177	0.76886	0.912749	0.725799	0.832995	0.799835	0.905246

Table A1.8. P values derived from t tests comparing the disparity of holosteans and teleosts within and between each Mesozoic time bin for a) the full dataset of 356 species, b) full dataset with Dapedidae assigned to Holostei, c) full dataset with Dapedidae assigned to Holostei in 50 of 100 replicates, d) *Lagerstätten* removal 1 (most diverse site from each bin removed), e) *Lagerstätten* removal 2 (sites with 10 or more species removed), f) genus range data. Stratigraphic interval abbreviations: AOI, Induan-Anisian; CL, Ladinian-Carnian; RN, Norian-Rhaetian; PSH, Hettangian-Pliensbachian; BAT, Toarcian-Bajocian; OCB, Bathonian-Oxfordian; TiKi, Kimmeridgian-Tithonian; ValBer, Berriasian-Valanginian; BarHau, Hauterivian-Barremian; Apt, Aptian; Alb, Albian. H=Holostei, T= Teleostei.

References

Adams, D. C. 2014. Quantifying and Comparing Phylogenetic Evolutionary Rates for Shape and Other High-Dimensional Phenotypic Data. Systematic Biology 63(2):166-177.

Adams, D. C., F. J. Rohlf, and D. E. Slice. 2004. Geometric morphometrics: ten years of progress following the 'revolution'. Italian Journal of Zoology 71(1):5-16.

Alfaro, M. E., D. I. Bolnick, and P. C. Wainwright. 2004. Evolutionary dynamics of complex biomechanical systems: An example using the four-bar mechanism. Evolution 58(3):495-503.

Alfaro, M. E., C. D. Brock, B. L. Banbury, and P. C. Wainwright. 2009a. Does evolutionary innovation in pharyngeal jaws lead to rapid lineage diversification in labrid fishes? Bmc Evolutionary Biology 9.

Alfaro, M. E., F. Santini, C. Brock, H. Alamillo, A. Dornburg, D. L. Rabosky, G. Carnevale, and L. J. Harmon. 2009b. Nine exceptional radiations plus high turnover explain species diversity in jawed vertebrates. Proceedings of the National Academy of Sciences of the United States of America 106(32):13410-13414.

Alfaro, M. E., F. Santini, and C. D. Brock. 2007. Do reefs drive diversification in marine teleosts? Evidence from the pufferfish and their allies (order tetraodontiformes). Evolution 61(9):2104-2126.

Alroy, J., M. Aberhan, D. J. Bottjer, M. Foote, F. T. Fuersich, P. J. Harries, A. J. W. Hendy, S. M. Holland, L. C. Ivany, W. Kiessling, M. A. Kosnik, C. R. Marshall, A. J. McGowan, A. I. Miller, T. D. Olszewski, M. E. Patzkowsky, S. E. Peters, L. Villier, P. J. Wagner, N. Bonuso, P. S. Borkow, B. Brenneis, M. E. Clapham, L. M. Fall, C. A. Ferguson, V. L. Hanson, A. Z. Krug, K. M. Layou, E. H. Leckey, S. Nuernberg, C. M. Powers, J. A. Sessa, C. Simpson, A. Tomasovych, and C. C. Visaggi. 2008. Phanerozoic trends in the global diversity of marine invertebrates. Science 321(5885):97-100.

Alroy, J., C. R. Marshall, R. K. Bambach, K. Bezusko, M. Foote, F. T. Fursich, T. A. Hansen, S. M. Holland, L. C. Ivany, D. Jablonski, D. K. Jacobs, D. C. Jones, M. A. Kosnik, S. Lidgard, S. Low, A. I. Miller, P. M. Novack-Gottshall, T. D. Olszewski, M. E. Patzkowsky, D. M. Raup, K. Roy, J. J. Sepkoski, M. G. Sommers, P. J. Wagner, and A. Webber. 2001. Effects of sampling standardization on estimates of Phanerozoic marine diversification. Proceedings of the National Academy of Sciences of the United States of America 98(11):6261-6266.

Amores, A., A. Force, Y. L. Yan, L. Joly, C. Amemiya, A. Fritz, R. K. Ho, J. Langeland, V. Prince, Y. L. Wang, M. Westerfield, M. Ekker, and J. H. Postlethwait. 1998. Zebrafish hox clusters and vertebrate genome evolution. Science 282(5394):1711-1714.

Anderson, P. S. L., and M. Friedman. 2012. Using cladistic characters to predict functional variety: experiments using early gnathostomes. Journal of Vertebrate Paleontology 32(6):1254-1270.

Anderson, P. S. L., M. Friedman, M. D. Brazeau, and E. J. Rayfield. 2011. Initial radiation of jaws demonstrated stability despite faunal and environmental change. Nature 476(7359):206-209.

Anderson, P. S. L., M. Friedman, and M. Ruta. 2013. Late to the Table: Diversification of Tetrapod Mandibular Biomechanics Lagged Behind the Evolution of Terrestriality. Integrative and Comparative Biology 53(2):197-208.

Arnegard, M. E., D. J. Zwickl, Y. Lu, and H. H. Zakon. 2010. Old gene duplication facilitates origin and diversification of an innovative communication system-twice. Proceedings of the National Academy of Sciences of the United States of America 107(51):22172-22177.

Arratia, G. 2000a. New teleostean fishes from the Jurassic of southern Germany and the systematic problems concerning the 'pholidophoriforms'. Palaeontologische Zeitschrift 74(1-2):113-143.

Arratia, G. 2000b. Remarkable teleostean fishes from the Late Jurassic of southern Germany and their phylogenetic relationships. Mitteilungen aus dem Museum fuer Naturkunde in Berlin Geowissenschaftliche Reihe 3:137-179.

Arratia, G. 2004. Mesozoic halecostomes and the early radiation of teleosts. Mesozoic fishes 3: Systematics, paleoenvironments and biodiversity: proceedings of the 3rd International Meeting, Serpiano, 2001.:279-315.

Arratia, G. 2008. The varasichthyid and other crossognathiform fishes, and the Break-up of Pangaea. Fishes and the Break-up of Pangaea 295:71-92.

Arratia, G. 2013. Morphology, taxonomy, and phylogeny of triassic pholidophorid fishes (actinopterygii, teleostei). Journal of Vertebrate Paleontology 33:1-138.

Arratia, G., and H. Tischlinger. 2010. The first record of Late Jurassic crossognathiform fishes from Europe and their phylogenetic importance for teleostean phylogeny. Fossil Record 13(2):317-341.

Arratia, G., and Schultze, H. P. 2013. Outstanding features of a new Late Jurassic pachycormiform fish from the Kimmeridgian of Brunn, Germany and comments on current understanding of pachycormiforms. Mesozoic Fishes 5, 87-120.

Barel, C. D. N. 1983. Towards a constructional morphology of cichlid fishes (Teleostei, Perciformes). Netherlands journal of zoology, 33(4), 357-424.

Bainbridge, R. 1960. Speed and stamina in three fish. Journal of Experimental Biology, 37(1), 129-153.

Baum, B. R. 1992. Combining trees as a way of combining data sets for phylogenetic inference, and the desirability of combining gene trees. Taxon 41(1):3-10.

Bellwood, D., and A. Hoey. 2004. Feeding in Mesozoic fishes: a functional perspective. Mesozoic fishes 3: Systematics, paleoenvironments and biodiversity: proceedings of the 3rd International Meeting, Serpiano, 2001.:639-649.

Bellwood, D. R. 2003. Origins and escalation of herbivory in fishes: a functional perspective. Paleobiology 29(1):71-83.

Bellwood, D. R., C. H. R. Goatley, S. J. Brandl, and O. Bellwood. 2014a. Fifty million years of herbivory on coral reefs: fossils, fish and functional innovations. Proceedings of the Royal Society B-Biological Sciences 281(1781).

Bellwood, D. R., A. S. Hoey, O. Bellwood, and C. H. R. Goatley. 2014b. Evolution of long-toothed fishes and the changing nature of fish-benthos interactions on coral reefs. Nature Communications 5.

Bellwood, D. R., P. C. Wainwright, C. J. Fulton, and A. S. Hoey. 2006. Functional versatility supports coral reef biodiversity. Proceedings of the Royal Society B-Biological Sciences 273(1582):101-107.

Benson, R. B. J., R. J. Butler, J. Lindgren, and A. S. Smith. 2010. Mesozoic marine tetrapod diversity: mass extinctions and temporal heterogeneity in geological megabiases affecting vertebrates. Proceedings of the Royal Society B-Biological Sciences 277(1683):829-834.

Benson, R. B. J., N. E. Campione, M. T. Carrano, P. D. Mannion, C. Sullivan, P. Upchurch, and D. C. Evans. 2014a. Rates of Dinosaur Body Mass Evolution Indicate 170 Million Years of Sustained Ecological Innovation on the Avian Stem Lineage. Plos Biology 12(5).

Benson, R. B. J., R. A. Frigot, A. Goswami, B. Andres, and R. J. Butler. 2014b. Competition and constraint drove Cope's rule in the evolution of giant flying reptiles. Nature Communications 5.

Benson, R. B. J., and J. N. Choiniere. 2013. Rates of dinosaur limb evolution provide evidence for exceptional radiation in Mesozoic birds. Proceedings of the Royal Society B-Biological Sciences 280(1768).

Benson, R. B., and Druckenmiller, P. S. 2014. Faunal turnover of marine tetrapods during the Jurassic–Cretaceous transition. Biological Reviews, 89(1), 1-23.

Benton, M. J. 1991. Extinction, biotic replacements, and clade interactions. The unity of evolutionary biology. Dioscorides Press, Portland, Oregon, 89-102.

Benton, M. J. 1996. Testing the roles of competition and expansion in tetrapod evolution. Proceedings of the Royal Society B-Biological Sciences 263(1370):641-646.

Benton, M. J., and F. J. Ayala. 2003. Dating the tree of life. Science 300(5626):1698-1700.

Betancur-R, R., R. E. Broughton, E. O. Wiley, K. Carpenter, J. A. Lopez, C. Li, N. I. Holcroft, D. Arcila, M. Sanciangco, J. C. Cureton Ii, F. Zhang, T. Buser, M. A. Campbell, J. A. Ballesteros, A. Roa-Varon, S. Willis, W. C. Borden, T. Rowley, P. C. Reneau, D. J. Hough, G. Lu, T. Grande, G. Arratia, and G. Orti. 2013. The tree of life and a new classification of bony fishes. PLoS currents 5.

Bininda-Emonds, O. R. P. 2004. The evolution of supertrees. Trends in Ecology and Evolution 19(6):315-322.

Bininda-Emonds, O. R. P., J. L. Gittleman, and M. A. Steel. 2002. The (Super)tree of life: Procedures, problems, and prospects. Annual Review of Ecology and Systematics 33:265-289.

Bininda-Emonds, O. R. P., and M. J. Sanderson. 2001. Assessment of the accuracy of matrix representation with parsimony analysis supertree construction. Systematic Biology 50(4):565-579.

Blazek, R., M. Polacik, and M. Reichard. 2013. Rapid growth, early maturation and short generation time in African annual fishes. Evodevo 4.

Bookstein, F. L. 1986. Size and shape spaces for landmark data in two dimensions. Statistical Science, 181-222.

Bowler, P. J. 1989. Evolution: The History of an Idea. University of California Press. p. 268.

Braasch, I., F. Brunet, J.-N. Volff, and M. Schartl. 2009. Pigmentation Pathway Evolution after Whole-Genome Duplication in Fish. Genome Biology and Evolution 1:479-493.

Braasch, I., J. N. Volff, and M. Schartl. 2008. The evolution of teleost pigmentation and the fish-specific genome duplication. Journal of Fish Biology 73(8):1891-1918.

Braasch, I., and Postlethwait, J. H. 2012. Polyploidy in fish and the teleost genome duplication. In Polyploidy and genome evolution (pp. 341-383). Springer Berlin Heidelberg.

Broughton, R. E., R. Betancur-R, C. Li, G. Arratia, and G. Orti. 2013. Multi-locus phylogenetic analysis reveals the pattern and tempo of bony fish evolution. PLoS currents 5.

Brusatte, S. L., M. J. Benton, M. Ruta, and G. T. Lloyd. 2008. Superiority, competition, and opportunism in the evolutionary radiation of dinosaurs. Science 321(5895):1485-1488.

Britton, J.R., Davies, G.D., Brazier, M. & Pinder, A. C. A case study on the population ecology of a topmouth gudegeon (*Pseudiasbora parva*) population in the UK and the implications for native fish communities. *Aquatic Conserv. Mar. Freshw. Ecosyst.* 17, 749-759 (2007).

Bush, A. M., and R. K. Bambach. 2011. Paleoecologic Megatrends in Marine Metazoa. Annual Review of Earth and Planetary Sciences, Vol 39 39:241-269.

Butler, R. J., P. M. Barrett, S. Nowbath, and P. Upchurch. 2009. Estimating the effects of sampling biases on pterosaur diversity patterns: implications for hypotheses of bird/pterosaur competitive replacement. Paleobiology 35(3):432-446.

Cailliet, G. M., A. H. Andrews, E. J. Burton, D. L. Watters, D. E. Kline, and L. A. Ferry-Graham. 2001. Age determination and validation studies of marine fishes: do deep-dwellers live longer? Experimental Gerontology 36(4-6):739-764.

Cañestro, C. 2012. Two rounds of whole-genome duplication: evidence and impact on the evolution of vertebrate innovations. In Polyploidy and genome evolution (pp. 309-339). Springer Berlin Heidelberg.

Cavin, L. 2010. Diversity of Mesozoic semionotiform fishes and the origin of gars (Lepisosteidae). Naturwissenschaften 97(12):1035-1040.

Cavin, L., U. Deesri, and V. Suteethorn. 2013. Osteology and relationships of Thaiichthys nov gen.: a Ginglymodi from the Late Jurassic - Early Cretaceous of Thailand. Palaeontology 56(1):183-208.

Cavin, L., and P. L. Forey. 2001. Osteology and systematic affinities of Palaeonotopterus greenwoodi Forey 1997 (Teleostei : Osteoglossomorpha). Zoological Journal of the Linnean Society 133(1):25-52.

Cavin, L., and P. L. Forey. 2007. Using ghost lineages to identify diversification events in the fossil record. Biology Letters 3(2):201-204.

Cavin, L., P. L. Forey, and C. Lecuyer. 2007. Correlation between environment and Late Mesozoic ray-finned fish evolution. Palaeogeography Palaeoclimatology Palaeoecology 245(3-4):353-367.

Cavin, L., A. Longbottom, and M. Richter. 2008. Fishes and the Break-up of Pangaea: an introduction. Fishes and the Break-up of Pangaea 295:7-8.

Chakrabarty, P. 2005 Testing conjectures about morphological diversity in cichlids of Lakes Malawi and Tanganyika. Copeia 2005, 359–373.

Ciampaglio, C. N., M. Kemp, and D. W. McShea. 2001. Detecting changes in morphospace occupation patterns in the fossil record: characterization and analysis of measures of disparity. Paleobiology 27(4):695-715.

Clarke, J. T., R. C. M. Warnock, and P. C. J. Donoghue. 2011. Establishing a time-scale for plant evolution. New Phytologist 192(1):266-301.

Colbert, E. H. 1969. Evolution of the Vertebrates. 2nd ed. Wiley, New York.

Collar, D. C., T. J. Near, and P. C. Wainwright. 2005. Comparative analysis of morphological diversity: Does disparity accumulate at the same rate in two lineages of centrarchid fishes? Evolution 59(8):1783-1794.

Collar, D. C., and P. C. Wainwright. 2006. Discordance between morphological and mechanical diversity in the feeding mechanism of centrarchid fishes. Evolution 60(12):2575-2584.

Collazo, A. 1996. Evolutionary correlations between early development and life history in plethodontid salamanders and teleost fishes. American Zoologist 36(2):116-131.

Collazo, A., J. A. Bolker, and R. Keller. 1994. A phylogenetic perspective on teleost gastrulation. American Naturalist 144(1):133-152.

Cowman, P. F., and D. R. Bellwood. 2011. Coral reefs as drivers of cladogenesis: expanding coral reefs, cryptic extinction events, and the development of biodiversity hotspots. Journal of Evolutionary Biology 24(12):2543-2562.

Davies, T. J., V. Savolainen, M. W. Chase, P. Goldblatt, and T. G. Barraclough. 2005. Environment, area, and diversification in the species-rich flowering plant family Iridaceae. American Naturalist 166(3):418-425.

Darwin, C. 1859. On the Origin of Species by Means of Natural Selection, or the Preservation of Favoured Races in the Struggle for Life 1 edn. John Murray.

de Pinna, M. C. C. 1996. Teleostean monophyly. Interrelationships of fishes.:147-162.

Deesri, U., K. Lauprasert, V. Suteethorn, K. Wongko, and L. Cavin. 2014. A new species of the ginglymodian fish Isanichthys from the Late Jurassic Phu Kradung Formation, northeastern Thailand. Acta Palaeontologica Polonica 59(2):313-331.

Depczynski, M., and D. R. Bellwood. 2005. Shortest recorded vertebrate lifespan found in a coral reef fish. Current Biology 15(8):R288-R289.

Dornburg, A., J. P. Townsend, M. Friedman, and T. J. Near. 2014. Phylogenetic informativeness reconciles ray-finned fish molecular divergence times. Bmc Evolutionary Biology 14.

Drake, A. G., and C. P. Klingenberg. 2010. Large-Scale Diversification of Skull Shape in Domestic Dogs: Disparity and Modularity. American Naturalist 175(3):289-301.

Eastman, J. M., M. E. Alfaro, P. Joyce, A. L. Hipp, and L. J. Harmon. 2011. A novel comparative method for identifying shifts in the rate of character evolution on trees. Evolution 65(12):3578-3589.

Edgecombe, G. D., and D. A. Legg. 2014. Origins and early evolution of arthropods. Palaeontology 57(3):457-468.

Edwards A.W.F., Cavalli-Sforza L.L. 1964. Reconstruction of evolutionary trees. In: Heywood V.H., McNeill J., editors. Phenetic and phylogenetic classification. London: Systematics Assocaition Publications. pp. 67–76.

Eimer, T. 1888. Die Entstehung der Arten auf Grund von Vererbnen erworbener Eigenschaften nach den Gesetzen organischen Wachsens. Verlag von Gustav Fischer, Jena.

Erwin, D. H. 2007. Disparity: Morphological pattern and developmental context. Palaeontology 50:57-73.

Faircloth, B. C., L. Sorenson, F. Santini, and M. E. Alfaro. 2013. A Phylogenomic Perspective on the Radiation of Ray-Finned Fishes Based upon Targeted Sequencing of Ultraconserved Elements (UCEs). Plos One 8(6).

Farrell, B. D. 1998. "Inordinate fondness" explained: Why are there so many beetles? Science 281(5376):555-559.

Felsenstein J. 1973. Maximum-likelihood estimation of evolutionary trees from continuous characters. Am. J. Hum. Genet. 25:471–492.

Felsenstein J. 1981. Evolutionary trees from gene frequencies and quantitative characters: finding maximum likelihood estimates. Evolution 35:1229–1242.

Felsenstein J. 1985. Phylogenies and the comparative method. Am. Nat. 125:1–15.

Felsenstein J. 2004. Inferring phylogenies. Sunderland (MA): Sinauer Associates.

Finarelli, J. A., and J. J. Flynn. 2006. Ancestral state reconstruction of body size in the Caniformia (Carnivora, Mammalia): The effects of incorporating data from the fossil record. Systematic Biology 55(2):301-313.

Fine, M. L., M. H. Horn, and B. Cox. 1987. Acanthonus-armatus, a deep-sea teleost fish with a minute brain and large ears. Proceedings of the Royal Society Series B-Biological Sciences 230(1259):257-+.

Fletcher, T., J. Altringham, J. Peakall, P. Wignall, and R. Dorrell. 2014. Hydrodynamics of fossil fishes. Proceedings of the Royal Society B-Biological Sciences 281(1788).

Foote, M. 1990. Nearest-neighbor analysis of trilobite morphospace. Systematic Zoology 39(4):371-382.

Foote, M. 1992. Rarefaction analysis of morphological and taxonomic diversity. Paleobiology 18(1):1-16.

Foote, M. 1993. Contributions of individual taxa to overall morphological disparity. Paleobiology 19(4):403-419.

Foote, M. 1997. The evolution of morphological diversity. Annual Review of Ecology and Systematics 28:129-152.

Foth, C., S. L. Brusatte, and R. J. Butler. 2012. Do different disparity proxies converge on a common signal? Insights from the cranial morphometrics and evolutionary history of Pterosauria (Diapsida: Archosauria). Journal of Evolutionary Biology 25(5):904-915.

Freeling, M., and B. C. Thomas. 2006. Gene-balanced duplications, like tetraploidy, provide predictable drive to increase morphological complexity. Genome Research 16(7):805-814.

Friedman, M. 2009. Ecomorphological selectivity among marine teleost fishes during the end-Cretaceous extinction. Proceedings of the National Academy of Sciences of the United States of America 106(13):5218-5223.

Friedman, M. 2010. Explosive morphological diversification of spiny-finned teleost fishes in the aftermath of the end-Cretaceous extinction. Proceedings of the Royal Society B-Biological Sciences 277(1688):1675-1683.

Friedman, M., and M. D. Brazeau. 2011. Sequences, stratigraphy and scenarios: what can we say about the fossil record of the earliest tetrapods? Proceedings of the Royal Society B-Biological Sciences 278(1704):432-439.

Friedman, M. 2012. Parallel evolutionary trajectories underlie the origin of giant suspension-feeding whales and bony fishes. Proceedings of the Royal Society B: Biological Sciences 279: 944-951. doi:10.1098/rspb.2011.1381

Friedman, M., and L. C. Sallan. 2012. Five hundred million years of extinction and recovery: a phanerozoic survey of large-scale diversity patterns in fishes. Palaeontology 55:707-742.

Gardiner, B. G. 1993. Osteichthyes: basal actinopterygians. The fossil record 2.:611-619.

Garland T.J., Ives A.R. 2000. Using the past to predict the present:confidence intervals for regression equations in phylogenetic comparative methods. Am. Nat. 155:346–364.

Gartner, J. V., Jr., Crabtree, R. E. and Sulak, K. J. 1997. Feeding at depth. Pp 115-193 in Randall, D. J. and Farrell, A. P., eds. Deep-sea Fishes. Academic Press, San Diego.

Gerber, S. 2013. On the Relationship between the Macroevolutionary Trajectories of Morphological Integration and Morphological Disparity. Plos One 8(5).

Gingerich, P. D. 2001. Rates of evolution on the time scale of the evolutionary process. Genetica 112:127-144.

Goatley, C. H. R., D. R. Bellwood, and O. Bellwood. 2010. Fishes on coral reefs: changing roles over the past 240 million years. Paleobiology 36(3):415-427.

Goloboff, P. A., J. S. Farris, and K. C. Nixon. 2008. TNT, a free program for phylogenetic analysis. Cladistics 24(5):774-786.

Gorzelak, P., Salamon, M.A., & Baumiller, T.K. (2012). Predator-induced macroevolutionary trends in Mesozoic crinoids. Proceedings of the National Academy of Sciences, 109(18). 7004-7007.

Goswami, A., and P. D. Polly. 2010. The Influence of Modularity on Cranial Morphological Disparity in Carnivora and Primates (Mammalia). Plos One 5(3).

Gould, S. J. 1989. Wonderful Life. New York: Norton. 347 pp.

Gould, S. J. 1991. The disparity of the burgess shale arthropod fauna and the limits of cladistic-analysis - why we must strive to quantify morphospace. Paleobiology 17(4):411-423.

Gould, S. J., D. M. Raup, J. J. J. Sepkoski, T. J. M. Schopf, and D. S. Simberloff. 1977. The shape of evolution a comparison of real and random clades. Paleobiology 3(1):23-40.

Graham, J. B. 1973. Terrestrial life of amphibious fish mnierpes-macrocephalus. Marine Biology 23(1):83-91.

Grande, L. 2010. An empirical synthetic pattern study of gars (lepisosteiformes) and closely related species, based mostly on skeletal anatomy. The resurrection of holostei. Copeia (2A):1-863.

Grande, L., and W. E. Bemis. 1998. A comprehensive phylogenetic study of amiid fishes (Amiidae) based on comparative skeletal anatomy. An empirical search for interconnected patterns of natural history. Journal of Vertebrate Paleontology 18(1):1-+.

Hallam, A. 2002. How catastrophic was the end-Triassic mass extinction? Lethaia 35(2):147-157.

Harper, E. M. 2003. The mesozoic marine revolution. Predator-Prey Interactions in the Fossil Record 20:433-455.

Hay, J. M., S. Subramanian, C. D. Millar, E. Mohandesan, and D. M. Lambert. 2008. Rapid molecular evolution in a living fossil. Trends in Genetics 24(3):106-109.

Hedman, M. M. 2010. Constraints on clade ages from fossil outgroups. Paleobiology 36(1):16-31.

Herring, P. J. 1987. Systematic distribution of bioluminescence in living organisms. Journal of bioluminescence and chemiluminescence 1(3):147-63.

Hoegg, S., H. Brinkmann, J. S. Taylor, and A. Meyer. 2004. Phylogenetic timing of the fish-specific genome duplication correlates with the diversification of teleost fish. Journal of Molecular Evolution 59(2):190-203.

Hopkins, M. J. 2014. The environmental structure of trilobite morphological disparity. Paleobiology 40(3):352-373.

Hubbell, S. P. 2001. The unified neutral theory of biodiversity and biogeography. Monographs in Population Biology 32:i-xiv, 1-375.

Hulsey, C. D., and P. C. Wainwright. 2002. Projecting mechanics into morphospace: disparity in the feeding system of labrid fishes. Proceedings of the Royal Society B-Biological Sciences 269(1488):317-326.

Hunter, J. P., and J. Jernvall. 1995. The hypocone as a key innovation in mammalian evolution. Proceedings of the National Academy of Sciences of the United States of America 92(23):10718-10722.

Huxley, T. H. 1861. Preliminary essay upon the systematic arrangement of the fishes of the Devonian epoch. Mem. Geol. Surv. UK, Decade, 10: 1-40.

Jablonski, D. 2008. Biotic interactions and macroevolution: Extensions and mismatches across scales and levels. Evolution 62(4):715-739.

Jernvall, J., J. P. Hunter, and M. Fortelius. 1996. Molar tooth diversity, disparity, and ecology in cenozoic ungulate radiations. Science 274(5292):1489-1492.

Kelley, P. H., T. A. Hansen, D. E. G. Briggs, and P. R. Crowther. 2001. Mesozoic marine revolution. Palaeobiology II.:94-97.

Kerschbaumer, M., and C. Sturmbauer. 2011. The utility of geometric morphometrics to elucidate pathways of cichlid fish evolution. International journal of evolutionary biology 2011:290245-290245.

Kriwet, J. 2001. Feeding mechanisms and ecology of pycnodont fishes (Neopterygii, Pycnodontiformes). Mitteilungen aus dem Museum fuer Naturkunde in Berlin Geowissenschaftliche Reihe 4:139-165.

Labandeira, C. C. 2005. The fossil record of insect extinction: New approaches and future directions. American Entomologist 51(1):14-29.

Lamarck, J. 1815. Histoire naturelle des animaux sans vertèbres, I (Paris).

Lambers, P. H. 1995. The monophyly of the Caturidae (Pisces, Actinopterygii) and the phylogeny of the Halecomorphi. Geobios Memoire Special (Villeurbanne) 19:201-203.

Lê, S., J. Josse, and F. Husson. 2008. FactoMineR: An R package for multivariate analysis. Journal of Statistical Software 25(1):1-18.

Levit, G. S., and Olsson, L. 2006. Evolution on rails: mechanisms and levels of orthogenesis. Ann Hist Philos Biol, 11, 99-138.

Lidgard, S., F. K. McKinney, and P. D. Taylor. 1993. Competition, clade replacement, and a history of cyclostome and cheilostome bryozoan diversity. Paleobiology 19(3):352-371.

Liem, K. F. 1973. Evolutionary strategies and morphological innovations - cichlid pharyngeal jaws. Systematic Zoology 22(4):425-441.

Lighthill, J. 1975. Mathematica. Biofluiddynamics. Society for Industrial and Applied Mathematics, US.

Lloyd, G. T. 2012. A refined modelling approach to assess the influence of sampling on palaeobiodiversity curves: new support for declining Cretaceous dinosaur richness. Biology Letters 8(1):123-126.

Lloyd, G. T., K. E. Davis, D. Pisani, J. E. Tarver, M. Ruta, M. Sakamoto, D. W. E. Hone, R. Jennings, and M. J. Benton. 2008. Dinosaurs and the Cretaceous Terrestrial Revolution. Proceedings of the Royal Society B-Biological Sciences 275(1650):2483-2490.

Lloyd, G. T., and M. Friedman. 2013. A survey of palaeontological sampling biases in fishes based on the Phanerozoic record of Great Britain. Palaeogeography Palaeoclimatology Palaeoecology 372:5-17.

Lloyd, G. T., S. C. Wang, and S. L. Brusatte. 2012. Identifying heterogeneity in rates of morphological evolution: discrete character change in the evolution of lungfish (sarcopterygii; dipnoi). Evolution 66(2):330-348.

Lombardo, C., and Tintori, A. 2005. Feeding specializations in Norian fishes. Museologia Scientifica e Naturalistica, 25-32.

Lopez-Arbarello, A. 2012. Phylogenetic Interrelationships of Ginglymodian Fishes (Actinopterygii: Neopterygii). Plos One 7(7).

Losos, J. B. 2011. Seeing the Forest for the Trees: The Limitations of Phylogenies in Comparative Biology. American Naturalist 177(6):709-727.

MacArthur, R. W. EO 1967. The theory of island biogeography. Princeton University Press, Monogr. Popul. Biol, 1, 202.

Maddison, W. P. and D.R. Maddison. 2008. Mesquite: a modular system for evolutionary analysis. Version 2.75 http://mesquiteproject.org

Mantel, N. 1967. Detection of disease clustering and a generalized regression approach. Cancer Research 27(2P1):209-and.

Marshall, C. R. 1990. Confidence-intervals on stratigraphic ranges. Paleobiology 16(1):1-10.

May, R. M. 1973. Stability and complexity in model ecosystems. Monographs in population biology 6:1-235.

May, R. M. 1994. Conceptual aspects of the quantification of the extent of biological diversity. Philosophical Transactions of the Royal Society of London Series B-Biological Sciences 345(1311):13-20.

Mayr, E. 1963. Animal species and evolution. Animal species and their evolution.

Mayrose, I., S. H. Zhan, C. J. Rothfels, K. Magnuson-Ford, M. S. Barker, L. H. Rieseberg, and S. P. Otto. 2011. Recently Formed Polyploid Plants Diversify at Lower Rates. Science 333(6047):1257-1257.

McShea, D. W. 1998. Possible largest-scale trends in organismal evolution: Eight "live hypotheses". Annual Review of Ecology and Systematics 29:293-318.

McPeek, M. A. and Brown, J. M. 2007. Clade age and not diversification rate explains species richness among animal taxa. Am. Nat., 169, E97–E106.

Meyer, A., and Y. Van de Peer. 2005. From 2R to 3R: evidence for a fish-specific genome duplication (FSGD). Bioessays 27(9):937-945.

Mora, C., Tittensor, D. P., Adl, S., Simpson, A. G., and Worm, B. 2011. How many species are there on Earth and in the ocean?. PLoS biology, 9(8), e1001127.

Motta, P. J. 1984. Mechanics and functions of jaw protrusion in teleost fishes - a review. Copeia (1):1-18.

Muller, J. 1844. Ueber den Bau und die Grenzen der Ganoiden und uber das natürliche System der Fische, Ber. Akad. Wiss. Berlin. 416-422

Muller, J. 1846a. Fernere Bemerkungen über den Bau der Ganoiden, Ber. Akad. Wiss. Berlin. 67-85 (English translation by J.W. Griffith, in Scient, Mem., 4:543-558

Muller, J. 1846b. Ueber den Bau und die Grenzen der Ganoiden und uber das natürliche System der Fische. Phys. Math. Abh. K. Akad. Wiss. Berlin, 1846: 117-216.

Nägeli, C. 1884. Mechanisch-physiologische Theorie der Abstammungslehre. R. Oldenbourg.

Near, T. J., R. I. Eytan, A. Dornburg, K. L. Kuhn, J. A. Moore, M. P. Davis, P. C. Wainwright, M. Friedman, and W. L. Smith. 2012. Resolution of ray-finned fish phylogeny and timing of diversification. Proceedings of the National Academy of Sciences of the United States of America 109(34):13698-13703.

Nilsson, G. E. 1996. Brain and body oxygen requirements of Gnathonemus petersii, a fish with an exceptionally large brain. Journal of Experimental Biology 199(3):603-607.

Olsen, P. E., and McCune, A. R. 1991. Morphology of the Semionotus elegans species group from the Early Jurassic part of the Newark Supergroup of Eastern North America with comments on the family Semionotidae (Neopterygii). Journal of Vertebrate Paleontology, 11(3), 269-292.

O'Meara, B. C., C. Ane, M. J. Sanderson, and P. C. Wainwright. 2006. Testing for different rates of continuous trait evolution using likelihood. Evolution 60(5):922-933.

O'Meara B.C. 2012. Evolutionary inferences from phylogenies: a review of methods. Ann. Rev. Ecol. Evol. Syst. 43:267–285.

Patterson, C. 1973. Interrelationships of holosteans. Pages 233–305. in PH Greenwood, RL Miles and C. Patterson, eds. Interrelationships of fishes.

Patterson, C. 1977. The contribution of paleontology to teleostean phylogeny. In Major patterns in vertebrate evolution (pp. 579-643). Springer US.

Patterson, C. 1981. Significance of fossils in determining evolutionary relationships. Annual Review of Ecology and Systematics 12:195-223.

Patterson, C. (Ed.). 1987. Molecules and morphology in evolution: conflict or compromise? Cambridge University Press.

Patterson, C. 1993a. An overview of the early fossil record of acanthomorphs. Bulletin of Marine Science 52(1):29-59.

Patterson, C. 1993b. Osteichthyes: Teleostei. The fossil record 2.:621-656.

Peng, Z., R. Diogo, and S. He. 2009. Teleost fishes (Teleostei). The timetree of life.:335-338.

Penney, D. 2004. Does the fossil record of spiders track that of their principal prey, the insects? Transactions of the Royal Society of Edinburgh-Earth Sciences 94:275-281.

Pietsch, T. W. 2005. Dimorphism, parasitism, and sex revisited: modes of reproduction among deep-sea ceratioid anglerfishes (Teleostei : Lophiiformes). Ichthyological Research 52(3):207-236.

Piper, R. 2007. Extraordinary Animals: An Encyclopedia of Curious and Unusual Animals, Greenwood Press.

Postlethwait, J., A. Amores, W. Cresko, A. Singer, and Y. L. Yan. 2004. Subfunction partitioning, the teleost radiation and the annotation of the human genome. Trends in Genetics 20(10):481-490.

Pough, F. H., J. B. Heiser, and W. N. McFarland. 1996. Vertebrate life. Fourth edition. Vertebrate life. Fourth edition.:i-xvii, 1-798.

Prentice, K. C., M. Ruta, and M. J. Benton. 2011. Evolution of morphological disparity in pterosaurs. Journal of Systematic Palaeontology 9(3):337-353.

Price, S. A., L. Schmitz, C. E. Oufiero, R. I. Eytan, A. Dornburg, W. L. Smith, M. Friedman, T. J. Near, and P. C. Wainwright. 2014. Two waves of colonization straddling the K-Pg boundary formed the modern reef fish fauna. Proceedings of the Royal Society B-Biological Sciences 281(1783).

Price, S. A., P. C. Wainwright, D. R. Bellwood, E. Kazancioglu, D. C. Collar, and T. J. Near. 2010. Functional innovations and morphological diversification in parrotfish. Evolution 64(10):3057-3068.

Quental, T. B., and C. R. Marshall. 2010. Diversity dynamics: molecular phylogenies need the fossil record. Trends in Ecology and Evolution 25(8):434-441.

Rabosky, D. L. 2009a. Ecological limits and diversification rate: alternative paradigms to explain the variation in species richness among clades and regions. Ecology Letters 12(8):735-743.

Rabosky, D. L. 2009b. Ecological Limits on Clade Diversification in Higher Taxa. American Naturalist 173(5):662-674.

Rabosky, D. L. 2010. Primary Controls on Species Richness in Higher Taxa. Systematic Biology 59(6):634-645.

Rabosky, D. L. 2014. Automatic Detection of Key Innovations, Rate Shifts, and Diversity-Dependence on Phylogenetic Trees. Plos One 9(2).

Rabosky, D. L., F. Santini, J. Eastman, S. A. Smith, B. Sidlauskas, J. Chang, and M. E. Alfaro. 2013. Rates of speciation and morphological evolution are correlated across the largest vertebrate radiation. Nature Communications 4.

Rabosky, D. L., G. J. Slater, and M. E. Alfaro. 2012. Clade Age and Species Richness Are Decoupled Across the Eukaryotic Tree of Life. Plos Biology 10(8).

Ragan, M. A. 1992. Phylogenetic Inference Based on Matrix Representation of Trees. Molecular Phylogenetics and Evolution 1(1):53-58.

Raup, D. M., S. J. Gould, T. J. M. Schopf, and Simberlo.Ds. 1973. Stochastic-models of phylogeny and evolution of diversity. Journal of Geology 81(5):525-542.

Regan, C. TATE, 1923. The skeleton of Lepidosteus, with remarks on the origin and evolution of the lower neopterygian fishes. Proc. zool. Soc. Lond., 1923: 445-461.

Renous, S., J. P. Gasc, V. L. Bels, and J. Davenport. 2000. Six-legged walking by a bottom-dwelling fish. Journal of the Marine Biological Association of the United Kingdom 80(4):757-758.

Revell, L. J. 2012. phytools: an R package for phylogenetic comparative biology (and other things). Methods in Ecology and Evolution 3(2):217-223.

Ricklefs, R. E., and D. B. Miles. 1994. Ecological and evolutionary inferences from morphology: An ecological perspective. Ecological morphology: Integrative organismal biology:13-41.

Rohlf, F. J., and L. F. Marcus. 1993. A revolution in morphometrics. Trends in Ecology and Evolution 8(4):129-132.

Rohlf, F. J. 2010. tpsRelw, v. 1.49. Stony Brook, NY: Department of Ecology and Evolution, SUNY Stony Brook.

Rohlf, F. J. 2012. tpsUtil, v. 1.55. Stony Brook, NY: Department of Ecology and Evolution, SUNY Stony Brook.

Rohlf, F. J. 2013. tpsDig2, v. 2.17. Stony Brook, NY: Department of Ecology and Evolution, SUNY Stony Brook.

Romer, A. S. 1966. Vertebrate paleontology, 3rd ed. Univ of Chicago Press, Chicago

Rook, D. L., N. A. Heim, and J. Marcot. 2013. Contrasting patterns and connections of rock and biotic diversity in the marine and non-marine fossil records of North America. Palaeogeography Palaeoclimatology Palaeoecology 372:123-129.

Rosen, D. E. 1982. Teleostean interrelationships, morphological function and evolutionary inference. American Zoologist 22(2):261-273.

Ross, R. M. 1990. The evolution of sex-change mechanisms in fishes. Environmental Biology of Fishes 29(2):81-93.

Roy, K., D. Jablonski, J. W. Valentine, and G. Rosenberg. 1998. Marine latitudinal diversity gradients: Tests of causal hypotheses. Proceedings of the National Academy of Sciences of the United States of America 95(7):3699-3702.

Ruta, M., K. D. Angielczyk, J. Froebisch, and M. J. Benton. 2013. Decoupling of morphological disparity and taxic diversity during the adaptive radiation of anomodont therapsids. Proceedings of the Royal Society B-Biological Sciences 280(1768).

Sallan, L. C. 2014. Major Issues in the Origins of Ray-finned Fish (Actinopterygii) Biodiversity. Biological Reviews. Early View.

Sanderson, S. L., and R. Wassersug. 1993. Convergent and alternative designs for vertebrate suspension feeding. The Skull, Vol. 3; Functional and evolutionary mechanisms:37-112.

Santini, F., L. J. Harmon, G. Carnevale, and M. E. Alfaro. 2009. Did genome duplication drive the origin of teleosts? A comparative study of diversification in ray-finned fishes. Bmc Evolutionary Biology 9.

Schaeffer, B., and D. E. Rosen. 1961. Major adaptive levels in the evolution of the actinopterygian feeding mechanism. American Zoologist 1(2):187-204.

Schultze, H. P., and Wiley, E. O. 1984. The neopterygian Amia as a living fossil. In Living fossils (pp. 153-159). Springer New York.

Schweitzer, C. E., and R. M. Feldmann. 2010. The decapoda (crustacea) as predators on mollusca through geologic time. Palaios 25(3-4):167-182.

Semon, M., and K. H. Wolfe. 2007. Reciprocal gene loss between Tetraodon and zebrafish after whole genome duplication in their ancestor. Trends in Genetics 23(3):108-112.

Sepkoski, J. J. 1978. A kinetic model of Phanerozoic taxonomic diversity. I. Analysis of marine orders. Paleobiology 4 (3): 223–251.

Sepkoski, J. J. 1979. A kinetic model of Phanerozoic taxonomic diversity. II. Early Phanerozoic families and multiple equilibria. Paleobiology 5 (3): 222–251.

Sepkoski, J. J. 1998. Rates of speciation in the fossil record. Philosophical Transactions of the Royal Society of London Series B-Biological Sciences 353(1366):315-326.

Sepkoski, J. J., F. K. McKinney, and S. Lidgard. 2000. Competitive displacement among post-Paleozoic cyclostome and cheilostome bryozoans. Paleobiology 26(1):7-18.

Sepkoski, J. J. J. 1976. Species diversity in the phanerozoic species area effects. Paleobiology 2(4):298-303.

Sidlauskas, B. 2007. Testing for unequal rates of morphological diversification in the absence of a detailed phylogeny: A case study from characiform fishes. Evolution 61(2):299-316.

Sidlauskas, B. 2008. Continuous and arrested morphological diversification in sister clades of characiform fishes: a phylomorphospace approach. Evolution 62(12):3135-3156.

Sivak, J. G. 1976. Optics of eye of 4-eyed fish (anableps-anableps). Vision Research 16(5):531-and.

Slater, G. J., L. J. Harmon, and M. E. Alfaro. 2012. Integrating fossils with molecular phylogenies improves inference of trait evolution. Evolution 66(12):3931-3944.

Smith, A. B., and A. J. McGowan. 2007. The shape of the phanerozoic marine palaeodiversity curve: How much can be predicted from the sedimentary rock record of western Europe? Palaeontology 50:765-774.

Soin, S. G. 1981. A new classification of the structure of mature eggs of fishes according to the ratio of yolk to ooplasm. Soviet Journal of Developmental Biology (English Translation of Ontogenez) 12(1):13-17.

Soltis, D. E., M. C. Segovia-Salcedo, I. Jordon-Thaden, L. Majure, N. M. Miles, E. V. Mavrodiev, W. Mei, M. B. Cortez, P. S. Soltis, and M. A. Gitzendanner. 2014. Are polyploids really evolutionary dead-ends (again)? A critical reappraisal of Mayrose et al. (2011). New Phytologist 202(4):1105-1117.

Staab, K. L., R. Holzman, L. P. Hernandez, and P. C. Wainwright. 2012. Independently evolved upper jaw protrusion mechanisms show convergent hydrodynamic function in teleost fishes. Journal of Experimental Biology 215(9):1456-1463.

Stanley, S. M. 1972. Functional morphology and evolution of byssally attached bivalve mollusks. Journal of Paleontology 46(2):165-212.

Stanley, S. M. 1984. Does Bradytely Exist?. In Living Fossils (pp. 278-280). Springer New York.

Stayton, C. T. 2008. Is convergence surprising? An examination of the frequency of convergence in simulated datasets. Journal of Theoretical Biology 252(1):1-14.

Stebbins, G. L. 1974. Adaptive shifts and evolutionary novelty a compositionist approach. Ayala, Francisco Jose and Theodosius Dobzhansky (Ed.). Studies in the Philosophy of Biology. Reduction and Related Problems. Symposium. Bellagio, Italy, Sept. 9-16, 1972. Xix+390p. Illus. University of California Press: Berkeley, Calif., U.S.a. Isbn 0-520-02649-7:285-306.

Stephens, P. R., and J. J. Wiens. 2003. Explaining species richness from continents to communities: The time-for-speciation effect in emydid turtles. American Naturalist 161(1):112-128.

Stiassny, M. L. J., and J. S. Jensen. 1987. Labroid intrarelationships revisited morphological complexity key innovations and the study of comparative diversity. Bulletin of the Museum of Comparative Zoology 151(5):269-319.

Stubbs, T. L., S. E. Pierce, E. J. Rayfield, and P. S. L. Anderson. 2013. Morphological and biomechanical disparity of crocodile-line archosaurs following the end-Triassic extinction. Proceedings of the Royal Society B-Biological Sciences 280(1770).

Sundberg, F. A. 1996. Morphological diversification of Ptychopariida (Trilobita) from the Marjumiid biomere (Middle and Upper Cambrian). Paleobiology 22(1):49-65.

Taverne, L. 2011. Osteology and phylogenetic relationships of Steurbautichthys ("Pholidophophorus") aequatorialis gen. nov (Teleostei, "Pholidophoriformes") from the Middle Jurassic of Kisangani, Democratic Republic of Congo. Bulletin de l'Institut Royal des Sciences Naturelles de Belgique Sciences de la Terre 81:129-173.

Taylor, J. S., Y. Van de Peer, I. Braasch, and A. Meyer. 2001. Comparative genomics provides evidence for an ancient genome duplication event in fish. Philosophical Transactions of the Royal Society of London Series B-Biological Sciences 356(1414):1661-1679.

Thomas GH. Freckleton RP. 2012. MOTMOT: models of trait macroevolution on trees. Methods Ecol. Evol. 3:145–151.

Thorne, P. M., M. Ruta, and M. J. Benton. 2011. Resetting the evolution of marine reptiles at the Triassic-Jurassic boundary. Proceedings of the National Academy of Sciences of the United States of America 108(20):8339-8344.

Tintori, A. 1998. Fish biodiversity in the marine Norian (Late Triassic) of northern Italy: the first Neopterygian radiation. Italian Journal of Zoology 65:193-198.

Tintori, A. 2011. Comment on "The vertebrates of the Anisian/Ladinian boundary (Middle Triassic) from Bissendorf (NW Germany) and their contribution to the anatomy, palaeoecology, and palaeobiogeography of the Germanic Basin reptiles" by C. Diedrich Palaeogeography, Palaeoclimatology, Palaeoecology 273 (2009) 1-16. Palaeogeography Palaeoclimatology Palaeoecology 300(1-4):205-207.

Van de Peer, Y. 2004. Tetraodon genome confirms Takifugu findings: most fish are ancient polyploids. Genome Biology 5(12).

Van de Peer, Y., S. Maere, and A. Meyer. 2009. OPINION The evolutionary significance of ancient genome duplications. Nature Reviews Genetics 10(10):725-732.

Venkatesh, B., M. V. Erdmann, and S. Brenner. 2001. Molecular synapomorphies resolve evolutionary relationships of extant jawed vertebrates. Proceedings of the National Academy of Sciences of the United States of America 98(20):11382-11387.

Vermeij, G. J. 1987. Evolution and escalation an ecological history of life. Vermeij, G. J. Evolution and Escalation: an Ecological History of Life. Xv+527p. Princeton University Press: Princeton, New Jersey, USA; Surrey, England, Uk. Illus:XV+527P-XV+527P.

Vogel, S. 2003. Comparative biomechanics: life's physical world. Comparative biomechanics: life's physical world.:i-xii, 1-580.

Vogt, C. 1845. Quelques observations sur les caractères qui servent à la classification des poisons ganoïdes. Annls Sci. nat., (Zool.), (3)4: 53-68

Volff, J. N. 2005. Genome evolution and biodiversity in teleost fish. Heredity 94(3):280-294.

Wagner, P. J. 1996. Contrasting the underlying patterns of active trends in morphologic evolution. Evolution 50(3):990-1007.

Wainwright, P. C. 1988. Morphology and ecology: the functional basis of feeding constraints in Caribbean labrid fishes. Ecology 69, 635–645.

Wainwright, P. C. 2007. Functional versus morphological diversity in macroevolution. Annual Review of Ecology Evolution and Systematics 38:381-401.

Wainwright, P. C., and D. R. Bellwood. 2002. Ecomorphology of feeding in coral reef fishes. Coral reef fishes: dynamics and diversity in a complex ecosystem.:33-55.

Wainwright, P. C., and S. W. Day. 2007. The forces exerted by aquatic suction feeders on their prey. Journal of the Royal Society Interface 4(14):553-560.

Wainwright, P. C., and Richard, B. A. 1995. Predicting patterns of prey use from morphology of fishes. In Ecomorphology of fishes (pp. 97-113). Springer Netherlands.

Wainwright, P. C., W. L. Smith, S. A. Price, K. L. Tang, J. S. Sparks, L. A. Ferry, K. L. Kuhn, R. I. Eytan, and T. J. Near. 2012. The Evolution of Pharyngognathy: A Phylogenetic and Functional Appraisal of the Pharyngeal Jaw Key Innovation in Labroid Fishes and Beyond. Systematic Biology 61(6):1001-1027.

Walford, L. A. 1937. Marine game fishes of the Pacific coast from Alaska to the equator. Contrib. Santa Barbara Mus. Nat. Hist., Univ. Calif. Press, Berkeley. xxix, 69.

Waltzek, T. B., and P. C. Wainwright. 2003. Functional morphology of extreme jaw protrusion in neotropical Cichlids. Journal of Morphology 257(1):96-106.

Ward, P. 1980. Comparative shell shape distributions in jurassic-cretaceous ammonites and jurassic-tertiary nautilids. Paleobiology 6(1):32-43.

Watson, W., and H. J. Walker. 2004. The world's smallest vertebrate, Schindleria brevipinguis, a new paedomorphic species in the family Schindleriidae (Perciformes : Gobioidei). Records of the Australian Museum 56(2):139-142.

Weir, J. T., and D. Schluter. 2007. The latitudinal gradient in recent speciation and extinction rates of birds and mammals. Science 315(5818):1574-1576.

Wesley-Hunt, G. D. 2005. The morphological diversification of carnivores in North America. Paleobiology 31(1):35-55.

Westneat, M. W. 1994. Transmission of force and velocity in the feeding mechanisms of labrid fishes (teleostei, perciformes). Zoomorphology 114(2):103-118.

Westneat, M. W. 2004. Evolution of levers and linkages in the feeding mechanisms of fishes. Integrative and Comparative Biology 44(5):378-389.

Westneat, M. W., and P. C. Wainwright. 1989. Feeding mechanism of epibulus-insidiator (labridae, teleostei) - evolution of a novel functional system. Journal of Morphology 202(2):129-150.

Wiens, J. J. 2011. The causes of species richness patterns across space, time, and clades and the role of "ecological limits. Quarterly Review of Biology 86(2):75-96.

Wiley, E. O., and Schultze, H. P. 1984. Family Lepisosteida (gars) as living fossils. In Living Fossils (pp. 160-165). Springer New York.

Wilkinson, M. 1995. Coping with abundant missing entries in phylogenetic inference using parsimony. Systematic Biology 44(4):501-514.

Wilkinson, M., Pisani, D., Cotton, J. A., and Corfe, I. 2005. Measuring support and finding unsupported relationships in supertrees. Systematic Biology, 54(5), 823-831.

Wills, M. A., D. E. G. Briggs, and R. A. Fortey. 1994. Disparity as an evolutionary index - a comparison of cambrian and recent arthropods. Paleobiology 20(2):93-130.

Wills, M. A., and R. A. Fortey. 2000. The shape of life: how much is written in stone? Bioessays 22(12):1142-1152.

Wilson, M. V. H., and A. M. Murray. 2008. Osteoglossomorpha: phylogeny, biogeography, and fossil record and the significance of key African and Chinese fossil taxa. Fishes and the Break-up of Pangaea 295:185-219.

Wittbrodt, J., A. Meyer, and M. Schartl. 1998. More genes in fish? Bioessays 20(6):511-515.

Xu, G.-H., and M.-M. Chang. 2009. Redescription of dagger Paralycoptera wui Chang and Chou, 1977 (Teleostei: Osteoglossoidei) from the Early Cretaceous of eastern China. Zoological Journal of the Linnean Society 157(1):83-106.

Zelditch, M. L., D. L. Swiderski, and H. D. Sheets. 2012. Geometric Morphometrics for Biologists: A Primer, 2nd Edition. Geometric Morphometrics for Biologists: a Primer, 2nd Edition:1-478.

Zhang, J. Y. 2004. New fossil osteoglossomorph from Ningxia, China. Journal of Vertebrate Paleontology 24(3):515-524.

Zhan, S. H., Glick, L., Tsigenopoulos, C. S., Otto, S. P., and Mayrose, I. 2014. Comparative analysis reveals that polyploidy does not decelerate diversification in fish. Journal of evolutionary biology, 27(2), 391-403.